Application of A Microfluidic Tool for the Determination of Enzyme Kinetics

Ringborg, Rolf H.

Publication date:
2015

Document Version
Publisher's PDF, also known as Version of record

Application of a Microfluidic Tool for the Determination of Enzyme Kinetics

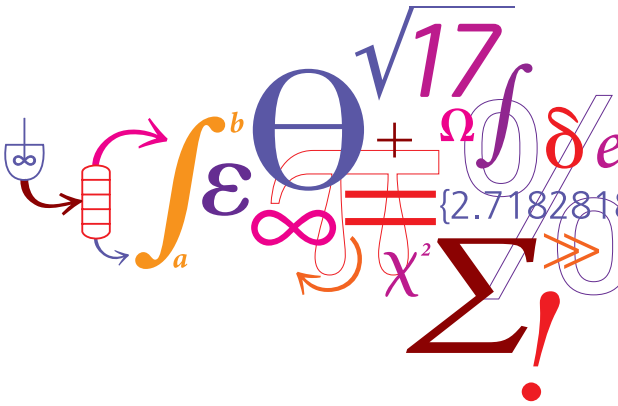

Rolf H. Ringborg

PhD Thesis

February 2016

DTU Chemical Engineering
Department of Chemical and Biochemical Engineering

Application of a Microfluidic Tool for the Determination of Enzyme Kinetics

Rolf H. Ringborg

Ph.D Thesis

February 2016

DTU Chemical Engineering
Department of Chemical and Biochemical Engineering

APPLICATION OF A MICROFLUIDIC TOOL FOR THE DETERMINATION OF ENZYME KINETICS

Ph.D Thesis

Rolf H. Ringborg

CAPEC-PROCESS Center

Department of Chemical and Biochemical Engineering

Technical University of Denmark

Supervisors:

Professor John M. Woodley

Co-supervisors:

Professor Krist V. Gernaey

Associate Professor Ulrich Krühne

This dissertation is submitted for the degree of Doctor of Philosophy

February 2016

PREFACE

This thesis is the main result of my Ph.D studies, which was performed at the CAPEC-PROCESS Research Center. The center is a part of the Department of Chemical and Biochemical Engineering at the Technical University of Denmark (DTU). The project was carried out in the period from September 2012 until November 2015. The project was partially funded by the BIOINTENSE project, financed by the European Union through the 7th Framework Programme (grant agreement n^o.: 312148). Furthermore, the project received co-funding by DTU.

During the course of the work presented in this thesis, a number of people have provided their help and support, for which I am truly grateful. First of all, I would like to thank my main supervisor, John M. Woodley, for his fantastic guidance and support. I am deeply appreciative for his ability to create an environment where it has been possible to discuss aspects far exceeding that of this Ph.D. A special thanks to my co-supervisor Ulrich Krühne, whom always took the time to discuss, reminded me to put things into perspective and after discussion left me with both solutions and twice as many questions. I would also like to thank co-supervisor Krist V. Gernaey that has always had an open door for my queries.

I would like to thank my former and present colleagues at CAPEC-PROCESS for making the past three years so enjoyable. This work has been part of a larger project, BIOINTENSE, and two other students has accompanied me on the journey, thanks Ines P. Rosinha and Søren Heintz. I would like give a special thanks to Søren, who has always been available for discussions surrounding the project. Every day the office has been full of a good mood, and therefore, many thanks Jason Price, Kresimir Janes, and Asbjørn T. Pedersen.

Finally, I am deeply grateful to my wife Nicole and my son Benjamin whose unconditional support has kept me going strong, thanks so much.

I enjoy learning and investigating new things, and I have been very fortunate to be able to do so all of my life. I would like to thank everyone that has helped me to make this a possibility. I hope that I can give as much in return as I have received.

Rolf H. Ringborg, November 2015

If I have seen further, it is by standing on the shoulders of giants.

– Isaac Newton

ABSTRACT

Biocatalysis offers the ability to carry out important synthesis and production of valuable chemicals at benign conditions. In the development of new processes, enzymes are being engineered towards specific products with great success. Currently, mutations are introduced into enzymes, and a search among the formed mutants is conducted. High throughput screening can deliver screening of mutants in the order of millions a day. Enzyme mutants with increased performance are therefore likely to be found.

Here, the enzyme amine transaminases is evaluated since it offers a unique way of producing chiral amines. These amines are important as building blocks for pharmaceuticals and agrochemicals. A promising enzyme has been found, but it has been a problem to assess its performance and give process development direction. Common limitations are substrate and product solubility, unfavourable thermodynamics, inhibition and stability. It is a difficult task to assess where the current bottleneck is for a desired process. Moreover, it cannot be expected that a single solution to the limitations can be found and rather an integrated solution of all of the problems should be the future aim. All the limitations surround the reactor of a process, and with the performance of this being unknown, it is almost impossible to direct development. A focal point must therefore lie in the determination of kinetic models and how kinetic data can be obtained in a robust and generic way. Models for many enzymes already exist and can be found in common text books. These models do however require mutant specific data and must be collected with the target reaction.

In this thesis a novel way of collecting kinetic data is created, this is carried out by combining existing technology and enables the analysis of aqueous solutions on-line. Furthermore, the use of a size exclusion column enables the simultaneous detection of the enzyme and UV/VIS-active compounds. The size exclusion chromatography does not provide baseline separated results, nor is this required. The application of chemometric tools enable detection of compounds in the collected retention time wavelength data. A major improvement over traditional techniques is the quantification of enzyme concentration and this makes it possible to use specific activities for model fitting. The setup takes advantage of microfluidic features and delivers semi-automatic experimentation, overall reducing both consumption of precious materials and costly labor.

DANSK RESUME

Med biokatalyse er det muligt at syntetisere og producere værdifulde kemikalier under milde betingelser. Ved udvikling af nye processer, bliver enzymer modificeret til at katalysere ønskede produkter med stor succes. Nu om dage introduceres mutationer i enzymer, derved dannes mange nye mutanter og der søges herefter iblandt disse. Med high throughput screening kan man udføre screening af millioner af mutanter pr. dag. Der er derfor høj sandsynlighed for at finde enzym mutanter med egnede egenskaber.

Specielt bliver enzymet amin transaminase her evalueret, da disse enzymer giver mulighed for en unik vej til fremstilling af chirale aminer. Chirale aminer er vigtige byggesten både i lægemidler og i kemikalier til landbrug. Et lovende enzym er blevet isoleret, men det har været vanskeligt at vurdere dets ydeevne samt at give retningslinier for en procesudvikling. Almindeligt kendte begrænsninger i processer er opløselighed af substrat og produkt, ufordelagtig termodynamik¸ inhibering samt stabilitet. Det er vanskeligt at vurdere, hvor flaskehalsen i en given proces vil være. Desuden kan man ikke forvente, at der kun er en enkelt løsningsmodel til afhjælpning af flaskehalse, og man bør i fremtiden have som mål at finde frem til integrerede problemløsninger. Alle de nævnte begrænsninger vedrører reaktoren i en proces, og når ydeevnen af et enzym er ukendt, er det næsten umuligt at opstille forslag til procesudvikling. Et fokuspunkt må derfor i fremtiden være at udvikle kinetiske modeller og metoder til at registrere kinetiske data på en robust og generisk måde. Modeller for mange enzymer eksisterer allerede og findes beskrevet i lærebøger omhandlende enzym kinetik. For at tilpasse modellerne er der brug for kinetisk data der er specifik for den enkelte mutant og skal være opsamlet med reaktionen der har interesse.

I denne afhandling beskrives en ny måde hvormed man kan opsamle kinetiske data. Det er blevet opnået ved en kombination af eksisterende teknologier og giver mulighed for online analyse af vandige opløsninger. Endvidere er det muligt at kvantificere enzym og UV/VIS aktive molekyler ved kombineret af størrelseskromatografi og UV/VIS detektion. Størrelseskromatografi giver ikke basislinie separation, hvilket heller ikke er nødvendigt. Brug af kemometriske metoder gør det nemlig muligt at detektere forbindelser på baggrund af opsamling af retentionstids- og bølgelængde data. Et stort fremskridt har været at kunne kvantificere enzymkoncentration, da man herigennem kan anvende specifik aktivitet til modeltilpasning. Dette setup udnytter fordelene ved mikrofluidiske skala og leverer semi-automatisk experimentmuligheder. Alt i alt reducerer dette setup både forbrug af dyrebart materiale og arbejdstid.

LIST OF PUBLICATIONS

Papers are attached as Appendix C

- Rosinha, P. I., **Ringborg, R. H.**, Heintz, S., Tufvesson, P., Krühne, U., Gernaey, K. V. and Woodley, J. M., Miniaturized experimental toolbox for ω-transaminase technology (BIOINTENSE). 1st International Symposium on Transaminase, Stockholm, Sweden, 28 Feb. – 1 Mar. (2013)
  Type: Poster
- **Ringborg, R. H.**, Krühne, U., Gernaey, K. V. and Woodley, J. M., Using micro technology in process screening for improved ω-transaminases. Implementation of Microreactor Technology into Biotechnology, Cavtat, Croatia, 5-8 May (2013)
  Type: Poster
- Mitic, A., Heintz, S., **Ringborg, R. H.**, Bodla, V., Woodley, J. M. and Gernaey, K. V., Applications, benefits and challenges of flow chemistry. Chimica Oggi – Chemistry Today, 31, 4, 4-8, (2013)
  Type: Mini-review paper
- **Ringborg, R. H.**, Heintz, S., Rosinha, P. I., Tufvesson, P., Krühne, U., Gernaey, K. V. and Woodley, J. M., Using micro technology in process screening for improved ω-transaminases, The Next Generation of Biocatalsis for Industrial Chemical Synthesis, Brussels, Belgium, 3 Dec, (2013)
  Type: Poster
- Krühne, U., Heintz, S., **Ringborg, R. H.**, Tufvesson, P., Gernaey, K. V. and Woodley, J. M., Biocatalytic process developments using microfluidic miniaturized systems., Green Process Synthesis, 3, 23-31, (2014)
  Type: Review paper
- **Ringborg, R. H.**, Krühne, U. and Woodley, J. M., *Enzyme characterisation in microreactors by multivariate data analysis*, 13th International conference on microreaction technology, Budapest, Hungary, 23-25 Jun (2014)
  Type: Poster
- Krühne, U., Larsson, H., Heintz, S., **Ringborg, R. H.**, Rosinha, P. I., Bodla, V. K., Santacoloma, P. A., Tufvesson, P., Woodley, J. M. and Gernaey, K. V., Systematic Development of Miniaturized (Bio)Processes using Process Systems Engineering (PSE) Methods and Tools. Chemical and Biochemical Engineering Quarterly, 28, 2, 203-214 (2014.)
  Type: Full journal article
- **Ringborg, R. H.**, Krühne, U. and Woodley, J. M, *Enzyme characterization in microreactors by UV-Vis*, Transam 2.0 - Chiral Amines Through (Bio)Catalysis, Greifswald, Germany, 4-6 March, 2015
  Type: Poster
- **Ringborg, R. H.** and Woodley, J. M., *The Application of Reaction Engineering to Biocatalysis*. Reaction Chemistry & Engineering, 1, 10 – 22, (2016)
  Type: Review paper

CONTENTS

LIST OF TABLES

LIST OF FIGURES

LIST OF ABBREVIATIONS AND ACRONYMS

Abbreviation	Description
A	First substrate to bind with enzyme
ACE	Acetone
ACP	Acetophenone
ALA	Alanine
API	Active Pharmaceutical Ingredient
AU	Absorbance units
B	Second substrate to bind with enzyme
BA	Benzyl acetone
CFD	Computational fluid dynamics
CONCORDIA	Core consistency diagnostic
DAD	Diode array detector
DKR	Dynamic Kinetic Resolution
DOF	Degrees of freedom
DSC	Differencial scanning calorimetry
E	Enzyme
EC	European commission
E-factor	Environmental-factor
Enz	Enzyme
EX	Enzyme - X complex
FIM	Fisher Information Matrix
FT-IR	Fourier transform infrared spectroscopy
GDH	Glucose dehydrogenase
HPLC	High performance liquid chromatography
HTS	High Throughput Screening
IPA	Isopropylamine
IR	Infrared spectroscopy
ISPR	In-situ product removal
ISSS	In-situ substrate supply
ITC	Isothermal titration calorimetry
IUBMB	International Union of Biochemistry and Molecular Biology
KR	Kinetic Resoltuion
LDH	Lactate dehydrogenase
LFR	Laminar flow reactor
LLE	Liquid-Liquid extraction
MBA	Methylbenzylamine
MBDoE	Model-based design of experiments
MCR-ALS	Multi curve resolution alternating least squares
MPPA	1-Methyl-3-phenylpropylamine
MUO	micro unit operation
NAD(P)	Nicotinamide adenine dinucleotide (phosphate)
P	First product to dissociate from enzyme
PARAFAC	Parallel factor analysis
Abbreviation	**Description**
PBS	Phosphate buffer solution

PBR	Packed bed reactor
PCA	Principal component analysis
PCR	Principal component regression
PFR	plug flow reactor
PMP	Pyridoxamine-5-'phosphate
PTFE	Polytetrafluoroethylene
PYR	Pyruvate
Q	Second product to dissociate from enzyme
R	Reactor
RTD	Residence time destribution
Sol	Solution
UV	Ultra violet
VIS	Visible

LIST OF NOMENCLATURE

Nomenclature	Description	Unit
a	Surface to volume ratio	$m^2 \cdot m^{-3}$
A	Area	m^2
Bo	Bodenstein number	$-$
C_i	Concentration of component i	$M\ (mol \cdot L^{-1})$
$C_{p,m}$	Mass based heat capacity	
d_H	Hydraulic diameter, the hydraulic diameter for tubes are the inner diameter of the tube	m
d_p	Particle diameter	
d_t	Diffusion distance	m
D	Taylor dispersion coefficient	$m^2 \cdot s^{-1}$
D_{ab}	Diffusion coefficient of solute a in b	$m^2 \cdot s^{-1}$
$E_{\theta,oo}$	Exit age distribution	$-$
Eo	Eötvös number	$-$
F_{oo}	F curve	$-$
g	Standard gravity = 9.81	$m \cdot s^{-2}$
h_0	Thermal conductivity	
ΔH_r	Reaction enthalpy	$kJ \cdot mol^{-1}$
I	Intensity	$-$
$I.D.$	Inner diameter	m
k	1st or 2nd order rate constant	s^{-1} or $L \cdot mol^{-1} \cdot s^{-1}$
k_{tef}	Thermal conductivity for teflon	
K_{eq}	Reaction equilibrium constant	$-$
K_m	Michaelis-Menten constant	mM
K_i	Inhibition constant	mM
K_{si}	Dead-end inhibiton constant	mM
K_d	Dissociation constant	mM
l	Path length	
L	Length	m
$log\ P$	Octanol-water partition coefficient	$-$
m	Mass	g
$\dot{m}$	Mass flow rate	$kg \cdot s^{-1}$
$M\ (M_w)$	Molecular weight	$g \cdot mol^{-1}\ or\ kDa$
$O.D.$	Outer diameter	
pK_a	Acid dissociation constant	$-$
q	Volumetric flow rate	$m^3 \cdot s^{-1}$
Q	Heat	J
R_G	Radius of gyration	Å
Re	Reynolds number	$-$
S	Slope of τ versus t_f	
t	Time	s
t_f	Fluid element entry time	s
t_f	Fluid element exit time	s
T	Temperature	$°K\ or$ ℃
T_0	Flowing liquid temperature	$°K$
T_b	Bulk temperature	$°K$
v	Rate of reaction	$mol \cdot s^{-1}$
v	Linear flow rate	$m \cdot s^{-1}$
Nomenclature	**Description**	**Unit**
v	Frequency	s^{-1}

$\boldsymbol{v_0}$	Fluid velocity based on an empty channel	$m \cdot s^{-1}$
$\boldsymbol{v_{avg}}$	Average linear flow rate	$m \cdot s^{-1}$
$\boldsymbol{V}$	Volume	m^3
$\boldsymbol{V_f}$	Forward V_{max} reaction rate	$mol \cdot s^{-1}$
$\boldsymbol{V_r}$	Reverse V_{max} reaction rate	$mol \cdot s^{-1}$
$\boldsymbol{V_{max}}$	Maximum reaction rate	$mol \cdot s^{-1}$
$\boldsymbol{U}$	Local heat transfer coefficient	$w \cdot K^{-1} \cdot m^{-2}$
$\boldsymbol{We}$	Weber number	$-$
$\boldsymbol{x}$	Length direction and fragment length	m
$[\boldsymbol{X}]$	Concentration of X	M
$\boldsymbol{\alpha}$	Ramp time coefficient	$-$
$\boldsymbol{\beta}$	Channel specific parameter for estimation of the Taylor dispersion coefficient (48 for a tube)	$-$
$\boldsymbol{\eta}$	Viscosity	$Pa \cdot s$
$\boldsymbol{\varepsilon}$	Molar absorption coefficient	$L \cdot mol^{-1} \cdot cm^{-1}$
$\boldsymbol{\varepsilon}$	Particle porosity	$L \cdot mol^{-1} \cdot cm^{-1}$
$\boldsymbol{\mu}$	Dynamic viscosity	$-$
Φ	Charged/uncharged distribution	$-$
$\boldsymbol{\rho}$	Density	$kg \cdot m^{-3}$
$\boldsymbol{\sigma}$	surface tension	N/m
$\boldsymbol{\tau}$	Residence time	$\min or\ h$
$\boldsymbol{\tau_0}$	Initial residence time	$\min or\ h$
$\boldsymbol{\tau_{mix}}$	Characteristic diffusion controlled mixing time	s
$\boldsymbol{\theta}$	Dimensionless residence time	$-$

1 INTRODUCTION

As scientists it is required that we incorporate the metrics of a sustainable process into our development. Anastas and Warner created the twelve principles of green chemistry[1] as a roadmap and further instruments have also been introduced by Sheldon[2], such as E(nvironmental)-factor and atom-efficiency. Biocatalysis is widely considered as one of the key technologies in respect of sustainability, but this claim should be confirmed through calculation of the E-factor[3]. More specifically, the motivation for the application of biocatalysts stems from their ability to perform highly selective chemistry under mild conditions in water based solutions, making them attractive as 'green' catalysts[3]. The replacement of organic solvents with water is of special interest as these solvents can have detrimental effects on the environment[4–6]. The sustainability of biocatalysts are further emphasized as they are themselves renewable, this is opposed to inorganic catalysts that are often made from rare earth elements which are facing depletion[7]. Biocatalysis uses enzymes to catalyze interesting reactions for the production of valuable molecules and has in recent decades been established as a growing branch of synthetic and process chemistry[8,9]. Today this method finds use in the synthesis and production of many chemical products, ranging from bulk commodities to pharmaceutical intermediates[10–12]. Several hundred industrial processes have already been implemented, mostly in the pharmaceutical industry, with more in development[10,13]. During the last decade the ability to alter the properties of an enzyme via protein engineering[14–17] has enabled the synthesis of entirely new molecules and reactions (without precedent in Nature)[15,18]. Multi-step sequences of enzymes, operating sequentially or in tandem[19,20], as well as chemo-enzymatic combinations[21,22] have now also been established. Likewise, also in synthesis, the exchange of multiple steps with a single step[23,24] has been carried out. In short, biocatalysis provides a valuable tool to complement many established synthetic approaches. Despite these scientific developments biocatalysis is still often limited in application due to a poor transition from the laboratory scale to the process plant. There are several clear reasons for this, but amongst the most important is the complexity of enzyme kinetics, combined with the fact that enzymes need to carry out synthetic reactions under conditions far away from those found in Nature. This makes the collection of kinetic data at process relevant conditions and model fitting especially difficult.

For conventional chemical reactions (including catalytic conversions), reaction engineering has for a long period provided an efficient and effective methodology for the design and sizing of appropriate reactors in order to synthesize valuable industrial chemicals[16–19]. At the heart of the discipline lies the determination of reaction rate laws, collection of kinetic parameters and the application of these models to obtain process stream mass balances. The model essentially enables in-silico prediction of product concentration and reactant conversion as a function of residence time. It is a vital activity that enables chemical engineers charged with the design of a pilot-scale or a full scale plant.

In order to move the development of biocatalytic processes forward, a change is needed in how development is approached. Suitable methods should be established for deriving kinetic expressions, not solely aimed at the mechanistic understanding that is required by biochemists, but of appropriate accuracy for the use of (bio)chemical engineers to design (bio)reactors. The designs will here enable implementation of substrate feeding strategies, investigation of required product removal and definition of suitable biocatalyst concentrations (g/L). Moreover, it can also be applied in the optimization of retrofitting existing equipment, which is often the requirement of the pharmaceutical industry. Finally, it will also enable considerations for improvement of the enzyme itself[29] (via protein engineering).

In order for the new biocatalytic synthesis routes to reach industrialization it is necessary to have models describing the kinetic properties of the biocatalyst. Chemical engineering tools can then be used to scale and design facilities. For the biocatalyst to reach this stage several requirements need to be met.

- An enzyme has been developed to thrive in the operational conditions required in the industrial process, frequently much harsher than those found in Nature.
- The enzyme has been characterized comprehensively in terms of kinetics and stability.
- A process concept has been made to define targets for the performance of the enzyme.

These three requirements are linked and often iteratively developed. Systematic procedures would be far more preferable and give the opportunity to assess the feasibility of processes quickly and where appropriate development strategies can be deployed. Enzyme kinetics lies at the center of this procedure.

Enzymes have excellent selectivity and hold the possibility of tailoring them to specific reactions. This is perhaps only surpassed by their multitude and the mere quantity of possible mutants makes High Throughput Screening (HTS) a necessity for the identification of viable enzyme. Methods of screening can now handle tens of millions of mutants a day[30,31]. This does however not change the requirements for process engineering. The possibility of a tailored enzyme makes it unique to the process that it is designed for. In order to carry out the job of process design it is required to have a mass balance of the reactor. The change of the in and out streams of the reactor is purely related to the kinetics of the reaction and the model for this is consequently essential. One of the initial steps of process design will therefore always be to develop a kinetic model for the reaction. A tool for the collection of kinetic data in a fast and reliable manner is desired as well as a protocol for fitting the models. Reaction engineering in microscale has really developed a lot over the last decade[26,32,33] and the application of microfluidics for development of biocatalytic processes has a great potential.

One clear benefit of applying microfluidics is the low consumption of scarce and valuable resources, especially in the early development phase where for example only mg to a few grams of the catalyst is available [34]. More importantly, the information gathered per mass of biocatalyst spent is much higher. Consequently, investigations that are more detailed in the comparison to conventional lab-scale studies can be carried out.

The real potential of biocatalysis is yet to be reached and the improved and new ways of synthesis must be brought to an industrial setting. A central bottleneck is the transfer from laboratory to large scale, and it is directly correlated with the difficulty of obtaining a reliable kinetic model and in turn the data required for the fitting of these. A solution must therefore be provided in order to move the integration of biocatalysis forward.

1.1 Scope of thesis

The goal of reducing development time of biocatalytic processes is at the very heart of this thesis. The development of such a process is divided into 3 phases and it is important to know where this work fits in. The starting point of any process development is usually surrounding a specific reaction and in this example it will be carried out by a biocatalyst, this is the “discovery phase” (1). An “improvement phase” (2) is hereafter initiated, where the biocatalyst is developed through protein engineering[16]. High throughput screening is well developed for this specific purpose and the likelihood of an improved enzyme mutant hit is ever increasing. Screening in an end point type of way will continue until a handful, i.e. about 10 candidates are left. This stage is termed the “process phase” (3). Protein engineering could here continue to introduce mutations and screen with increasingly relevant process concentrations until a final mutant has been identified[35]. However, it is expected that more processes could be developed through integration of protein engineering with process engineering. At this phase (3) it is uncertain in which direction development should continue and a tool is here required to assess this. In reality this is reaction engineering at its core, and the question is rather about how the biocatalyst can be exploited to the highest degree. The only way to answer such a question is by deriving rate laws and conducting optimization. The mathematical description of enzyme mechanisms, in the form of derived rate laws, has been studied for over a century[36] and has been elucidated in several text books[37–39]. Nonetheless, a large bottleneck for fitting these rate laws is the availability of kinetic data. The goal of this thesis is therefore the development of a microfluidic tool that can be used to collect enzyme kinetic data. In order to achieve such an instrument several items require consideration.

The following objectives are addressed in this thesis:

- Describe the kinetic models of enzymes with particular value for synthesis and production
- Investigate the current technology for rate determination of enzymatic reactions
- Apply microfluidic theory to describe phenomena important for carrying out reactions with enzymes.
- Design and construct a microfluidic setup with integrated analytics that can collect enzyme kinetic data in an automated fashion
- Reflection on how reaction engineering can aid biocatalytic process development

1.2 Structure of thesis

This section will give an overview of how the objectives will be presented with the final aim of developing a microfluidic setup for the collection of enzymatic rate data. The tool is based on considerations of three individual pieces of background, chapter 3, 4 and 5. In these chapters the background material will be displayed with the application in mind, this means that plots and calculations surrounding the set-up will be given here. The information from the three chapters are then combined in chapter 6. The set-up is then validated in chapter 7. An overview of how this information relates is given in Figure 1.1.

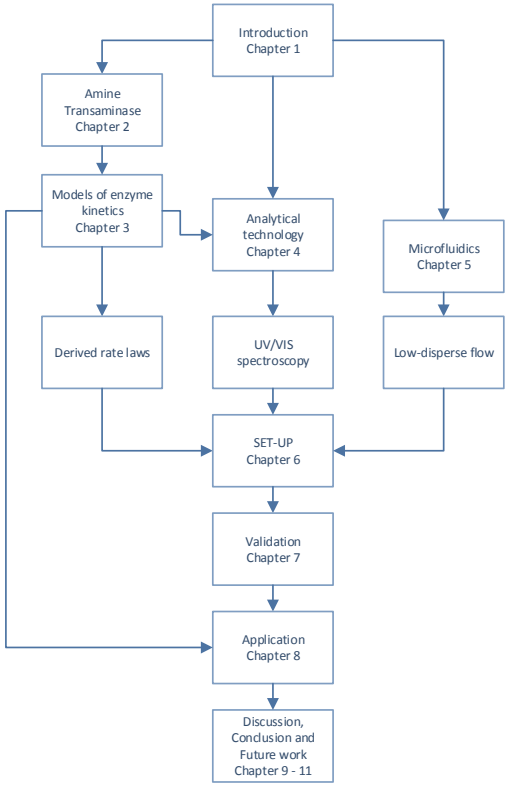

Figure 1.1 – Structure of thesis

Chapter 1

Here an introduction to the thesis is described.

Chapter 2

The enzyme, amine transaminase, will be used as an applied case throughout the thesis, the motivation for its use, its catalytic ability and process development problems are here presented.

Chapter 3

In order to develop a tool with the specific purpose of generating data for kinetic models of enzymes, it was necessary to explain the structure of such models. This chapter will therefore

investigate models of enzymes with particular value to synthesis and production. In this regard, the amine transaminases kinetic model and a method for fitting this type of model is described.

Chapter 4

This chapter reviews the current technologies for collecting the kinetic data of an enzymatic reactions. These technologies consist of two parts, one part is the reactor, and the other part is the detection method. The parts can be separated or integrated, and the review describes the applied combinations. The methods of continuous measurements are of particular interest and spectroscopic methods are further investigated.

Chapter 3 and 4 forms the basis for the publication: Ringborg, R. H., Woodley, J. M., *The Application of Reaction Engineering to Biocatalysis*, Reaction Chemistry and Engineering, 1, 10-22, 2016.

Chapter 5

A critical parameter for characterization of an enzyme is the quantity available for analysis. In the case of being limiting, it will determine the extent of which investigations can be carried out. It is therefore desired to keep consumption of materials to a minimum, this can be accomplished by using dimensions of microscale. The physical effects of operating at this scale is therefore explained and categorized in this chapter. Furthermore, the possibilities of applying a microfluidic platform for process development was investigated.

This chapter has been written as a joint chapter with Søren Heintz. This was carried out, since microfluidic effects are a core element in both our theses and by combining efforts a more comprehensive understanding was achieved.

Chapter 6

The combined findings and calculations of chapter 3, 4 and 5 is hereafter applied to develop the setup. Here, both the setup and the method will be developed and the methods used for testing the setup is explained.

Chapter 7

Before applying the setup for the collection of kinetic data, it is required to validate that it indeed produces the intended information. Some problems with the set-up is also described here as it is closely related with operation.

Chapter 8

To illustrate the application of a kinetic model for process development a general description is given in this chapter.

Chapter 9-11

A specific discussion of the aspects evaluated in this thesis is given. After this a conclusion of the work is presented and future work suggest the further development of the setup in the end.

Contributions to papers

The papers that has been co-authored include parts and discussions that have a basis in the background described in this thesis.

2 AMINE TRANSAMINASES

Here the case used for development are introduced and explained.

The enzyme amine transaminase (EC 2.6.1.18) is chosen as a case study. The enzyme is of particular interest as it produces chiral amines with high enantiomeric excess. Nevertheless, this enzyme presents itself with many difficulties and the developed techniques and technology handling the problems can be transferred to other enzyme cases. Problems with activity, substrate supply, product removal and unfavourable thermodynamics are here encountered as such difficulties.

2.1 Chiral amines

Chiral amines are important for the pharmaceutical, agro-chemical and chemical industry. They are represented in many Active Pharmaceutical Ingredients (APIs)[40–44], and in antibacterials for the agrochemical industry[40]. There are many routes to the synthesis of chiral amines achieved by chemo- and/or bio-catalysis[40,41,45], the biocatalytic routes are outlined in Figure 2.1.

The preparation of chiral amines from biocatalysis has recently gained much attention. The routes that are considered here are 1) kinetic resolution (KR) of racemic mixtures, using e.g. Lipases, 2) dynamic kinetic resolution (DKR) of racemic mixtures, using e.g. Amine oxidases coupled with ammonia borane and 3) asymetric synthesis, using e.g. Amine transaminases.

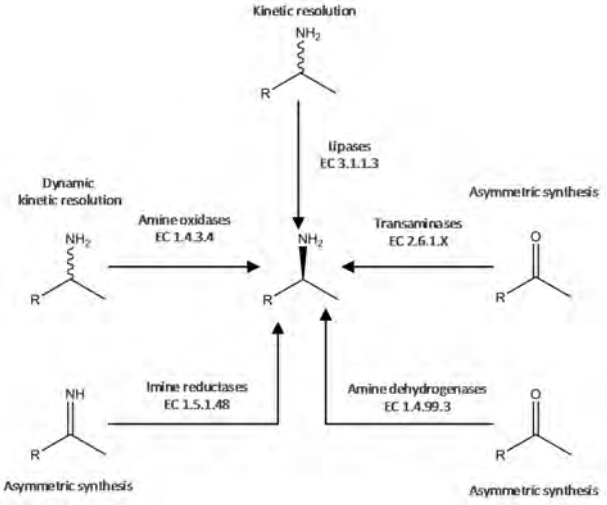

Figure 2.1 – Biocatalytic routes for the synthesis of chiral amines, based on Ghislieri and Turner[45] and Höhne and Bornscheuer[40]

Kinetic resolution and dynamic kinetic resolution is used for differentiating and in the end separating enantiomers in a racemic (50/50) mixture. The two enantiomers are both eligible for the reaction but are converted with different reaction rates. This results in an enantio-enriched sample of the less reactive enantiomer[46]. This classic method has a theoretical maximum yield of 50%. It is however possible to circumvent this by coupling the reaction with a bio/chemocatalytic racemization step, where the undesired product is returned to the racemic state, enabling further conversion. This makes it possible to get a 100% yield from a racemic mixture and the method is termed dynamic kinetic resolution (DKR). The other way, namely asymmetric synthesis, is the direct synthesis of a single enantiomer. Transaminases, more specifically amine transaminases, conducts this type of synthesis. The possibility of directly obtaining the chiral product is very appealing and motivates the use of amine transaminases. These enzymes will therefore be a focus in this thesis.

2.2 Amine transaminases

The enzyme utilized for this study is a transaminase. This group of enzymes (EC 2.6.1.X) are used in the synthesis of chiral amines. More specifically the subgroup of amine transaminases (EC 2.6.1.18) is investigated here as this subgroup, in principle, can accept a broad range of ketones and amines even without a carboxyl group[40,47–49], can potentially achieve 100% yield at mild operating conditions[48] and can be engineered to have very high enantiomeric excess.

The enantiomeric excess is of particular value due to the inherent problem of separating racemic mixtures. Furthermore the cost of downstream processing in the pharmaceutical industry can amount to 80-90% of the production cost[43]. This is understandable, since traditional methods of separation cannot be applied when molecules only differ by rotation of one chiral center. The strategies to resolve the separation problem are chromatography[50], deracemisation[51], dynamic kinetic resolution[51] or asymmetric synthesis[35,47].

Another aspect of the enantiomeric purity is drug safety as it is known that the one of the enantiomers can cause deleterious effects[52] whereas the other enantiomer is the active pharmaceutical ingredient. The apparent advantages and economic benefits, in terms of reduced downstream processing, justifies a direct biocatalytic route to optically pure amines.

A amine transaminase process at large scale has been demonstrated[35] and other processes should therefore also be realisable. Amine transaminase catalyses the exchange of an amine (-NH_2) and pro-chiral keto-group (=O) yielding a chiral amine stereospecifically. The reaction can be seen in Figure 2.2. Specific details of the reaction mechanism will be explained later.

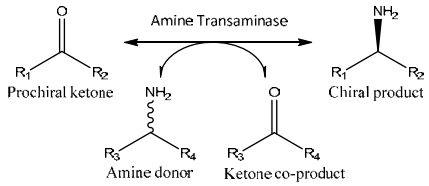

Figure 2.2 – Asymmetric synthesis of chiral amines using ω-transaminase

2.2.1 Cases

It is desired to develop technology that can be applied in a wider sense and in order to assess common problems in relation to process development following model reactions were selected:

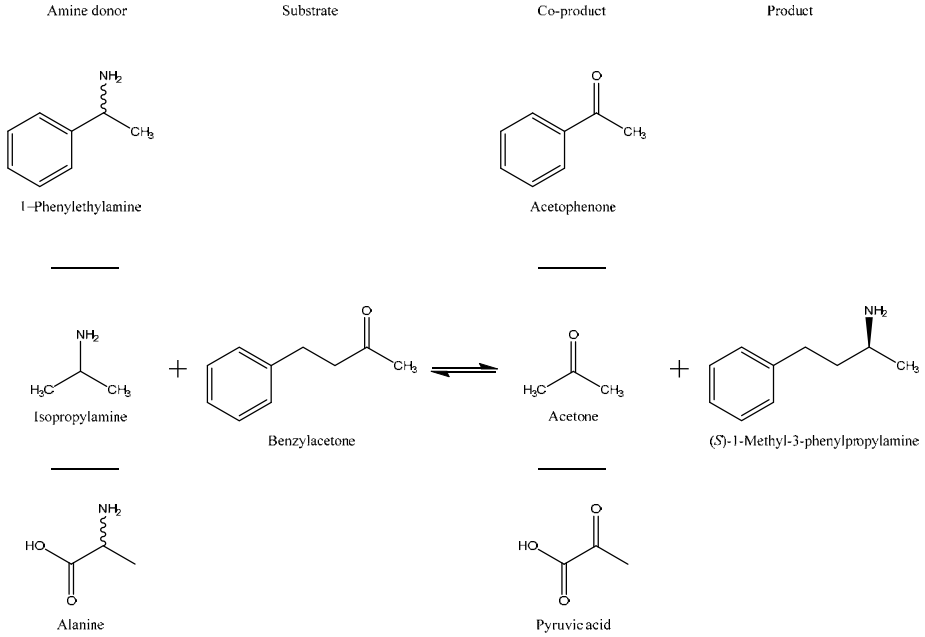

Figure 2.3 – Model reactions with the core transformation of Benzylacetone (BA) to 1-Methyl-3-phenylpropylamine (MPPA) carried out with different donors and their respective products

The desired target is 1-Methyl-3-phenylpropylamine (MPPA) which can be obtained from benzyl acetone (BA). To show possible solution strategies different amine donors have been

chosen as cases, i. e. 1-Phenylethylamine (PEA), isopropylamine (IPA) and alanine (ALA). Each of the donors offers different in-situ product removal (ISPR) and downstream challenges due to favourable, equal and unfavourable equilibrium scenarios. The thermodynamic equilibrium of each of the reactions is roughly: ~30/1 (PEA-donor), ~1/1 (IPA-donor) and ~1/1000 (ALA-donor)[53]. Removing a product selectively will always benefit thermodynamically challenged reactions, but often comes with a trade-off.

In the case of MBA the reaction equilibrium is favourable, so the motivation for ISPR implementation are more related to product inhibition. Nonetheless, difficulties can arise in the downstream product recovery as a consequence of the great similarities between MBA, ACP (Acetophenone), MPPA and BA.

In the case of IPA as donor the low boiling point of (ACE) acetone directs development towards evaporation but the IPA has a similar vapour pressure and will be removed simultaneous. Furthermore, for the IPA reaction system it will be necessary to both influence the equilibrium, by an excess, and the effects of main product inhibition. Evaporation of the amine donor will therefore add considerable cost to the process, as it is operated with excess.

The ALA reaction system has a very unfavourable reaction equilibrium, so for this case it will be required to shift first the equilibrium and thereafter consider inhibition issues. In general, a cascade is applied to this system, Lactate Dehydrogenase/Glucose Dehydrogenase[20] which can drive reactions to completion, but adds considerable cost to the process[54], making it the most cost heavy of the three amine donor processes.

It is expected that ISPR will never become a simple solution[54,55]. A number of general physicochemical properties of the different reaction species are listed in Appendix 1 and in Table 2.1 an overview of some of the general challenges.

Table 2.1 - Challenges related to the reaction systems.

	PEA - system	**IPA - system**	**ALA-system**
Challenges [S]/[P] Inhibition [S]/[P] Solubility	**All compounds have similar properties**	**Equilibrium and Volatility**	**Equilibrium**
Potential options	Excess ISPR (extraction) (Im-)Miscible solvent	Excess ISPR (extraction) IScPR (evaporation) (Im-)Miscible solvent	Excess ISPR (extraction) IScPR (cascade) (Im-)Miscible solvent
Required solutions	Excess	Excess or ISPR or IScPR	IScPR

The relatively simple case of Down Stream Processing (DSP) of the IPA case and the manageable thermodynamics connected, makes it a favourable system to investigate. This is further motivated by the economical assessment of amine donors[54]. Here it was found that among the amine donors, IPA would be adding the least to the production costs. In this thesis it has therefore been chosen to investigate the kinetic dynamics of enzyme catalyzed reaction $IPA + BA \rightleftharpoons ACE + MPPA$.

Subjects still to be discussed is the influence of the actual concentration of protonated amine in solution. This is of interest as it is common that the enzyme has an optimal pH setpoint lower than the pKa of the amine. In the proposed mechanism[56–58] for ω-transaminase, the un-protonated amine is the true substrate. The protonation of species occurs according to

standard pH-theory and isotherms can be calculated accordingly. From Figure 2.4 it can be seen that species goes from charged to uncharged at higher pH. Consequently, both substrate and product will be available for the mechanism to a higher extend at higher pH. Hydrazine and ammonia cannot be used directly as amine donors, ammonia can however be used in combination with Alanine Dehydrogenase to regenerate alanine from pyruvate[59]. Hydrazine and ammonia are included as they could be better donors, at pH 8 their uncharged concentration is higher than the donor presented earlier.

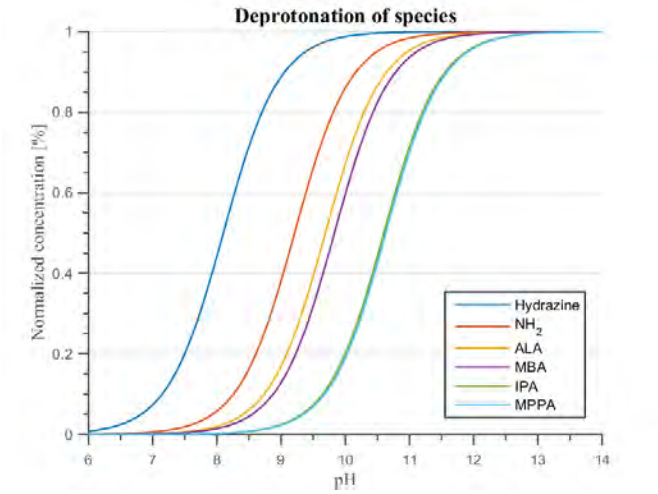

Figure 2.4 – Deprotonation of different amines

Table 2.2 – pKa of selected amines

Amine	pKa
Hydrazine	8.10
Ammonia	9.21
ALA	9.69
MBA	9.83
IPA	10.6
MPPA	10.63

This pH analysis can be extended to calculate the percentages of true substrate available, Φ. The results at different pH can be observed in Table 2.3. These values can be added onto their respective compounds in the K_{EQ} formula, see Eqn. 2.1 and Eqn. 2.2. For the ALA/MPPA system it can be observed that a theoretical 3 fold improvement can be obtained by operating at pH 10. This can be expected when pKa of the amine donor is lower than the product. The reverse effect is observed when the amine donor has a pKa value higher than the product, but as the uncharged amine is the true substrate, the equilibrium effect would drown in lower reaction rate due to a miniscule substrate concentration. Reported K_{EQ} does not take protonation effects into account and should be adjusted in order to display correct values. In the case of IPA/MPPA where pKa is more or less equal, more substrate will become available by increasing pH and this should directly influence the reaction rate. Moving from pH 8 to 10 should make a 100 fold more substrate available to the enzyme. In this regard it is required to consider the components that can inhibit the enzyme. This might be both the uncharged and charge versions of the amines. It would be very interesting to find an enzyme, stable in the region pH 8-10, and then generate a substrate/product profile at different pH. It is expected that at higher pH K_M will decrease and that this can be attributed to the charged/uncharged distribution of the amines. This could become an explanation for the low rate that is often observed in relation to the amine transaminase enzymes, and could aid as a target for biocatalyst engineering.

$$K_{EQ,pH=8} = \frac{\Phi_{MPPA,pH=8}[MPPA][PYR]}{\Phi_{ALA,pH=8}[BA][ALA]} = \frac{0.23_{pH=8}[MPPA][PYR]}{2_{pH=8}[BA][ALA]} \approx \frac{1}{10}\frac{[MPPA][PYR]}{[BA][ALA]} \quad \text{Eqn. 2.1}$$

$$K_{EQ,pH=10} = \frac{19_{pH=10}[MPPA][PYR]}{60_{pH=10}[BA][ALA]} \approx \frac{1}{3}\frac{[MPPA][PYR]}{[BA][ALA]} \quad \text{Eqn. 2.2}$$

Table 2.3 - Percentage of uncharged amine at different pH

Amine	pH = 7	pH = 8	pH = 9	pH = 10
Hydrazine	7.36%	44.27%	88.82%	98.76%
Ammonia	0.61%	5.81%	38.15%	86.05%
ALA	0.20%	2.00%	16.96%	67.13%
MBA	0.15%	1.46%	12.89%	59.66%
IPA	0.03%	0.25%	2.45%	20.08%
MPPA	0.02%	0.23%	2.29%	18.99%

3 ENZYME KINETICS

In order to generalize, the scope of this chapter is an investigation regarding the mechanisms of important enzymes for synthesis and production chemistry. Three common mechanisms are identified and a method for identification is presented. The case enzyme, amine transaminase, has a ping pong bi bi mechanism. Currently, the best way of modelling this mechanism is by steady-state assessment of the reaction network, this is not to be confused with steady state of a flow reactor. The fitting method is described and a possible way of optimizing this method is presented.

3.1 Nomenclature

Reactants are designated by the letters A and B in the order in which they are added to the enzyme. Products are designated the letters P and Q in the order in which they leave the enzyme. Stable enzyme forms are designated E and F, complexes between e.g. E and A are designated EA. K_{i_X} is the dissociation constant of EX, K_{M_X} is the Michaelis-Menten constant for the individual compound X. The number of kinetically important reactants in a given direction is indicated by the prefix or postfix Uni, Bi, Ter and Quad. A reaction with two reactants and two products is therefore termed a bi-bi reaction.

3.2 Operational window for kinetic studies

Historically, in biocatalysis, activity assays have been used for the investigation of enzyme kinetics. These preliminary studies include an investigation of the effect on reaction rate with changes in temperature, pH, ionic strength, enzyme and component concentration. The results have not always been presented in a rate law, but have most often provided a useful starting point for more detailed studies by fixing some of the surrounding variables such as ionic strength, pH and temperature. Experiments have usually been carried out by mixing all components together at the same time and thereafter monitoring the development of the individual component concentrations. The rate of reaction has then been defined as either the disappearance or production of a component over time. The initial testing of enzymes usually includes an investigation of the linear activity/enzyme concentration range and the optimal

pH. After this has been established enzyme concentration can be fixed so as to obtain subsequently measured initial rates in a reasonable time period. pH is then also fixed in accordance with the highest activity observed, although care should be taken here to investigate the protonation of the different compounds in solution, as described in section 2.2.1. The activity dependence on temperature for enzymes is similar to that of chemo-catalysts. Here also the empirical rule of a 10 °C increase in temperature resulting in a two-fold increase in rate holds true[60]. However, with enzymes denaturation can also occur at higher temperatures resulting in a trade-off of activity and stability – most usually reported as an optimum temperature. The temperature at which an enzyme is fully denaturated is termed its melting temperature[61]. Technology for measuring this is available and can be performed either with Differential Scanning Calorimetry (DSC)[62] or the recently developed thermal shift methodology[63]. Denaturation will still occur at temperatures below the melting temperature but at a slower rate and this fact can easily be mistaken for inhibition of the enzyme. An optimal temperature will require a minimum enzyme stability and will therefore lie significantly below the melting temperature. In order to avoid stability issues experiments are therefore often carried out at ambient temperatures similar to these in their natural environment. After fixing the enzyme concentration, pH and temperature, the concentration of the different compounds can be investigated.

In short, the items of interest are:

- Kinetics
    - Initial rate on pH (optimal pH)
    - Initial rate vs. [E] (linear range)
    - Initial rate on [S][cS] (forwards rate)
    - Initial rate on [P][cP] (backwards rate)
    - Full reaction profile
- Activity stability of E
    - Degradation under standard conditions
    - Thermal (melting point measurement)

3.3 Enzymatic reaction schemes

For multi-substrate biocatalytic reactions the identification of empirical rate laws are complex as they display mixed order kinetics. The strategy has therefore been to elucidate reaction mechanisms and in turn develop models, based on rigorous experimental data. Not surprisingly, the field of biocatalytic model construction has therefore produced several textbooks covering the common mechanisms[37,38].

Enzyme classification has long been based on chemical function and according to the convention of the International Union of Biochemistry and Molecular Biology, IUBMB nomenclature falls into 6 categories, each of which with 3 further levels of sub-classes. In this way each enzyme can be characterized by a 4 digit number (e.g. Transketolase is EC 2.2.1.1). The generalized reactions that are carried out by these enzymes in the 6 categories are summarized in Table 3.1.

Table 3.1 - Enzyme commission categories with generalized reaction schemes

Group	Reaction catalyzed	Typical reaction	Enzyme example(s) with trivial name
EC 1 Oxidoreductases	To catalyze oxidation/reduction reactions; transfer of Hydrogen and Oxygen atoms.	$AH + B \rightleftharpoons A + BH$ $A + O_2 \rightleftharpoons P + H_2O_2$	Dehydrogenase, Oxidase
EC 2 Transferases	Transfer of a functional group from one substance to another. The group may be methyl-, acyl, amino- or phosphate	$A + B \rightleftharpoons P + Q$	Transaminase, Transketolase
EC 3 Hydrolases	Formation of two products from a substrate by hydrolysis	$A + H_2O \rightleftharpoons P + Q$	Lipase, amylase, peptidase
EC 4 Lyases	Non-hydrolytic addition or removal of groups from substrates. C-C, C-N, C-O or C-S bonds may be cleaved	$A \rightleftharpoons P + Q$	Aldolase Decarboxylase
EC 5 Isomerase	Intramolecular rearrangement, i.e. isomerization changes within a single molecule	$A \rightleftharpoons P$	Isomerase, mutase
EC 6 Ligases	Join together two molecules by synthesis of new C-O, C-S, C-N or C-C bonds with simultaneous breakdown of ATP	$A + B + ATP \rightleftharpoons XY + ADP + Pi$	Synthetase

The third column of Table 3.1 indicates the stoichiometric equation of these conversions. This is important in order to identify the basic structure of the rate law. For synthetic purposes, the emphasis lies with classes EC 1-4[8,9,12], where typical reaction schemes involve two reactants and two products (with the exception of EC 4 that in the synthesis direction only has a single product). General models for EC 1-3 are summarized in Figure 3.1 and represent so-called ordered, random and ping pong bi-bi mechanisms, reflecting the order in which multiple substrates and products are bound to or released from the enzyme complex, respectively. Enzymes in class EC 4 have a simpler form. Examples of synthetically useful enzymes from these different EC categories are listed in Table 3.1. It is well known that the three mechanisms listed do not represent all enzymes, and both more complex as well as simpler mechanisms exist. Nonetheless, for synthetic purposes these are the most common and further discussion will therefore be based on the identification and parameter fitting of these models in particular.

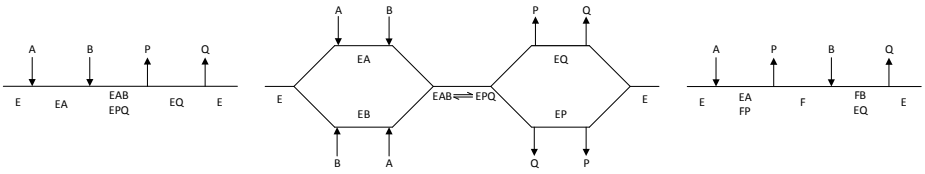

Ordered Random Ping pong

Figure 3.1 – Cleland representation of ordered bi-bi, random bi-bi and ping pong bi-bi, substrates are denoted A and B, products are denoted P and Q, free enzyme species are denoted E, F, enzyme complexes are denoted EA, EB, EP, EQ, EAB, EPQ.

Table 3.2 - Kinetic mechanisms of different enzymes in different EC categories.

EC category	Sub EC #	Reactive group	Case enzyme	Kinetic mechanism	ref
EC 1 Oxidoreductases		**Acting on**			
	1.1	Alcohol groups	Alcohol dehydrogenase	Random bi-bi, Ordered bi-bi, Theorell-Chance	[64–66]
	1.1	Alcohol groups	Galactose oxidase	Ping pong bi-bi	[67]
	1.2	Aldehyde or oxo groups	Pyruvate dehydrogenase	Ping pong bi-bi	[68]
	1.4	Amino groups	Mono amino oxidase	Ping pong bi-bi	[69]
EC 2 Transferases		**Transferring**			
	2.7	phosphorous-containing groups	Non-specific protein-tyrosine kinase	Random bi-bi	[70]
	2.4	Glycosyl groups	Glycogen phosphorylase	Random bi-bi	[71]
	2.1	one-carbon groups	Thymidylate synthase	Ordered bi-bi	[72]
	2.3	Acyl groups	histone acetyltransferases	Ordered bi-bi	[73]
	2.6	nitrogenous groups	Transaminases	Ping pong bi-bi	[74–76]
	2.2	Carbon-carbon	Transketolase	Ping pong bi-bi	[77,78]
EC 3 Hydrolases		**Acting on**			
	3.1	Ester bonds	Lipase	Ping pong bi-bi	[79]
	3.2	Glycosyl bonds	Amylase	Ping pong bi-bi	[80]
	3.5	Carbon-nitrogen bonds	Amidase	Ping pong bi-bi	[81,82]
EC 4 Lyases		**Acting on**			
	4.1	Keto acid	Aldolase	Random bi-uni Ordered bi- uni	[83]
	4.3	Carbon-nitrogen	methylaspartate ammonia-lyase	Ordered bi-uni	[84]

In cases where no mechanism has previously been determined for an enzymatic catalyst of interest, it can be determined by an inhibition study. The initial rates are studied under the conditions where one substrate is varied while the other is kept constant. The mechanism can hereafter be identified by plotting them in a Lineweaver-Burk plot, see Figure 3.2. The relative position of the intercept depends on whether the substrates hinder or favour one another, resulting in an intercept above or below the abscissa, respectively. Commonly, the intercept will appear to the left of the ordinate above the abscissa. If both substrates bind independently of one another the intercept should lie on the abscissa, indicating a random mechanism. When parallel lines are observed, then a ping-pong mechanism is inferred.

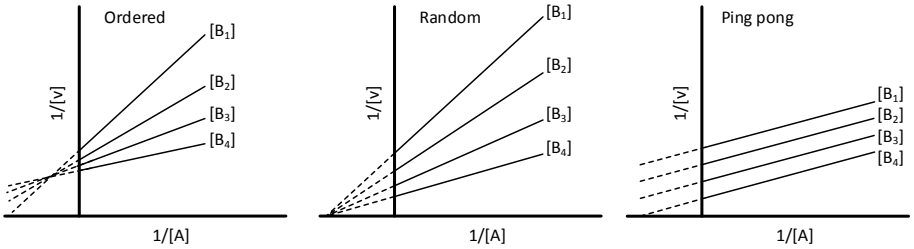

Figure 3.2 – Lineweaver-Burk plots for the determination of Ordered, Random and Ping pong bi-bi mechanisms, [A] and [B] denotes the substrate concentration of A and B, v denotes the initial rate.

Lineweaver-Burk plots are still used for fitting and this cannot be advised. This is because the inverse of the substrate is used as independent variable, increased emphasis will therefore be on the low concentration experiments. This is unfortunate as error usually correlates inversely with concentration. A better method is by least squares regression where such error are avoided.

3.4 Mechanistic models

In the fitting of models a question one must address is dealing with precision and detail. It is desired to generate high detail biocatalytic models at the micro-kinetic level, with rate laws as functions of rate constants and compound concentration. This would indeed reveal the limiting step in a biocatalytic reaction network, and could hypothetically guide protein engineers to target residues with effect on that step in the mechanism. The term 'Reaction progress kinetic analysis', coined by Blackmond[25,85], stresses the importance of on- or in-line analysis to elucidate mechanisms of catalytic systems. Ideally, this would also be routinely applied to the study of enzyme kinetics and Johnson[86] has reported an excellent case applying this to determine the micro-kinetic parameters for the rate law of Invertase and the more complex case of EPSP synthase[87]. The technology of fluorescence[86,88] was applied, but also radiolabeling[87] can be used in order to measure the different enzymatic species, nonetheless, these methods add significant complexity to the studies. Furthermore, the goal of such research is to investigate the structure-activity relationship, which is quite different from the process engineering objective, that is the primary target here. In principle, for process design and development all that is desired is a sufficiently accurate model that can describe the kinetic dynamics of a biocatalytic reaction. Short of the ability to measure the individual species it will be impossible to derive unique rate constants for the individual rates of the intermediate reactions even though precision would be high. This micro-kinetic problem has therefore been circumvented by the steady state assumption, which states that the concentration of enzymatic species reaches steady state after milliseconds of reaction henceforth termed as state-state models. Additionally, the rate constants are collected together in the form of equilibrium-like constants, K, which are termed macro-kinetic constants. These constants have the same physical meaning as the ones from the simple uni Michaelis-Menten rate law, see Eqn. 3.1, where $K_{M_X}{}'s$ designates the concentration of X at which the initial rate will be half of the maximum rate, V_{max}. Similarly, inhibition constants $K_{i_Y}{}'s$ designate the concentration of Y that will saturate half the active sites. Experiments for steady-state models need to be designed such that the substrate concentration greatly

exceeds that of the enzyme. This is not required in order to saturate the enzyme but rather to have a negligible amount of the substrate bound to the enzyme[89].

$$v = \frac{V_{max}[A]}{K_{M_A} + [A]} \qquad \text{Eqn. 3.1}$$

The mechanism of the case enzyme amine transaminase has been shown to follow a ping pong bi-bi mechanism[47,56,75]. The analogue to a ping pong game gives name to the mechanism where two substrate/product pairs enters and leaves the active site consecutively, one at a time. The full name is termed ping pong bi-bi, where bi denotes a substrate/product pair. For derivative purposes following King-Altman representation is used in Figure 3.3:

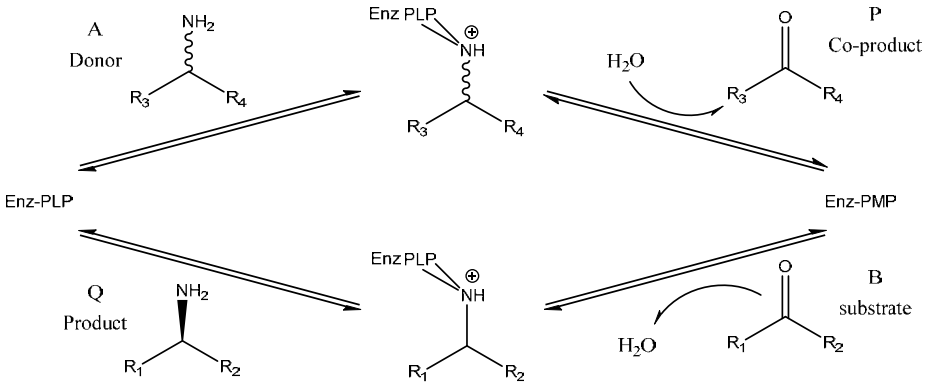

Figure 3.3 – Scheme of the ω-Transaminase mechanism

The enzyme operates with the co-factor pyridoxal-5'-phosphate (PLP)[40] and uses this as a shuttle to facilitate the transfer of the amine group. The co-factor is regenerated in every reaction cycle and will not cause problems in this regard. In this type of mechanism all substrates and products can potentially bind to the respectively wrong form of the enzyme, i.e. dead-end complexes illustrated by orange arrows in Figure 2.8. This leads to following King-Altman representation of the kinetic model, see Figure 3.4.

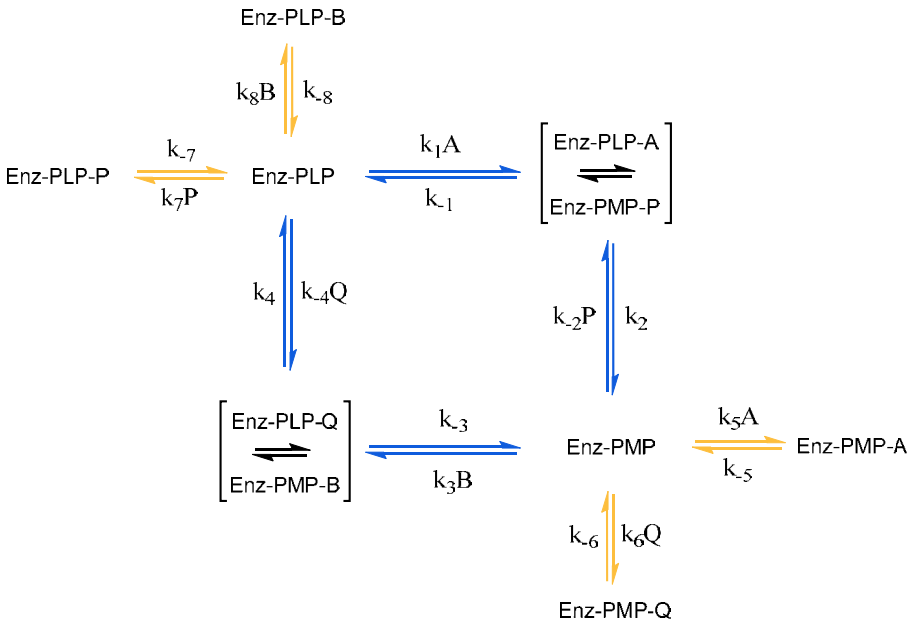

Figure 3.4 – King-Altman representation of the model

The procedure of King-Altman lists interconversion patterns making it possible to describe each enzyme specie proportional to the total enzyme.

$$\frac{[EX]}{[E]_t} = \frac{interconversion\ pattern}{denominator} \qquad \text{Eqn. 3.2}$$

The total enzyme, $[E]_t$, is equal to the sum of all enzyme species

$$denominator = [E]_t = [E] + [EA + FP] + [FB + EQ] + [\mathrm{F}] \qquad \text{Eqn. 3.3}$$

The steady-state net velocity is then given by the difference between the forward and reverse velocities of any step. By applying the King-Altman procedure to the "blue" part of Figure 3.4 it is possible to derive following rate:

$$v = \frac{k_1k_2k_3k_4[E]_t[A][B] - k_{-1}k_{-2}k_{-3}k_{-4}[E]_t[P][Q]}{\begin{array}{c} k_1k_2(k_{-3}+k_4)[A] + k_3k_4(k_2+k_{-1})[B] + k_{-1}k_{-2}(k_{-3}+k_4)[P] \\ +k_{-3}k_{-4}(k_{-1}+k_2)[Q] + k_1k_3(k_2+k_4)[A][B] + k_1k_{-2}(k_{-3}+k_4)[A][P] \\ +k_{-2}k_{-4}(k_{-1}+k_{-3})[P][Q] + k_3k_{-4}(k_{-1}+k_2)[B][Q] \end{array}} \qquad \text{Eqn. 3.4}$$

The equation is reduced according to Table 3.3, note that this is only applicable to the bi bi ping pong mechanism. Here the num1 denotes the positive term of the numerator and num2 the negative. The coefficients of A is $k_1k_2(k_{-3}+k_4)$ and so forth.

Table 3.3 – King-Altman transfer of model parameters

Parameter	Definition	Representing
V_f	$\frac{num1}{CoefAB}$	$\frac{k_2 k_4 [E]_t}{k_2 + k_4}$
V_r	$\frac{num2}{CoefPQ}$	$\frac{k_{-1} k_{-3} [E]_t}{k_{-1} + k_{-3}}$
K_{m_A}	$\frac{CoefB}{CoefAB}$	$\frac{(k_{-1} + k_2) k_4}{k_1 (k_2 + k_4)}$
K_{m_B}	$\frac{CoefA}{CoefAB}$	$\frac{k_2 (k_{-3} + k_4)}{(k_2 + k_4) k_3}$
K_{m_P}	$\frac{CoefP}{CoefPQ}$	$\frac{(k_1 + k_2) k_{-3}}{(k_{-1} + k_{-3}) k_{-2}}$
K_{m_Q}	$\frac{CoefQ}{CoefPQ}$	$\frac{k_{-1} (k_{-3} + k_4)}{(k_{-1} + k_{-3}) k_{-4}}$
K_{iA}	$\frac{CoefP}{CoefAP}$	$\frac{k_{-1}}{k_1}$
K_{iB}	$\frac{CoefQ}{CoefBQ}$	$\frac{k_{-3}}{k_3}$
K_{iP}	$\frac{CoefA}{CoefAP}$	$\frac{k_2}{k_{-2}}$
K_{iQ}	$\frac{CoefB}{CoefBQ}$	$\frac{k_4}{k_{-4}}$
K_{eq}		$\frac{V_f K_{mQ} K_{iP}}{V_r K_{iA} K_{mB}} = \frac{V_f K_{mP} K_{iQ}}{V_r K_{iB} K_{mA}} = \frac{K_{iP} K_{iQ}}{K_{iA} K_{iB}} = \left(\frac{V_f}{V_r}\right)^2 \frac{K_{mP} K_{mQ}}{K_{mA} K_{mB}}$

The model can now be presented on following form.

$$v = \frac{V_f V_r \left([A][B] + \frac{[P][Q]}{K_{eq}}\right)}{V_r K_{m_B}[A] + V_r K_{m_A}[B] + \frac{V_f K_{m_Q}[P]}{K_{eq}} + \frac{V_f K_{m_P}[Q]}{K_{eq}} + V_r[A][B] + \frac{V_f K_{m_Q}[A][P]}{K_{eq} K_{iQ}} + \frac{V_f [P][Q]}{K_{eq}} + \frac{V_r K_{m_A}[B][Q]}{K_{iQ}}} \quad \text{Eqn. 3.5}$$

The transfer of the rate constant based model to a Michaelis-Menten meaningful domain has turned 8 degrees of freedom (DOF) into 11. The Haldane equilibriums are then applied and reduces the model back to 8 DOF. Here both forward and reverse rates, all $K_M{}'s$ and only K_{iQ} are included, with the remaining $K_i{}'s$ described through the Haldanes. Nonetheless, one must consider whether the model fitting yields a unique fit. Otherwise the physical parameters will be arbitrary and only valid within the parameter space investigated. Optimally one must reduce the model until a unique fit is obtained, but this will make parts of the model empirical and the physical meaning will be lost.

Dead-end enzyme complex inhibition, orange part of Figure 3.4, can be added to the model by multiplying e.g. $\left(1 + \frac{k_5 A}{k_{-5}}\right) = \left(1 + \frac{A}{K_{siA}}\right)$ to the denominator of the enzymatic specie of attack see Eqn. 3.3. Dead-end complexes are only occurring on the free enzyme species E-PLP and E-PMP, as the enzyme can contain only one molecule at a time. In the derivation of the model, as an example, the description of E-PLP contains one addend with factor B and another with

factor P, see Figure 3.4. It is therefore relatively easy to add this type of inhibition here, and because both A and Q can inhibit, $\left(1+\frac{A}{K_{siA}}+\frac{Q}{K_{siQ}}\right)$ is multiplied to the terms B and P. The full inhibition model can hence be described by Eqn. 3.6.

$$v=\frac{V_fV_r\left([A][B]+\frac{[P][Q]}{K_{eq}}\right)}{\begin{matrix}V_rK_{m_B}[A]\left(1+\frac{[B]}{K_{siB}}+\frac{[P]}{K_{siP}}\right)+V_rK_{m_A}[B]\left(1+\frac{[A]}{K_{siA}}+\frac{[Q]}{K_{siQ}}\right)\\+\frac{V_fK_{m_Q}[P]}{K_{eq}}\left(1+\frac{[A]}{K_{siA}}+\frac{[Q]}{K_{siQ}}\right)+\frac{V_fK_{m_P}[Q]}{K_{eq}}\left(1+\frac{[B]}{K_{siB}}+\frac{[P]}{K_{siP}}\right)+V_r[A][B]\\+\frac{V_fK_{m_Q}[A][P]}{K_{eq}K_{iQ}}+\frac{V_f[P][Q]}{K_{eq}}+\frac{V_rK_{m_A}[B][Q]}{K_{iQ}}\end{matrix}} \qquad \text{Eqn. 3.6}$$

This type of inhibition adds another 4 DOF to the model and in regards of regression this is not desirable. It is imagined that rather than adding all the terms at once one should add them one at a time in the model fitting.

Recently, Al-Haque and co-workers have published a stepwise approach for the fitting of the ping pong bi-bi mechanism[76] based on deriving the rate equations for the forward and backward rates independently Eqn. 3.7 and Eqn. 3.8. The remaining model parameters are then adjusted and validated against high conversion experiments. In total, one can expect to carry out a minimum of 45-55 different experiments to have a robust platform for fitting such a mechanism[76]. The forward rate equation:

$$v_{forward}=\frac{V_f[A][B]}{K_{m_B}[A]\left(1+\frac{B}{K_{siB}}\right)+K_{m_A}[B]\left(1+\frac{A}{K_{siA}}\right)+[A][B]} \qquad \text{Eqn. 3.7}$$

The reverse rate equation:

$$v_{reverse}=\frac{V_r[P][Q]}{K_{m_Q}[P]\left(1+\frac{Q}{K_{siQ}}\right)+K_{m_P}[Q]\left(1+\frac{P}{K_{siP}}\right)+[P][Q]} \qquad \text{Eqn. 3.8}$$

However, the methodology is not yet complete as strong correlation between some parameters still persists. A change in one parameter can therefore be compensated by another, i.e. the parameters become unidentifiable.

In the scientific literature makro-kinetic reaction networks with sequential, competitive or consecutive steps are models recognized to have highly correlated parameters[90]. This causes problems with finding a global minimum for the objective function, and consequently a unique solution. The estimated parameters from the previously described method rely on "independent estimation", first fitting the forwards rate, then fitting the backwards rate and finally fitting the remaining parameters. However, because correlation persists, further measurements need to be taken. Model-based design of experiments (MBDoE) uses the model to design new experiments which will yield information in terms of reducing uncertainty or correlation[90,91]. In order for this method to be applicable it is necessary to have a good initial

guess of the individual model parameters. The stepwise approach is currently the best way of fitting the data and thus the best "initial-guess" available. MBDoE aims at devising experiments that will yield the most informative data, in a statistical sense, for use in parameter estimation and model validation. The method applies the maximization of the Fisher Information Matrix (FIM) or minimization of the covariance matrix, which is the inverse of the FIM. The calculated experimental conditions required to reach this point can then be identified and tested. Specifically, The anti-correlation criteria for experimental design can be applied here and has been described by Franceschini et al.[92]. In the case where correlation cannot be eliminated, the parameters should be collapsed into a new variable. This variable may lose physical meaning but, as with the case of the rate and equilibrium constants described previously, it is better to have a practically identifiable model.

3.5 Binding experiments.

An indirect way of reducing the model's DOF is to measure dissociation constants, K_d. This is defined in the same way as K_i's and K_{Si}'s, see Eqn. 3.9.

$$K_d = \frac{k_{-1}}{k_1} = \frac{off - rate}{on - rate} = \frac{[S][E]}{[ES]} \qquad \text{Eqn. 3.9}$$

MicroScale Thermophoresis (MST)[93] is a technique that allows K_d to be measured. This currently surpasses any other known measurement techniques as it measures directly on features of the enzyme. It is somewhat independent of the actual concentration of enzyme, as long as the signal is strong enough to be measured. More specifically, it measures the rate of which the protein moves in a thermal gradient and does this over a wide range of compound concentration. The measurements results in a fully unbound state, a fully saturated state and a gradient between the two. An isotherm can hereafter be fitted to the data revealing K_d. Please re-evaluate the model in Figure 3.4, here one can observe that it only possible to measure the inverse of $K_{iA}, K_{iQ}, K_{SiB}, K_{SiP}$ unless isolation of the E-PMP is possible. The MST experiments were carried out in corporation with NanoTemper and revealed the results presented in Table 3.4.

Table 3.4 – Results of the MST experiments

	Model parameter	Wild type	Mutant
Substrate (BA)	$K_{dB} = K_{SiB}$	0.35 mM	1.97 mM
Product (MPPA)	$K_{dQ} = K_{iQ}$	6.78 mM	1 mM

The results of Table 3.4 show that the affinity of the substrate, B, to enzyme form, E, is decreased between the wild type enzyme and the mutant increased. This indicates that dead-end substrate inhibition is decreased. For the target product, Q, the affinity is increased, which indicates that the reverse reactions is faster to reach maximum. It would be very interesting to see the dissociation constant of the substrate, B, with enzyme form, F.

4 TECHNOLOGY FOR OBTAINING KINETIC DATA

In this chapter the current methods for collecting kinetic data are reviewed. The stepwise fitting procedure presented in chapter 3 is heavily reliant upon data in the form of initial rate as a function of initial concentration of substrates or products. A technology is therefore found suitable when it can be used to reliably determine initial rates at low conversion and likewise have the possibility of conducting high conversion experiments. The high conversion experiments determine the remaining parameters after forward and backward rates are fitted and locked.

The described technologies consist of two parts, one part is the reactor, and the other part is the detection method. The parts can be either separated or integrated, and the review describes the applied combinations. Recent developments include exciting new ways of collecting data at microscale[33,94–96], although the associated FT-IR and Raman spectroscopy do not yet deliver the required concentration sensitivity. All the methods are summarized in Table 4.1. After this comparison, special focus will be put on spectroscopy. This is of particular interest since the technology can be coupled on-line to the setup or even in-line as with Raman[95]. The different spectroscopic methods are therefore investigated and compared.

Table 4.1 - Comparison of the different methods for collection of enzyme kinetics, 'continuous' data acquisition refers to that measurement can be obtained in-line/on-line whereas 'discontinuous' data acquisition refers to the transfer of samples between instruments.

Technology	Micro wells	Spectrophotometric assays	Batch	Continuous flow	Stopped-flow	Isothermal titration calorimetry
Detection method	-UV-plate reader -HPLC	-UV-Vis	-HPLC	NIR, IR, Raman	-Spectro-photometric	-Heat flow
Advantages	-Automated -Mixing -Running many reactions in parallel	-In-line -Cheap	-omnipotent -Mixing -Running many reactions in parallel	-Automated batch kinetics -Controlled environment	-Studying reactions in the millisecond range	-Direct non-destructive measurement -Constant error -Determination of ΔH_r
Disadvantages	-Generally not sealed	-Generally not sealed -No mechanical mixing	-Manual handling	-Long term experiments	-Long term experiments	-Expensive -External validation for ΔH_r -Fitting of heat flow
Examples of application	-Oxygen dependent systems -Small quantity of consumables	-Kinetics at benign conditions	-Long term experiments	-Exo and endothermic reactions -Small quantity of consumables	-Very fast reactions -Assays	-Complex and opaque solutions
Time range	Seconds - hours	Seconds - few hours	Minutes – days	Few minutes –few hours	Millisecond- few minutes	Second – few hours
Time resolution	Single wavelenght: 1/10 Hz for 96 wells	Up to 100 Hz	minutes	1-1/15 Hz	Up to 300 Hz	Up to 100 Hz
Data acquisition	Parallel-semi-continuous	Single-continuous	Parallel-Discontinouos	Single-continuous	Single-continuous	Single-continuous
Ref.	97–99	64–66,68,74,75,100–103	76,78,80,83,98	33,94–96	69,104–108	109–112

4.1 Spectrophotometric assays, in cuvettes

Historically, this has been the most important method for the study of enzyme kinetics which can be seen from the extensive encyclopedia-like chapters and textbooks[64–66,68] describing such methods. The method involving the cofactor $NAD(P)^+$ has been central to the success. Upon reduction to NAD(P)H it forms a new absorption band at 340 nm[113]. This is not only an easily accessible region but has the great advantage that the oxidized form does not absorb at this wavelength, meaning that any observed change in absorption is directly proportional to the reaction rate. This technique is directly applicable to dehydrogenases[64–66,68] and these enzymes can also be coupled with other reactions in cascades[114–116]. The reaction conditions of such 'coupled assays' are rather complex to ensure that the test reaction and not the 'indicator' reaction becomes limiting. In general, coupled assays are helpful for the determination of enzyme activity, but cannot be recommended for enzyme kinetic studies for this exact reason. In an analogous way, oxidases can be used to produce hydrogen peroxide which can then oxidize phenol red[117] or xylenol orange[118] detected at 610 and 560 nm, respectively.

4.2 Batch reactors

The slowest and most labour intensive method for collecting kinetic data is by batch experiments. This is also the most robust in terms of wide applicability. Vessels can range from micro wells to lab scale equipment. Most often vessels are chosen in the scale of a few mLs. They fit into thermoshakers and aliquots can be drawn without affecting the reaction. The samples can then be measured off-line, most commonly by HPLC. The frequency of sampling is usually quite high for measuring initial rates and 5-10 points can be collected within an hour. Many batch experiments can be carried out in parallel and for a prolonged time, making them ideal for the measuring of progress curves. Here the sampling frequency is in the order of hours. In general, the batch reactor is considered to be superior at collecting kinetic data, and this mainly comes from the ability to continuously sample from the same reactor at different time points[119]

4.3 Flow reactors

More recently, systems based on the principles of flow chemistry have been developed to ensure rapid, low-volume and high precision analysis. This can replace many tedious and high volume requirements of conventional analysis. Use of flow systems implies the use of pumps and this environment is quite naturally leading towards automation. The implications of computer controlled liquid handling can give rapid characterization throughputs and cost savings. Furthermore, automated operation can remove manual errors and in principle will give more reliable results.

Flow strategies can best be classified dependent upon how the reacting stream is manipulated after merging the reactant with the enzyme. The different types considered here are a) "continuous flow" which is a non-interrupted flow from introduction to waste, b) "stopped flow" which holds the mixture in a chamber that is fit for spectrophotometric measurements and c)"quench flow" which involves either physically or chemically stopping of the reaction at the exit of the system and thereafter analyzing the samples off-line.

Generally flow systems struggle to circumvent the problem of laminar flow, which introduces dispersion into the system. Dispersion elongates the flow profile and hence the time required to reach steady state. This is a problem because the concentration profile in the reactor will change over time until steady-state is reached. A comparison of the different performance under non-steady state reactor conditions should therefore only be made when the flow conditions are exactly the same, such as constant residence time and Reynolds number. Flow injection analysis (FIA) solves this to some extent by measuring pulses of samples. Here the distribution of the sample is followed over time and the area of the pulse is measured. This method is very similar to that of an HPLC and it is calibrated likewise.

What further complicates things for enzymes are their size, which in solution translates to a factor 100 slower diffusivity compared to small molecules (10^{-11} to 10^{-9} m2/s)[120,121]. The dispersion of enzymes will therefore be much more pronounced, meaning they are more dispersed along the length of the channel compared to the small molecule reactants and resulting products. Homogeneity of the pulses is therefore questionable for FIA applied to enzyme catalysis. The effect of enzyme diffusion in 83-283 µm wide channels with side-by-side flow has been investigated by Swarts and co-workers[122]. A Michaelis-Menten model was constructed for a β-galactopyranoside enzyme ($V_{max_{specific}}$ = 20.9 µmol/(s g_{enzyme}), K_M = 1.04 mM), the model was combined with a Computational Fluid Dynamics (CFD) model. The pure model and the CFD model were subsequently compared to understand the effects of diffusion. Even though the enzyme only occupies half of the reactor volume, the reaction rate was not limiting due to the short characteristic mixing time of the reactant. Consequently, only at high enzyme concentrations, (>1 g/L) in this case, would rate limiting effects be observed. Clearly, this is very dependent on the kinetic constants of the enzyme of interest. The investigation was assumed to have been carried out at steady-state, and so the impact of enzyme diffusion on non-steady state methods is yet to be described.

4.4 Microfluidic flow reactors

Developments towards carrying out chemical reactions in flow micro-reactors has in recent years received much attention[123–127]. This can also be applied to the collection of kinetic data. In many cases it is likely that this will replace the traditionally used flasks or stirred vessels operated in batch mode. The small scale makes it possible to conduct experiments with low material input but yielding the same degree of information about the reaction performance. There are three methods reported in the scientific literature used for conducting such investigations, namely: (1) steady-state end-point, (2) measurements at multiple positions at steady-state and (3) non-steady state. The measurements at non-steady-state are made possible by reconsidering low disperse flow[128] that was originally described by Taylor[129,130]. Low-disperse flow behaves similar to that of plug flow but at relatively small flow rates. What makes this so interesting is that a plug-flow reactor has the same integrated mass balance model as a batch reactor, and the performance in flow can hence be used directly to elucidate kinetics.

4.4.1.1 Steady-state

Steady-state measurements of “continous flow” should represent the kinetic behaviour of batch systems. The method will generally be slower for measuring kinetics compared to that of a batch reactor as one will have to wait for steady-state to be attained, prior to making

measurements. Normally, operational steady state is measured as a dependence on substrate or product concentration, a small drift might be neglected but could indicate that the mass balance of the enzyme is yet to reach steady state. Looking through the literature this is often not considered and it is expected that this is commonly attributed to uncertainty of the experiments.

4.4.1.2 Steady state multi point readings

Making microfluidic reactor designs in transparent materials offers the possibility of probing the concentration at different locations along the length of the reactor. These locations represent different residence times according to the flowrate and channel dimensions. Such a combination was recently reported by Fagaschewski and co-workers[96] using IR-spectroscopy. Absorption saturation of water was avoided by substitution with deuterium oxide.

4.4.1.3 Non-steady state

Mozharov and co-workers have developed a method in which the contents of the reactor are quickly pushed out and measured[94]. It was subsequently possible to correlate concentrations with residence times. The Jensen group at Massachusetts Institute of Technology has reconsidered the low-disperse flow[128], and investigated a method to exploit this region further by implementing a flow ramp after obtaining steady-state. This gradually changes the residence time of the fluid elements in the reactor and in this way makes it possible to monitor the development of the reaction by coupling the system to FT-IR analysis[33]. The obtained progress curve was compared to steady-state values and hereby validated. The method has already been adopted and has been shown to work using Raman spectroscopy as well[95].

4.5 Stopped-flow techniques

This technique has been developed for the study of reactions in the millisecond to minutes time range. Transient kinetics can be measured in the lower time range[131–133] if the method is in place. The system can otherwise be used to study steady-state kinetics with the common assays as described previously. Experiments can be carried out by rapidly injecting solutions into a mixing device. The liquid is then led into the flow cell from the mixer, replacing the previous sample, the displaced liquid then fills a stop syringe moving the plunger towards the trigger leaf. After hitting the leaf, the flow is stopped and measurement begins. The flow cell is illuminated and data is collected over time. The usual properties exploited are absorbance and fluorescence measurements, as well as application of light scattering, turbidity and fluorescence anisotropy technologies see Figure 4. In the absence of a spectrophotometric method, quench flow can be applied. Directly after mixing, the solution is be chemically quenched, which can be used to study reactions in the millisecond range. Instead of holding the solution in an observation cell, the quenched sample is collected and analyzed elsewhere (e.g. by HPLC).

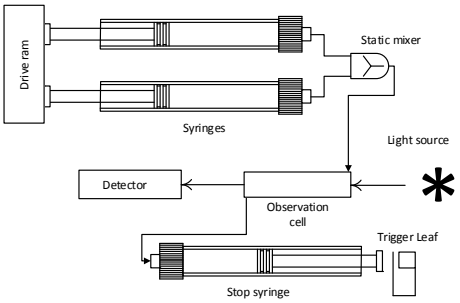

Figure 4.1 – Concept of stopped flow methods

4.6 Isothermal titration calorimetry (ITC)

In contrast to spectral methods, measurements performed with ITC, are independent of the optical properties of the solution. ITC instruments have the objective of keeping the temperature constant in the reaction chamber, this is achieved either by heating or cooling the chamber. The required energy added or subtracted is logged and can be directly translated into a reaction rate by relating the heat flow (dQ/dt) to the enthalpy change of reaction (ΔH_r)[134]. From a practical perspective this is usually done with a single injection experiment where reactant is inserted into the reaction chamber. In the chamber it is possible to follow the burst of energy as the reaction initiates. From this point the reaction will follow a 1st order reaction development until the returns to steady state (zero energy flow). It is here necessary to know the exact amount of reactant converted, and this is done by performing an independent concentration determination. The enthalpy change of reaction can thereafter be calculated by dividing the total heat transferred to the measurement cell by the total number of moles of substrate converted, $n_{sub,converted}$, see Eqn. 4.1.

$$\Delta H_r = \frac{\int_{t=0}^{t=\infty} \frac{dQ}{dt} dt}{n_{sub,converted}} \qquad \text{Eqn. 4.1}$$

The reaction rate can thereafter be determined, see Eqn. 4.2.

$$v = \frac{1}{V \Delta H_r} \frac{dQ}{dt} \qquad \text{Eqn. 4.2}$$

Where V denotes the volume of the reaction chamber.

The technique of ITC is particularly potent since it can essentially measure any event occurring in a reaction chamber. This is also its problem, since dilution, binding events, interaction of impurities and buffer protonation effects[135] will influence the readout. Pure formulations and materials for experiments are therefore required to ensure accurate measurements. Furthermore, dialysis of macromolecular solutions is also recommended, and preparation of small molecule solutions should be made from the dialysate. After satisfying the rather high entrance requirements, it is necessary to match the energy development (rate of reaction) with the lower and upper detection limits. The enthalpy changes for most enzyme-catalyzed reactions range from -40 to -400 kJ/mol, allowing reaction rates from 10 to 100 pmol/sec to be accurately measured[136]. Despite the fact that ITC has been used to measure enzymatic

activity[109,111,112] and that the technology dates back to the 1960s[137,138], the method is not found to be frequently applied in the field of enzyme kinetics. The advantage of a direct non-invasive measurement is though obvious and could be applied to a greater extent.

4.7 Summary of the current methods

Many spectrophotometric assays require alterations to the original reaction in order to be carried out effectively. This can be achieved either by derivation of the reactant with a chromophore or by an analytical enzyme cascade. The widely used indirect spectrophotometric assays rely on the stability of the enzymes and cofactors (e.g. NAD(P)H). Testing rather harsh conditions requires an especially robust assay and this should therefore be carefully considered in the experimental planning phase. The industrial development environment is rarely able to conduct comprehensive investigations, so both speed and resources are important factors, driving automated and flexible methods similar to those that have been developed for classic organic synthesis at microscale[33,95]. However, more sensitive methods of concentration measurement are required and preferably in the order of 0.1 mM. Either UV/VIS or ITC can here be used, but the economic entry boundary for ITC in Denmark is around 130 k€. The technology of UV/VIS is examined further and will be compared to other spectroscopic methods in the following section.

4.8 Spectroscopic Analysis techniques

Absorption spectroscopy is defined by any technique that can detect photons being absorbed by either atoms or molecules. This causes a transition from a low-energy state to a higher energy state or excited state (violet liness in Figure 4.2). The number of photons passing through a sample decreases through absorbance. The extend of this is varied across wavelengths and yields different spectra according to the compounds in a sample. This information can be used to quantify the concentration of a compound in solution.

All spectroscopic methods rely on electromagnetic radiation. The spectrum of different wavelengths is illustrated in Figure 4.3. The mentioned methods in the figure are here presented as a function wavelength. In order to give a quick overview of the output from these different methods, examples of spectra is given as a function of reaction time. It is in this regard good to consider the relation between frequency and wavelength. It is described by $v = c/\lambda$, where v is the frequency, λ is the wavelength and c is the speed of light, $c = 3.00 \times 10^8\ m/s$. The shorter the wavelength the higher the frequency and the higher the energy. Infrared spectroscopy does not cause shifts in energy levels but in vibrational energy (red lines in Figure 4.2) This technology is hence good for the study of different functional groups of a compound. Comparing Infrared and UV/VIS spectroscopy, the former tends to show a detailed map of the compound in solution whereas UV/VIS will display significantly broader bands. This is because compounds in UV/VIS radiation not only changes energy levels but also transition between vibrational levels.

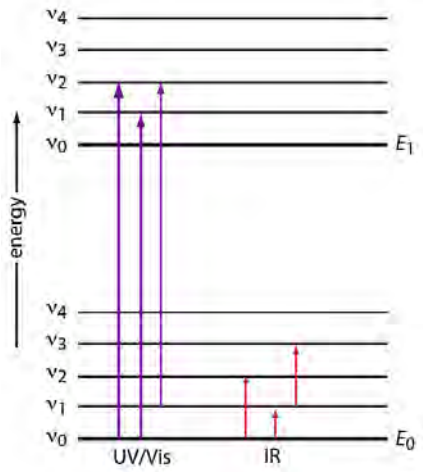

Figure 4.2 – Schematic drawing of the energy levels E_0 and E_1 each with vibrational levels v_0-v_4. violet lines represent absorption of ultraviolet and visible radiation, red lines represent vibrational absorption of infrared radiation

The commonly applied methods in analytical chemistry are ultraviolet spectroscopy (UV, 10-380 nm), visible spectroscopy (vis, 380-750 nm), shortwave near-infrared spectroscopy (SW-NIR 750-1100 nm), longwave near-infrared spectroscopy (LW-NIR, 1100-2500 nm), infrared spectroscopy (2500 nm – 25000 nm) and Raman spectroscopy.

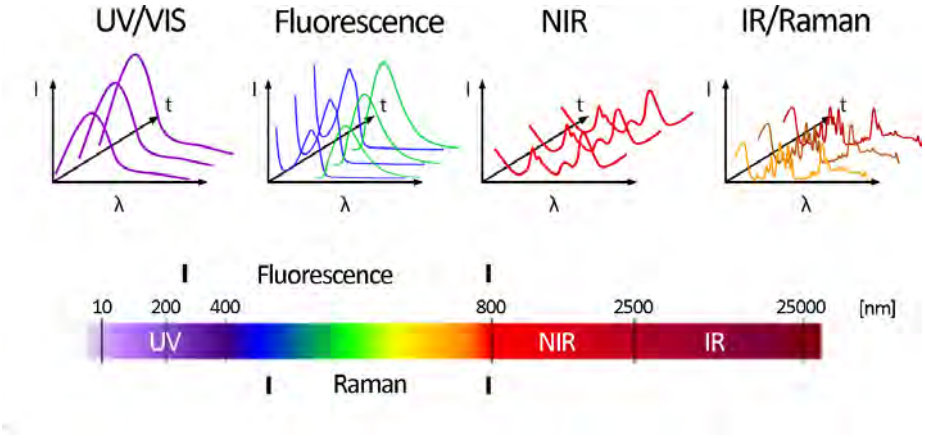

Figure 4.3 – The different analytical methods as a function of wavelength, inspired by Kessler[139]

4.8.1 Lambert-Beers law

When a matter is irradiated the radiation can either be reflected, transmitted or absorbed. Lambert Beers law states that the concentration is directly proportional to the absorbance at a given wavelength and path length at a specified temperature and pressure, with the extinction coefficient for scaling.

$$A = \varepsilon C l \qquad \text{Eqn. 4.3}$$

where C is the molar concentration, l (cm) is the path length and ε (L/(mol cm)) is the molar absorption coefficient. The absorbance (A) is related to the intensity of the light before (I_0) and after (I) passage through the sample. It can be seen that the absorbance unit is measured on a log scale which translates to that for 100 to 10 % transmittance (I/I_0) one will observe 0-1 absorbance units (AU), for 10-1 % transmittance 1-2 AU, and so forth. For this reason one should avoid measuring above 2 AU.

$$A = -\log_{10}\left(\frac{I}{I_0}\right) \qquad \text{Eqn. 4.4}$$

A comparison of the mentioned spectroscopic methods is given as Table 4.2. Please keep in mind, that this table is created with the scope of on-line measurements.

The resolution is the ability to distinguish between analytes and techniques such as NIR and UV/VIS will typically have low spectral resolution. Conversely, analytical methods such as IR and Raman show fingerprints of molecules and have higher spectral resolution. The high resolution makes it possible to selectively choose peaks related to the desired analyte. In order to use low spectral resolution methods such as UV/VIS or NIR it is common to apply chemometric methods of resolving the spectral data mathematically, this will be described later.

The selectivity in Table 4.2 is a measure for how independent samples are of their mixtures. Raman and IR can achieve quantification with a modest set of calibration, this is due to their spectral resolution. This is not the case for UV/VIS and NIR that require larger calibration sets in order to asses natural variation of different chemical species, this is due to the overlapping bands of the different solutes. IR and to some extend NIR is limited to non-aqueous systems, because the molecular extinction coefficient of water in the mid-infrared region is extremely large. In most cases this will saturate the absorption associated with the analytes, shading the possibility of detection. Raman can be saturated by fluorescence and its high price for a robust equipment limits the widespread use of this technology. In short, UV can operate with aqueous systems as water renders invisible, but compared to NIR/IR/Raman the peaks are broad and overlap.

Table 4.2 – comparison of different spectroscopic methods, inspired by Kessler[140] and Lyndgaard [141]

	NIR absorption	Raman scattering	IR absorption	UV/VIS absorption	HPLC w/ UV/VIS detector
Ref.	[142]	[143]	[144]	[145]	
Resolution	Low	Medium	Medium	Low	High
Sensitivity	Low	Medium	Medium	High	High
Selectivity	Medium	High	High	Low	High
'Main interferences'	Water	Fluorescence	Water	Scattering	Saturation
Path length	1 mm – 1 cm	-	0.01 – 1 mm	6 – 60 mm	6 – 60 mm
Limit of quantification	0.1 M	50 mM	10 mM[146]	10 µM[146]	10 µM[146]
Sample preparation	None	None	None	None	Dilution
Typical analysis time	Seconds	Seconds - minutes	Seconds - minutes	Seconds	Minutes
Price of robust instrument [140,147]	++	++++	++	+	++
Molecular phenomena	Combination and overtones of molecular vibrations	Fundamental molecular vibrations	Fundamental molecular vibrations	Valence electron transitions	Valence electron transitions
Other characteristics	-Nearly all molecules absorb -Quartz transparent -PTFE transparent -describes X-H chemistry	-Nearly all molecules scatter -Quartz transparent -Large signal for C=C and C≡C	-Nearly all molecules absorb -Quartz transparent -PTFE transparent -Very sensitive for C=O	-Not all molecules absorb -Quartz transparent	-Separates molecules by chromato-graphy making it possible to conduct quantification as if it was on an isolated solution

4.8.2 UV/VIS detection

For determination of enzyme kinetics both the absolute absorption and spectral changes must be considered. From the perspective of synthesis, many small molecules which absorb in the mid-UV region (200-300 nm) are used. For reference some of the molecules relevant to this thesis are listed in Table 4.3. It can be seen that very small molecules have small molar absorption coefficients, whereas compounds with aromatic rings have a factor 10-100 higher coefficients. Conjugated aromatic rings top this list with a factor 1000 higher coefficients compared to acetone. From the absorption coefficients and Eqn. 4.3 it is possible to calculate the maximum allowed concentration in a flow cell with path length 1 cm. This can be done by setting the absorption to a maximum of 2 Absorbance Units (AU) and is motivated by the small difference in transmittance above this value as described previously. There are two ways to increase this maximum, either by decreasing the path length or by diluting the sample. The wavelength at which a compound has maximum absorbance and is denoted λ_{max} and is defined to be the analytical wavelength. Conjugation usually moves the analytical wavelength to higher values, an example could be Ethene at $\lambda_{max} = 180 - 200\ nm$ and 1,3-Butadiene at $\lambda_{max} = 217\ nm$. Methods also exists for calculating the analytical wavelength and can be found in textbooks such as Lampman[148].

Table 4.3 – Analytical wavelengths and molar absorption coefficients of selected compounds, prim. denotes primary and sec. denotes secondary

Compound	Acetone	Benzoic acid	Aceto-phenone	NADH	PLP
Ref.	149	148	148	150	151
Structure		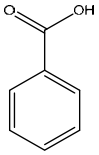	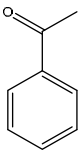	-	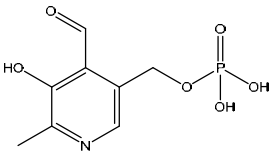
Analytical wavelenght [nm]	260	Prim. 230 Sec. 273	245	340	415
Molar Absorption coefficient [L $mol^{-1}cm^{-1}$]	15.4	Prim. 8600 Sec. 1430	11400	6317	5380
Maximum concentration Abs= 2 AU, path lengt= 1 cm [mM]	130	Sec. 2.1	0.18	0.32	0.37

Enzymatic reactions often require stable pH and buffers are introduced for the same reason. In the desire to investigate the middle and far UV regions it is best to use inorganic buffers as they do not interfere with the absorbance spectra because of their low wavelength cut-offs. Applied buffers could be as phosphate, borate or Cacodylate. These three compounds cover a suitable pH range (5.27-10.24) for the investigation of enzymatic reactions, see Table 4.4. Proteins usually show secondary λ_{max} between 275 and 280 nm which is mainly due to the absorbance of the two aromatic amino acids tryptophan and tyrosine and to a small extend to the absorbance of cysteine. As mentioned before, the molecules used for synthesis usually absorbs in the mid-UV region, it is also necessary to use solvents that has a low wavelength cut-off, see Table 4.5.

Table 4.4 – buffer compounds suitable for investigation of the middle UV spectra.

Buffer	pKa	Range
Phosphate	2.12	1.12-3.12
	7.21	6.21-8.21
Borate	9.24	8.24-10.24
Cacodylate	6.27	5.27-7.27

Table 4.5 – wavelength cutoff in the application of solvent[146,148,152]

solvent	Lower wavelength limit, nm
Water	190
Methanol	205
Ethanol	205
Hexane	200
Cyclo Hexane	200
Isopropyl alcohol	210

In summary, UV/VIS provides a sensitive and economic way of measuring many important molecules for organic synthesis in aqueous solutions. The remaining challenge is to increase

resolution. In many cases the spectral differences in solutions with enzyme, substrate(s) and product(s) are not very large and only small shifts can be observed. For this reason chemometrics will be applied as part of the detection method and the concepts will be explained in the next section.

4.9 Chemometrics background

As stated above, chemometrics can be used to mathematically resolve spectral data. Chemometrics is a combination of chemistry, mathematics and statistics that is used to analyse and convert collected data into quantifiable observations. As computational power continues to become cheaper, the field sees more and more implementation and wider awareness. Data in this thesis will be 3-way (spectral x retention time x samples) and will be converted into compound concentrations.

The objective of this thesis is not to develop the field of chemometrics but rather the application of it. The concepts applied will therefore be explained but not the extensive theory behind. Knowledge of principal component analysis (PCA) and principal component regression (PCR) will help in understanding the following but will not be explained here.

4.9.1 Nomenclature

Scalars are indicated by lowercase italics, vectors by bold lower-case characters, bold capitals are used for two-way matrices, and underlined bold capitals for three-way arrays. The letters I, J, K, L and M are reserved for indicating the dimension of different modes. The *ijk*th element of $\underline{\mathbf{X}}$ is hence called x_{ijk}. The terms mode, way and order are used more or less interchangeably.

4.9.2 Multi decomposition methods

Multi decomposition methods, such as parallel factor analysis (PARAFAC) or multi curve resolution alternating least squares (MCR-ALS), are used to extract scores and loadings and hereby describe modelled data in a more compact form. Loadings should ideally represent the different chemical species present in the mixture. Imagine that loadings are puzzle pieces added together and scaled by the scores to fit the individual dataset. The scores therefore represent the quantity of a loading present in a dataset, and can be calibrated against concentration to extract quantitative information. This can conceptually be compared to bilinear PCA, but instead of one score vector and one loading vector, a (PARAFAC) component has one score vector and two or more loading vectors. The expansion from PCA to a two loadings (**F**actor) PARAFAC model can be seen in Figure 4.4.

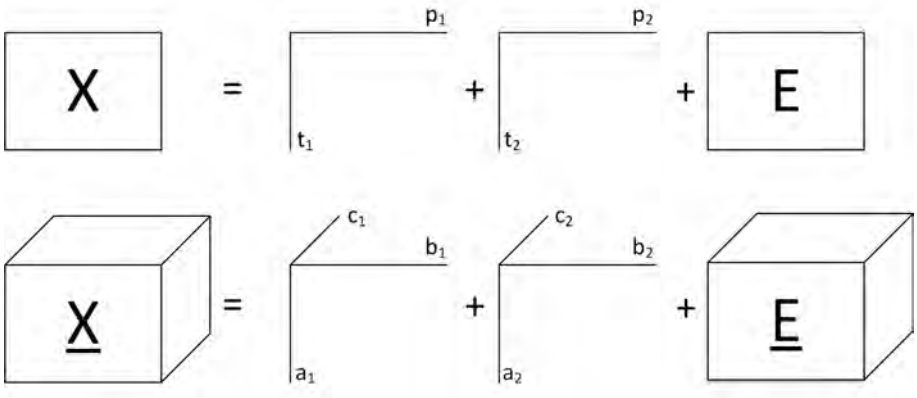

Figure 4.4 – graphical representation of the expantion from PCA to PARAFAC, F=2

The graphical representation of Figure 4.4 can also be written in equation form, see Eqn. 5.1

$$x_{ij} = \sum_{f=1}^{F} t_{if} p_{jf} + e_{ij} \qquad \text{Eqn. 4.5}$$

Where x_{ij} is original data point in the position given by indices i and j. t denotes the scores and p the loadings, e_{ij} is the residuals that the model does not fit. The PARAFAC model can be written as follows

$$x_{ijk} = \sum_{f=1}^{F} a_{ij} b_{if} c_{kf} + e_{ijk} \qquad \text{Eqn. 4.6}$$

The objective of the models is to minimize the sum of squares of the residual e by change in the scores and loadings. After convergence is achieved e should ideally only contain the noise of the data.

Modelling data in a bi-linear way has a well known challenge with rotational freedom. This is because the loadings always will be orthogonal. This can be understood best by drawing an analogy with a coordinate system where the x-axis is independent of y-axis due to orthogonality. Imagine a 3D-space of data points that can be described to some extend by an axis (1st loading) by points, an addition of a second axis (2nd loading) will describe the data even better by coordinates. The objective of describing data in the best possible way forces the two loadings to be orthogonal. The loadings (axis) now span a plane and can be rotated in this plane without losing descriptive power, but this will of course change the scores (coordinates) accordingly[153]. The loadings may therefore reflect pure spectra though this is not a given and cannot be confirmed without external information. This is not a problem for a PARAFAC model. If the data is tri-linear it will find the true underlying spectra if the right number of components are used [154]. This makes PARAFAC an excellent tool for curve-resolution. In the fitting of the PARAFAC model, it is possible to apply constraints to the different modes. Most commonly applied is the non-negativity which also have physical meaning. Neither background corrected spectra nor concentrations can be negative. Another constraint is Uni-modality. Here loadings are allowed to only monotonically increase to a maxima and here after

monotonically decrease. The constraint is therefore restricting the individual components to have only one peak. This is excellent in the sense of chromatography, where molecules of a specific compound are grouping and eluting together. In order to fit a PARAFAC model it is required to have strict parallelization. This is understandable as any shift in either of the modes could represent an actual difference in the sample. In normal HPLC the shift and variation of retention times are handled by giving an interval for where a peak is expected and hereafter integrating the peak to determine the area. The peak area is then correlated with concentration and quantification can be obtained. This way of analysis is robust but requires complete baseline separation to provide reliable results. Shift and variation in retention times is here handled by peak alignment. This was made possible with the help of algorithms developed at the department of Food Science, University of Copenhagen. Firstly, iCoshift was utilized on all samples to align the retention time mode by the substrate peak. The intervals and indexes were hereafter transferred to the apply iCoShift script and applied to the 3-way data. The data could then be fitted with PARAFAC model in the N-way toolbox also from KU.

In order to address the problem of strict parallelization, PARAFAC2 was developed. This model allows of shifts in loadings of one mode, here the time mode. This is however much more computational heavy as it evaluates every single sample separately and not by whole matrix operations.

4.10 Summary of spectroscopic techniques

Aqueous solutions are difficult to measure spectrophotometrically, this can be explained by water saturation of the NIR or IR spectrum or spectral resolution problems with UV/VIS. Saturation and sensitivity of infrared technologies makes these a poor choice in this regard. UV/VIS technology has the desired sensitivity and is a relatively affordable solution. Nonetheless, the problem of resolution must be solved. One solution is to introduce a crude separation of the different compounds, where the overlapping retention time-wavelenght data can then be chemometrically quantified by a PARAFAC model.

5 MICROFLUIDICS

Application of microfluidics in the development of biocatalytic processes, where the main advantage is the low consumption of scarce and valuable resources has great potential. However, to fully exploit this potential requires a fundamental understanding of the dominating phenomena and effects at a microfluidic scale.

It is therefore the aim here to give an overview of these dominating phenomena and effects in order to highlight how to exploit them in the development of biocatalytic processes. Special emphasis is given to microfluidic mixing/mass transfer effects, which is considered the most important feature for successful application of microfluidics for development of biocatalytic processes. Furthermore, the concept of combining microfluidic modules in a plug-and-play manner is described and introduced as a novel option for testing complex biocatalytic process strategies that otherwise are very difficult to test with conventional methods. Complex biocatalytic process concepts are of interest as potential solutions for biocatalytic processes that are particularly challenging to operate as conventional batch processes.

5.1 Introduction

Microfluidics is in this context referred to as the analysis, control and manipulation of fluids in geometrically constrained channels, having characteristic dimensions in the micrometer range[126,155]. Microfluidics can be classified as a sub-category of flow chemistry, which covers continuous reactions conducted in microreactors, and is currently being considered an improvement and greener alternative compared to conventional batch processing in organic synthesis[124,156]. Furthermore, it has been pointed out several times that the use of microfluidics is in accordance with the 12 principles of green chemistry [157,158], in terms of improved safety[126,159], reduced waste generation [160] and energy efficiency to name a few metrics[161]. All these features are also considered requirements of efficient processes [156].

In 2007, a roundtable with the pharmaceutical industry ranked the most important research topics as being continuous processing, bioprocesses and separation and reaction technologies[162]. Hence, it is the focus of this work to address these topics and apply microfluidics as a tool in doing so.

Jensen and co-workers[160] presented the most recent developments in the microfluidic toolbox and further addressed major challenges for the technology. The Jensen group has published many papers regarding the field of microscale technology, and most relevant here are the operational window for plug flow conditions at microscale[163], batch-like reaction time courses[33], automatic reaction optimization[164], and automatic kinetic model validation[165]. Furthermore, there is increased focus on the application of microfluidics for multistep synthesis systems [166,167] and continuous-flow chemical [168] and biochemical [169] processing, which is considered highly relevant as well.

The application of microfluidics for development of biocatalytic processes has a great potential. In fact, the main product resulting from the application of microfluidic process technology is information and fundamental knowledge that can be channeled towards accelerated process development. The exception to this is when reactions are difficult to control in conventional batch systems, causing microfluidics to be a suitable production method[170,171], which is in fact rarely the case for biocatalytic processes. For biocatalytic processes, one clear benefit of applying microfluidics is the low consumption of scarce and valuable resources, especially in the early development phase where for example only a few milligrams to a few grams of the catalyst is available [34]. More importantly, the information gathered per mass of biocatalyst spent is much higher in micro-scale reactors. Consequently, investigations that are more detailed can be carried out in comparison to conventional lab-scale studies. Furthermore, the small characteristic length scale and the large surface-to-volume ratio in microsystems enable faster heat and mass transfer. Compared to larger scale equipment this enables better control of concentration and temperature gradients in the microfluidic systems [126,161].

To fully exploit microfluidics for biocatalytic process development it is essential to have a fundamental understanding of the physical effects at the scale of interest. The dimensional effects are the majority of what is changing by using microscale technology as opposed to conventional lab scale and large scale equipment. In particular the smaller intrinsic volume, large surface to volume ratio and small hydraulic diameter are worth mentioning[172]. Microsystems commonly operate in well-defined laminar flow conditions, where heat and mass transfer will mainly be governed by diffusion and convection. Especially the mass

diffusion time in microfluidic modules has a significant impact on the development of biocatalytic processes as it dictates the ideality of the mixing in the system. The diffusion time can be calculated by Eqn. 5.1.

$$\tau_{mix} = \frac{d_t^2}{4D_{ab}} \qquad \text{Eqn. 5.1}$$

, where $d_t[m]$ is the diffusion distance, τ_{mix} [s] is the characteristic mixing time and D_{ab} [m^2s^{-1}] is the diffusion coefficient of solute a in b.

Therefore, an important tool for understanding the phenomenal behavior at microscale, is to perform dimensional analysis which gives insights into opportunities that can emerge from miniaturization. Examples of different effects of miniaturization are displayed in Table 5.1. For example, the short distances in microsystems cause the transport times of mass and heat to be shortened, where especially short mixing times are important when testing biocatalytic processes. The highly increased surface to volume area gives fast energy control and important operation parameters can be regulated precisely. The model assumption of ideal conditions are therefore approached, and modeling of the system will be more accurate. Microfluidic systems are expected to form the practical tool that will make us realize high-speed, functional, and compact instrumentation[173]. This will aid in improving and accelerating the characterization and development of biocatalytic processes. After investigating the effect of miniaturization, different dimensionless numbers will be introduced in this chapter, in order to better understand the fluid dynamic behavior occurring at this scale. These numbers can also be used to define regions of operation where desired behavior can be exploited.

Table 5.1 – Effects of miniaturization, the hydraulic diameter for tubes are the inner diameter of the tube

Parameter	Factor change	Macroscale	Mesoscale	Microscale
Hydraulic diameter	d_H	1 m	1 cm	100 µm
Surface	d^2	1 m^2	1 cm^2	10^4 μm^2
Volume	d^3	1000 L	1 mL	1 nL
Surface / Volume (m^2/m^3)	$d^2/d^3 = 1/d$	1	10^2	10^4
Diffusion time over d ($D_{ab} = 10^{-5}$ cm^2s^{-1})	d^2	8 y	7 h	2.5 s
Diffusion time over d ($D_{ab} = 10^{-6}$ cm^2s^{-1})		80 y	70 h	25 s
Example: in flowing systems				
Linear flow rate	d	1 m/s	1 cm/s	1 mm/s
Re (µ = 0.001 kg m^{-1} s^{-1}, ρ = 1000 kg m^{-3})		10^6	10^3	0.1
Volume / Experiment		>1 m^3	]1000: 1[mL	<<1 mL

In order to get a better feeling for the ranges one applies in the different overall flow regimes, typical values are given in

Table 5.2, these values were thereafter plotted as boxes in a hydraulic diameter and logarithmic flowrate plot along with a Re number as a contour in Figure 5.1.

Table 5.2 – Typical values for the hydraulic diameter (d_H) and the flow rate (q)

	d_H [mm]	q
Plug flow	6.4	>100 L/min
Laminar flow	1-3	1-500 mL/min
Low-dispersed flow	0.1-0.5	50-400 µL/min

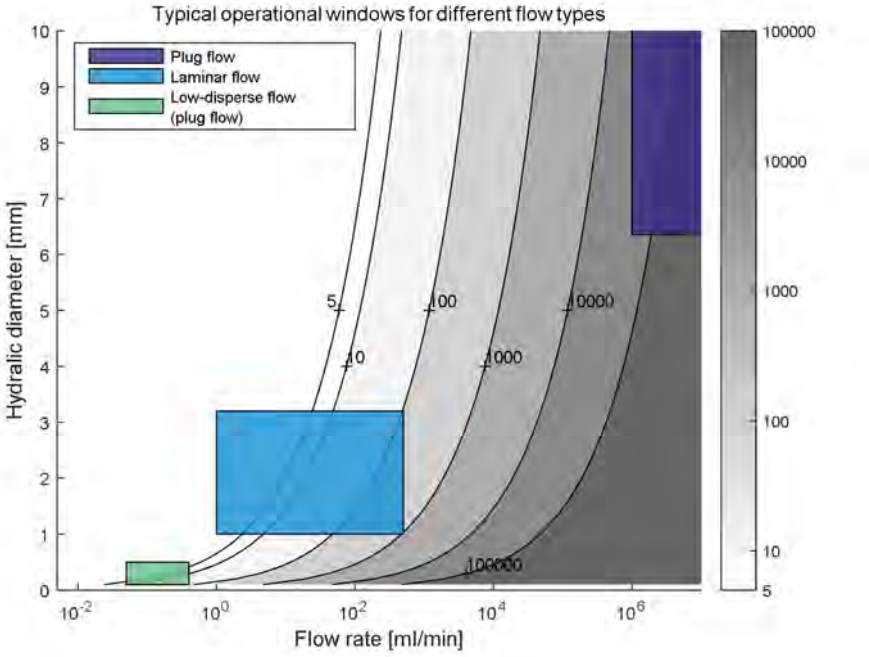

Figure 5.1 – Illustration of typical values for different types of flow, Re numbers are indicated by the grey contour.

5.2 Phenomena at the microfluidic level

A core element in the development of processes is to develop a proper understanding of the transport phenomena across scales, i.e. small scale in the development phase and large scale for industrial implementation. In order to efficiently use the information collected at the different scales such differences must be accounted for. It is therefore essential to understand the dominating transport phenomena in the microfluidic regime, relative to large-scale applications, when applying microfluidics for process development.

The topic of transport phenomena is a well-developed branch of physics with many standardized methods to calculate the dominating physical phenomena at the given scale and operational conditions, i.e. through dimensionless numbers[174,175]. Here a brief overview is given of common dimensionless numbers that are applied to understand the transport phenomena in microfluidics. The dimensionless numbers are crucial when dimensioning microfluidic modules for specific applications.

5.2.1 Reynolds number

The Reynolds number is applied to describe the ratio of momentum forces relative to viscous forces. The Reynolds number is calculated by Eqn. 5.2.

$$Re = \frac{momentum\ force}{viscous\ force} = \frac{\rho v d_h}{\mu} = \frac{\rho \left(\frac{q}{A}\right) d_H}{\mu} \qquad \text{Eqn. 5.2}$$

, where $\rho\ [kg/m^3]$ is the fluid density, $d_h[m]$is the hydraulic diameter, $\mu\ [kg/(m \cdot s)]$ is the dynamic viscosity, $v\ [m/s]$ is the average linear flow velocity in the channel, $A\ [m^2]$ is the cross-sectional area and $q\ [m^3/s]$ is the volumetric flow rate in the channel.

At low Reynolds numbers, viscous forces become dominant, which causes the fluid to move with a laminar flow profile, i.e. a parabolic velocity profile. At high Reynolds numbers, the momentum forces become dominant causing chaotic mixing effects, i.e. turbulent flow. The two types of flow regime are illustrated in Figure 5.2. In the scientific literature different regions of Reynolds numbers are applied to identify where the two types of flow regimes are dominant. It is stated in the literature that the different flow regime regions are in the ranges of [161,174]:

Turbulent flow regime: $Re > 3000$

Transition from turbulent flow to laminar flow: $1500 < Re < 3000$

Laminar flow regime: $Re < 1500$

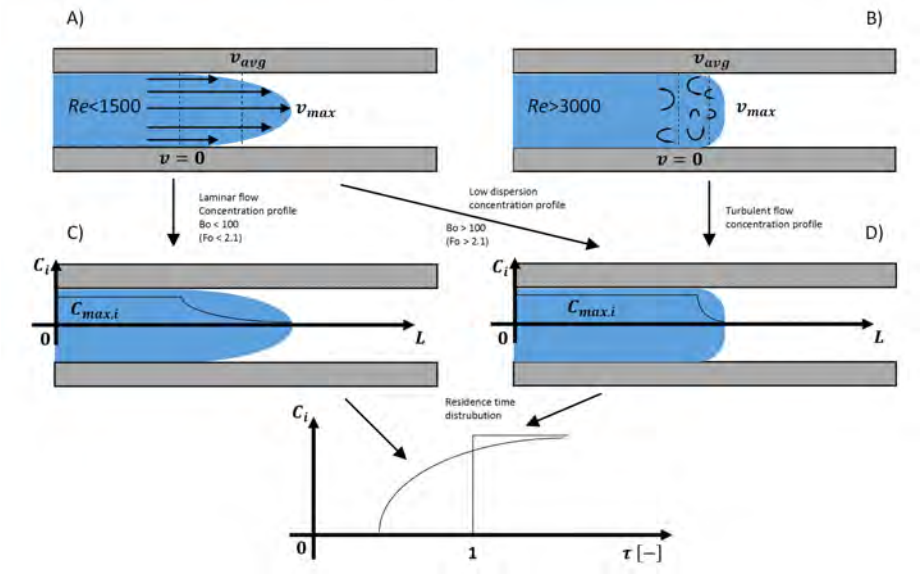

Figure 5.2 – Overview of flow characteristics and concentration distribution profile scenarios. A) Laminar flow velocity profile. B) Turbulent flow velocity profile. C) Laminar flow concentration profile, where convection is dominating over radial dispersion. D) Turbulent flow concentration profile, which will appear similar to laminar flow when radial dispersion is dominating. E) Residence time concentration profiles of laminar flow and plug-flow dominated systems.

In Figure 5.3, the Reynolds number is calculated for a range of tube diameters and flow rates that are commonly applied for microsystems. Also highlighted in the figure are the Reynolds numbers, at various flow rates, for standard PTFE tubes, which are easily applicable in microsystems. The calculated Reynolds numbers clearly indicate that microsystems operate in the laminar flow regime, i.e. $Re \ll 1500$. In comparison, it is common that large-scale systems

operate in the turbulent flow regime, which causes some fundamental differences in the mixing behavior across scales. This also makes it challenging to scale up processes based on knowledge obtained in microfluidic systems.

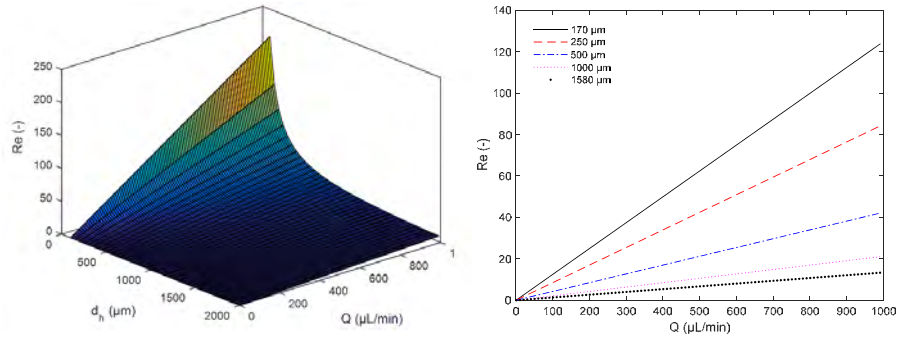

Figure 5.3 – Left) Reynolds numbers for various inner tube diameters at various flow rates. Right) Reynolds numbers at various flow rates for standard PTFE tube dimensions.

5.2.2 Bodenstein & Fourier numbers

The Reynolds number only indicates the flow regime at the specified dimensions and flow conditions. Therefore, in order to get an idea about the mixing effects and concentration profiles in the microsystem of interest at various process conditions, it is essential to consider the Bodenstein, Fourier and/or Péclet numbers. The Bodenstein number is applied to describe the ratio of convection relative to that of dispersion. The Bodenstein and Péclet numbers both describe momentum transfer relative to molecular mass transfer. Consequently, the focus here is solely on the Bodenstein number. The Bodenstein number is described as Eqn. 5.3.

$$Bo = \frac{total\ momentum\ transfer}{molecular\ mass\ transfer} = \frac{vL}{\mathbf{D}} \qquad \text{Eqn. 5.3}$$

, where $\mathbf{D}$ is the Taylor dispersion coefficient [163,175]. Convection dominates most small scale flow systems and as a result the diffusive portion of the expression can be neglected, see Eqn. 5.4.

$$\mathbf{D} = D_{AB} + \frac{v^2 d_H^2}{4\beta D_{AB}} \cong \frac{v^2 d_H^2}{4\beta D_{AB}} \qquad \text{Eqn. 5.4}$$

, where $\beta[-]$ is a channel specific parameter, i.e. 48 for cylindrical channels [163].

Large Bodenstein numbers indicate low dispersion and operation will resemble that of a plug-flow reactor. At low Bodenstein numbers, dispersion will be dominant and the flow profile will be that of a laminar flow reactor. This is illustrated in Figure 5.4, where the flow profile will develop towards parabolic flow if convection is dominant (small Bo numbers), whereas radial dispersion will move the behavior towards plug flow when diffusion becomes significant.

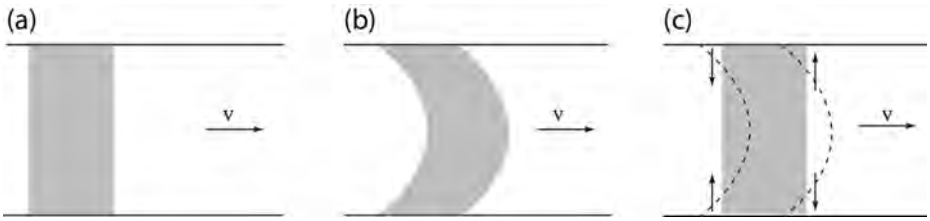

Figure 5.4 – Explaining convection with and without diffusion, (a) impulse injected, (b) convection of impulse without diffusion and (c) convection of impulse with diffusion

Both concentration profile scenarios and their relative system response times (retention time distributions, RTD) are schematically presented in Figure 5.2. The inverse of the Bodenstein number can be said to describe the intensity of dispersion, and follows the inverse explanation of the Bodenstein numbers. Nagy et al. [163], coupled the Bodenstein number with the Fourier number, the ratio of residence time relative to the time to diffuse halfway across the channel, described by Eqn. 5.5.

$$Fo = \frac{residence\ time}{transverse\ diffusion\ time} = \frac{4D_{AB}\tau}{d_t^2} \qquad \text{Eqn. 5.5}$$

This coupling made it possible to specify ranges of the Bodenstein number, which resembles plug-flow dynamics and the transition to Taylor dispersion/convective flow dynamics. The specified ranges are as follows for step changes in the flow rate and/or concentration composition [163]:

Convective profile:	$Bo < 10$	$(Fo < 0.16)$
Large deviations from plug-flow profile:	$10 < Bo < 100$	$(0.16 < Fo < 2.1)$
Small deviations from plug-flow profile:	$100 < Bo < 1000$	$(2.1 < Fo < 21)$
Plug-flow profile:	$1000 < Bo$	$(21 < Fo)$

Based on the specified regions it was possible to make predictions about the magnitude of dispersion effects and the corresponding flow characteristics for different diffusion coefficients. These predictions are presented in Figure 5.5, inspired by Nagy et al. [163]. The location of the different regions, relative to residence time and tube diameter, is greatly dependent on the diffusion coefficient of the solute. Practically, this means that slowly diffusing compounds are prone to having flow dynamics which are dominated by axial dispersion. The main problem of having such flow dynamics is the time it takes to reach steady state, which is greatly increased compared to plug-flow dynamics. This can be observed in Figure 5.6, the region of interest is either C or D.

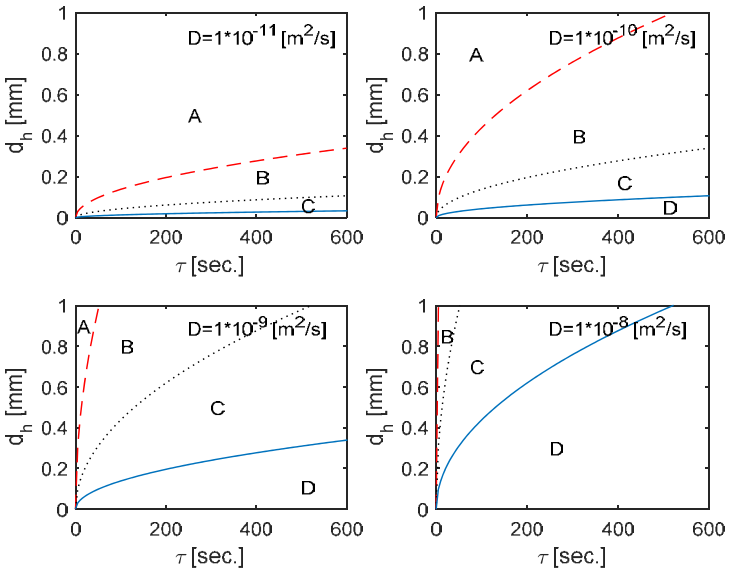

Figure 5.5 – Influence of the diffusion coefficient on the flow dynamics/mixing dynamics of the system. A) fully developed laminar flow dynamics, B) large deviations from plug-flow dynamics, C) small deviations from plug-flow dynamics, and D) plug-flow dynamics

Enzymes and other proteins are known for having low diffusivities, which as earlier stated makes it time consuming to achieve steady state. This problem is repeated for each step change with regard to the enzyme concentration. However, it is possible to circumvent this by acquiring a steady state condition profile for the enzyme in the system and hereafter only introduce step changes to the substrate composition. In other words, the mass balance over the reactor for the enzyme is kept constant. It can hereby be assumed that the system operation will depend on the substrates diffusion coefficient, as shown in Figure 5.5. The substrates applied for enzymatic reactions are commonly very small molecules, and consequently also fast diffusing molecules.

Estimation of the time required to reach the initial steady state shows that this time is still highly dependent on the specific diffusion coefficient of the investigated enzyme. Significant research efforts have been invested into development of quick and robust methods and models for predicting protein diffusion coefficients. He et al. [176], for example, included the radius of gyration [177] to the molecular weight correlation [121] to get within 15% deviation of most experimentally determined values. The addition of gyration radius gives a correction for non-globular shaped proteins, which is for example important in the case of rod shaped proteins. The radius of gyration needs to be calculated and should not be looked up as a general value. It can be calculated directly from protein database files by applying the HYDROPRO software [178]. It is suitable to apply the HYDROPRO software when the protein crystal structure is available, as the software not only calculates the radius of gyration, but also directly calculates the diffusion coefficient. For globular proteins, it is possible to correlate the diffusion coefficient directly to the molecular weight of the protein. The molecular weight correlation [121] and the model including the radius of gyration [176] are defined as Eqn. 5.6 and Eqn. 5.7

$$D_{AB} = 8.34 \cdot 10^{-11} \left(\frac{T}{\mu \cdot M^{1/3}}\right) \quad \text{Eqn. 5.6}$$

$$D_{AB} = \frac{6.85 \cdot 10^{-15} T}{\mu \cdot \sqrt{M^{1/3} \cdot R_G}} \quad \text{Eqn. 5.7}$$

, where $T\ [K]$ is the absolute temperature, $\mu\ [PA \cdot s]$ is the dynamic viscosity, $M\ \left[\frac{g}{mol}\right]$ is the molecular weight and $R_G[\text{Å}]$ is the radius of gyration. HYDROPRO requires knowledge of the specific volume, $\bar{\nu}$, or inverse density, which can be estimated based on the following correlation, see Eqn. 5.8[179]s.

$$\rho(M) = \left[1.410 + 0.145 \exp\left(-\frac{M}{13}\right)\right] = \frac{1}{\bar{\nu}} \quad \text{Eqn. 5.8}$$

, where the molecular weight M is expressed in kDa units.

Predicted diffusion coefficients from the above-mentioned models and correlations for two transaminases are presented in Table 5.3. It was assumed for the calculations that $T = 303.15\ K$ (30°C) and $\eta = 0.001\ Pa \cdot s$.

Table 5.3 – Predicted diffusion coefficients of two transaminases obtained from various models and correlations.

PDB ID.	Enzyme	M	R_G (from hydropro)	$\bar{\nu}$	$D_{AB,calc}$ Young et al. [121]	$D_{AB,calc}$ He et al. [176]	$D_{AB,calc}$ HYDROPRO [178]
Units:	-	g/mol	Å	cm^3/g	$10^{-11} m^2/s$		
3A8U	ω-ATA-monomer	48916	23.1	0.71	6.91	7.14	7.23
4A72	ω-ATA-tetramer	205613	40.7	0.71	4.28	4.23	4.49

The Taylor dispersion coefficient described earlier (equation 3.4) can be combined with dispersion models to predict the exit age distribution. For open-open systems, where the system boundaries represent similar flow dynamics as that of the control volume, the exit age distribution can be described by Eqn. 5.9[180].

$$\mathrm{E}_{\theta,\mathrm{oo}} = \frac{1}{\sqrt{4\pi \mathrm{D}/\mathrm{v}L}} \exp\left[-\frac{(1-\theta)^2}{4\theta\, \mathbf{D}/vL}\right] \quad \text{Eqn. 5.9}$$

, where $\theta\ [-]$ is the mean residence time.

The F curve can then be calculated by Eqn. 5.10[180].

$$\mathrm{F}_{\mathrm{oo}} = \int_0^{\theta} \mathrm{E}_{\theta,\mathrm{oo}}\, dt \quad \text{Eqn. 5.10}$$

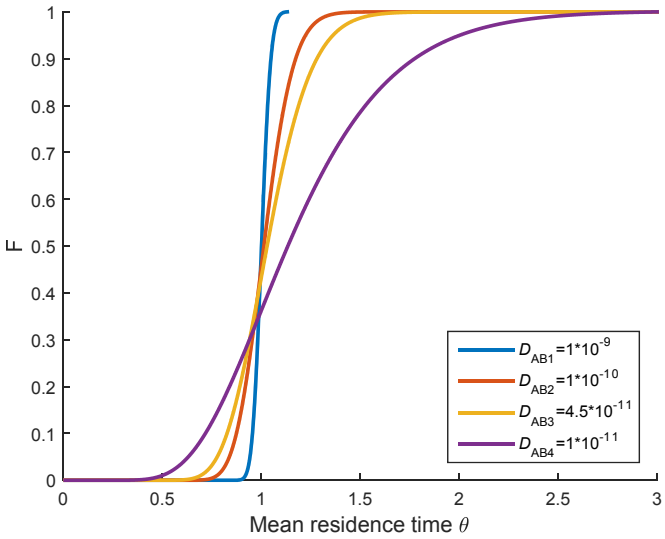

Figure 5.6 – F curve as a function of mean residence time accounting for different diffusion coefficients, D_{AB1}=1·10^{-9}, D_{AB2}=1·10^{-10}, D_{AB1}=4.5·10^{-11} and D_{AB1}=1·10^{-11}. The curves were calculated with v=0.023 m/s, L= 7 m, beta = 48 and ID=200 µM

From Figure 5.6, it is clear that the substrates (D_{AB} = 10^{-9} m^2/s) and enzymes (D_{AB} = 10^{-11} m^2/s) move very different through the reactor, as expected. The required times to reach steady state have been estimated and can be observed in Table 5.4. Levenspiel[180] states that for dispersion numbers above $\mathbf{D}/\bar{v}L = 0.01$ other models should be applied to calculate the exit age distribution. For the diffusion coefficient $D_{AB} = 1 \cdot 10^{-11}\ m^2/s$, the steady state calculation can therefore only be used as a guidance.

Table 5.4 – Required time to reach steady state (ss) dependent on diffusion coefficient. Calculations were done with v=0.023 m/s, L= 7 m, beta = 48 and ID=200 µM

Diffusion coefficient $D_{AB}\ [m^2/s]$	Dispersion number $D/\bar{v}L$	95% ss	99% ss	Region defined above
$1 \cdot 10^{-9}$	0.0006	1.06θ	1.09θ	"plug-flow"
$1 \cdot 10^{-10}$	0.0066	1.22θ	1.32θ	Small deviations from plug flow
$4.5 \cdot 10^{-11}$	0.015	1.36θ	1.52θ	Large deviations – mixed flow
$1 \cdot 10^{-11}$	0.066	2.00θ	2.47θ	Dispersed flow.

In the cases where the dispersion number is high more complex numerical models, i.e. computational fluid dynamics (CFD) solving the Navier-Stokes equations, are required to describe the dispersion in the system. As an example, such CFD calculations were done for a specific cylindrical tube with the characteristic dimensions of 1 mm Inner diameter and a length of 10 cm. Various diffusion coefficients were applied and the flow rate was fixed to 21 µL/min. The given flow rate was specified as that flow rate was applied for some experimental investigations, which are not included in this thesis. The commercial software ANSYS CFX 14.0 was applied to solve this problem, and the results are shown in Figure 5.7. Additionally, the

analytical solutions are compared with the step responses of an ideal continuous stirred tank reactor (CSTR) and a plug-flow reactor (PFR).

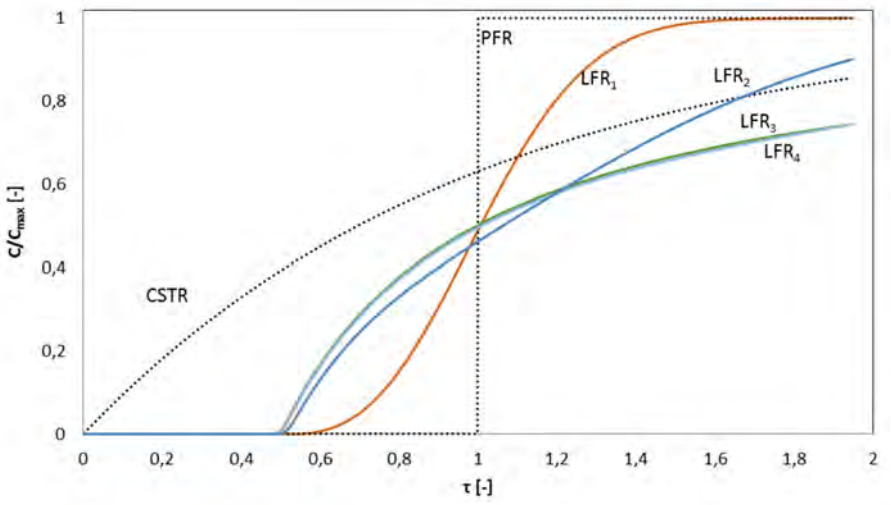

Figure 5.7 – Mapping of compounds with different diffusion velocities, i.e. D_{ab} = 1·10^{-9} m^2/s (orange), D_{ab} = 1·10^{-10} m^2/s (blue), D_{ab} = 1·10^{-11} m^2/s (light blue) and D_{ab} = 1·10^{-12} m^2/s (green), based on CFD simulations. The curves for the two latter diffusion coefficients are very similar to one another in the simulated time interval. The length of the simulated tube is in this case 10 cm, and the tube has a diameter of 1 mm. The initial concentration was set to 1 kg/m^3 and the mass flow rate was specified to be 3.5·10^{-7} kg/s. Nomenclature: PFR - plug flow reactor, CSTR - continuous stirred tank reactor, LFR - laminar flow reactor

Regarding the similarities of the dispersion profiles for slowly diffusing solutes presented in the figure, $D_{AB} \geq 1 \cdot 10^{-11} \frac{\mathrm{m}^2}{\mathrm{s}}$, it is obviously difficult to distinguish between them in the given modelling framework. However, it should be possible to distinguish between them. This can be done by extending the RTD experimental time which will cause the difference in the profiles to become more prominent as $time \rightarrow \infty$. Based on the performed experiments the dispersion numbers were also calculated, and the values are presented in Table 5.5. It can be seen that the numbers are all significantly higher than the boundary specified by Levenspiel[180].

Table 5.5 – Diffusion coefficients, dispersion coefficients and dispersion intensity of the simulation examples in Figure 5.7.

$\mathbf{D_{AB}}$	$\boldsymbol{D}$	$\frac{\boldsymbol{D}}{\boldsymbol{vL}}$
10^{-9}	$1.04 \cdot 10^{-6}$	0.023
10^{-10}	$1.03 \cdot 10^{-5}$	0.232
10^{-11}	$1.03 \cdot 10^{-4}$	2.323
10^{-12}	$1.03 \cdot 10^{-3}$	23.210

5.2.3 Capillary, Eötvös (Bond) and Weber numbers (for two-phase flow)

Another application in microfluidics is to operate with immiscible fluids, e.g. gas-liquid or liquid-liquid. This type of application is beneficial for the development of separation processes and/or biocatalytic processes where it is required to feed and/or remove various compounds

during the reaction course. The interfacial behavior in this type of application can be described through a different set of dimensionless numbers [181,182]. Two of the numbers are the Eötvös number (also known as the Bond number) and the Weber number.

The Eötvös number represents the ratio of gravitational forces relative to surface tension forces. It is described by Eqn. 5.11.

$$Eo = \frac{\Delta\rho g d_H^2}{\sigma} \qquad \text{Eqn. 5.11}$$

, where $\Delta\rho$ $[kg/m^3]$ is the density difference between two immiscible fluids and σ $[N/m]$ is the surface tension.

The Weber number represents the ratio of the fluids inertia relative to its surface tension. It is described by Eqn. 5.12.

$$We = \frac{\rho\mu^2 d_H}{\sigma} \qquad \text{Eqn. 5.12}$$

However, the Weber number is usually not the most important dimensionless number for microfluidic applications, i.e. the Reynolds number is small for such applications which means that the inertial effects can be neglected. Furthermore, the Eötvös number is only essential when operating with two immiscible fluids with significant density differences, like gas-liquid systems [183,184]. Besides these two numbers, which are not used for microfluidic liquid-liquid applications, there is a third dimensionless number that is commonly applied. This is the Capillary number which describes the ratio of viscous forces, shear stresses, relative to surface tension forces [184]. The Capillary number is defined by Eqn. 5.13.

$$Ca = \frac{viscous\ force}{surface\ tension\ force} = \frac{\mu v}{\sigma} \qquad \text{Eqn. 5.13}$$

The Capillary number is an important parameter for understanding the droplet formation, size and shape in microsystems [185]. Dependent on the magnitude of the Capillary number it is possible to predict different droplet formation regimes, i.e. squeezing, dripping and jetting [186,187]. The different droplet formation regimes are illustrated in Figure 5.8. At low Capillary numbers, e.g. $Ca \leq 0.01$, the system operates in the squeezing regime, which causes the formation of slug-like droplets [183,184,186], as shown as (a) Figure 5.8**Error! Reference source not found.**. Larger Capillary numbers, e.g. $Ca \geq 0.02$, cause formation of dripping droplets, which have a significantly lower droplet volume than the slugs [183,184,186], as shown as (b) of Figure 5.8. As the Capillary number increases in the dripping regime, the behavior of the system moves towards the jet regime. Here the detachment in the dripping regime gradually moves further down the channel. This trend is then further amplified with increasing Capillary number and increasing ratio of the continuous flow phase relative to the droplet phase ratio, as shown as (c) of Figure 5.8.

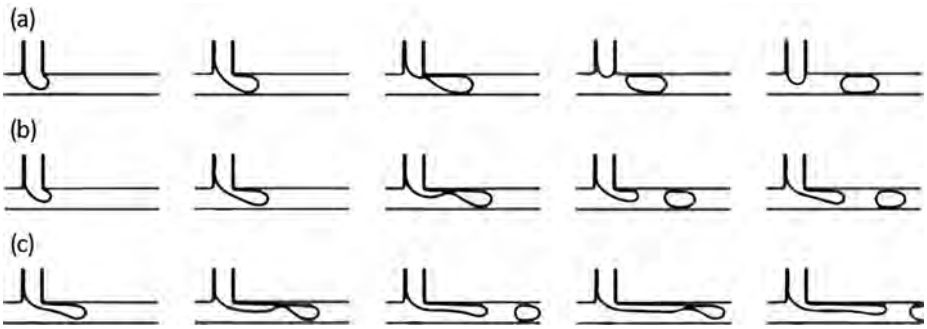

Figure 5.8 – Squeezing (a), dripping (b) and jetting (c) based droplet formation mechanisms.

Dependent on the channel dimensions, flow rates, surface tensions etc. it is possible to achieve different types of multi-phase flow patterns in the channels [188]. In addition, modifying the wetting properties of the wall surfaces will enable to operate with fluid streams in co- or counter side-by-side flow [189]. Maintaining this type of flow is dependent on stabilizing the pressure gradient between the two phases by the Laplace pressure at the interface [168]. These different types of flow are sketched in Figure 5.9[188,190]. The shape of the liquid-liquid interphase is dependent on the interfacial tension between the two phases.

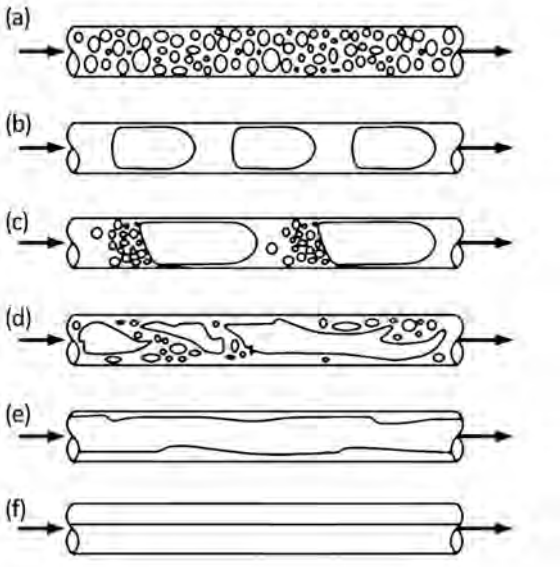

Figure 5.9 – Overview of different multi-phase flow scenarios: (a) bubble flow, (b) slug flow, (c) transitional slug/churn flow, (d) churn flow, (e) annular flow, (f) side-by-side flow.

Table 5.6 - Overview of important dimensionless numbers and their ranges for various applications.

	Re	Bo	Ca	Application	Comments
Plug flow	>3000	N/A	N/A	Production	
Laminar flow	<1500	<10	N/A	Transport of homogenous solution	Well-defined flow regime and easy to simulate through CFD.
Low dispersed flow	<10	>100	N/A	Determine kinetics	Laminar flow regime where concentration profiles appear similar to plug flow profiles.
Slug flow (sweeping)	N/A	N/A	≤ 0.01	Study of LLE, GLE, ISSS, ISPR, individual batch reactors	Formation of slugs is greatly dominated by the inlet diameter and the diameter of the operating channel – for microfluidic channels it is common to talk about slugs/droplets for this range of capillaries
Side-by-side flow	N/A	N/A	N/A	Study of LLE, ISSS, ISPR	Note: Requires that the pressure gradient is stabilized between the two phases by the Laplace pressure and/or by modifying the channel hydrophobicity.
Droplet flow (dripping)	N/A	N/A	≥ 0.02	Study of LLE, GLE, ISSS, ISPR	Similar to slug flow.

In Table 5.6, an overview is given of the different dimensionless numbers, along with ranges that are of interest for different applications. The different highlighted applications of interest in relation to the development and application of biocatalytic processes are:

- **Plug-flow:** Plug-flow mixing characteristics are commonly experienced at large scale (larger hydraulic diameters and flow rates) and thereby such flow dynamics are relevant for production purposes. The required dimensions and flow rates to achieve plug flow dynamics make this flow regime unsuited for development purposes, as it would be too costly.
- **Laminar flow:** For development purposes, it is common to operate with laminar flow dynamics, due to the small scale and flow rates. This gives however some challenges for scale-up as the flow dynamics change with increasing scale. Transport of homogenous solutions and steady state measurements are here the direct application. However, the study of dynamic responses with such a flow profile is either relative to the system, or should be corrected by residence time distributions. Nonetheless, it is here possible to quickly assess the dynamics of various flows and operating conditions on the biocatalyst performance and/or separation. The comparison of similar systems with different units can thereby still be quite useful for process optimization.
- **Low dispersed flow:** The application of this regime is for simulating plug-flow dynamics of a system, and as the plug-flow reactor has an identical behaviour as a batch reactor, it is here possible to determine kinetics in flow.
- **Slug, side-by-side and droplet flow:** These microfluidic flow applications are useful for testing and optimizing separation based processes, such as liquid-liquid extraction, gas-liquid extraction, in-situ substrate supply (ISSS) and in-situ product removal (ISPR). Furthermore, droplet and slug flow can also be operated as single reactors making it possible to perform high-throughput reaction screening and characterization. A limitation to side-by-side flow is that its application is restricted to small scale

applications and that its main purpose is to gain knowledge about mass transfer between phases. It is also dependent on phase separation at the end of the module. The advantage of slug flow over droplet flow is the possibility to apply optical analytical methods to follow the progress in the slugs, which is significantly more difficult with freely flowing droplets. For development of extraction methods, droplet and/or slug flow applications are more appropriate than side-by-side flow. This is because the high throughput characterization of such applications is easily adaptable to a broad range of different operating conditions.

5.3 Pressure drop

When designing a specific microfluidic module it is important to consider the limitations of the pumps available to operate the specific system, i.e. not all pumps can operate at high pressure. It is therefore important to evaluate the pressure drop in each module and in combined modules. The Hagen-Poiseulle equation, Eqn. 5.14, describes pressure drop in laminar flow with incompressible and Newtonian fluids, where the length of the channel is much greater than the diameter [161].

$$\Delta P = \frac{128 \eta L q}{\pi d_H^4} \qquad \text{Eqn. 5.14}$$

, where $\Delta P\ [Pa]$ is the pressure drop across length L $[m]$ of the channel diameter, for a flow $q\ [m^3/s]$ of a fluid with viscosity $\eta\ [Pa \cdot s]$. As the hydraulic diameter ($d_H\ [m]$) decreases, the pressure needed to achieve the same flow increases dramatically. In Figure 5.10, the influence of flow rates and channel diameters on the pressure drop can be seen for various tube lengths, assuming a maximum allowable pressure drop of 3 bar, which was indeed the pressure limit of the pumps utilized in this project.

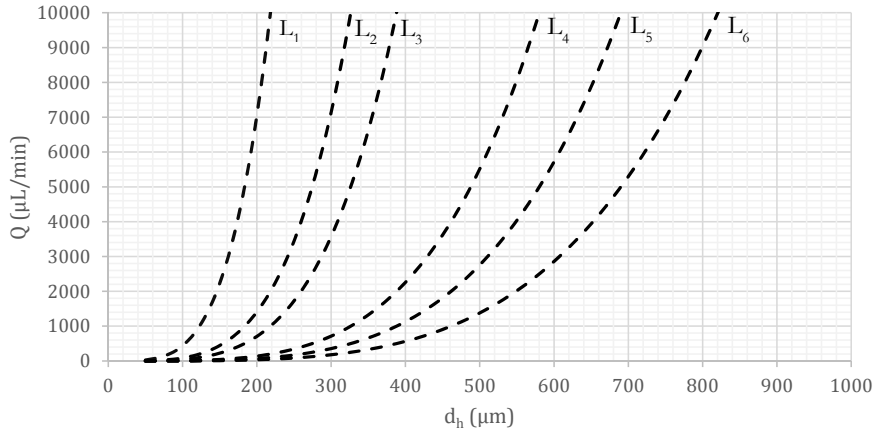

Figure 5.10 – Representation of a 3 bar pressure drop in microfluidic modules with changing flow rates and diameter at various tube lengths, i.e. L_1=0.1 m, L_2=0.5 m, L_3=1 m, L_4=5 m, L_5=10 m and L_6=20 m. Everything to the left of the curves corresponds to regions where the pressure drop is higher than 3 bar.

For modules with porous domains, e.g. packed bed reactors, one can apply Erguns equation to describe the pressure drop [191]. Erguns equation is defined as Eqn. 5.15.

$$\Delta P = 1.75 \frac{v_0^2 \rho L(1-\varepsilon)}{\varepsilon^3 d_p} + 150 \frac{v_0 \eta L(1-\varepsilon)^2}{\varepsilon^3 d_p^2} \qquad \text{Eqn. 5.15}$$

, where $\varepsilon\ [-]$ is the particle porosity, $v_0\ [m/s]$ is the fluid velocity based on an empty channel, and $d_P\ [m]$ is the diameter of the spherical particles. However, in many cases it might be difficult to get an exact prediction of the pressure drop in porous domains. For example, there can be many variations in packing densities, whereas particles come in a range of sizes and shapes, and are rarely completely spherical[192].

5.4 Microfluidic reactor and separation modules

The development of biocatalytic processes is greatly dominated by lab scale batch process based technologies. Liquid handling at lab scale for batch type experiments requires manual handling. This type of liquid handling is directly related to the amount of labor required to run an experiment. Furthermore, conducting reaction and separation sequentially in different containers requires that people are available to conduct the transfer of liquid. It is clear that this form of experimentation is laborious and requires relatively large volumes for every cycle. The alternative is to conduct microfluidic experiments in a continuous fashion by connecting reactors with separation directly and by handling the liquids by pumps. The labor requirement for constructing such a setup is of course much larger compared to the sequential “batch” lab scale. Therefore, such an effort should only be done when more than a couple of experiments are required. Flow chemistry has evolved a lot in the recent years, and has moved into microscale and microfluidics, where many unit operations have been translated to this scale. It is possible to mix[193], introduce an extraction phase, phase separate[194], distil[195], adsorb/absorb[181] and implement optical analytical methods. The available microfluidic modules enable the testing of various unit operations in combination (plug-and-play combination of the microfluidic modules). An advantage of this type of testing is that it will be possible to test complex biocatalytic process options, where reactor modules and separation modules are integrated to some extent. In order to really understand the simplicity of combining units at this scale, different unit operations relevant for biocatalytic processes have been sketched and can be seen in Figure 5.11.

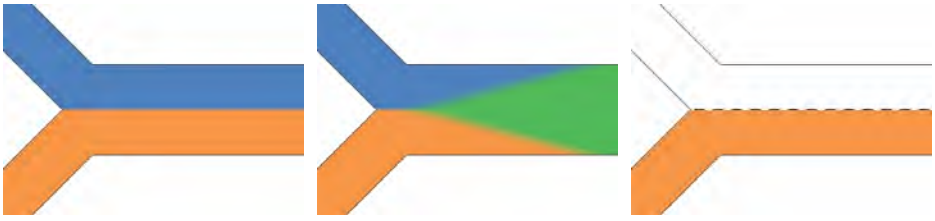

Side-by-side flow | Mixing | Membrane separation

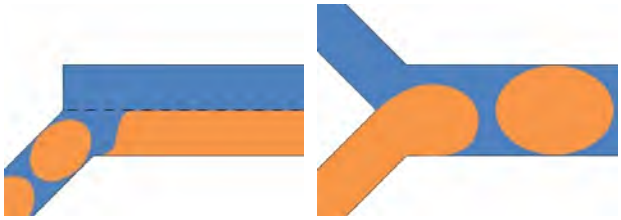

Liquid-liquid separator Droplet flow

Figure 5.11 – Different unit operations at µ-scale.

The sketched unit operations can be combined rather easily with a simple interface consisting of tubing and fittings. The realization that this is possible makes the hurdle of continuous setup construction less time consuming. To illustrate this, a PI diagram (Figure 5.11) describing a generalized process flow for synthesis of chiral amines catalyzed by aminotransferases (ATAs) [196] has been translated to microscale unit operations (MUO's), as shown in Figure 5.13.

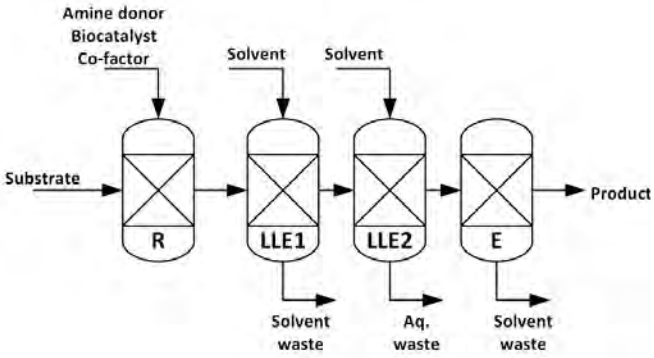

Figure 5.12 – Generalized aminotransferase (ATA) process flow chart for synthesis and recovery of chiral amines. The generalized scheme consists of a reactor (R), two liquid-liquid extraction steps (LLE1 and LLE2) and an evaporation step (E).

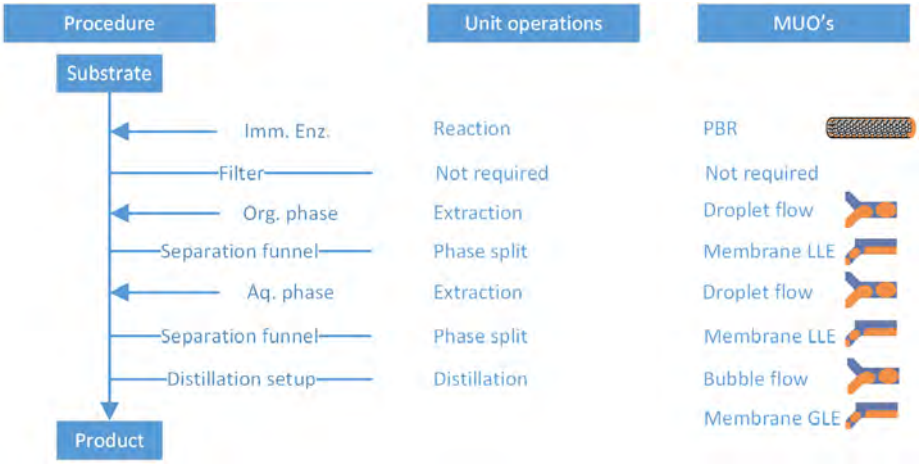

Figure 5.13 – Translation from standard sequential batch processing to continuous microscale unit operations.

The concept of modularity is not new, and creating a framework for such modularization has been attempted a number of time [197–199]. Projects defined with the specific objective of developing generic approaches to somewhat different operating regimes compared to the one investigated in this thesis are summarized in the list below. However, applications of such modules in a plug-and-play manner for biocatalytic applications has to date only been attempted a few times [167].

The European project BIOINTENSE intended to design units with fixed dimensions to fit all purposes for biocatalytic applications, and an obviously clear result is that this is impossible. In order to navigate the space of microfluidics, as outlined in this chapter, one should be able to manipulate the characteristic dimension, length and flow rate of the modules. Commercialization of the technology for flow chemistry, which can be adopted to biocatalytic applications, is becoming more widespread and platforms are available such as the Lonza flow plate [200], the Syrris system [201], Fluidgent [202] or Chemtrix [203]. The increasing number of industrial producers of such systems can be considered as a direct proof of the commercial importance of this research, and can be extended to how relevant this work is to the wider world. Along with the history of other international projects, this indicates that this type of work is a relatively high priority in industry.

5.5 Materials and fabrication

It is from a qualitative point of view nice to work with systems that are easy to manufacture, and from a quantitative point of view systems characterized by complete inertness are important. Polymers are relatively easy to manipulate, and 3D printing lightens the burden of constructing a microscale reactor even further[204]. It is within such a flexible design space that rapid investigations of geometry can take place. Several trade-offs can be observed in Table 5.7. Glass is the preferred material for inert reactor construction, and can be made at microscale to have a high pressure rating and fair heat transfer capacity as well. Unfortunately, glass has a rather rough surface and adsorption is therefore unavoidable when working with proteins. It is possible to work around this by using poly-ethylene glycol, or by working with an enzyme concentration that is high enough to make monolayer surface coverage insignificant. A semi-quantitative comparison of different materials is given in Table 5.7.

Table 5.7 – Comparison of materials for construction of microreactors

	Chemical Resistance	**Transparency for optical measurements**	**Heat transfer**	**Prototype cost**	**Mass produced device cost**
Polymers (PDMA, PMMA)	Very Low	Good	Poor	Low	High
Hard Polymers (COP, COPF)	Low	Good	Medium	Medium	Low
Glass (SiO_2)	High	Very good	Good	High	Medium
Quartz (SiO_4)	High	Excellent	Good	Very high	Medium - High
Metal (steel)	High	N/A	Very good	Medium	Medium
Silicon	High	N/A	Good	Very high	Medium
Tubing (PTFE, Glass capillary)	High	PTFE is IR transparent, but pathlength is small	Good	Low-medium	Low

Based on the experience gained from working with microfluidics it has become clear that when experimental methods are established and experiments are to be reproduced hundreds of times it is suggested to apply microfluidic chip designs. This is exactly what Lab-on-a-chip has been about, i.e. scaling down analysis with a fixed method. When the method is being developed and while working with complex fluid dynamics (precise droplet flow, side by side flow) or extremely small volumes it is suggested to use 'standard' options from chip manufacturers. In general, for research purposes, it is desired to be as flexible as possible and unless it is required to have optical readout it is suggested to do experiments in tubing. In the latter approach, changing the length of the reactor is as simple as cutting a new piece of tubing.

A decision roadmap for when to use which technique or tool has previously been described, but this was in relation to organic chemistry where fast reactions and high temperatures and pressures are present[205,206]. The following paragraph will focus on describing where experiments should be conducted in relation to the specific goals of a project. Three different goals can be distinguished to categorize the different efforts which are carried out in the course of biocatalytic process development, namely discovery, development/optimization and production. For biocatalyst discovery, testing is usually conducted as end point measurements and for that reason the use of containers in parallel provides an easy accessible platform. In the biocatalyst development and optimization phase, it is very important to have proper control of the experimental conditions. Microfluidics as described in this chapter, displays these qualities along with small resource consumption. Well plates also have small resource consumption but applies same conditions to all experiments in one plate. Thus allowing less control over the individual reaction, this is however great for testing many different solution compositions. Microfluidic and well plate methods require automation for efficient and precise handling of the small volumes. In such an automated set-up, samples are directly drawn from the reactors, be it wells or channels, and injected into the analysis system. Without this automated handling and analysis ability one should probably stick to working on a slightly larger scale, such as small vials (4 mL) in thermoshakers. For production is it obvious that the smaller type equipment will have problems handling very large scale. With microfluidics, one of the major advantages is that one can set up systems in parallel, and numbering up can in this way generate a considerable throughput. The main elements of the discussion in this last paragraph have been summarized in Table 5.8.

Table 5.8 – Considerations on when to use microfluidic technology

Goals	Labscale batch >1 mL	Well plates <400 µL	Labscale continous >1mL	Microfluidic <1 mL
Discovery	Good	Good	Poor	Poor
Development and optimization	Fair	Good	Poor - Fair	Good +
Production	Fair	Poor	Good	Bad-fair

6 DESIGN OF EXPERIMENTAL SETUP

At the process phase (3) described in the scope of this thesis, it is expected that up to 10 enzymatic mutants would require kinetic characterisation. A tool for conducting this investigation must therefore be automatic. From chapter 3 it was found that a technology for the collection of kinetic data would be suitable when it could be used to determine initial rates at low conversion reliably. Additionally, it would be preferable if it could conduct high conversion experiments as well. The different technologies were reviewed in chapter 4 and UV/VIS spectroscopy coupled with chemometrics was here identified as a solution. From chapter 3 it was also found that over 55 experiments would be needed in order to have a robust dataset for fitting. Experiments should therefore be conducted at microscale to conserve scarce materials. The different physical effects of this small scale were investigated in chapter 5. Here it was found that low disperse flow provides an excellent opportunity for collection of kinetic data, since the application of this regime introduces plug-flow dynamics. Plug-flow reactors have identical behaviour to that of a batch reactors and it will therefore be possible to use concentration residence time data, without modification, for the calculation of rate. In this chapter the above information is utilized as a foundation from which a setup is designed and constructed.

6.1 Mode of operation

As stated in the Microfluidics chapter, operating in plug flow like region is highly desirable for investigation of kinetics in flow. Moore and Jensen[33] has recently published a method to exploit this operational region. This manipulation is only possible since the concentration profile of batch reactors with respect to time is identical to that of plug flow with respect to residence time. The batch reactor is, as described, often considered to be superior at collecting kinetic data, by being able to sample from the same reactor at different time points[119]. This ability has now be replicated for μ-scale flow reactors and must influence the choice of reactor

for the collection of kinetic data of homogenous mixtures. The method is briefly presented and will also be applied in this thesis.

The system is set to operate in a steady state, and a small residence time has therefore been selected to rapidly reach steady state. The flow rate will hereafter be decreased linearly and the systems instantaneous residence time will be know from Eqn. 6.1.

$$\tau_{ins} = \tau_0 + \alpha t = \frac{V_r}{q(t)} \qquad \text{Eqn. 6.1}$$

Each fluid element exiting the reactor will therefore have a unique residence time. This can be calculated from the time it exits the reactor, t_f, substrated by the time it enters, t_i, see Eqn. 6.2.

$$\tau = t_f - t_i \qquad \text{Eqn. 6.2}$$

In order to relate the inlet time to the exit time, the instantaneous flow rate is integrated over the fluid elements residence time, then isolated and substituted in Eqn. 6.2, the final relation can be seen in Eqn. 6.3. The full derivation can be found in supporting information of Moore and Jensens article[207].

$$\tau = t_f - t_i = \frac{S}{\alpha}\tau_0 + St_f \qquad \text{Eqn. 6.3}$$

Where S is the slope of τ versus t_f and given by Eqn. 6.4.

$$S = (1 - e^{-\alpha}) \qquad \text{Eqn. 6.4}$$

By adjusting α it is possible to set S and thereby choose the slope with which the flow rate is changing. Effectively this means that it is possible to control the space-time difference between samples (e.g. If the ramp is set to half the real time one could measure every space-time minute with a 2 minute analysis).

6.2 Setup

The sensitivity required can only be obtained spectrophotometrically with either UV/VIS or fluorescence spectroscopy. Many more chromophores exist compared to fluorophores and the applicability of UV/VIS is therefore wider when compared to fluorescence. Furthermore, fluorescence is usually detected on a single compound, whereas if a substrate is absorbing in the UV/VIS range, it is likely that its product will as well, these can then be detected at the same time if they can be separated, either physically or mathematically. The setup is developed to detect reactions in the 0.1 mM range, aromatic substrates commonly have a molar absorption coefficient in the range of 100-1000 $L\,mol^{-1}cm^{-1}$ and will hence have maximum allowed concentrations in the range of 1-10 mM. In order to increase this range a dilutions is required to avoid saturation. With the aim of having in-line measurements, the outlet stream of the reactor is diluted with a carrier phase. After investigation of this setup, it was realised that the enzyme covered the unique features of the substrate and products spectra, making curve resolution impossible. Many attempts were hereafter made to remove the enzyme from the outlet stream, with membranes and filters, and a solution was found

with a guard size exclusion column. After connecting the column to the setup it was discovered that the small molecules also partly separated. The size exclusion column did however introduce back pressures of 8 bar and above, which is much higher than the specified maximum for the syrringe pumps, namely 3.5 bar. A flow injection analysis approach was therefore taken, and an 8-port injection valve was integrated with the system. The problem of backpressure was thereby removed as the valve splits the system in two, an analysis part and a reactor part. An 8-port valve was chosen over a 6-port valve as it offers a configuration with two sample loops, the outlet of the reactor is hereby always connected to a sample loop. This is important since with high residence times, the inlet will have very low flow rates. The small outlet stream is therefore used optimally and is never just waste. The final setup is presented in Figure 6.1 and Figure 6.2.

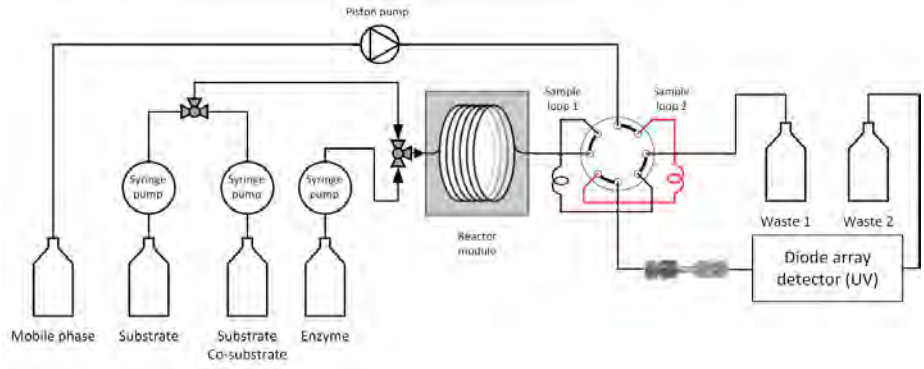

Figure 6.1 – Schematics of the experimental setup

Black lines in Figure 6.1 indicates tubing, PTFE 1/16'' O.D. and 170 µm I.D, except for the PTFE tubing connected to the pumps where liquid is drawn through, here 1/16'' O.D., 500 µm I.D was used. The reactor module consist of 710 cm PTFE 1/16'' O.D. and 170 µm I.D tubing submerged into a water bath. The other instruments used are listed in Table 6.1. The size exclusion column used was a Phenomenex BioSep-Sec-2000 30x4.5mm. 3 syrringe pumps were integrated with the system, and made it possible to combine two stock solutions to vary one concentration while keeping the other constant.

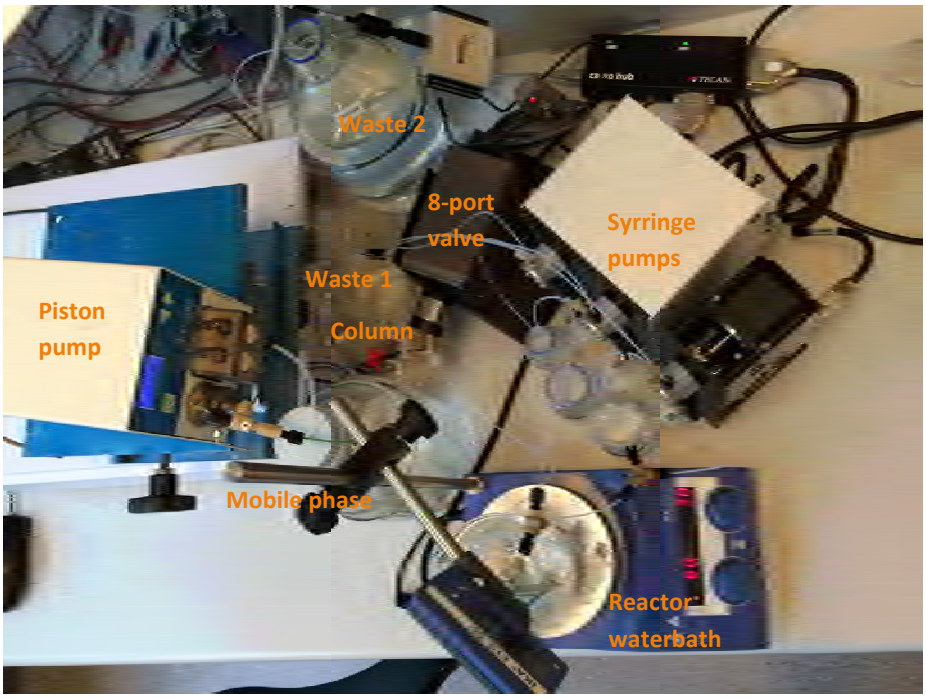

Figure 6.2 – Picture of experimental setup

6.3 Control of the setup

HPLC's are operating with microscale phenomena and detectors developed for this type of analytical setup is therefore also ideal here. The precision of UV/VIS detectors is readily 0.1 mAU and can reach sampling speeds of 200 Hz. The only problem in the utilization of these detectors are that they are linked to specific software. Timing of the system is essential and it was therefore a necessity to have an integrated control over all the components of the system. This could be obtained with LabVIEW, which is short for Laboratory Virtual Instrument Engineering and is a development environment for a visual programming language by National Instruments. In short, it is a program in which it is possible to combine the control of many different instruments and hereby create a single virtual one. Many companies sees the strength of this and delivers LabVIEW drivers for their instruments alongside the hardware. In this thesis the program has been used to combine the items of Table 6.1

Table 6.1 – instruments of experimental setup

Type of instrument	Model	Communication	Driver
1 UV detector	Agilent G1315AR	Ethernet	AG1100
3 Syringe pumps	Tecan Cavro XLP6000	USB-Serial	Constructed in this work
1 HPLC pump	Knauer smartline 100	USB-Serial	Constructed in this work
1 Injection 8-port valve	VICI E45-230 - CR2 head	NI USB-6008	Constructed in this work

6.3.1 Automation

The system was automated to follow a setpoint sequence for the pumps, this will be described later in the experimental methods section. In order to reach this automation it was required to

develop controls of the individual parts. These parts were hereafter integrated in a master virtual instrument. The entirety of the LabVIEW scripts developed is too complex and too large to be shown on paper, however the front panel and the block diagram of the final virtual instrument is displayed in Appendix D. A link is also provided granting access to all the developed virtual instruments.

6.3.2 UV detector

The driver AG1100 was obtained from National Instruments driver network[208], a new framework for the existing virtual instruments were created. Following protocol for connectivity was applied:

1. Open connection to instrument
2. Set parameters such as slit width (2nm), stepwidth (1 nm) , fixed wavelength 1 (240 nm), fixed wavelength 2 (260 nm), collection frequency (2.5 Hz), spectra acquisition mode (All)
3. Balance detector (baseline adjustment)
4. Start analysis
5. Parse recorded signals / transfer recorded signals
6. Stop analysis
7. Collect spectral data
8. Close connection

Unknown errors forces the driver to stop the VI and it was required to reset the detector in a separate software, Agilent Lab Advisor, which was purchased from Agilent alongside the detector. Critical errors were reduced to a minimum at the end of the project, but did still occur, further development could remove this entirely.

6.3.3 Syringe pumps

TECAN provides text commands in their manual for the XLP 6000 OEM pumps. A virtual instrument was therefore constructed based on these commands. The controls of the syringe pumps involve:

- Slow priming
- Bypass initialization and stopping
- Continuous flow in the form of drawing liquid fast and delivering at a target flow rate.
- Ramp mode on top of continuous operation

6.3.4 HPLC pump

Commands for the pump where obtained through a KNAUER driver from the NI driver network. These commands could then be used to construct a virtual instrument for this device. The instrument were able to monitor delivered pressure over time, which is a good measure to see what the status of the column is. Chromatographic columns can collapse when too much force is applied instantly. It is therefore required to slowly ramp the flowrate to reach operating conditions. This was therefore added to the control of the HPLC pump.

6.3.5 Injection port valve

The injection port valve has 2 positions, A and B. The drive motor switches between these by a 5 volt on-off signal, control of this could be obtained by coupling the valve with a NI USB-6008, which is a data acquisition device that has an analog output of 5 volts. The virtual instrument was set to induce a change immediately after the UV/VIS instrument started analysis.

6.4 Description of the different parts of the setup

Here each part of the instrument vital for the operation of the setup is presented and issues are considered.

6.4.1 UV Detector

The Agilent G1315A is equipped with a 13 µL flow cell that has a 10 mm path length. It is capable of measuring full spectra in the range of 190-950 nm with 20 Hz. However, the instrument is an over 10 year's old model and the LabVIEW driver could not continuously extract the full spectra data. This made it necessary to stop collection and extract data between sample injections. The instrument could collect 202 full spectra before the memory buffer was full. To circumvent this, the collection rate was set to 2.5 Hz which enabled collection of 80.8 seconds of data. Within this time it was possible to turn the valve, inject the sample and completely elute it through the column.

6.4.2 Syringe pumps

The step motor of the XLP 6000 syringe pumps has 48000 steps and controls flow rate in steps per second. Different syringe sizes can therefore determine the range of flow rate, 50 µL syringes were used for the experimental work in this thesis. The ramp operation calculates flow rate setpoints as a function of time, these are translated into exact frequency numbers.

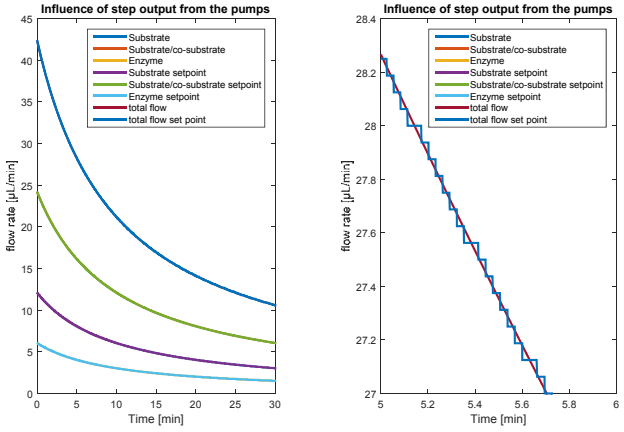

Figure 6.3 – Influence of step change, investigated with syringes 50 µL, the actual setpoint is covering the target in the left figure and an exploded view of the total flow and the total flow setpoint is presented on the right.

The syringe pump can however only read round frequency numbers and this will cause an error by letting the flow enter the reactor in a step change form, and this can be observed in

Figure 6.3. The maximum deviation from the setpoint is calculated to be 0.5 % and is neglected from this point forward.

6.4.3 Reactor

The ramp method relies on the low disperse flow assumption and this is questionable for the enzyme as discussed in chapter 5. The smallest I.D tubing of 170 µm was chosen to minimize dispersion and residence time experiments were carried out in order to assess the extent of such, see Figure 6.4, the experiments are described in the methods section later in this chapter. As predicted, Benzyl acetone has plug flow behaviour, and the enzyme deviates significantly from such behaviour. The enzyme is therefore the limiting factor for how quickly steady state can be reached. It is assumed that when the enzyme mass balance over the reactor is constant, that the concentration profile through the reactor will be as well. Step changes in small molecule concentrations can then be introduced without disturbing the enzyme concentration profile. The residence time distribution was used to calculate the reactor volume by the method described in Fogler[209]. Here the average volume was found to be 212 µL, this is within the tolerance of a 7.1 meter tube with 170 µm I.D ±50 µm. The I.D of the tube must therefore be on average 195 µm, this was calculated by isolating the diameter in the formula for a cylinders volume, $d_{\mathrm{H}} = 2\sqrt{V/L\pi}$.

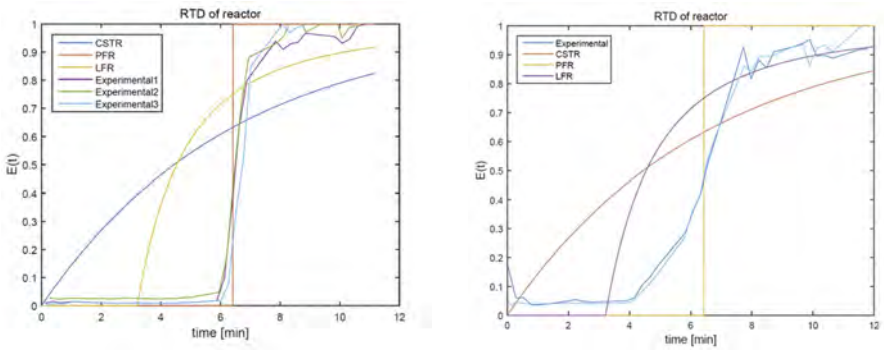

Figure 6.4 – Residence time experiments with Benzyl Acetone on the left and with the enzyme on the right.

6.4.4 Heat transfer

The steady state energy balance for a constant wall temperature reactor can be described by Eqn. 6.5 [174].

$$\dot{m}C_{p,m}\frac{dT_b}{dz} = U\pi D_0(T_0 - T_b) \qquad \text{Eqn. 6.5}$$

Where $\dot{m}$ is the mass flow rate, $C_{p,m}$ is the heat capacity based on mass and is assumed to be equal to that of water, T_b is the bulk temperature of the flowing liquid, T_0 is the wall temperature, D_0 is the inner diameter, U is a local heat transfer coefficient, here used for the transfer of water bath temperature over teflon tubing to flowing liquid. This can be described by Eqn. 6.6[174].

$$\frac{1}{D_0 U} = \left(\frac{1}{D_0 h_0} + \frac{\ln(D_1/D_0)}{2k_{tef}} + \frac{1}{D_1 h_0}\right) \qquad \text{Eqn. 6.6}$$

Where D_1 is outer diameter, h_0 is thermal conductivity of water, k_{tef} is thermal conductivity of teflon. Thermal conductivities are given in Table 6.2.

Table 6.2 – Thermal conductivity of different materials

Material	Thermal conductivity [W/(mK)]	Ref.
Stainless steel	16	[210]
Glass (SiO_2)	1	[210]
Water	0.6	[211]
Teflon	0.35	[212]

The temperature profile can now be calculated as a function of reactor length. The poor thermal conductivity of PTFE and a wall thickness of 700 µm, was thought to be a heat transfer problem. This is not the case, as the large surface area to volume ratio ensures that operational temperature is reached rapidly after entering the reactor, see Figure 6.5. The temperature is reached after 10 cm and with a total length of the reactor being 710 cm, the non-isothermal area represents a 1/71 of the reactor. It can therefore be concluded that the setup allows for a good control of the temperature.

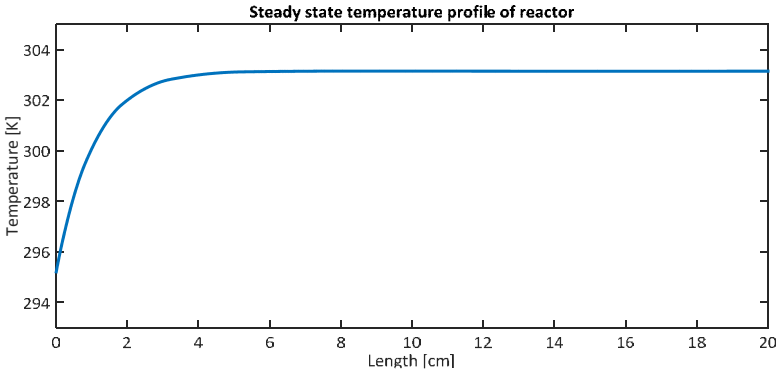

Figure 6.5 – Steady state temperature profile of the first 20 cm of the reactor.

6.5 Experimental materials and methods

In this section materials and methods are described.

6.5.1 Materials

Chemicals:

Following chemicals were bought from Merck KGaA: Benzylacetone (BA; synthesis grade; Cas no. 2550-26-7), Phosphoric acid (analytical grade, cas no. 7664-38-2), Dipotassium Phosphate (analytical grade, cas no. 7758-11-4), Monopotassium phosphate (analytical grade, cas no. 7778-77-0). Following chemicals were purchased from Sigma-Aldrich: 1-Methyl-3-phenylpropylamine (MPPA; 98%; Cas no. 22374-89-6). Pyridoxal 5'-phosphate monohydrate (PLP; ≥97.0%; Cas no. 41468-25-1). Acetone (ACE; ≥99.5%; Cas no. 67-64-1). Isopropylamine (IPA; ≥99.5%; Cas no.75-31-0).

Parts of the setup:

Tubing and fittings was acquired from Microlab Aarhus which supplies VICI, IDEX-HS and BOLA, the tubing was a combination from the three suppliers, and the fittings were from IDEX. The BioSep-Sec-2000 30x4.5mm was purchased from Phenomenex. The magnetic stirrer used for heating the water bath was a IKA RCT basic with a ETS-D5 that serves as both temperature probe and PID controller. The signal generator for the VICI injection valve was a National instruments USB-6008. Two 5 µL loops were purchased through mikrolab from VICI. The XLP6000 OEM syringe pumps were purchased from TECAN and power and connectivity was achieved through a Cavro hub, also from TECAN. The HPLC smartline 100 pump with a 10 mL/min ceramic pump head was purchased through from KNAUER.

6.5.2 Solutions

Substrate stock solutions were made by the following procedure. 40 mL 20 mM pH 8 phosphate buffer solution (PBS) was added to a 100 mL volumetric flask, the compound of interest was hereafter added by weight. The pH was readjusted to 8 and buffer was added until the indicator on the volumetric flask was reached. For IPA and MPPA solutions equimolar H_3PO_4 was added to the 40 mL buffer before the addition of amine, this forces the amine to be on ionic form and reduces evaporation.

The enzyme solution was made by weighing the enzyme in a porcelain weighing boat and hereafter transferring it to a 5-10 mL volumetric flask with 20 mM pH 8 PBS buffer. After solubilisation, the solution was filtered on a 25 mm 0.45µm syringe disk filter. Typical enzyme concentrations were 1-2 mg/mL

The Mobile phase was prepared in a 2 L volumetric flask by adding 200 mL PBS stock solution pH 3 or pH 7, 1 M made with 19.4 µS/cm water and hereafter filling the flask to its 2 L indicator with 19.4 µS/cm water.

6.5.3 Batch method

Batch experiments were carried out in 4.5 mL vials in duplicates, the vials where heated and shaken in a thermoshaker HLC Biotech MKR13. A substrate stock solution of 9 mM BA and 100 mM IPA was mixed 1:1 with 2 mg/mL enzyme solution. A zero point measurement was made by adding buffer in a 1:1 ratio with the substrate stock. Samples of 100 µL were drawn at times 0, 5, 10, 15, 30 and 60 minutes and diluted in 900 µL 0.05 M NaOH. The analytical method for these samples can be found in Appendix B.

6.5.4 Residence time destribution experiments

The setup was modified slightly for carrying out these experiments. Because only one component were introduced at a time, the column could be removed. The detector was set to collect single wavelenght measurements, and collection could be done for up to an hour without exceeding the capacity of the memory buffer. The HPLC pump was set to 0.600 mL/min and the syringe pumps were set to pump with 33 µL/min. Injections where carried out every 15 seconds and the time point of the valve turning was taken as the time of measurement. The Y-connector with tubing leading to the reactor was disconnected and primed with buffer in one stream and stock solution in the other. After priming, the Y-connector was reattached and the reactor was purged with buffer solution for 10 minutes. The

detector was started and upon 3rd injection the buffer pump was stopped and the stock solution pump started. Here a 10 mM BA stock solution and a 1 mg/mL Enz stock solution was used.

6.5.5 Steady state method

Only the reactor part of the setup is used here. The flow rate is adjusted to obtain residence times of 5, 10 and 20 minutes. A sample was taken by submerging the outlet tube into a 900 µL filled HPLC vial. At the time of submersion a dial was started on the computer to show the dispensed liquid of the pumps and the tubing was removed after 100 µL had been collected. The samples were hereafter analysed by the HPLC method attached as Appendix B.

6.5.6 Ramp method

A typical experiment started by turning on the lamps of the UV detector, and the flow rate of the HPLC pumps was set to ramp up from overnight flow of 0.100 mL/min to 0.600 mL/min. The water bath was turned on and set to 30 °C. Pumps were hereafter primed with the prepared stock solutions, visual inspection of the syringes could easily detect if there was any air in them. Air in the syringes was handled by removing the syringe from the pump and hereafter prime it manually. In order to conserve enzyme solution priming was done at 50 µL/min drawing in and pushing out, this was repeated for 15 minutes. After all equipment reports ok, the LabVIEW control sequence was initiated. The pumps were started to reach a steady state setpoint. As described in chapter 5, the enzyme is here the limiting factor and for the first setpoint, 4 residence times were used to ensure a steady state throughput of the enzyme. The following setpoints were set to use only 2 residence times to reach steady state. The system would then automatically collect data for the setpoint sequence. Sampling is carried out in such a way that the first sample is collected at the steady state and the ramp is hereafter initiated immediately. A sample could be taken roughly every two minutes. The time of the valve turning is taken as the sampling time. The difference in sampling time to initiation time can then be used to translate the recorded real time points into space time points. This is carried out via the method described in the supporting information of Moore and Jensen's article[207].

As an example consider the following setpoint sequence, here three stock solutions where made in 20 mM PBS buffer pH 8, solution 1) consisted of enzyme 2 mg/mL. Solution 2) consisted of 45 mM MPPA and 115 mM ACE and solution 3) consisted of 115 mM ACE. The concentration for the enzyme is held constant. Desired concentration of substrates were set by mixing x flow rate of solution 2 plus y flow rate of solution 3, see Table 6.3. The concentration of ACE was in this was kept constant while MPPA was varied.

Table 6.3 – Concentration and flow rate setpoints for the three pumps

	Solution 1	**Solution 2**		**Solution 3**	**Pump 1**	**Pump 2**	**Pump 3**	
#	E [mg/ml]	MPPA [mM]	ACE [mM]	ACE [mM]	[µL/min]	[µL/min]	[µL/min]	sum [µL/min]
1	0.25	40	100	0	5.3	37.1	0.0	42.4
2	0.25	34.29	85.71	14.29	5.3	31.8	5.3	42.4
3	0.25	28.57	71.43	28.57	5.3	26.5	10.6	42.4
4	0.25	22.86	57.14	42.86	5.3	21.2	15.9	42.4
5	0.25	17.14	42.86	57.14	5.3	15.9	21.2	42.4
6	0.25	11.43	28.57	71.43	5.3	10.6	26.5	42.4
7	0.25	5.71	14.29	85.71	5.3	5.3	31.8	42.4
8	0.25	2.50	6.25	93.75	5.3	2.3	34.8	42.4

6.5.7 Experimental plan for the kinetic characterization of an enzyme

A full overview over the experimental plan can be seen in Table 6.4, an assessment of the required time to conduct the investigation is also given. Here it can be seen that the data for an enzyme could be kinetically characterized within 3 work days. In comparison to batch experiments, it is assumed that a skilled labuser would be able to carry out 20-30x2 thermoshaker experiments in a workday. The experimental workload for carrying out a characterization is therefore expected to take 4 workdays. The preparation time for both methods is expected to be equally time demanding and is left out of the comparison. The method is therefore assessed to be able to characterize an enzyme faster and with much less manual labor compared to the traditional method.

Table 6.4 – Full experimental plan for the kinetic characterisation of amine transaminase, the total experiments suggested are summarized by initial rates x 2 and high conversion experiments x 2

Type of Labor	Type of experiment	description	number of samples	Time for analysis	accumulated time [min]
Semi-auto	Calibration of PARAFAC model	E, S, cS, P, cP	-	240	240
auto	Initial rates at different enzyme concentrations	[E] 1,2,3,4 g/L	4 x 2	4x4xτ_0 20minx8	480
manual	Change bottles			10 min	490
semi-auto	Initial rates at different pH	pH 5-9 in 1 increments	5 x 2	20minx10	690
auto	Initial rates at different T	30-50 °C in 5 °C increments	5 x 2	20minx10	890
manual	Change bottles			10 min	900
auto	Initial rates at different substrate concentrations	[S]: 1-10 mM in 6 steps [cS]: 100,300,500 mM	6 x 3 x 2	20minx36	1620
manual	Change bottles			10 min	1630
auto	Initial rates at different product concentrations	[P]: 1-40 mM in 8 steps [cP]: 50, 100, 500 mM	8 x 3 x 2	20minx48	2590
manual	Change bottles			10 min	2600
auto	Progress curves at different substrate/product concentrations	[S] optimum [cS] optimum [P] 0-5 mM [cP] -	**2x2**	120minx4	3080
	Total		103x2+**2x2**		51.3 h

6.5.8 Calibration

Calibration was done by having stock solutions of MPPA/ACE, BA, ACE and enzyme. A calibration would then be the following combination, MPPA/ACE and ACE, BA and ACE and ACE and enzyme. Everything could then be aligned according to acetone, explained later. In an 11 step 0-100% way the two solutions were used to dilute each other, see Table 6.5. This type was done to insure that interaction of the different compounds would be reflected in the calibration curve.

Table 6.5 – Step settings for a calibration curve

Step:	1	2	3	4	5	6	7	8	9	10	11
Sol. A.	100	90	80	70	60	50	40	30	20	10	0
Sol. B.	0	10	20	30	40	50	60	70	80	90	100

6.6 Chemometric data treatment

The aim of the chemometric data treatment is to transfer the retention time wave length data into sample quantity data. A standard sample can be seen in Figure 6.6.

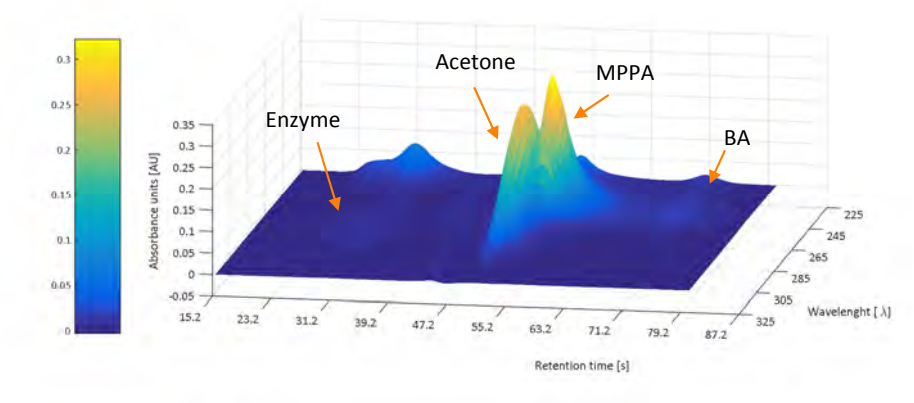

Figure 6.6 – Standard sample

As stated in the chemometric background section, strict alignment is required for the PARAFAC method. It is desired to align samples in either unique spectral regions or where complete baseline separation is available. For this system ACE and MPPA overlap in the retention time region, see the right part of Figure 6.7. At wavelength $\lambda = 285\ nm$ BA, ACE and ENZ overlap, see left part of Figure 6.7, but are baseline separated and alignment is therefore carried out here, see Figure 6.8. The shifts in retention time and relatively low collection rate, $2.5\ Hz$, was a problem in relation to alignment as it could result in a slight skew of peaks. In order to assist alignment, interpolation between each 0.4 sec spectral sample was introduced and this effectively doubled the sample points in the retention time direction. Alignment could then be carried out in a satisfactory fashion and the aligned data was hereafter resampled in order to bring the data back to a physical domain, effectively removing every second data point.

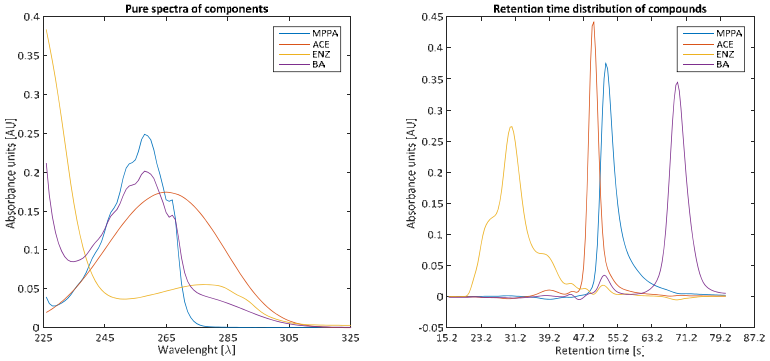

Figure 6.7 – Pure spectra and residence time distribution of the compounds

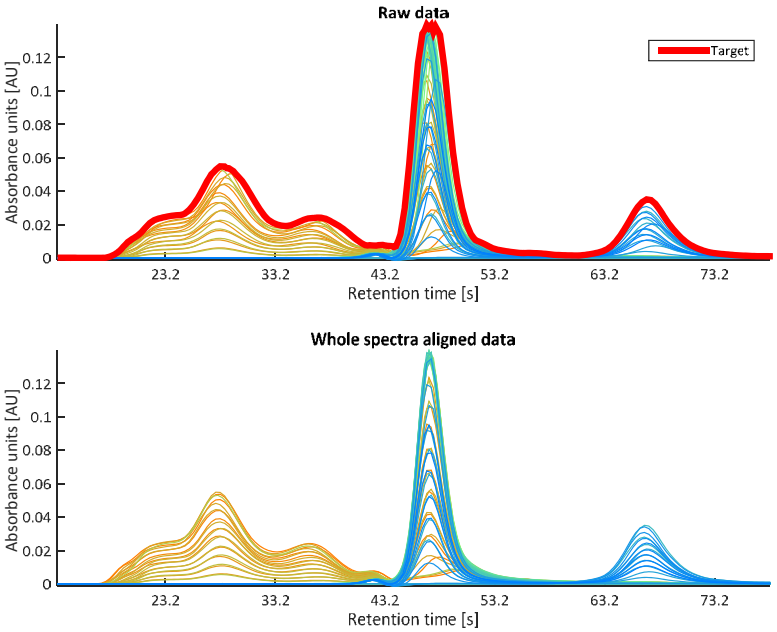

Figure 6.8 – Alignment of samples, here the max of λ = 285-460 nm in the spectral direction of each sample is shown

A PARAFAC model with 4 components could then be fitted. A quick tool for the evaluation of the models ability to describe tri-linearity in the data is the core consistency diagnostic, CONCORDIA, which evaluates the 'appropriateness' of the model[213]. For these data the CONCORDIA was 100, verifying that the data is indeed tri-linear. The scores of the model could then be calibrated with the concentrations of the stock solutions. The calibration curves obtained for this model can be seen in Figure 6.9. The matlab code for calibration can be found in appendix E.

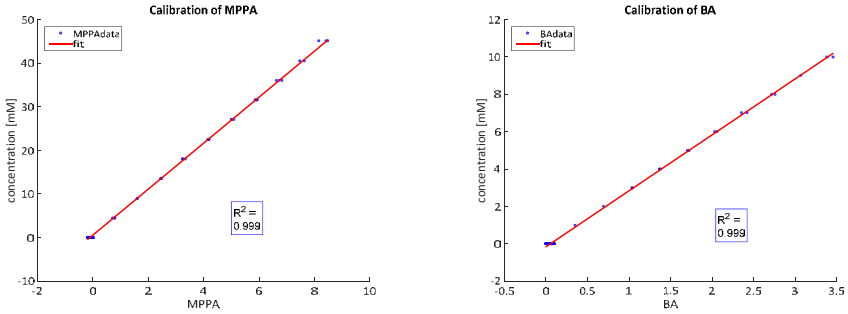

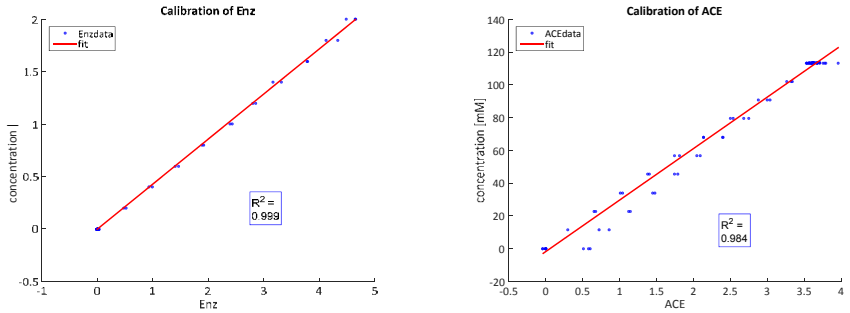

Figure 6.9 – Calibration curves of the different compounds

6.7 Error analysis

Sensitivity is a key element of the setup, and therefore an error analysis of the setup is therefore evaluated. The HPLC pump does have a small oscillation, this can be seen in the spectral data. It is difficult to quantify the effect of the pump alone. The combined error of pump and UV instrument is therefore assessed. The error is found by making a moving average of blank samples and calculating the standard deviation of this. Examples of blank spectra can be seen in Figure 6.10, it can be seen that there is a drift of 0.1 mAU over the 80 seconds retention time. The standard deviation from the moving average was averaged over 14 samples to be 0.015 mAU. The error caused by the pump and spectrophotometer is very small and signals of 1 mAU will therefore have a signal to noise ratio of 65. What cannot be detected is if the pump oscillations cause retention time shifts, elongating or narrowing the peaks.

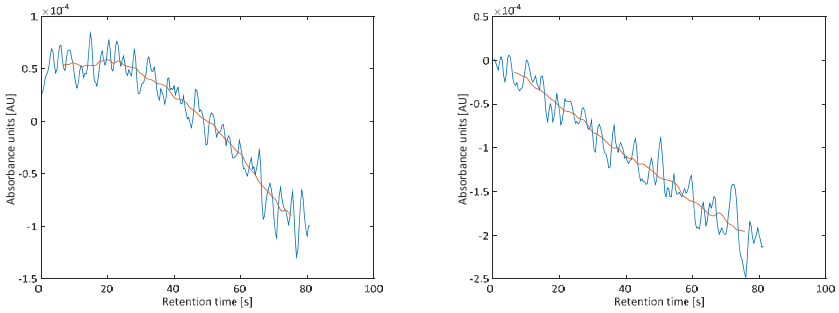

Figure 6.10 – Examples of blank spectra at λ = 210 nm, raw data – blue line and moving average – orange line.

The HPLC pump delivered printed values with a ± 1% deviation throughout all experiments. Syringe pumps delivered set values with a ± 0.1%. In calibration of compounds MPPA, BA, and ENZ, even absorbance differences between samples is seen in the spectral data of Figure 6.8. This data also shows very good linear correlation between scores and concentration, see Figure 6.9. Nonetheless, there seems to be two groupings in the acetone calibration, this is with and without enzyme. At 0 ACE the deviation is maximal, here the enzyme concentration is 2 mg/ml. There is a correlation between the ENZ and ACE however as enzyme concentration is set to 0.25 mg/ml the deviation should be minimal. At the zero and maximum values of the calibration curves there are some variance in the scores. The zero concentration variance are artefacts in the PARAFAC model which can be seen in Figure 6.7 to the right. BA, the purple

line, has a small peak in the MPPA due to their similarities. This could be removed by enforcing unimodality and this will also remove the enzymes influence on ACE and MPPA. It is nonetheless clear that the enzyme is absorbing at these retention times and it would be incorrect to zero this effect. Please compare the spectral data in Figure 6.8 with Figure 6.7 for reference. The repeated ACE measurement at 113 mM is the most uncertain, here the score is 3.6428 ± 0.0865, which corresponds to 112.8 ± 2.7 mM. It should be noted that the molar absorption coefficient for acetone is quite low at 15.4. Overall it can be concluded that the method is very accurate.

The time of the valve turning is taken as the sampling time, the liquid in the sample loop will therefore contain an average of τ_{t_f} and $\tau_{t_f - t_l}$ where t_l is the sample loop filling time, see Table 6.6. The uncertainty of the space time is a maximum of 1.2%, and is neglected in the calculations of initial rate.

Table 6.6 – Time it takes to fill the sample loop as a function of flowrate, α = 0.5, *S* = 0.393.

Time, t_f [min]	**0**	**5**	**10**	**15**	**20**
Space time [min]	5	5.9	7.9	9.8	11.8
Flowrate [µL/min]	42.40	28.30	21.20	16.96	14.13
Sample loop filling, t_l [min]	0.116	0.177	0.237	0.293	0.355
Maximum deviation in space time	Steady state	0.25%	1.2%	1.2%	1.2%

6.8 Cost of setup

Earlier it was suggested that the steep price of equipment will prevent it from wide application. It has therefore been a concern to keep the price of the total instrument low. The purchased Agilent detector is refurbished and a new model will naturally cost considerably more money. The LabVIEW driver has however only been developed for G1315A and B, and in order to use the developed software instrument, a new user would be forced to buy one of the two models, refurbished, as they are discontinued. The current setup's individual cost is displayed in Table 6.7.

Table 6.7 – Individual cost of the setups different elements.

Part of instrument	**Details**	**Cost [k€]**	**Total [k€]**
1 UV detector	Agilent G1315AR	4	4
4 Syringe pumps	Tecan Cavro XLP6000	1	3
1 HPLC pump	Knauer smartline 100	3.5	3.5
1 Injection 8-port valve	VICI E45-230 – CR2 head	2	2
Pre-column-filter holder	-	0.3	0.3
1 SEC column	SEC-BioSep-2000	0.5	0.500
Matlab licence	2015a	2.	(2)
PARAFAC and iCoShift scripts	Department of food science, University of Copenhagen	-	-
Standalone LabVIEW application	For development	5.5	(5.5)
Total			13.3 + (7.5)

For comparison a new HPLC system roughly starts at 70k € and an ITC 130 k€. Instead of relying on a finish product, it is possible to build a detector from the bottom up where one acquires a light source, optical fibers, flow cell and detector, see Figure 6.11.

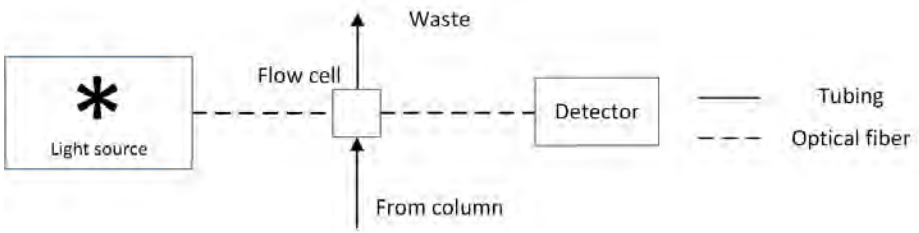

Figure 6.11 – Schematics of a spectrophotometric detector.

Ocean Optics[214] has taken such an approach where it is possible to fit light sources with the detectors of a specific need. Ocean Optics furthermore sells LabVIEW drivers for all its detectors and these can readily be incorporated into the software instrument. Flow cells can also be purchased at Ocean Optics or alternatively at KNAUER[215]. The common fluid connectors can be purchased at e.g. IDEX[216]. The reason this approach was not applied here, was that the DAD detector has integrated the all the different parts. This integration makes it possible to avoid the use of optical fibers and no light intensity is lost in this way. The instrument can also temperature control the entire system and it is in general built for high sensitivity and reliability. This combined, is believed to provide more robust measurement over the modular instrument.

7 VALIDATION OF THE TOOL

Similar to the analytical instruments of chapter 4, the setup also has a reactor part and a detection method. The reactor part consists of a PTFE tube with a narrow inner diameter facilitating low disperse flow. This flow regime generates plug flow conditions for the fast diffusing compounds such as substrates and products. Nonetheless, the enzyme dispersion sets a limit for how fast steady state can be obtained, this is handled by keeping the enzyme concentration constant after this state has been reached. The plug flow conditions makes it possible to apply a ramp mode of operation, enabling collection of samples as residence time is dynamically increased.

The detection method is a diode array UV/VIS detector coupled with a size exclusion column, which separates, enzyme, substrates and products. The species are not baseline separated and this is neither a requirement. The collected residence time – wavelength data is analysed with chemometrics and yields concentrations of a given sample.

Before discussing the possible application of the tool, it is necessary to validate that it indeed produces the intended information. Some problems with the set-up are also described here since they are closely related with operation.

7.1 Comparison with batch and steady state

In order to validate the method it was necessary to see that the operation of steady state, ramp mode and batch yielded the same results. The experimental methods for the different operational modes are given in the experimental methods section in chapter 6. All methods are described in the experimental methods section. As expected no deviation was found between batch and ramp operation, see Figure 7.1. Steady state flow has a small deviation from the other two and it is expected that manual error is the source of this.

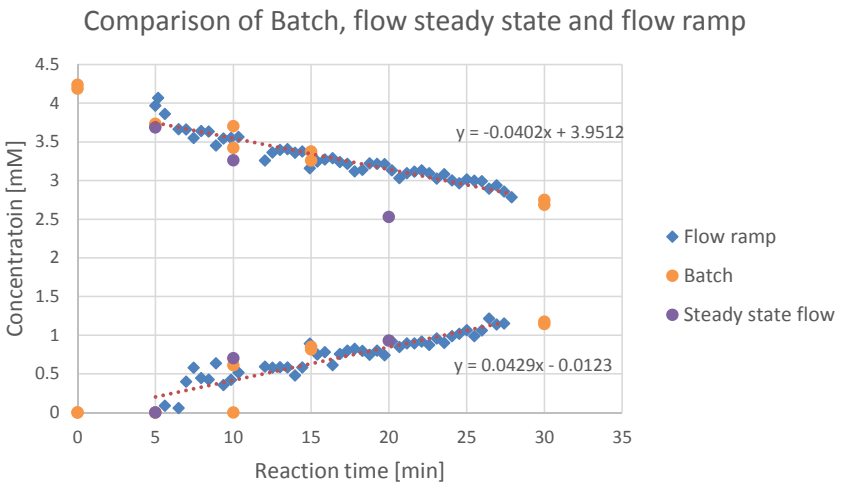

Figure 7.1 – Comparison of batch, steady state flow and ramp flow, [BA] = 4.5 mM, [IPA] = 50 mM, [PLP] = 0.1 mM, [Enz] = 1 mg/mL, T= 30 °C, the different methods for obtaining the data are described in the experimental methods section, dotted lines are linear regression of the flow ramp data.

7.2 A co-factor problem

Initially the reaction was run in the synthetic direction, BA->MPPA. The projects assay conditions were defined by the University of Lund and included excess PLP, which was added in order to saturate the active site in case of leakage from the active site of the enzyme. A concentration of 0.1 mM was indentified to be ideal, along with 20 mM PBS buffer pH 8, 100 mM IPA and 10 mM BA. What was not realized until late in the project was that PLP changes protonation in the size exclusion column depending on the concentration of MPPA. Because PLP and MPPA elutes together, the relative high concentration of MPPA inside the column increases pH and thereby changes the spectral output of PLP. The mobile phase was a phosphate buffer at pH 7 as this was suggested by the producer of the column. The buffer was substituted for a pH 3 phosphate buffer to suppress this pH change. However, even at high concentrations, $0.1\ M$, it was not possible to change the pH effect of MPPA on PLP. The effect can be seen in Figure 7.2, where PLP without MPPA, green, and with MPPA, purple, is plotted. A mixture of the two PLP species appear at low MPPA concentrations, roughly around $K_M \approx 2\ mM$, which is exactly the region of interest, this can be seen later in the inhibition profile.

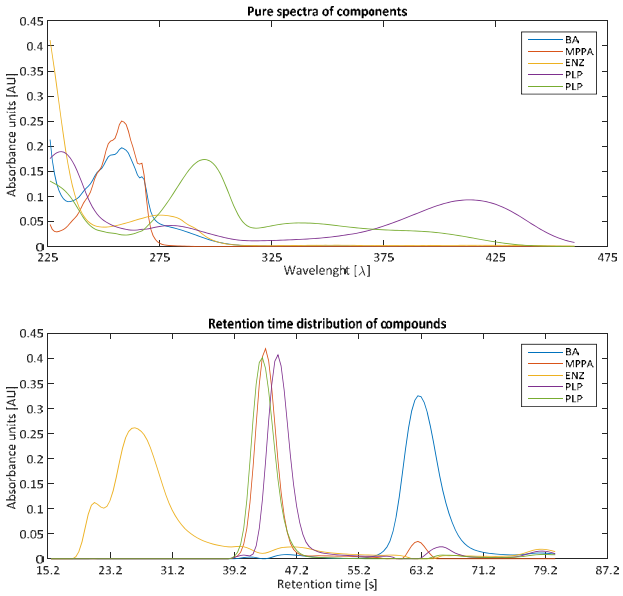

Figure 7.2 – Spectral change of PLP

Moreover it was extremely difficult to obtain a unique model, which is otherwise the hallmark of the PARAFAC model. The CONCORDIA of the model displayed in Figure 7.2 was zero and from the paper of Bro[213], this implies an invalid model.

7.3 A column problem.

It is generally known that column performance is bound to decrease, the rate of the decrease defines the stability of a detection method. HPLC is somewhat immune to peak drifting and widening as long as peaks do not collide or become so wide that sensitivity is lost. The method here can also handle drift in peaks, as alignment forces the retention time to be shifted into the correct position, see Figure 7.3. However the method performs poorly with widening of peaks, and this forces the user to make calibrations relatively often. In particular, small particulates and protein agglomerates is a problem. Filtering is therefore substantially increasing the lifetime of this column, the carrier phase was filtered by adding a filter to the drawing tube of the piston pump. In order to keep dead volume after the reactor as low as possible no filtering was done of the substrate stock solutions. The enzyme was filtered but agglomerated over time, also in the tubes. This is really a problem as the constructed set-up is not yet error proof and a critical errors can stop the setup, which in turn gives the protein time to aggregate. A column filter could assist in solving this, and should have been added in hindsight. It was however not added as it would have widened the peaks.

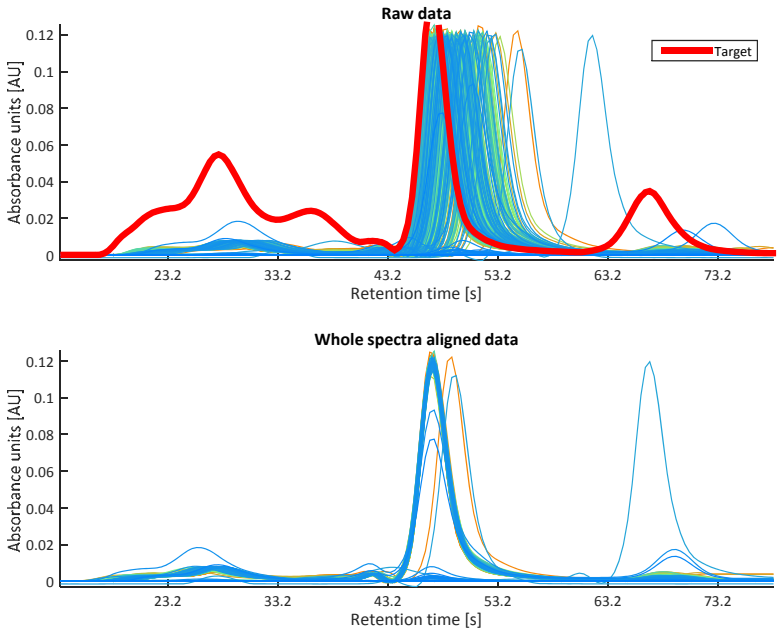

Figure 7.3 – Shift in peaks and resulting alignment

7.4 Inhibition profile of MPPA

Late in the project, University of Lund discovered that the applied enzyme ATA-50 and ATA-82 had PLP tightly bound, and did not leak for the first hours of reaction. PLP could therefore be removed from the reaction mixture and it was then possible to fit the PARAFAC model with a CONCORDIA of 100 as described in section 6.6. The buffer was switched back to PBS pH 7 0.1 M and data collection could start. In the effort to circumvent the PLP problem the direction of the reaction was shifted to MPPA->BA, but this ended out in having no effect on the actual problem. Nonetheless, this reaction direction was kept for the remainder of the project. In order to really see the utility of the system it is desired to inspect the sensitivity of the calculated initial rates. Experimental triplicates of a full inhibition profile for MPPA was then designed and set to run, see result in Figure 7.4. The data collected is very consistent and the ACE concentration is close to 100 mM throughout the experimental design. There is a slight increase in the individual sets of ACE and this is due to the ACE concentration being a little higher in the pure ACE solution than in the MPPA/ACE solution. What is more interesting is to see the enzyme profile, which is significantly increasing from 0.2 mg/ml to 0.3 mg/ml in the first set of experiments, 0-110 samples. This first set of data was collected over 300 minutes and the phenomena experienced here must be very slow. In set 2 and 3 little to no enzyme build up was seen 0.26 – 0.28 and 0.25 – 0.27 mg/ml respectively. The mass balance of the enzyme must therefore be in steady state. This verifies the assumption about being able to step change the input of substrates without disturbing the enzyme concentration profile. It does still not explain the 50% increased observed initially. A clear statement can be made from these experiments: it is very important to measure enzyme concentration, since it makes it

possible to use the actual concentration of the enzyme in the calculation of specific initial rates, see Figure 7.5. This will increase reliability and reduce uncertainty in activity data.

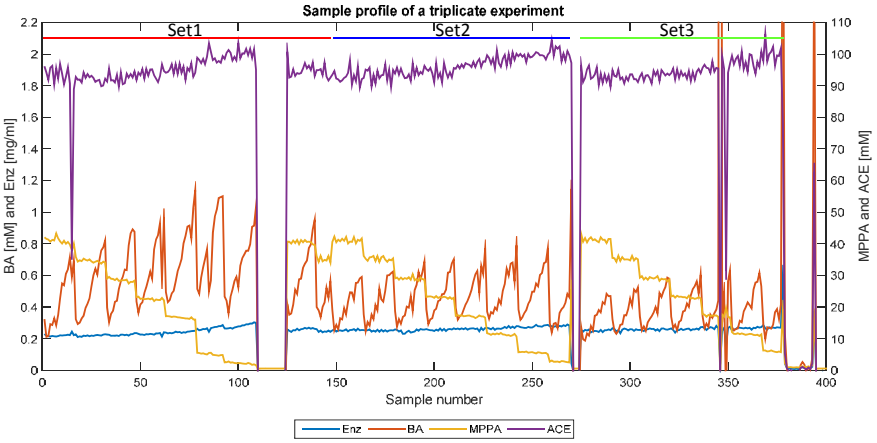

Figure 7.4 – Sample profile of the triplicate experiment, the different sets are indicated by red – set 1, blue – set 2, green – set 3

The data is cut out into individual subsets representing the different setpoints. Linear regression of the concentration and space time data yields the initial rates of the setpoints. By plotting the initial rates versus substrate concentration one obtains the substrate inhibition curve, see Figure 7.5, the MatLab scripts for calculating the intial rates can be found in Appendix E. The scatter plot is divided into set 1, red, set 2, blue, and 3, green. At sample 124 and 147 the UV instrument made critical errors which could only be overwritten manually. The system was therefore standing still for 9 hours, and explains the much lower rate experienced in set 2 and is even slightly lower in 3. The activity stability is here a problem and will be discussed later. From the figure it can be observed that the apparent $K_{M_{MPPA}}$ is in the range$1 - 3\ mM$, and that MPPA is inhibiting the reaction. In order to fit Eqn. 3.8 with inhibition it requires that more data is collected, where different levels of ACE are tested.

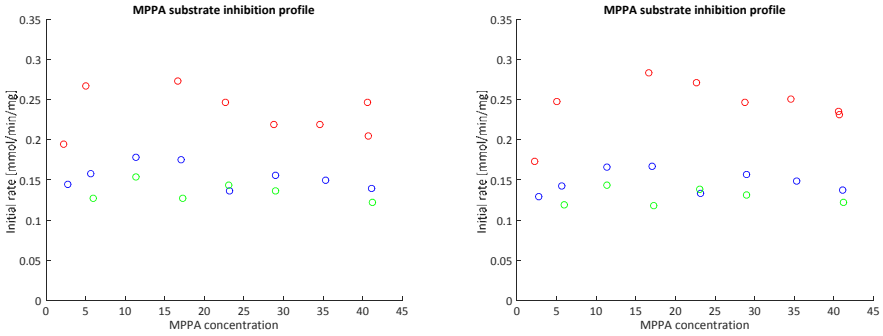

Figure 7.5 – MPPA substrate inhibition profile displayed to the left with specific initial rate [mmol/min/mg] with assumed enzyme concentration and to the right with specific initial rate [mmol/min/mg] with measured enzyme concentration, experimental set 1 - red, set 2 - blue, set 3 - green as illustrated in Figure 7.4

The method was validated against steady state flow data and batch and it was found that under the applied flow conditions, there was no discrepancy between the different modes of operation. The robustness of the detection method still requires improvement and will be discussed in future work. Even though activity was lost over time the method delivered consistency in the inhibition profile, it therefore suggests that an automated protocol for collection of enzyme kinetic data is within reach. Further analysis was put to a stop by column fouling of protein aggregates. Even though the column is build for eluting larger molecules, tight binding can occur. It is also hypothesized that the change of buffer from pH 3 to pH 7 decreased column performance much faster.

8 Biocatalytic Reaction Engineering

A tool for the collection of kinetic data, that can be used to fit a mechanistic model, has been described. In the following chapter, the possibilities of having a model available for process design will be presented.

8.1 Economic frame

A powerful tool in assessing how a process can be developed is by coupling mass balances in a process design. This can only be carried out if kinetic and thermodynamic models for all the different parts of the process are available. Theoretical evaluation is then possible and requirements for the different elements of a process can be set. In the development of new processes one of the most difficult parts is to assess where the bottleneck lies. Recent reviews on the application of biocatalytic models[217,218], show that models are applied to find performance limitations, to define optimal operating conditions, different reactor choices and compare different process configurations. For example, Berendsen and co-workers[219] combined models of two enzymes to optimize the enantiomeric excess as a function of conversion. Schaber and co-workers[220] carried out an economic assessment of a full process. It is therefore clear that these models provide very valuable information for process design. All processes are developed from an economical perspective and for a biocatalytic process that produces fine chemicals, the metrics of Table 8.1 can be used.

Table 8.1 – Economic feasibility of a biocatalytic process for fine chemicals[48]

Biocatalyst formulation	
Retention of activity	High
Stabilization	Improve catalyst productivity > 5 times
Reaction	
Product concentration	>50 g/L
Catalyst productivity	100-250 g product/ g free enzyme (crude)
Stereoselectivity	> 98% ee
Yield	>90%

Initially, when little information on the unit operation dynamics are available, simplified designs can be made in order to set an overall economic boundary. Rather than dynamically responding to concentrations of inlet streams, splits are predefined and for example 100% substrate comes into the reactor and splits into 90% product and 10% substrate. Recently, Tufvesson and co-workers published guidelines for selection of amine donors through simplified generic process design[54]. Here product prices define different regions of operation, such information can be applied directly here. In the introduction this provided insights to the economics of using the different donors. Here it is evaluated how early biocatalytic reaction engineering can be used as an input to such designs in order to guide development.

8.2 Reaction engineering tools

The bottleneck can be, poor rate of reaction, substrate inhibition, product inhibition and enzyme stability. After collecting all the data, and assuming that the mechanistic model is fitted uniquely, modelling can begin. It is assumed here that the enzyme has been engineered to have at least mediocre activity and that activity stability is kept for minimum of 8 hours. Process design and reaction engineering cannot alter the intrinsic rate of reaction, it can however assist in maximum performance by engineering the reaction environment. With such a perspective, substrate and product inhibition as well as stability will be considered.

8.2.1 Substrate inhibition

Competitive and non-competitive Substrate inhibition[76,97] can be handled by a feeding strategy where substrate is supplied corresponding to the maxima of the inhibition curve. The curves maxima moves depending on the product concentration, and this can only be calculated if a kinetic model is available, see example in Figure 8.1. This is different from keeping the substrate level constant at the initial maxima and will show suboptimal performance. In the formulation of economic constraints for a feasible process, the intensity is listed to be 50 g/L product. A natural incentive, without model insight, is therefore to add 50 g/L molar equivalent of the substrate. This is catastrophic in terms of activity as is clearly illustrated in the figure, as substrate is consumed one will move from upper right to bottom left. When competitive or non-competitive substrate inhibition is observed protein engineers ought to screen at lower concentrations where higher resolution should be observed.

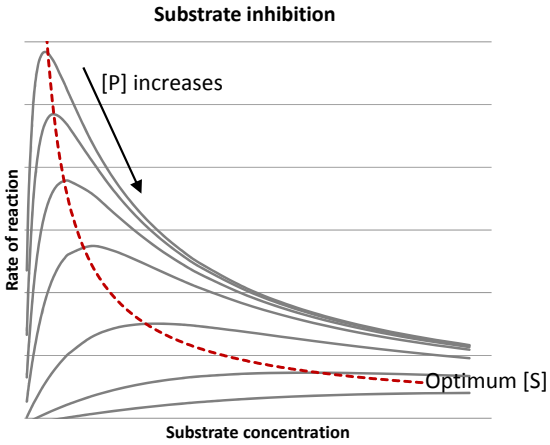

Figure 8.1 – Substrate inhibition profile as concentration of P increases

When uncompetitive- or no substrate-inhibition is experienced, it is desired to run at the highest possible concentration. For the substrates of Amine Transaminase namely ketones, poor water solubility is often experienced. Substrates must therefore also here be fed to the solution, and should be done in the most concentrated form to avoid dilution. Another solution is to add organic solvent to the reaction mixture thereby increasing the solubility of the substrate. As enzyme dynamics are very dependent on their milieu, extrapolation of kinetic investigations cannot be advised and a whole new set of data should be collected if the solvent composition is changed. Substrate toxicity is also an issue and high substrates can significantly alter the half-life of enzymes[221]. Substrate toxicity is handled by feeding to highest possible concentration where the half-life of the enzyme is tolerable. A microfluidic fluidic setup for the study of this was made by Lawrence and co-workers[222].

8.2.2 Product inhibition

Picking solutes out of a solution has always been a challenging task for process chemist. Unfortunately, dealing with product inhibition seems also to be an equally demanding task for protein engineers and only one example is found where K_i of the product is modified[223]. Modifying the active site of an enzyme is possible and increasing substrate scope has been carried out by a technique called substrate walking[35,224]. Once the active site has been opened to a different substrate, the corresponding product must also be able to freely enter and leave the site. Specifically, the products of transferases will likely show inhibition as they are very similar to the substrates. It is different to oxidases, where hydrogen peroxide can be removed effectively with catalase or to hydrolases that splits or condenses their products thereby substantially changing the structure of the molecule. It is thereby, in some cases, possible to prevent product inhibition by derivatizing it, and this is one of the pillars of multi-step onepot synthesis. This type of synthesis is challenged by very complex solutions that can be even more difficult to separate compared to the obtained benefit of product removal[22]. The case studied here with IPA, BA, ACE and MPPA is purposely chosen purposely to avoid such complex mixtures. Product inhibition curves are different to that of a substrate as they asymptotically decreases the rate as a function of product concentration. As the product concentration

increases, the cost of removing it decreases. A trade-off must therefore almost always be made, connecting lost activity with economy of removal. This trade-off at hand can be expressed if models for both kinetics and ISPR are available and will reveal feasibility of the combination. Most importantly, is the kinetic model as ISPR can be artificially introduced and used to set a required target. This ISPR target would assist process engineering in terms of rapidly discarding non-feasible methods.

8.3 An overview

The different strategies that can be used to overcome generic problems of biocatalytic processes can be observed in Figure 8.2. Blue text marks process engineering options whereas green text marks protein engineering options.

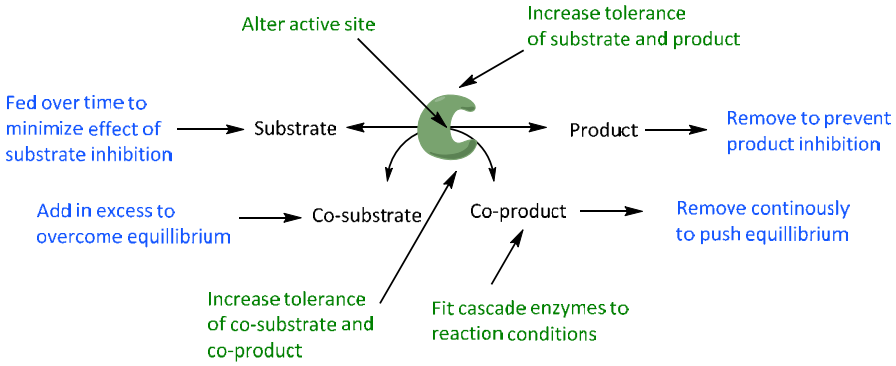

Figure 8.2 – Strategies for different bottlenecks of the process, blue text marks process engineering options whereas green text marks protein engineering options

All the presented process strategies can be added to the kinetic model and studied in-silico. Reaction time, enzyme concentration, donor/substrate excess, productivity can then be fed to the process model and only here, will it be apparent whether an enzymes performance is meeting the economic criteria. For development, extrapolation of the results by artificially increasing rate, optimal substrate feeding, decreasing product inhibition or improving ISPR can guide development and set formal targets. In order to gain a perspective to the work effort of the strategies, an attempt to rank them according to simple (green), complex (orange) and necessary (blue) is done in Table 8.2. Protein engineering is separated into two parts where direct engineering is associated with changes in the active site and in-direct is associated with the stability of the enzyme.

Table 8.2 – Strategies of process engineering and protein engineering, simple (green), complex (orange) and necessary (blue)

	Process engineering	Direct protein engineering	In-direct protein engineering	Driver
Substrate	Feed substrate	Increase tolerance	Positive solvent effect on activity	Maximum rate([S]) Price of enzymes
Amine donor	Add in excess		Increase tolerance and stability	Yield
Co-product	In-situ product or co-product removal	Fit cascade enzymes to reaction conditions	Increase tolerance, stability and temperature stability.	Yield
Product	In-situ product removal	Increase tolerance	Solvent and pH tolerance	Product concentration

9 Discussion

In this chapter the different aspects evaluated in this thesis will be discussed.

The development of a new biocatalytic process, most often comes with a new catalyst and which consequently has unknown kinetics. It is argued here, that in order to rationally develop a biocatalytic process it is necessary to have a kinetic model for the biocatalyst. Nonetheless, for the case of amine transaminase, none of the literature reports of process feasibility[48] involve the use of a kinetic models. Rather the direct implementation of the process or protein engineering options is seen, Truppo reports on enzymatic cascades and ISPR[225]. Whereas two others report protein engineering in which productivity and substrate tolerance was increased[35,226]. Process options such as changing donor, cascades and IScPR can also be screened by brute force in a well plate fashion[227]. It is clear that modelling of bi-substrate systems yields complex correlated models and insights as to why they should be applied in early development is not so apparent. The academic community of biocatalysis is very focussed on new chemistry and the industrial development environment is rarely able to conduct detailed kinetic investigations. The brute force approach is therefore preferred since it delivers direct results. However, the benefits of having a kinetic model available are so appealing that anyone developing a biocatalytic process should be interested in developing a kinetic model as one of the first steps.

The continued interest in biocatalytic processes and the constant change of catalysts justifies a more streamlined development. Enzymes applied for synthetic and production chemistry are of particular interest for industrial use, and the most important enzyme categories for such chemistry typically carry out two substrate and consequently two product reactions. It therefore seems possible to streamline model development as few models fit large groups of enzymes. Namely the models, ordered bi-bi, random bi-bi and ping pong bi-bi, and these are fully described in textbooks[37–39]. Variation of such models are found in how enzymes are inhibited and after identification of this, algebraic terms can be added to the model. This is an attainable task as the types of inhibition are well known and can be identified graphically[37–39]. The different kinds of inhibition are revealed by carrying out inhibition profile experiments, and such data is the same as what is required for model fitting, it therefore serves as a two in one investigation. The latest protocol for estimation of a bi-substrate model is the method of

Al-Haque[76]. In this method, the parameters are estimated from the forward and reverse direction independently. Their local correlation should therefore be transferred to the final correlation matrix and parameters that could not have had an influence on the determined parameters should be set to zero. The remaining correlation must still be dealt with, and Methods of MBDoE should here be applied. This can be used to design experiments that will provide maximum information on a parameter, thereby distinguishing it from its correlated parameters. Targeting of parameters can be done by the anti-correlation criteria described by Franceschini and co-workers[92]. If correlation between parameters cannot be removed, condensation of these can be done but this also clears them of physical meaning.

Parameter correlation is however not a problem for evaluating process options within the operating space of the collected data. In such a case substrate feeding and product removal dynamics are well within the boundaries of a model. This is however not the limit of what a model can be used for and it is desired to guide protein engineering with actual targets for V_{max} of the reaction as well as K_M and K_i for the different compounds. It is important to understand that the catalyst is a fully dynamic protein, and that exchanging a residue will inevitably result in a different dynamic of the enzyme as a whole. Nonetheless, mutations in parent enzymes often yields children with anchored properties. It is therefore assumed to be within the boundaries of a unique model to modify its parameters and set order of magnitude targets for these.

The different parts of the development required is combined into a methodology as proposed in Figure 9.1. Theory and protocols has already been developed, but appropriate models are yet to be produced as a basic step in biocatalytic process development.

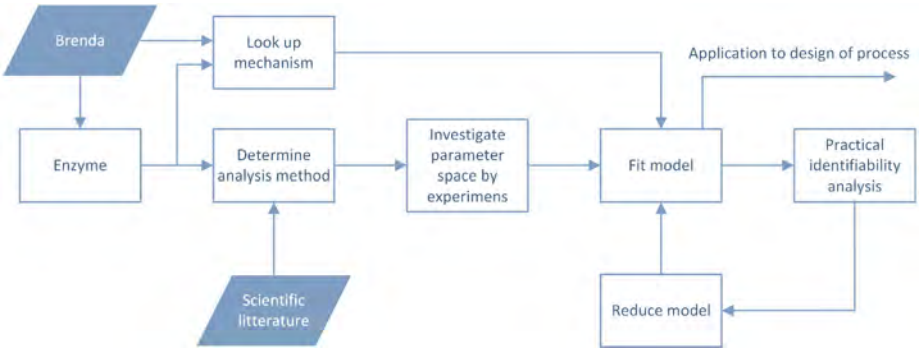

Figure 9.1 – A proposed approach to fitting of enzyme kinetics, here Brenda refers to the database[228]

The motivation is clear and the models are available, but a discussion of the experimental methods are required. The most generic method available is HPLC and is without a doubt a very robust method, but it requires substantial manual labor for experimentation. Automated sample preparation for HPLC's exists but is not a common type of equipment. Stopped flow apparatus can be used to deliver samples in an autonomous way, it is however designed for investigation of reactions at a small time scale. Each time setpoint is additive towards a total analysis time. A set of samples that should be taken at 2, 4 6, 8 and 10 minutes will therefore make a sum of minimum 30 minutes to collect. The samples can hereafter be transferred to an analytical method. The standard spectrophotometric assays have the desired feature of continuous detection, but many spectrophotometric assays require alterations to the original

reagents in order to be carried out effectively. This is can be achieved either by derivation of the reactant with a chromophore or by an analytical enzyme cascade. The widely used indirect spectrophotometric assays rely on the stability of the enzymes and cofactors (e.g. NAD(P)H). Testing rather harsh conditions should therefore be carefully considered in the experimental planning phase. ITC, also has the benefit of continuously detecting the rate of heat development and is suited for thermodynamic favourable reactions. The method can be used by adjusting the enzyme concentration to fit the conditions required for sensitive measurements. As stated in the section describing the technology it is not clear why this method is not applied more frequently, but it could very well be the steep price of the instrument. The readily available methods are therefore not prevalent to that of batch combined with HPLC. New methods must therefore be developed and the refreshed suggestion of using low disperse flow in microfluidics[33,128] provides a way. Microfluidics can only be carried out in connection with pumps, and because these are controlled by a computer these systems are designed to be automated from birth. Very sophisticated algorithms can be made and even computational fluid dynamics can be coupled with the setup making it possible to operate without the low-disperse methodology. Schaber and co-workers[229] algorithm would automatically try to fit suggested models and then propose experiments in the parameter space (e.g. concentration, temperature) based on the FIM. This seems only possible to carry out for relatively simple rate laws as carried out by Schaber[229]. It is suggested, for biocatalytic model development, that focus is on applying the low disperse flow regime rather than coupling it with CFD. Furthermore, for biocatalytic models it is not sufficient to just describe the concentration-time relationship, but rather derived data in the form of initial rates as a function of substrate or product concentration is required. Nonetheless, the merits of microfluidics are clear and much of future reaction engineering and process development is envisaged to be carried out at this scale. Collecting kinetic data by microfluidic low-dispersed flow is smart and can be recommended here.

The sensor technology is now discussed. A robust continuous detection system with Hz order frequency is highly desired as it will provides optimal experimental time resolution. Much of the experimental plan is carried out with the method of initial rates, and as soon as a robust rate determination has been carried out the next setpoint could be investigated. In-line sensors should therefore be programmed to shift to the next setpoint directly after a rate was determined. However, as investigated, few technologies had the sensitivity and none had the resolution in aqueous solutions. Furthermore, In-line UV/VIS without dilution would too sensitive and saturation would readily occur. Typically the limit of undiluted systems is 1-10 mM for aromates, a dilution of the outlet is therefore a requirement. The process feasible intensity described above and has a target of 50 g/L product, which corresponds to 333 mM MPPA. The interplay between path length and sample volume makes it possible to span a very large operational window for detection. Path lengths of flow cells that can be used in the G1315A DAD span from 3 to 10 mm, for other devices, this can be expanded up to 60 mm e.g. with Agilents Max-Light cartridges. For an $\varepsilon = 200\ Lmol^{-1}cm^{-1}$ like MPPA the concentration-absorbance dependence with a dilution of 10 can be viewed in Figure 9.2. The method developed here can handle concentrations of approximately 100 mM. In order to further increase the range one could change the flow cell to one with a 0.3 mm path length, this would increase the range up to 333 mM. Furthermore, with a reduction in sample loop from 5 to 2 µL (minimum with current valve) the range could go up to approximately 800 mM. This is of

course very dependent on the molar absorption coefficient and increased uncertainty is proportional with the increasing range to some extend.

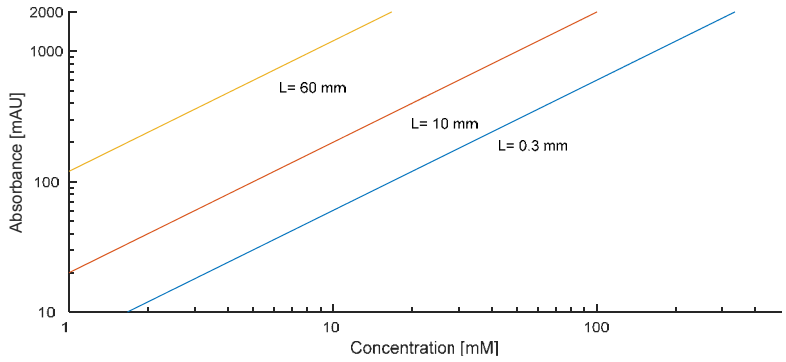

Figure 9.2 – Concentration-absorbance dependence of a molecule with ε = 200 $Lmol^{-1}cm^{-1}$ diluted by a factor 10 at different path lengths, L.

The error analysis reveals only small deviation on all fronts, it is therefore interesting why the output data shows sudden spikes. The massive spikes are due to data that could not be aligned, where the detector and injection valve was not synchronised. It is especially interesting that a drop in BA is validated with an increase of MPPA, which indicates that less reaction has taken place. If concentration would have been consistently lower for MPPA and BA it could mean that the sample loop was improperly filled, but this is not the case. There are some correlation in the PARAFAC model but even with the unimodality constraint applied the irregularities are seen. Furthermore, the enzyme concentration is very consistent and does neither justify these changes. After a spike the concentration jumps back to the progress of the reaction. For the majority of the data, the progress is smooth and consistent, but further investigation of this subject should be carried out. There are problems in reliable determination of MPPA for estimation of rate, but BA can here be used. When the reaction was driven in the other direction, the detection of MPPA formation was more reliable as can be observed in Figure 7.1. It is therefore assumed that there will be no problem in investigating both forward and reverse rates of the reaction with this setup.

The stability of the activity is a general problem for enzymes and after solubilizing them they become more prone to destabilisation. Enzyme solutions are therefore often made just an hour before application to ensure homogeneity and the most stable solution. The method here requires that a stock solution is made from which the pumps can draw liquid. Normally, enzyme solutions are refrigerated to increase stability, a small ice box or cooling water bath should hence be applied here. Because the enzyme stream is relatively small (1/7 nth of 45 µL/min) the glass syringe will most likely heat it up to room temperature before it is pushed out. If not it will be merged with the liquid of the two other stock solutions and hereafter transferred to the heated reactor.

10 Conclusion

This chapter will summarize the conclusions that can be drawn from this thesis.

The kinetic models of important enzymes for synthesis and production chemistry were identified to be a variation of three mechanisms. Namely, ordered bi bi, ping pong bi bi and random bi bi. A method for identification of these and a protocol to fit such models were presented.

After reviewing methods of collecting kinetic data, following items are observed the spectrophotometric assays requires benign conditions, stopped-flow is designed for short reaction times, ITC is too expensive and requires external validation for thermodynamically challenged reactions, batch and HPLC is labor intensive and prone to manual errors. It can therefore be concluded that none of the methods were deemed fit for the purpose that this thesis aims at. Furthermore, it was desired to use a method that would have a small consumption of the scarce biocatalyst and experiments at microscale was found to be a solution. Only by on-line measurements is it possible to utilize the small flows applied at this scale. Spectroscopic methods were therefore investigated and UV/VIS spectroscopy coupled with chemometrics was found to be suitable. This detection method has both the required sensitivity and can be used for aqueous solutions.

The study of microfluidic phenomena revealed that low disperse flow satisfies low consumption as well as plug flow conditions. The low consumption makes it possible to collect a high quantity of information per mass of catalyst spent. The plug flow condition makes it possible to incorporate a ramp mode of operation that will yield concentration-time data at much higher rate compared to steady state measurements. The enzymes diffusivity was found to be the limiting factor for the time required to obtain initial steady state in the low dispersed flow regime. However, after this initial state was obtained, the composition of the substrates could be changed without impact on the enzymes mass balance over the reactor.

After finding and collecting the equipment, the set-up was built. A software instrument was then programmed, which connect and control the different instruments. The control offers automatic collection of concentration time data in a setpoint sequence. Drastically reducing the required labor for obtaining this kind of data. The implementation of a size exclusion

column, effectively isolated the enzyme from the rest of the compounds. As a very positive side effect to this, separation of the mixtures other compounds also occurred. In order to quantify the concentrations of a sample by the spectral-retention time data, PARAFAC, a chemometric tool, was applied. This tool requires strict parallelisation and alignment could be carried out with algorithms developed at department of Food Science, University of Copenhagen. It was hereafter possible to calibrate a PARAFAC model with high CONCORDIA and R^2 values for regression of the scores with actual concentrations in samples. The triplicate experiments for the MPPA inhibition curve displays the current state of the setup, see Figure 10.1. It can here be seen that the activity stability was not as good as anticipated and activity dropped as a consequence. 9 hours separates the stop of experimental set 1 and start of 2. After another 5 hours of experiments the activity is further decreased as can be seen with set 3. By comparing the two graphs in Figure 10.1 it is possible to see a reduction in data scatter as the rate is normalised by the actual concentration of the enzyme.

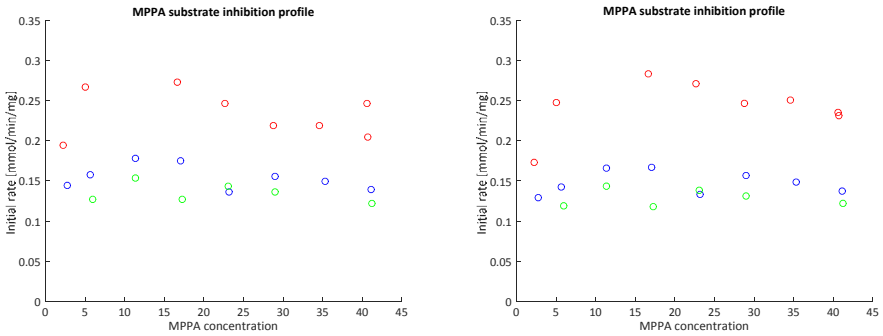

Figure 10.1 – MPPA substrate inhibition profile displayed to the left with specific initial rate [mmol/min/mg] with assumed enzyme concentration and to the right with specific initial rate [mmol/min/mg] with measured enzyme concentration, experimental set 1 - red, set 2 - blue, set 3 - green as illustrated in Figure 7.4

A new method for collecting kinetic data in aqueous solutions was made. It is generic, cheap and automated, making it ideal for conducting kinetic investigations of enzymes. The method is completely novel in the way that it measures both the enzyme concentration as well as component concentrations. It is especially applicable to process development since it can be run at process relevant conditions and can determine concentrations in a wide range.

The entry barrier for developing biocatalytic kinetic models is therefore lowered, and this enables others to find bottlenecks, quantify the process problems and conduct a fast feasibility analysis of what is at hand. In this way the application of validated models will therefore be able to drive the field of biocatalytic process development, as a whole, forward. Hence the input from the process engineering gives direction for protein engineering, which in turn drives a better process. While the order of the necessary tasks in process development is still not fixed[230] it remains certain that in order to move the field forward, collaboration between chemical engineers and protein engineers must be emphasized.

11 FUTURE WORK

Amine transaminases and the developed tool can both be further improved. In this chapter the necessary developments are outlined.

1 Amine transaminases

For the current case of amine transaminase, the low solubility of BA requires that it is supplied continuously, this can be either by an auxiliary phase or by a substrate feeding strategy if inhibition or toxicity is discovered. Furthermore, the thermodynamics are unfavourable and IPA must therefore be added in excess to drive the equilibrium. A product removal strategy should also be implemented to remove effects of product inhibition. Additionally, it is required that the enzyme is engineered to achieve higher rates. A process will only be realised by the combination of the above items, but in order to guide development it is required to develop and fit a kinetic model. The dependency of uncharged and charged amines species needs further investigation. It might be very beneficial to screen for mutants with activity at higher pH where the donors are uncharged.

2 The tool

The tool has several items that can be improved and these will be described in the following. It is desired to scope out the developments required to obtain a fully automatic and robust method.

2.1 Column performance

Aggregates of the protein decrease column performance at a pace that one can cope with at pH 3. Switching the mobile phase buffer to pH 7, along with aggregated enzyme fouled the column and increased backpressure at much higher rate. It is therefore suggested to apply the pH 3 buffer for future investigations and add a pre-column filter. The filter will disturb the separation currently experienced, but method robustness is a key issue. Furthermore, the chemometric fitting can handle overlapping spectra as long as they are consistent. Daily or more frequent washes of the column could be applied, but automatic implementation would require another pump or motorized valve. Even though it is not imagined that air bubbles

disturb the system, installation of a degasser could give additional stability as it guarantees that there is no channelling inside the column caused by bubbles.

2.2 Activity stability

Activity stability needs to be preserved, and measures to ensure this must be applied. It is suggested to cool down the enzyme stock solution or add agents that will promote protein solubility and avoid aggregation[231]. It is desired to stabilize the stock solution for at least 16 hours, which is the unattended operating time. Any duration less than this would result in standby time.

2.3. Optimize setup towards faster collection of data

Most of the experimental plan revolves around the determination of initial rates, the primary focus is therefore to obtain these, as fast and reliable as possible. In the method, the increase of the ramp slope, S, increases the difference in space time between measurement points. The impact of increased S should be used to optimize the rate at which the machine can collect the derived data. A bigger change in space time will result in a bigger change in concentration, a trade-off between space time resolution (magnitude of S) and regression reliability (amount of sample points) will have to be made.

2.4. Initial concentration measurements and full automation

To get more certainty of the inlet composition, a zero time concentration determination of the different setpoints should be done immediately before running the experiments. This can be implemented by substituting the valve heads of the pumps. In the exchange of valve heads one could as well add ports for different stock solutions, so that both product and substrate solutions would be connected. Ideally, one would like to have all substrates and products available in stock solution of high concentrations. Here stream composition could be made up as desired and diluted to the correction concentration with a buffer stream. As discussed above it is likely in the case of amine transaminases that the ketone substrate, BA in this case, has poor solubility. Here it would be required to have a port for each co-substrate concentration. BA 10 mM + 100, 300, 500 mM, so 3 substrate/co-substrate stocks and 3 co-substrate stocks. All in all, two pumps with a minimum of 7 ports + syringe port, and another two pumps with ports with 4 ports + syringe. An illustration of this can be seen in Figure 11.1.

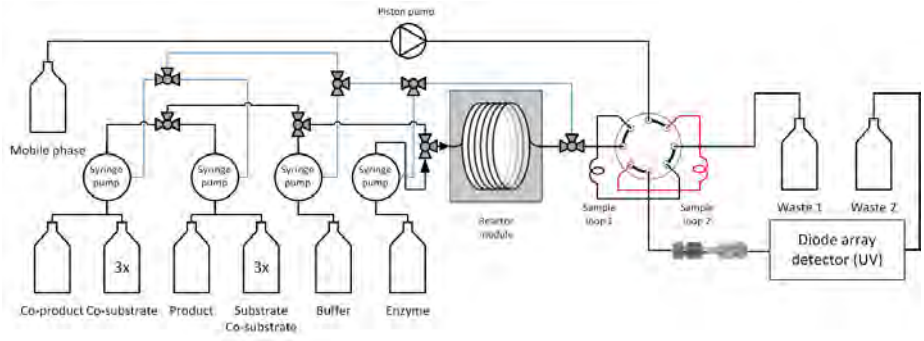

Figure 11.1 – Final experimental setup for full kinetic characterisation of a bi-substrate, bi-product enzyme reaction, note that there is a connection between the syringe pumps and waste 1 which is not shown

12 REFERENCES

1. Anastas, P. & Eghbali, N. Green Chemistry: Principles and Practice. *Chem. Soc. Rev.* **39,** 301–312 (2010).

2. Sheldon, R. A. E factors, green chemistry and catalysis: an odyssey. *Chem. Commun. (Camb).* 3352–3365 (2008). doi:10.1039/b803584a

3. Ni, Y., Holtmann, D. & Hollmann, F. How Green is Biocatalysis? To Calculate is To Know. *ChemCatChem* **6,** 930–943 (2014).

4. Alfonsi, K., Colberg, J., Dunn, P. J., Fevig, T., Jennings, S., Johnson, T. a., Kleine, H. P., Knight, C., Nagy, M. a., Perry, D. A. & Stefaniak, M. Green chemistry tools to influence a medicinal chemistry and research chemistry based organisation. *Green Chem.* **10,** 31 (2008).

5. Henderson, R. K., Jiménez-González, C., Constable, D. J. C., Alston, S. R., Inglis, G. G. a., Fisher, G., Sherwood, J., Binks, S. P. & Curzons, A. D. Expanding GSK's solvent selection guide – embedding sustainability into solvent selection starting at medicinal chemistry. *Green Chem.* **13,** 854 (2011).

6. Prat, D., Pardigon, O., Flemming, H.-W., Letestu, S., Ducandas, V., Isnard, P., Guntrum, E., Senac, T., Ruisseau, S., Cruciani, P. & Hosek, P. Sanofi's Solvent Selection Guide: A Step Toward More Sustainable Processes. *Org. Process Res. Dev.* **17,** 1517–1525 (2013).

7. Long, K. R., Gosen, B. S. V., Foley, N. K. & Cordier, D. *Non-Renewable Resource Issues*. *Non-Renewable Resource Issues Geoscientific and Societal Challenges* (Springer Netherlands, 2012). doi:10.1007/978-90-481-8679-2

8. Faber, K., Fessner, W.-D. & Turner, N. J. *Science of Synthesis: Biocatalysis in Organic Synthesis*. (Georg Thieme Verlag KG, 2015).

9. Drauz, K., Groger, H. & May, O. *Enzyme Catalysis in Organic Synthesis, Third, Completely Revised and Enlarged Edition*. (WILEY-VCH Verlag, 2012).

10. Pollard, D. J. & Woodley, J. M. Biocatalysis for pharmaceutical intermediates: the future is now. *Trends Biotechnol.* **25,** 66–73 (2007).

11. Nestl, B. M., Nebel, B. A. & Hauer, B. Recent progress in industrial biocatalysis. *Curr. Opin. Chem. Biol.* **15,** 187–193 (2011).

12. Meyer, H.-P., Eichhorn, E., Hanlon, S., Lütz, S., Schürmann, M., Wohlgemuth, R. & Coppolecchia, R. The use of enzymes in organic synthesis and the life sciences: perspectives from the Swiss Industrial Biocatalysis Consortium (SIBC). *Catal. Sci. Technol.* **3,** 29–40 (2012).

13. Schmid, A., Dordick, J. S., Hauer, B., Kiener, A., Wubbolts, M. & Witholt, B. Industrial biocatalysis today and tomorrow. *Nature* **409,** 258–268 (2001).

14. Turner, N. J. & Truppo, M. D. Biocatalysis enters a new era. *Curr. Opin. Chem. Biol.* **17,** 212–214 (2013).

15. Strohmeier, G. a., Pichler, H., May, O. & Gruber-Khadjawi, M. Application of designed enzymes in organic synthesis. *Chem. Rev.* **111,** 4141–4164 (2011).

16. Bornscheuer, U. T., Huisman, G. W., Kazlauskas, R. J., Lutz, S., Moore, J. C. & Robins, K. Engineering the third wave of biocatalysis. *Nature* **485,** 185–194 (2012).

17. Davids, T., Schmidt, M., Böttcher, D. & Bornscheuer, U. T. Strategies for the discovery and engineering of enzymes for biocatalysis. *Curr. Opin. Chem. Biol.* **17,** 215–220 (2013).

18. Siegel, J. B., Zanghellini, A., Lovick, H. M., Kiss, G., Abigail, R., Clair, J. L. S., Gallaher, J. L., Hilvert, D., Gelb, M. H., Stoddard, B. L., Houk, K. N., Michael, F. E. & Baker, D. Computational design of an enzyme catalyst for a stereoselective bimolecular Diels-Alder reaction. *Science (80-.).* **329,** 309–313 (2011).

19. Ricca, E., Brucher, B. & Schrittwieser, J. H. Multi-enzymatic cascade reactions: Overview and perspectives. *Adv. Synth. Catal.* **353,** 2239–2262 (2011).

20. Simon, R. C., Richter, N., Busto, E. & Kroutil, W. Recent developments of cascade reactions involving ω-transaminases. *ACS Catal.* **4,** 129–143 (2014).

21. Gröger, H. & Hummel, W. Combining the 'two worlds' of chemocatalysis and biocatalysis towards multi-step one-pot processes in aqueous media. *Curr. Opin. Chem. Biol.* **19,** 171–179 (2014).

22. Bruggink, A., Schoevaart, R. & Kieboom, T. Concepts of Nature in Organic Synthesis : Cascade Catalysis and Multistep Abstract : *Org. Process Res. Dev.* **7,** 622–640 (2003).

23. Dunn, P. J. The importance of Green Chemistry in Process Research and Development. *Chem. Soc. Rev.* **41,** 1452–1461 (2012).

24. Wohlgemuth, R. Asymmetric biocatalysis with microbial enzymes and cells. *Curr. Opin. Microbiol.* **13,** 283–92 (2010).

25. Blackmond, D. G. Kinetic Profiling of Catalytic Organic Reactions as a Mechanistic Tool. *J. Am. Chem. Soc.* **137,** 10852–10866 (2015).

26. Hessel, V., Kralisch, D., Kockmann, N., Noël, T. & Wang, Q. Novel process windows for enabling, accelerating, and uplifting flow chemistry. *ChemSusChem* **6,** 746–789 (2013).

27. McMullen, J. P. & Jensen, K. F. Integrated microreactors for reaction automation: new approaches to reaction development. *Annu. Rev. Anal. Chem.* **3,** 19–42 (2010).

28. Newman, S. G. & Jensen, K. F. The role of flow in green chemistry and engineering. *Green Chem.* **15,** 1456–1472 (2013).

29. Woodley, J. M. Protein engineering of enzymes for process applications. *Curr. Opin. Chem. Biol.* **17,** 310–316 (2013).

30. Agresti, J. J., Antipov, E., Abate, A. R., Ahn, K., Rowat, A. C., Baret, J.-C., Marquez, M., Klibanov, A. M., Grifiths, A. D. & Weitz, D. A. Ultrahigh-throughput screening in drop-based microfluidics for directed evolution. *Proc. Natl. Acad. Sci.* **107,** 6550–6550 (2010).

31. Fallah-Araghi, A., Baret, J.-C., Ryckelynck, M. & Griffiths, A. D. A completely in vitro ultrahigh-throughput droplet-based microfluidic screening system for protein engineering and directed evolution. *Lab Chip* **12,** 882 (2012).

32. Hartman, R. L., McMullen, J. P. & Jensen, K. F. Deciding whether to go with the flow: Evaluating the merits of flow reactors for synthesis. *Angew. Chemie - Int. Ed.* **50,** 7502–7519 (2011).

33. Moore, J. S. & Jensen, K. F. 'Batch' kinetics in flow: online IR analysis and continuous control. *Angew. Chem. Int. Ed. Engl.* **53,** 470–3 (2014).

34. Krühne, U., Heintz, S., Ringborg, R., Rosinha, I. P., Tufvesson, P., Gernaey, K. V & Woodley, J. M. Biocatalytic process development using microfluidic miniaturized systems. *Green Process Synth* **3,** 23–31 (2014).

35. Savile, C. K., Janey, J. M., Mundorff, E. C., Moore, J. C., Tam, S., Jarvis, W. R., Colbeck, J. C., Krebber, A., Fleitz, F. J., Brands, J., Devine, P. N., Huisman, G. W. & Hughes, G. J. Biocatalytic asymmetric synthesis of chiral amines from ketones applied to sitagliptin manufacture. *Science* **329,** 305–309 (2010).

36. Cornish-Bowden, A. History of Enzyme Chemistry. *eLS* (2011). doi:10.1002/9780470015902.a0003466

37. Segel, I. H. *Enzyme kinetics: behavior and analysis of rapid equilibrium and steady-state enzyme systems*. **2,** (John Wiley & Sons, 1975).

38. Cleland, W. W. in *The enzymes, vol II: kinetics and mechanism* (ed. Boyer, P. D.) 1–61 (Academic Press, 1970).

39. Cornish-Bowden, A. *Fundamentals of enzyme kinetics*. (Wiley-Blackwell, 2012).

40. Höhne, M. & Bornscheuer, U. T. Biocatalytic routes to optically active amines. *ChemCatChem* **1,** 42–51 (2009).

41. Nugent, T. C. & El-Shazly, M. Chiral Amine Synthesis - Recent Developments and Trends for Enamide Reduction, Reductive Amination, and Imine Reduction. *Adv. Synth. Catal.* **352,** 753–819 (2010).

42. Koszelewski, D., Lavandera, I., Clay, D., Rozzell, D. & Kroutil, W. Asymmetric synthesis of optically pure pharmacologically relevant amines employing ω-transaminases. *Adv. Synth. Catal.* **350,** 2761–2766 (2008).

43. Wenda, S., Illner, S., Mell, A. & Kragl, U. Industrial biotechnology—the future of green chemistry? *Green Chemistry* **13,** 3007 (2011).

44. Patel, R. N. Biocatalysis: Synthesis of key intermediates for development of pharmaceuticals. *ACS Catalysis* **1,** 1056–1074 (2011).

45. Ghislieri, D. & Turner, N. J. Biocatalytic Approaches to the Synthesis of Enantiomerically Pure Chiral Amines. *Top. Catal.* **57,** 284–300 (2014).

46. Kagan, H. B. & Fiaud, J.-C. Kinetic Resolution. *Top. Stereochem.* **18,** 249–330 (1988).

47. Malik, M. S., Park, E.-S. & Shin, J.-S. Features and technical applications of ω-transaminases. *Appl. Microbiol. Biotechnol.* **94,** 1163–71 (2012).

48. Tufvesson, P., Lima-Ramos, J., Jensen, J. S., Al-Haque, N., Neto, W. & Woodley, J. M. Process considerations for the asymmetric synthesis of chiral amines using transaminases. *Biotechnology and Bioengineering* **108,** 1479–1493 (2011).

49. Kroutil, W., Fischereder, E. M., Fuchs, C. S., Lechner, H., Mutti, F. G., Pressnitz, D., Rajagopalan, A., Sattler, J. H., Simon, R. C. & Siirola, E. Asymmetric preparation of prim -, sec -, and tert-amines employing selected biocatalysts. *Organic Process Research and Development* **17,** 751–759 (2013).

50. Okamoto, Y. & Yashima, E. Polysaccharide Derivatives for Chromatographic Separation of Enantiomers. *Angew. Chemie Int. Ed.* **37,** 1020–1043 (1998).

51. Turner, N. J. Enzyme catalysed deracemisation and dynamic kinetic resolution reactions. *Current Opinion in Chemical Biology* **8,** 114–119 (2004).

52. Smith, S. W. Chiral toxicology: It's the same thing only different. *Toxicological Sciences* **110,** 4–30 (2009).

53. Tufvesson, P., Jensen, J. S., Kroutil, W. & Woodley, J. M. Experimental determination of thermodynamic equilibrium in biocatalytic transamination. *Biotechnol. Bioeng.* **109,** 2159–62 (2012).

54. Tufvesson, P., Nordblad, M., Krühne, U., Schürmann, M., Vogel, A., Wohlgemuth, R. & Woodley, J. M. Economic Considerations for Selecting an Amine Donor in Biocatalytic Transamination. *Org. Process Res. Dev.* **19,** 652 – 660 (2015).

55. Woodley, J. M. in *Synthetic Methods for Biologically Active Molecules - Exploring the Potentials of Bioreductions* 263–284 (WILEY-VCH, 2013).

56. Cassimjee, K. E., Humble, M. S., Miceli, V., Colomina, C. G. & Berglund, P. Active site quantification of an ω-Transaminase by performing a half transamination reaction. *ACS Catal.* **1,** 1051–1055 (2011).

57. Łyskowski, A., Gruber, C., Steinkellner, G., Schürmann, M., Schwab, H., Gruber, K. & Steiner, K. Crystal structure of an (R)-selective ω-transaminase from Aspergillus terreus. *PLoS One* **9,** e87350 (2014).

58. Cassimjee, K. E., Manta, B. & Himo, F. A quantum chemical study of the ω-transaminase reaction mechanism. *J. Phys. Chem. B* **103,** 1193–1202 (1999).

59. Baldenius, K.-U., Ditrich, K., Breuer, M., Navickas, V., Janssen, D., Bartsch, S. & Grismaru, C. G. Method for the production of primary amines. (2014).

60. Bisswanger, H. Enzyme assays. *Perspect. Sci.* **1,** 41–55 (2014).

61. Vieille, C., Zeikus, G. J. & Vieille, C. Hyperthermophilic Enzymes : Sources , Uses , and Molecular Mechanisms for Thermostability Hyperthermophilic Enzymes : Sources , Uses , and Molecular Mechanisms for Thermostability. *Microbiol. Mol. Biol. Rev.* **65,** 1–43 (2001).

62. Bruylants, G., Wouters, J. & Michaux, C. Differential scanning calorimetry in life science: thermodynamics, stability, molecular recognition and application in drug design. *Curr. Med. Chem.* **12,** 2011–2020 (2005).

63. Alexander, C. G., Wanner, R., Johnson, C. M., Breitsprecher, D., Winter, G., Duhr, S., Baaske, P. & Ferguson, N. Novel microscale approaches for easy, rapid determination of protein stability in academic and commercial settings. *Biochim. Biophys. Acta - Proteins Proteomics* **1844,** 2241–2250 (2014).

64. Adolph, H. W., Maurer, P., Schneider-bernlöhr, H., Sartorius, C. & Zeppezauer, M. Substrate specificity and stereoselectivity of horse liver alcohol dehydrogenase. *Eur. J. Biochem.* **201,** 615–625 (1991).

65. Heinstra, P. W., Thörig, G. E., Scharloo, W., Drenth, W. & Nolte, R. J. Kinetics and thermodynamics of ethanol oxidation catalyzed by genetic variants of the alcohol dehydrogenase from Drosophila melanogaster and D. simulans. *Biochim. Biophys. Acta* **967,** 224–233 (1988).

66. Dalziel, K. & Dickinson, F. M. The kinetics and mechanism of liver alcohol dehydrogenase with primary and secondary alcohols as substrates. *Biochem. J.* **100,** 34–46 (1966).

67. Humphreys, K. J., Mirica, L. M., Wang, Y. & Klinman, J. P. Galactose oxidase as a model for reactivity at a copper superoxide center. *J. Am. Chem. Soc.* **131,** 4657–4663 (2009).

68. Tsai, C. S., Burgett, M. W. & Reed, L. J. α-Keto Acid Dehydrogenase Complexes. *J. Biol. Chem.* **248,** 8348–8352 (1973).

69. Suzuki, H., Ogura, Y. & Yamada, H. Kinetic Studies on the Amine Oxidase Reaction. *J. Biochem.* **72,** 703–712 (1972).

70. Adams, J. A. Kinetic and catalytic mechanisms of protein kinases. *Chemical Reviews* **101,** 2271–2290 (2001).

71. Maddaiah, V. T. & Madsen, N. B. Kinetics of Purified Liver Phosphorylase. *J. Biol. Chem.* **241,** 3873–3881 (1966).

72. Carreras, C. W. & Santi, D. V. The catalytic mechanism and structure of thymidylate synthase. *Annu. Rev. Biochem.* **64,** 721–762 (1995).

73. Roth, S. Y., Denu, J. M. & Allis, C. D. Histone acetyltransferases. *Annu. Rev. Biochem.* **70,** 81–120 (2001).

74. Henson, C. P. & Cleland, W. W. Kinetic Studies of Glutamic Oxaloacetic Transaminase Isozymes. *Biochemistry* **3,** 338–345 (1963).

75. Shin, J. S. & Kim, B. G. Kinetic modeling of omega-transamination for enzymatic kinetic resolution of alpha-methylbenzylamine. *Biotechnol. Bioeng.* **60,** 534–40 (1998).

76. Al-Haque, N., Santacoloma, P. a, Neto, W., Tufvesson, P., Gani, R. & Woodley, J. M. A robust methodology for kinetic model parameter estimation for biocatalytic reactions. *Biotechnol. Prog.* **28,** 1186–96 (2012).

77. Gyamerah, M. & Willetts, A. J. Kinetics of overexpressed transketolase from Escherichia. **20,** 127–134 (1997).

78. Chen, B. H., Hibbert, E. G., Dalby, P. A. & Woodley, J. M. A New Approach to Bioconversion Reaction Kinetic Parameter Identification. **54,** 3–5 (2008).

79. Paiva, A. L., Balcão, V. M. & Malcata, F. X. Kinetics and mechanisms of reactions catalyzed by immobilized lipases. *Enzyme Microb. Technol.* **27,** 187–204 (2000).

80. Van Der Veen, B. a., Van Alebeek, G. J. W. M., Uitdehaag, J. C. M., Dijkstra, B. W. & Dijkhuizen, L. The three transglycosylation reactions catalyzed by cyclodextrin glycosyltransferase from Bacillus circulans (strain 251) proceed via different kinetic mechanisms. *Eur. J. Biochem.* **267,** 658–665 (2000).

81. Maestracci, M., Thiery, A., Arnaud, A. & Galzy, P. A study of the mechanism of the reactions catalyzed by the amidase Brevibacterium sp. R312. *Agric. Biol. Chem.* **50,** 2237–2241 (1986).

82. Fournand, D., Bigey, F. & Arnaud, A. Acyl transfer activity of an amidase from Rhodococcus sp. strain R312: Formation of a wide range of hydroxamic acids. *Appl. Environ. Microbiol.* **64,** 2844–2852 (1998).

83. Wang, W., Baker, P. & Seah, S. Y. K. Comparison of two metal-dependent pyruvate aldolases related by convergent evolution: Substrate specificity, kinetic mechanism, and substrate channeling. *Biochemistry* **49,** 3774–3782 (2010).

84. Botting, N. P. & Gani, D. Mechanism of C-3 hydrogen exchange and the elimination of ammonia in the 3-methylaspartate ammonia-lyase reaction. *Biochemistry* **31,** 1509–1520 (1992).

85. Blackmond, D. G. Reaction progress kinetic analysis: a powerful methodology for mechanistic studies of complex catalytic reactions. *Angew. Chem. Int. Ed. Engl.* **44,** 4302–20 (2005).

86. Johnson, K. A. A century of enzyme kinetic analysis, 1913 to 2013. *FEBS Lett.* **587,** 2753–2766 (2013).

87. Anderson, K. S., Sikorski, J. a & Johnson, K. A. A tetrahedral intermediate in the EPSP synthase reaction observed by rapid quench kinetics. *Biochemistry* **27,** 7395–7406 (1988).

88. Kellinger, M. W. & Johnson, K. A. Role of Induced Fit in Limiting Discrimination against AZT by HIV Reverse Transcriptase. *Biochemistry* **50,** 5008–5015 (2011).

89. Schulz, A. R. *Enzyme Kinetics*. (Cambridge University Press, 1994). doi:http://dx.doi.org/10.1017/CBO9780511608438

90. Franceschini, G. & Macchietto, S. Model-based design of experiments for parameter precision: State of the art. *Chem. Eng. Sci.* **63,** 4846–4872 (2008).

91. Telen, D., Logist, F., Derlinden, E. Van, Tack, I. & Impe, J. Van. Optimal experiment design for dynamic bioprocesses : a multi-objective approach. *Chem. Eng. Sci.* **78,** 82–97 (2012).

92. Franceschini, G. & Macchietto, S. Novel Anticorrelation Criteria for Model-Based Experiment Design: Theory and Formulations. *AIChE J.* **54,** 1009–1024 (2008).

93. Jerabek-Willemsen, M., André, T., Wanner, R., Roth, H. M., Duhr, S., Baaske, P. & Breitsprecher, D. MicroScale Thermophoresis: Interaction analysis and beyond. *J. Mol. Struct.* **1077,** 101–113 (2014).

94. Mozharov, S., Nordon, A., Littlejohn, D., Wiles, C., Watts, P., Dallin, P. & Girkin, J. M. Improved method for kinetic studies in microreactors using flow manipulation and noninvasive raman spectrometry. *J. Am. Chem. Soc.* **133,** 3601–3608 (2011).

95. Schwolow, S., Braun, F., Rädle, M., Kockmann, N. & Röder, T. Fast and Efficient Acquisition of Kinetic Data in Microreactors Using In-Line Raman Analysis. *Org. Process Res. Dev.* **19,** 1286–1292 (2015).

96. Fagaschewski, J., Sellin, D., Wiedenhöfer, C., Bohne, S., Trieu, H. K. & Hilterhaus, L. Spatially resolved in situ determination of reaction progress using microfluidic systems and FT-IR spectroscopy as a tool for biocatalytic process development. *Bioprocess Biosyst. Eng.* **38,** 1399–1405 (2015).

97. Rios-Solis, L., Bayir, N., Halim, M., Du, C., Ward, J. M., Baganz, F. & Lye, G. J. Non-linear kinetic modelling of reversible bioconversions: Application to the transaminase catalyzed synthesis of chiral amino-alcohols. *Biochem. Eng. J.* **73,** 38–48 (2013).

98. Rios-Solis, L., Morris, P., Grant, C., Odeleye, A. O. O., Hailes, H. C., Ward, J. M., Dalby, P. a., Baganz, F. & Lye, G. J. Modelling and optimisation of the one-pot, multi-enzymatic synthesis of chiral amino-alcohols based on microscale kinetic parameter determination. *Chem. Eng. Sci.* **122,** 360–372 (2015).

99. Galgani, F., Cadiou, Y. & Bocquene, G. Routine Determination of Enzyme Kinetics Using Plate Reader. *Biotechnol. Bioeng.* **38,** 434–437 (1991).

100. Schätzle, S., Höhne, M., Redestad, E., Robins, K. & Bornscheuer, U. T. Rapid and sensitive kinetic assay for characterization of omega-transaminases. *Anal. Chem.* **81,** 8244–8 (2009).

101. DeLouise, L. a & Miller, B. L. Enzyme immobilization in porous silicon: quantitative analysis of the kinetic parameters for glutathione-S-transferases. *Anal. Chem.* **77,** 1950–1956 (2005).

102. Kim, Y., Tanner, K. G. & Denu, J. M. A continuous, nonradioactive assay for histone acetyltransferases. *Anal. Biochem.* **280,** 308–314 (2000).

103. Baker, P., Pan, D., Carere, J., Rossi, A., Wang, W. & Seah, S. Y. K. Characterization of an aldolase-dehydrogenase complex that exhibits substrate channeling in the polychlorinated biphenyls degradation pathway. *Biochemistry* **48,** 6551–6558 (2009).

104. Burke, B. J. & Regnier, F. E. Stopped-flow enzyme assays on a chip using a microfabricated mixer. *Anal. Chem.* **75,** 1786–1791 (2003).

105. Faller, B., Cadène, M. & Bieth, J. G. Demonstration of a two-step reaction mechanism for the inhibition of heparin-bound neutrophil elastase by alpha 1-proteinase inhibitor. *Biochemistry* **32,** 9230–9235 (1993).

106. Kintses, B., Simon, Z., Gyimesi, M., Tóth, J., Jelinek, B., Niedetzky, C., Kovács, M. & Málnási-Csizmadia, A. Enzyme kinetics above denaturation temperature: a temperature-jump/stopped-flow apparatus. *Biophys. J.* **91,** 4605–4610 (2006).

107. Hartwell, S. K. & Grudpan, K. Flow-based systems for rapid and high-precision enzyme kinetics studies. *J. Anal. Methods Chem.* (2012). doi:10.1155/2012/450716

108. Saunders, L. P., Cao, W., Chang, W. C., Albright, R. a., Braddock, D. T. & De La Cruz, E. M. Kinetic analysis of autotaxin reveals substrate-specific catalytic pathways and a mechanism for lysophosphatidic acid distribution. *J. Biol. Chem.* **286,** 30130–30141 (2011).

109. Todd, M. J. & Gomez, J. Enzyme kinetics determined using calorimetry: a general assay for enzyme activity? *Anal. Biochem.* **296,** 179–187 (2001).

110. Watt, G. D. A microcalorimetric procedure for evaluating the kinetic parameters of enzyme-catalyzed reactions: Kinetic measurements of the nitrogenase system. *Anal. Biochem.* **187,** 141–146 (1990).

111. Haq, I. & Hill, B. Calorimetry in the Fast Lane: The Use of ITC for Obtaining Enzyme Kinetic Constants. *Microcal, LLC Appl. note* **44,** (2002).

112. Bianconi, M. L. Calorimetry of enzyme-catalyzed reactions. *Biophys. Chem.* **126,** 59–64 (2007).

113. Burch, H. B., Bradley, M. E. & Lowry, O. H. The Measurement of Triphosphopyridine Nucleotide Erroneous Values * Nucleotide and the Role and Reduced Triphosphopyridine of Hemoglobin in Producing Triphosphopyridine Nucleotide. *October* **242,** (1967).

114. Passonneau, J. V. & Lowry, O. H. A Collection of Enzyme Assays. *Enzym. Anal. A Pract. Guid.* 229–305 (1993). doi:10.1007/978-1-60327-407-4_7

115. Bisswanger, H. *Practical Enzymology*. (Wiley-VCH Verlag GmbH & Co. KGaA, 2011).

116. Purich, D. L. & Allison, R. D. *The enzyme reference: a comprehensive guidebook to enzyme nomenclature, reactions, and methods*. (2003). doi:10.5860/CHOICE.41-0053

117. Pick, E. & Keisari, Y. A simple colorimetric method for the measurement of hydrogen peroxide produced by cells in culture. *J. Immunol. Methods* **38,** 161–170 (1980).

118. Erel, O. A new automated colorimetric method for measuring total oxidant status. *Clin. Biochem.* **38,** 1103–11111 (2005).

119. Valera, F. E., Quaranta, M., Moran, A., Blacker, J., Armstrong, A., Cabral, J. T. & Blackmond, D. G. The flow's the thing..or is it? Assessing the merits of homogeneous reactions in flask and flow. *Angew. Chem. Int. Ed. Engl.* **49,** 2478–85 (2010).

120. Cussler, E. L. *Diffusion: Mass Transfer in Fluid Systems*. *Engineering* **Second,** (1997).

121. Young, M. E., Carroad, P. A. & Bell, R. L. Estimation of diffusion coefficients of proteins. *Biotechnol. Bioeng.* **22,** 947–955 (1980).

122. Swarts, J. W., Kolfschoten, R. C., Jansen, M. C. A. A., Janssen, A. E. M. & Boom, R. M. Effect of diffusion on enzyme activity in a microreactor. *Chem. Eng. J.* **162,** 301–306 (2010).

123. Jähnisch, K., Hessel, V., Löwe, H. & Baerns, M. Chemistry in Microstructured Reactors. *Angewandte Chemie - International Edition* **43,** 406–446 (2004).

124. Wiles, C. & Watts, P. Continuous flow reactors: a perspective. *Green Chem.* **14,** 38 (2012).

125. Hartman, R. L. & Jensen, K. F. Microchemical systems for continuous-flow synthesis. *Lab Chip* **9,** 2495–2507 (2009).

126. Wohlgemuth, R., Plazl, I., Žnidaršič-Plazl, P., Gernaey, K. V. & Woodley, J. M. Microscale technology and biocatalytic processes: opportunities and challenges for synthesis. *Trends Biotechnol.* **33,** (2015).

127. Yoshida, J. I., Kim, H. & Nagaki, A. Green and sustainable chemical synthesis using flow microreactors. *ChemSusChem* **4,** 331–340 (2011).

128. Nagy, K. D., Shen, B., Jamison, T. F. & Jensen, K. F. Mixing and Dispersion in Small-Scale Flow Systems. *Org. Process Res. Dev.* **16,** 976–981 (2012).

129. Taylor, G. Dispersion of Soluble Matter in Solvent Flowing Slowly through a Tube. *Proc. R. Soc. London. Ser. A* **219,** 186–203 (1953).

130. Aris, R. On the dispersion of a solute in a fluid flowing through a tube. *Proc. R. Soc. London. Ser. A* **235,** 67–77 (1956).

131. Zechel, D. L., Konermann, L., Withers, S. G. & Douglas, D. J. Pre-Steady State Kinetic Analysis of an Enzymatic Reaction Monitored by Time Resolved ESI MS. **2960,** 7664–7669 (1998).

132. Lawson, S. L., Wakarchuk, W. W. & Withers, S. G. Positioning the acid/base catalyst in a glycosidase: Studies with bacillus circulans xylanase. *Biochemistry* **36,** 2257–2265 (1997).

133. Huddleston, J. P., Schroeder, G. K., Johnson, K. A. & Whitman, C. P. A pre-steady state kinetic analysis of the ??y60W mutant of trans-3-chloroacrylic acid dehalogenase: Implications for the mechanism of the wild-type enzyme. *Biochemistry* **51,** 9420–9435 (2012).

134. Thomson, J. A. & Ladbury, J. E. in *Biocalorimetry 2: Application of Calorimetry in the Biological Sciences* (eds. Ladbury, J. E. & Doyle, M. L.) (2004).

135. Fukada, H. & Takahashi, K. Enthalpy and heat capacity changes for the proton dissociation of various buffer components in 0.1 M potassium chloride. *Proteins Struct. Funct. Genet.* **33,** 159–166 (1998).

136. Freyer, M. W. & Lewis, E. A. Isothermal Titration Calorimetry: Experimental Design, Data Analysis, and Probing Macromolecule/Ligand Binding and Kinetic Interactions. *Methods in Cell Biology* **84,** 79–113 (2008).

137. Christensen, J. J., Izatt, R. M., Hansen, L. D. & Partridge, J. A. Entropy Titration. A Calorimetric Method for the Determination of ΔG, ΔH and ΔS from a Single Thermometric Titration. *J. Phys. Chem.* **70,** 2003–2010 (1966).

138. Hansen, L. D., Christensen, J. J. & Izatt, R. M. Entropy Titration. A Calorimetric Method for the determination of ΔG (K), ΔH and ΔS. *Chem. Commun.* **3,** 36–38 (1965).

139. Kessler, R. W. Perspectives in process analysis: Process analysis and technology. *J. Chemom.* **27,** 369–378 (2013).

140. Kessler, R. W. *Prozessanalytik: Strategien und Fallbeispiele aus der industriellen Praxis*. (WILEY-VCH Verlag, 2012).

141. Lyndgaard, L. B. Application of Raman Spectroscopy and Multivariate Data Analysis in Food and Pharmaceutical Sciences. (University of Copenhagen, 2013).

142. Simpson, M. B. in *Process Analytical Technology: Spectroscopic Tools and Implementation Strategies for the Chemical and Pharmaceutical Industries* (2010).

143. Jestel, N. L. in *Process Analytical Technology: Spectroscopic Tools and Implementation Strategies for the Chemical and Pharmaceutical Industries* (2010).

144. Coates, J. P. in *Process Analytical Technology: Spectroscopic Tools and Implementation Strategies for the Chemical and Pharmaceutical Industries* (2010).

145. Liauw, M. A., Baylor, L. C. & Rourke, P. E. O. in *Process Analytical Technology: Spectroscopic Tools and Implementation Strategies for the Chemical and Pharmaceutical Industries* (2010).

146. Skoog, D. A., Holler, J. F. & Crouch, S. R. *Principles of Instrumental Analysis*. (Brooks Cole, 2006).

147. Dickens, J. E. in *Process Analytical Technology: Spectroscopic Tools and Implementation Strategies for the Chemical and Pharmaceutical Industries* 1–15 (2010).

148. Lampman, G. M., Pavia, D. L., Kriz, G. S. & Vyvyan, J. R. in *Spectroscopy* 381–417 (Mary Finch, 2010).

149. Feigenbrugel, V., Loew, C., Le Calvé, S. & Mirabel, P. Near-UV molar absorptivities of acetone, alachlor, metolachlor, diazinon and dichlorvos in aqueous solution. *J. Photochem. Photobiol. A Chem.* **174,** 76–81 (2005).

150. McComb, R. B., Bond, L. W., Burnett, R. W., Keech, R. C. & Bowers, G. N. Determination of the molar absorptivity of NADH. *Clin. Chem.* **22,** 141–150 (1976).

151. Peterson, E. A. & Sober, H. A. Preparation of Crystalline Phosphorylated Derivatives of Vitamin B6. *J. Am. Chem. Soc.* **76,** 169–175 (1954).

152. Faust, B. *Modern Chemical Techniques : An Essential Reference for Students and Teachers*. (Royal Society of Chemistry).

153. Smilde, A. K., Bro, R. & Geladi, P. *Multi-way analysis with applications in the chemical sciences*. (J. Wiley, 2004).

154. Bro, R. PARAFAC. Tutorial and applications. in *Chemometrics and Intelligent Laboratory Systems* **38,** 149–171 (1997).

155. Sackmann, E. K., Fulton, A. L. & Beebe, D. J. The present and future role of microfluidics in biomedical research. *Nature* **507,** 181–9 (2014).

156. Newman, S. G. & Jensen, K. F. The role of flow in green chemistry and engineering. *Green Chem.* **15,** 1456 (2013).

157. Anastas, P. T. & Kirchhoff, M. M. Origins, current status, and future challenges of green chemistry. *Acc. Chem. Res.* **35,** 686–694 (2002).

158. Poliakoff, M., Fitzpatrick, J. M., Farren, T. R. & Anastas, P. T. Green chemistry: science and politics of change. *Science* **297,** 807–810 (2002).

159. Wegner, J., Ceylan, S. & Kirschning, A. Ten key issues in modern flow chemistry. *Chem. Commun. (Camb).* **47,** 4583–4592 (2011).

160. Jensen, K. F., Reizman, B. J. & Newman, S. G. Tools for chemical synthesis in microsystems. *Lab Chip* 3206–3212 (2014). doi:10.1039/c4lc00330f

161. Darvas, F., Dormán, G. & Hessel, V. *Flow Chemistry*. (De gruyter, 2014).

162. Jiménez-González, C., Poechlauer, P., Broxterman, Q. B., Yang, B. S., Am Ende, D., Baird, J., Bertsch, C., Hannah, R. E., Dell'Orco, P., Noorman, H., Yee, S., Reintjens, R., Wells, A., Massonneau, V. & Manley, J. Key green engineering research areas for sustainable manufacturing: A perspective from pharmaceutical and fine chemicals manufacturers. *Org. Process Res. Dev.* **15,** 900–911 (2011).

163. Nagy, K. & Jensen, K. Catalytic processes in small scale flow reactors. *Chem. Today* **29,** 29–31 (2011).

164. McMullen, J. P. & Jensen, K. F. An Automated Microfluidic System for Online Optimization in Chemical Synthesis. *Org. Process Res. Dev.* **14,** 1169–1176 (2010).

165. Schaber, S. D., Born, S. C., Jensen, K. F. & Barton, P. I. Design, Execution, and Analysis of Time-Varying Experiments for Model Discrimination and Parameter Estimation in Microreactors. *Org. Process Res. Dev.* **18,** 1461–1467 (2014).

166. Sahoo, H. R., Kralj, J. G. & Jensen, K. F. Multistep continuous-flow microchemical synthesis involving multiple reactions and separations. *Angew. Chemie - Int. Ed.* **46,** 5704–5708 (2007).

167. Fagaschewski, J., Bohne, S., Kaufhold, D., Müller, J. & Hilterhaus, L. Modular micro reaction engineering for carboligation catalyzed by benzoylformate decarboxylase. *Green Process. Synth.* **1,** 337–344 (2012).

168. Aota, A., Mawatari, K. & Kitamori, T. Parallel multiphase microflows: fundamental physics, stabilization methods and applications. *Lab Chip* **9,** 2470–2476 (2009).

169. Andrade, L. H., Kroutil, W. & Jamison, T. F. Continuous Flow Synthesis of Chiral Amines in Organic Solvents: Immobilization of E. coli Cells Containing Both ω-Transaminase and PLP. *Org. Lett.* **16,** 6092–6095 (2014).

170. Mitic, A., Heintz, So., Ringborg, R. H., Bodla, V., Woodley, J. M. & Gernaey, K. V. Applications, benefits and challenges of flow chemistry. *Chim. Oggi/Chemistry Today* **31,** 4–8 (2013).

171. Roberge, D., Noti, C., Irle, E., Eyholzer, M., Rittiner, B., Penn, G., Sedelmeier, G. & Schenkel, B. Control of Hazardous Processes in Flow: Synthesis of 2-Nitroethanol. *J. Flow Chem.* **4,** 1–9 (2013).

172. Klais, O., Westphal, F., Benaïssa, W. & Carson, D. Guidance on safety/health for process intensification including MS design Pat I: Reaction hazards. *Chem. Eng. Technol.* **32,** 1831–1844 (2009).

173. Whitesides, G. M. The origins and the future of microfluidics. *Nature* **442,** 368–373 (2006).

174. Bird, R. B., Stewart, W. E. & Lightfoot, E. N. *Transport Phenomena*. (2002).

175. Bruus, H. *Theoretical microfluidics*. (Oxford University Press, 2008).

176. He, L. & Niemeyer, B. A novel correlation for protein diffusion coefficients based on molecular weight and radius of gyration. *Biotechnol. Prog.* **19,** 544–548 (2003).

177. Feigin, L. A. & Svergun, D. I. *Structure Analysis by Small-Angle X-Ray and Neutron Scattering*. (Plenum Press, 1987).

178. Ortega, A., Amorós, D. & García De La Torre, J. Prediction of hydrodynamic and other solution properties of rigid proteins from atomic- and residue-level models. *Biophys. J.* **101,** 892–898 (2011).

179. Fischer, H., Polikarpov, I. & Craievich, A. F. Average protein density is a molecular-weight-dependent function. *Protein Sci.* **13,** 2825–2828 (2004).

180. Levenspiel, O. *Chemical reaction engineering*. *Chemical Engineering Science* (John Wiley and Sons inc., 1999). doi:10.1016/0009-2509(64)85017-X

181. Bolivar, J. M. & Nidetzky, B. Multiphase biotransformations in microstructured reactors: opportunities for biocatalytic process intensification and smart flow processing. *Green Process. Synth.* **2,** 541–559 (2013).

182. Hessel, V., Angeli, P., Gavriilidis, A. & Löwe, H. Gas - Liquid and Gas - Liquid - Solid Microstructured Reactors : Contacting Principles and Applications. *Ind. Eng. Chem. Res.* **44,** 9750–9769 (2005).

183. Liu, H. & Zhang, Y. Droplet formation in a T-shaped microfluidic junction. *J. Appl. Phys.* **106,** (2009).

184. Day, P., Manz, A. & Zhang, Y. *Microdroplet Technology: Principles and Emerging Applications in Biology and Chemistry*. *Springer* (Springer Science+Business Media, 2008). at <http://medcontent.metapress.com/index/A65RM03P4874243N.pdf>

185. Van Der Graaf, S., Nisisako, T., Schroën, C. G. P. H., Van Der Sman, R. G. M. & Boom, R. M. Lattice Boltzmann simulations of droplet formation in a T-shaped microchannel. *Langmuir* **22,** 4144–4152 (2006).

186. De Menech, M., Garstecki, P., Jousse, F. & Stone, H. A. Transition from squeezing to dripping in a microfluidic T-shaped junction. *J. Fluid Mech.* **595,** 141–161 (2008).

187. Nisisako, T., Torii, T. & Higuchi, T. Novel microreactors for functional polymer beads. *Chem. Eng. J.* **101,** 23–29 (2004).

188. Kreutzer, M. T., Kapteijn, F., Moulijn, J. A. & Heiszwolf, J. J. Multiphase monolith reactors: Chemical reaction engineering of segmented flow in microchannels. *Chem. Eng. Sci.* **60,** 5895–5916 (2005).

189. Günther, A. & Jensen, K. F. Multiphase microfluidics: from flow characteristics to chemical and materials synthesis. *Lab Chip* **6,** 1487–1503 (2006).

190. De Loos, S. R. A., Van Der Schaaf, J., Tiggelaar, R. M., Nijhuis, T. A., De Croon, M. H. J. M. & Schouten, J. C. Gas-liquid dynamics at low Reynolds numbers in pillared rectangular micro channels. *Microfluid. Nanofluidics* **9,** 131–144 (2010).

191. Ergun, S. Fluid flow through packed columns. *Chem. Eng. Prog.* **48,** 89 – 94 (1952).

192. Caulkin, R., Jia, X., Fairweather, M. & Williams, R. A. Predictions of porosity and fluid distribution through nonspherical-packed columns. *AIChE J.* **58,** 1503–1512 (2012).

193. Nguyen, N.-T. & Wu, Z. Micromixers—a review. *Journal of Micromechanics and Microengineering* **15,** R1–R16 (2004).

194. Zaiput Flow Technologies. doi:xxyy

195. Hartman, R. L., Naber, J. R., Buchwald, S. L. & Jensen, K. F. Multistep microchemical synthesis enabled by microfluidic distillation. *Angew. Chemie - Int. Ed.* **49,** 899–903 (2010).

196. Tufvesson, P., Nordblad, M., Kruhne, U., Schürmann, M., Vogel, A., Wohlgemuth, R. & Woodley, J. M. Economic considerations for selecting an amine donor in biocatalytic transamination. *Org. Process Res. Dev.* **19,** 652–660 (2015).

197. Blow, N. Microfluidics: the great divide. *Nat. Methods* **6,** 683–686 (2009).

198. Bieringer, T., Buchholz, S. & Kockmann, N. Future Production Concepts in the Chemical Industry: Modular - Small-Scale - Continuous. *Chemical Engineering and Technology* **36,** 900–910 (2013).

199. Jensen, K. F., Reizman, B. J. & Newman, S. G. Tools for chemical synthesis in microsystems. *Lab Chip* **14,** 3206–3212 (2014).

200. Ehrfeld. Mikrotechnik BTS. at <http://www.ehrfeld.com/home.html>

201. Syrris. at <http://syrris.com/>

202. Fluidgent. at <http://www.fluigent.com/>

203. Chemtrix. at <http://www.chemtrix.com/>

204. Poulsen, A., Heintz, S., Ringborg, R. H., Woodley, J. M., Gernaey, K. V. & Krühne, U. 3D-printer vejen til innovation? *Dansk Kemi* **94,** 32–34 (2013).

205. Hartman, R. L., McMullen, J. P. & Jensen, K. F. Deciding whether to go with the flow: Evaluating the merits of flow reactors for synthesis. *Angewandte Chemie - International Edition* **50,** 7502–7519 (2011).

206. Valera, F. E., Quaranta, M., Moran, A., Blacker, J., Armstrong, A., Cabral, J. T. & Blackmond, D. G. The flow's the thing...or is it? Assessing the merits of homogeneous reactions in flask and flow. *Angew. Chem. Int. Ed. Engl.* **49,** 2478–85 (2010).

207. Moore, J. S. & Jensen, K. F. Supporting Information to: Batch kinetics in flow: Online IR analysis and continuous control. *Angew. Chemie - Int. Ed.* **53,** 470–473 (2014).

208. National Instrument Driver Network. at <http://www.ni.com/downloads/instrument-drivers/>

209. Fogler, H. S. *Elements of Chemical Reaction Engineering*. (Pearson Education, Inc, 2005).

210. Haynes, W. M. (ed. . *CRC Handbook of chemistry and physics : a ready-reference book of chemical and physical data*. (CRC Press, 2012).

211. Ramires, M. L. V., Castro, C. A. N. De, Nagasaka, Y., Nagashima, a., Assael, M. J. & Wakeham, W. A. Standard Reference Data for Thermal Conductivity of Water. *Advances in Heat Transfer* **18,** 1377–1381 (1994).

212. Bergman, T. L., Lavine, A. S., Incropera, F. P. & DeWitt, D. P. *Introduction to heat transfer*. (WILEY, 2011).

213. Bro, R. & Kiers, H. A. L. A new efficient method for determining the number of components in PARAFAC models. *J. Chemom.* **17,** 274–286 (2003).

214. Ocean Optics. at <www.oceanoptics.com>

215. KNAUER. at <http://www.knauer.net/>

216. IDEX Health and Science. at <https://www.idex-hs.com>

217. Vasić-Rački, D., Findrik, Z. & Vrsalović Presečki, A. Modelling as a tool of enzyme reaction engineering for enzyme reactor development. *Appl. Microbiol. Biotechnol.* **91,** 845–56 (2011).

218. Sin, G., Woodley, J. M. & Gernaey, K. V. Application of modeling and simulation tools for the evaluation of biocatalytic processes: A future perspective. *Biotechnol. Prog.* **25,** 1529–1538 (2009).

219. Berendsen, W. R., Gendrot, G., Freund, A. & Reuss, M. A Kinetic Study of Lipase-Catalyzed Reversible Kinetic Resolution Involving Verification at Miniplant-Scale. *Biotechnol. Bioeng.* **96,** 883–892 (2006).

220. Schaber, S. D., Gerogiorgis, D. I., Ramachandran, R., Evans, J. M. B., Barton, P. I. & Trout, B. L. Economic analysis of integrated continuous and batch pharmaceutical manufacturing: A case study. *Ind. Eng. Chem. Res.* **50,** 10083–10092 (2011).

221. Chen, B. H., Baganz, F. & Woodley, J. M. Modelling and optimisation of a transketolase-mediated carbon–carbon bond formation reaction. *Chem. Eng. Sci.* **62,** 3178–3184 (2007).

222. Lawrence, J., O'Sullivan, B., Lye, G. J., Wohlgemuth, R. & Szita, N. Microfluidic multi-input reactor for biocatalytic synthesis using transketolase. *J. Mol. Catal. B. Enzym.* **95,** 111–117 (2013).

223. Urano, N., Fukui, S., Kumashiro, S., Ishige, T., Kita, S., Sakamoto, K., Kataoka, M. & Shimizu, S. Directed evolution of an aminoalcohol dehydrogenase for efficient production of double chiral aminoalcohols. *J. Biosci. Bioeng.* **111,** 266–271 (2011).

224. Chen, Z. & Zhao, H. Rapid Creation of a Novel Protein Function by in Vitro Coevolution. *J. Mol. Biol.* **348,** 1273–1282 (2005).

225. Truppo, M. D., Rozzell, J. D. & Turner, N. J. Efficient Production of Enantiomerically Pure Chiral Amine at Conc 50 g/L Using Transaminase. *J. Am. Chem. Soc.* **14,** 234–237 (2010).

226. Martin, A. R., DiSanto, R., Plotnikov, I., Kamat, S., Shonnard, D. & Pannuri, S. Improved activity and thermostability of (S)-aminotransferase by error-prone polymerase chain reaction for the production of a chiral amine. *Biochem. Eng. J.* **37,** 246–255 (2007).

227. Halim, M., Rios-Solis, L., Micheletti, M., Ward, J. M. & Lye, G. J. Microscale methods to rapidly evaluate bioprocess options for increasing bioconversion yields: Application to the ω-transaminase synthesis of chiral amines. *Bioprocess Biosyst. Eng.* **37,** 931–941 (2014).

228. Scheer, M., Grote, A., Chang, A., Schomburg, I., Munaretto, C., Rother, M., Söhngen, C., Stelzer, M., Thiele, J. & Schomburg, D. BRENDA, the enzyme information system in 2011. *Nucleic Acids Res.* **39,** 670–676 (2011).

229. Schaber, S. D., Born, S. C., Jensen, K. F. & Barton, P. I. Design, Execution, and Analysis of Time-Varying Experiments for Model Discrimination and Parameter Estimation in Microreactors. *Org. Process Res. Dev.* **18,** 1461–1467 (2014).

230. Tufvesson, P., Lima-Ramos, J., Haque, N. Al, Gernaey, K. V. & Woodley, J. M. Advances in the process development of biocatalytic processes. *Org. Process Res. Dev.* **17,** 1233–1238 (2013).

231. Bondos, S. E. & Bicknell, A. Detection and prevention of protein aggregation before, during, and after purification. *Anal. Biochem.* **316,** 223–231 (2003).

232. Chemspider - search and share chemistry. at <www.chemspider.com>

13 APPENDICES

APPENDIX A – PHYSICOCHEMICAL PROPERTIES OF SUBSTRATES AND PRODUCTS

Table 13.1 - Physicochemical properties of substrates and products from the model reactions [210,232]

	Cas no.	M_w	T_b	ρ	*Log P*	*aq. Sol.*	*pKa*	P_{vap}
		(g/mol)	°C	g/cm^3	-	g/L	-	mmHg (25 °C)
BA	2550-26-7	148.2	236	1±0.1	1.671	1.625		0.1±0.4
MPPA	22374-89-6	149.2	221	0.9±0.1	2.18±0.20	12.05	10.63	0.1±0.4
MBA	618-36-0	121.2	69-70	1±0.1	1.3	54.38	9.83	0.8±0.3
ACP	98-86-2	120.2	202	1±0.1	1.58	4.484		0.3±0.4
IPA	75-31-0	59.1	33-34	0.7±0.1	0.21±0.19	Miscible	10.6	460
ACE	67-64-1	58.08	56	0.8±0.1	-0.16±0.19	Miscible		180
ALA	302-72-7	89.09	-	1.2±0.1	-0.679	164	2.35/9.69	0.1±0.9
PYR	127-17-3	88.06	165	1.3±0.1	-1.24±0.39	High	2.5	1.0±0.6

APPENDIX B – HPLC ANALYTICAL METHODS

The HPLC was a Dionex Ultimate 3000 (Dionex, Sunnyvale, CA, USA), with an UV photodiode array detector, and was applied to determine the concentrations of MPPA and BA. The compounds were separated using a Gemini-NX 3µ C18 110Å (100 x 2 mm) column (Phenomenex, Torrance, CA, USA). The details on how the method was operated are listed in Table B..

Table B.1 - HPLC method for determination of 1-methyl-3-phenylpropylamine (MPPA), benzylacetone (BA),

Method settings	
Mode	Isocratic
Flow	0.450 mL/min
Mobile phase	35 % Acetonitrile
	65% H_2O pH-11 (adj. by NaOH)
Column	Gemini-NX 3µ C18 110Å (100 x 2mm)
T_{oven}	30 ℃
Detection	2.67 min (210 nm) - MPPA
	3.63 min (210 nm) - BA
Time of analysis	5 min
Std. Inj. Vol.	1 µL

An example of a spectrum of a sample containing both MPPA and BA is shown in Figure B.13.1.

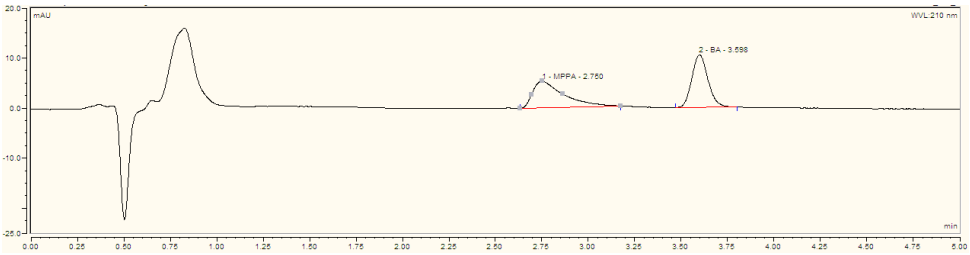

Figure B.13.1 - Spectrum obtained from a solution of MPPA, BA, IPA and Ace

The quantitative analysis was performed from peak areas by external standards. The generated standards are highlighted below in Figure B.13.2 and Figure B.13.3 for BA and MPPA, respectively.

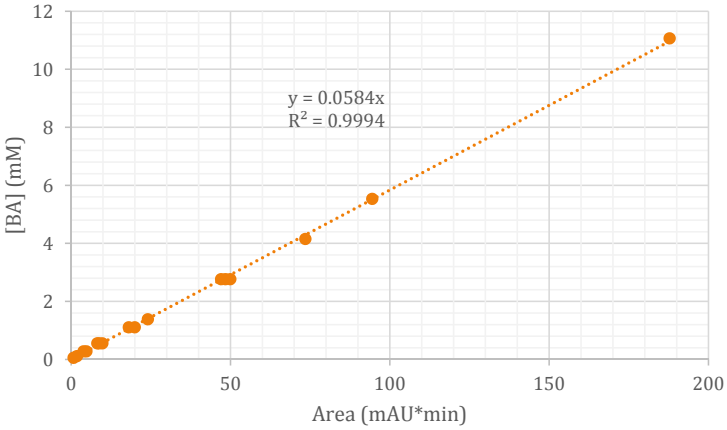

Figure B.13.2 - Standard curve for Benzyl Acetone (BA) at 210 nm

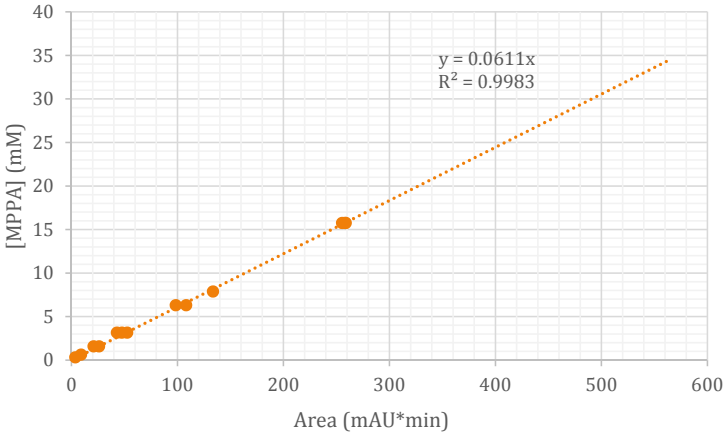

Figure B.13.3 - Standard curve for 1-Methyl-3-phenylpropylamine (MPPA) at 210 nm

APPENDIX C – PUBLICATIONS

Krist V. Gernaey

Applications, benefits and challenges of flow chemistry

PEER REVIEWED

ALEKSANDAR MITIC, SØREN HEINTZ, ROLF H. RINGBORG, VIJAYA BODLA, JOHN M WOODLEY, KRIST V. GERNAEY*

*Corresponding author

1. Technical University of Denmark (DTU), Department of Chemical and Biochemical Engineering, Søltofts Plads, Building 229, 2800 Kgs. Lyngby, Denmark

KEYWORDS

Flow chemistry; Organic Synthesis; Biocatalysis; Process Analytical Technology (PAT); Microreactor Technology.

ABSTRACT

Organic synthesis (incorporating both chemo-catalysis and biocatalysis) is essential for the production of a wide range of small-molecule pharmaceuticals. However, traditional production processes are mainly based on batch and semi-batch operating modes, which have disadvantages from an economic, environmental and manufacturing perspective. A potential solution to resolve these issues is to use flow chemistry in such processes, preferably with applications of micro- and mini-sized equipment. In addition, Process Analytical Technology (PAT) may be implemented in a very efficient way in such equipment due to the high degree of automation and process controllability that can be achieved in small scale continuous equipment.

INTRODUCTION

Continuous production is often cited as both eco-friendly and economic, mainly due to the higher energy efficiency and reduced consumption of resources that can be achieved in comparison with traditional batch production (1-4). Furthermore, continuous production fulfills very well the requirements defined by the regulatory bodies, such as the Food and Drug Administration (FDA). More particularly, the FDA has clearly indicated that it favors such processes – including on-line measurement and control – with the publication of the Process Analytical Technology (PAT) guidance in 2004 (5). PAT defines the key Initiative of cGMP (6) and is incorporated into the International Conference on Harmonization (ICH) Q8 guidance (7). The Initiative has shown many advantages in modern organic synthesis and biotechnology, and has consequently been applied in other industry sectors, such as food, chemical and life sciences (8). The objective of this manuscript is to briefly review applications of flow chemistry in modern organic synthesis. Furthermore, the focus will be on emphasizing the benefits of such processes and additionally on identifying the remaining challenges for further improvement.

MICRO-CHEMICAL PROCESSING IN ORGANIC SYNTHESIS

Organic synthesis can be performed in continuous mode by using mini- and micro-structured flow devices. Small scale continuous flow technology has many potential advantages, such as: rapid heat and mass transfer, increased safety, easy scale-up/scale-out, fast process characterization, potential for real-time release, operation with unstable reaction species, and so on (9, 10). Due to such advantages integration of these small scale devices in plant architectures has become more common in the last two decades (11). It is important to note here that not all chemical reactions are suited to such small-scale equipment. For example, according to Roberge et al. (12), chemical reactions with a half-life higher than 10 min should preferably be operated in batch manufacturing mode. However, it has been demonstrated that some of these reactions too could be drastically accelerated by downsizing the equipment to a micro-scale level (13). Furthermore, chemical reactions with very reactive substrates, such as Grignard exchange reactions and reactions with chloride, bromide and amine species are all very suitable for flow chemistry applications. These reactions, with typical half-lives below 1 s, can therefore be completed in the mixing zone alone (12, 14, 15). Finally, chemical reactions with half-lives from 1 s up to 10 min could also benefit from the micro-scale devices (16). Better control of heat flow and temperature are the main advantages of operating such reactions at micro-scale (12).

The kinetics of biocatalytic processes (mixed order, obeying Michelis-Menten) will always be best exploited in a batch or continuous plug flow mode, especially for reactions requiring a high conversion. For this reason, continuously stirred tank reactors are rarely used for biocatalytic reactions in industry. However, at reasonable concentrations for industrial implementation most biocatalytic reactions are limited by substrate inhibition, meaning that a fed-batch system becomes favorable. Often the product too is inhibitory which is most normally dealt with, by *in-situ* product removal (ISPR) (1, 3, 17-19). Such a combination of 'feed and bleed' combined with the mixed order kinetics, characteristic of an enzyme catalyzed reaction, implies that a batch with feed and ISPR, or alternatively a plug flow with multiple feed and product removal points down the column, would be attractive. Hence, we believe that flow chemistry also can be attractive to biocatalysis. Performing synthesis at micro-scale is even more attractive when one considers

the small amounts of material (both substrates and products) available at an early stage of biocatalytic process development. Operating in plug flow enables the effective testing of immobilized enzyme formats as well, and simplifies integration with the neighboring chemical operations (20). Besides the limiting effects of inhibitions at industrially relevant process conditions, there are also situations where the reaction equilibrium of the biocatalytic processes is unfavorable. In those situations it is necessary to use different methodologies to shift the equilibrium towards the desired products. For example *in-Situ* co-Product Removal (IScPR) is a potential solution enabling higher yields and productivities (21, 22).

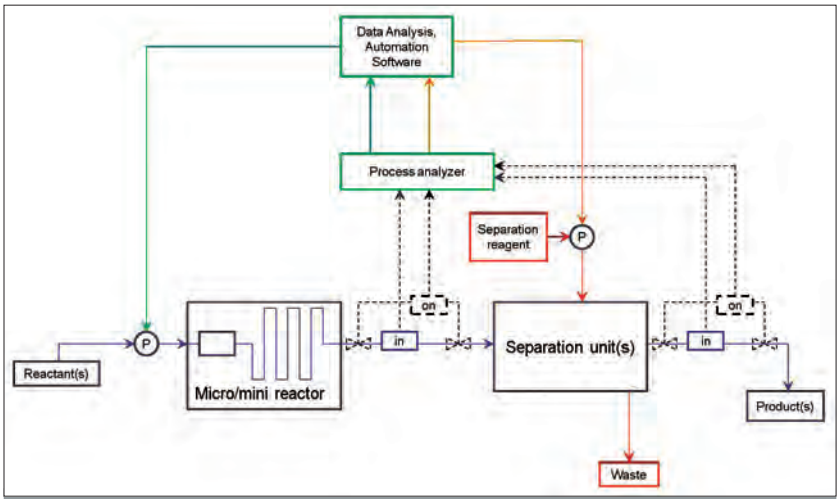

Figure 1. Simplified scheme of the Lab-on-a-chip system with implemented PAT requirements. Blue solid line – main flow; blue dashed line – process signal obtained by in-line process monitoring; black dashed line – on-line process monitoring and resulting process signal; green solid line – data from a process analyzer to data analysis section intended to establish process control and automation of the pumps for the reactor section; yellow solid lines – data from a process analyzer to data analysis section intended to establish process control and automation of the pumps for the separation section; red solid line – separation agent and waste material flow.

The benefits of flow systems have been reported to some extent in the scientific literature, for both simple and more complex systems. One example of relatively simple biocatalytic systems is using lipase (EC. 3.1.1.3). The enzyme is particularly robust in non-natural environments, e.g. high concentrations, organic solvents, etc. (3, 23, 24). An example of more complex biocatalytic systems is the use of ω-transaminase (ω-TA – EC. 2.6.1.1) to transfer an amine to a prochiral ketone. Transaminase based biocatalytic processes typically experience severe substrate and product inhibition, along with unfavorable reaction equilibrium depending on the choice of amine donor (21, 25). In preliminary work Bodla et al. (26) showed improved productivity in micro-scale systems compared to conventional batch methods for such a reaction.

INTEGRATION OF MICROREACTORS IN THE PLANT ARCHITECTURE

Even though they are only suited for micro-chemical processing, miniaturized total analysis systems (μ-TAS) or lab-on-a-chip systems are receiving increasing attention in the process industries. This approach integrates all analytical steps on the same platform (27), and could thereby successfully avoid unnecessary storage of intermediate products. In this way, faster manufacturing of a desired compound could be obtained, as well as circumventing significant losses in processes with very reactive substrates and intermediates. A simplified process flow scheme of such lab-on-a-chip system is shown in Figure 1, together with integrated process in-/on-line monitoring, process control and automation.

The previous section was entirely focused on the reaction step in continuous flow. However, incorporation of multi-step chemical synthesis in micro-scaled devices usually necessitates coupling the reaction step(s) with a subsequent continuous separation step. Traditional separation approaches for two immiscible liquids at macro-scale levels are mainly based on gravitational forces. However, if downsizing is applied, surface forces become dominant (9).

A recent lab-scale example with the use of a hydrophobic membrane separator (Figure 2) showed great efficiency for separating two immiscible liquids (28). However, it requires long-term tests at industrial scale before such membrane separators will be accepted by industry. While waiting for the results of such trials, development of separators without membranes is preferred (29). Furthermore, effective separation of two miscible liquids has been achieved by applying micro-evaporation principles (30), as well.

Solid particles form a major issue in meso- and especially in micro-scaled equipment. One successful approach for handling solids is to use acoustic irradiation, which is often applied in modern organic synthesis with the main purpose to avoid bridging inside the channels. Another phenomenon called constriction could also cause potential problems in small scale flow devices, and it is usually avoided by using different fluid velocities, or more precisely by applying periodical flushing actions. Assuming constant concentrations of starting materials or formed particles present inside micro-channels, the extent of such constriction phenomena could be predicted. Indeed, assuming constant inflow conditions, quantification of the constriction rates is possible on the basis of simple measurements of pressure drops along the microchannels (31).

For biocatalytic applications it will often be a necessity to operate these systems in the presence of solids, e.g. as a consequence of the biocatalyst formulation (see below), or in some cases due to reaction species with low solubilities (21, 24). Operating biocatalytic processes in these miniaturized modules can therefore, for many applications, be expected to give some precipitation and clogging problems, which have to be overcome (33, 34). Use of unconventional reaction media, e.g. organic solvents, can result in avoiding high concentrations of insoluble compounds. However, unconventional reaction media can have severe effects on the biocatalyst performance, e.g. toxic and denaturizing effects (34). Protein engineering here provides the means to modify the biocatalyst in a manner so it becomes more resistant to operation in non-conventional media (1, 2). Protein engineering is generally used for biocatalyst modifications to improve performance in process relevant conditions (22).

The formulation of the biocatalyst can also cause clogging.

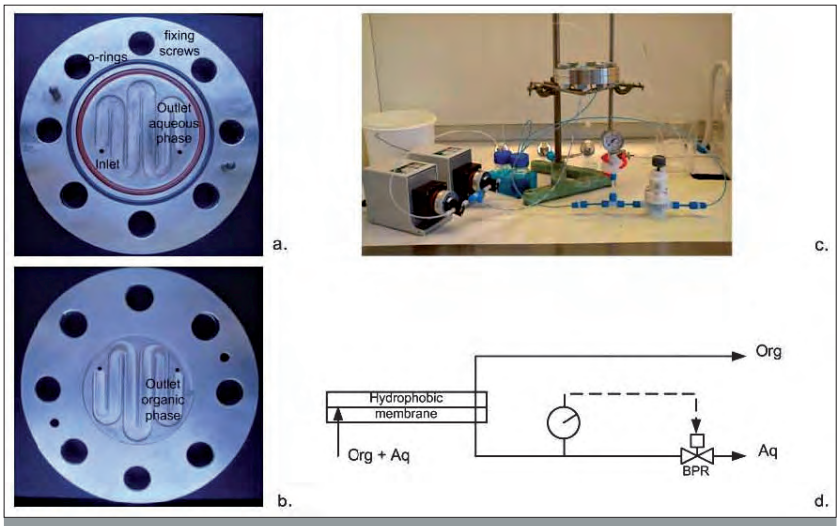

Figure 2. A PTFE membrane separator applicable for splitting two immiscible liquids. a. Part of the separator intended for the aqueous phase. b. Part of the separator intended for the organic phase. c. Image of the PTFE membrane separator with aqueous phase coloured in blue and uncoloured toluene phase. d. Scheme of the PTFE membrane separator setup (28).

The formulation of the biocatalyst is highly dependent on the process economics, e.g. the feasibility of a biocatalytic process can be greatly improved by applying the biocatalyst in the crudest possible form (35), as a consequence of reduced purification costs. It can therefore for some applications be necessary to use solutions potentially containing precipitate, polymers, cells, etc. resulting in clogging issues caused by adhesion of compounds or cells to surfaces (36). Also, for some applications the biocatalysts are immobilized onto solid supports with the purpose of improving the catalyst stability along with simplification of catalyst recirculation (37). For some biocatalytic applications, we expect that it will be ideal to use the biocatalyst directly from the fermentation, without any major purification steps beforehand. This could greatly improve process feasibility, but at the same time result in potential issues with regards to high solid concentrations in flow systems.

The majority of new synthetic pathways in organic chemistry involve chemical catalysts and in some cases biocatalysis as one step in the otherwise chemical synthetic sequence. Hence, removal of transition metals is still receiving considerable attention in pharmaceutical production. Due to the high toxicity of these chemical elements, the allowed concentrations in final products are usually very low (38) and thereby very efficient metal removal procedures are required. Currently, most procedures are based on batch processing (39), however, examples with packed-bed columns showed promising performance in flow, as described by Wiles et al. (40).

DOWNSTREAM PROCESSING

Besides developing efficient synthesis pathways in miniaturized systems, there is also a demand for efficient inline downstream methods in order to recover and purify products. The high surface-to-volume ratios attainable at micro-scale result in faster mass transfer suggesting improved effectiveness of such systems compared to macro-scale. Combining upstream with downstream unit operations in micro-chemical or biochemical processing enables testing entire processes on a bench – e.g. factory-on-a-bench. In some situations it might even be desired to run the actual process on a bench. However, there is a clear need for miniaturized equivalents of large scale downstream unit operations before this factory-on-a-bench concept can be fully realized. There has been some focus already on providing such miniaturized unit operations (41, 42). Here the main focus will be on continuous extraction in flow systems.

Liquid-liquid extraction (LLE) is a well-established product recovery method in the pharmaceutical industry. Laminar flow conditions experienced in micro-scale extraction units give the possibility to operate with both segmented and side-by-side flows. Side-by-side flow operation allows easy laminar flow splitting in a continuous manner, and both extraction in concurrent and counter current flow modes can be established. Segmented flow operation improves the mass transfer by diffusion, due to an even higher surface area than side-by-side flow. However, it is not possible to separate the segments by gravitational forces as in conventional methods, because surface tension forces are dominant in micro-scale. LLE with segmented flows requires other separation methods, e.g. membrane separation units have shown great potential for continuous separation in such flow systems (43). For biocatalytic applications there can be issues concerning biocompatibility and phase toxicity if streams are recycled, and specifically for such applications it would be necessary to modify biocatalysts to operate efficiently in the presence of organic solvents (protein engineering, see previous section).

Solid-liquid extraction using particles (resins etc) is an attractive alternative option to processes where organic solvents exhibit operational challenges, e.g. biocompatibility, phase toxicity, emulsification, etc. Porous resins, in general, are inert, easy to handle and simplify product isolation (filtration). In biocatalysis, resins can additionally be used to enhance the reaction performance for reactions with kinetic limitations. This is achieved by using them as an auxiliary phase for substrate supply and product removal (ISPR) by integrating the reaction and extraction steps. However, at micro-scale and more specifically in flow systems, one important limitation is that solid reagents are difficult to handle as they may clog micro-channels.

High surface-to-volume ratios attainable at microscale result in faster mass transfer suggesting the improved effectiveness of such systems compared to macro-scale. However, the increase in pressure drop needs to be addressed with a suitable reactor design solution. Losey et al. (44), for example, reported an increase in mass transfer by more than 2 orders of magnitude for cyclohexene hydrogenation in a micro packed bed reactor, using activated carbon catalyst,

compared to a macro scale counterpart. The increase in pressure drop was in that case addressed by splitting the flow into multiple channels and thus reducing the overall pressure drop while retaining the effective cross-sectional area and obtaining higher reactor throughput.

PROCESS MONITORING, CONTROL AND AUTOMATION

Efficient production of the desired compounds is the main goal in organic synthesis. Operating the processes in an efficient manner does however require a high degree of process understanding to enable improved monitoring and control. It is though very challenging to implement in-line monitoring in micro-scale systems because of the small dimensions required for the sensors, as well as the fact that analysis of very complex process signatures is needed. Traditional applications based on in- and on-line spectroscopic methods are desired even though they are difficult to obtain. A recent example of process monitoring and control in flow was published by Cervera-Padrell et al. (45).

Fulfilment of the PAT requirements involves automation of the established processes. Several successful case studies have been reported using different kinds of commercially available software (46). The most desired way is to perform in/on-line process monitoring and control due to the very fast response that can be obtained. Consequently, faster data analysis is achieved and, for example, corrective actions to avoid or reduce side reactions are performed easily, which is essential for fast reactions.

Besides using miniaturized systems for operation of complex biocatalytic processes, there is also the possibility of using these miniaturized systems for process development and research purposes. The micro-scale flow systems indeed have the potential of being powerful tools which can aid in detailed process screenings and biocatalyst characterization under realistic process conditions. Early, in the development of new biocatalytic processes, there is limited availability of resources, e.g. biocatalyst to be tested. The limited availability of resources puts some constraints on how many experiments can be performed. The level of system detail is therefore also determined by the available quantity of the biocatalyst to be tested, and this should be enough to evaluate the potential of a given process. The use of miniaturized systems for process investigations enables more detailed characterization with lower sample volumes and could be used to set up sophisticated models describing the systems. There are however limitations with regard to how low the sampling volumes can become before analytical limitations become a hindrance, as illustrated in Figure 3.

CONCLUSIONS AND FUTURE PERSPECTIVES

Flow chemistry in meso- and micro-scale devices has found many useful applications in modern organic synthesis and increasingly also in biocatalytic processes. Increased selectivity and yields, increased safety, and additional benefits lead to higher applicability of these processes in the modern pharmaceutical industry, especially in relation to complex processes. Furthermore, easier implementation of the requirements defined by the PAT Initiative has made flow chemistry into a key focus point.

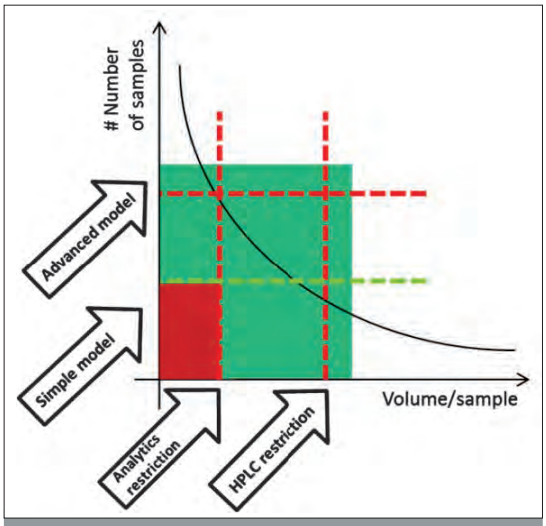

Figure 3. Illustration of the correlation between analytical limitations and model complexity, when availability of resources is scarce during process development. E.g. multiple data points are required for more sophisticated models, but the volume per sample for analytical measurements gives restrictions to the number of samples which can be obtained when having scarce resources.

However, obstacles in performing process monitoring and consequently process controls in micro-scaled devices are still a major challenge. Hence, further focus is on the development of better data analysis tools in order to facilitate efficient process control actions on the basis of the collected data.
Extrapolating from these miniaturized systems to larger production volumes can mainly be done in two ways, by means of scale-up or scale-out (numbering-up). When considering scale-up, this can introduce additional obstacles as a consequence of altered reaction and flow conditions. It is therefore essential to develop tools that can help to predict the cost to scale-up and scale-out, respectively, and to use such tools to support decision making when designing the production process.

ACKNOWLEDGEMENTS

The authors acknowledge the support of: (1) project BIOINTENSE, financed through the European Union 7th Framework Programme (Grant agreement no.: 312148); (2) the Danish Council for Independent Research | Technology and Production Sciences (project number: 10-082388).

REFERENCES AND NOTES

1. Pollard, D.J., Woodley, J.M., *Trends Biotechnol.*, **25(2)**, 66-73 (2006).
2. Bornscheuer, U.T., Huisman, G.W., et al., *Nature*, **485**, 185-194 (2012).
3. Schmid, A., Dordick, J., et al., *Nature*, **409**, 258-268 (2001).
4. Baughman E., *Process Analytical Chemistry: Introduction and Historical Perspectives*, Chapter 1, in *Process Analytical Technology-Spectroscopic Tools and Implementation Strategies for the Chemical and Pharmaceutical Industries*, Edited by Bakeev, K.E., Ed. Blackwell Publishing Ltd, Oxford, Iowa, USA (2005).
5. FDA, *Guidance for Industry. PAT - A framework for innovative pharmaceutical manufacturing and quality assurance*, U.S. Food and Drug Administration, U.S. Department of Health and Human Services, Rockville, USA (2004).
6. FDA, *Drug Applications and Current Good Manufacturing Practice (CGMP) Regulations*, U.S. Food and Drug Administration, U.S. Department of Health and Human Services, Rockville, USA (2004).
7. FDA, *Guidance for Industry. Q8 Pharmaceutical Development*. U.S. Food and Drug Administration, U.S. Department of Health and Human Services, Center for Drug Evaluation and Research (CDER), Center for Biologics Evaluation and Research (CBER), International Conference of on Harmonization (2006).
8. Workman, J., Koch, M., et. al., *Anal. Chem.*, **81(12)**, 4623-4643 (2009).
9. Hartman, R.L., Jensen, K.F., *Lab Chip*, **9(17)**, 2495-2507 (2009).
10. Hessel, V., Löb, P., et al., *Microstructured Reactors for Development and Production in Pharmaceutical and Fine Chemistry*, in *New Avenues to Efficient Chemical Synthesis: Emerging Technologies*. Edited by Seeberger, P.H., Blume, T., Ed. Springer-Verlag, Berlin, Heidelberg, Germany (2007).
11. Ehrfeld, W., Hessel, V., et al., *Microreactors*, Chapter 22, in *Ullmann's Encyclopedia of Industrial Chemistry*, Edited by Bohnet, M., Ullman, F., Ed. Wiley Online Library, Weinheim, Germany (2003).
12. Roberge, D.M., Ducry, L., et al., *Chem. Eng. Technol.*, **28(3)**, 318-323 (2005).
13. Damm, M., Glasnov, T.N., et al., *Org. Process Res. Dev.*, **14(1)**, 215-224 (2009).
14. Riva, E., Gagliardi, S., et al., *Tetrahedron*, **66(17)**, 3242-3247 (2010).
15. Wakami, H., Yoshida, J-I., *Org. Process Res. Dev.*, **9(6)**, 787-791 (2005).
16. Wiles, C., Watts, P., *Expert Opin. Drug Discovery*, **2(11)**, 1487-1503 (2007).
17. Carstensen, F., Apel, A., et al., *J. Membr. Sci.*, **394-395**, 1-36 (2012).
18. Truppo, M.D., Turner, N.J., *Org. Biomol. Chem.*, **8**, 1280-1293 (2010).
19. Truppo, M.D., Rozzell, J.D., et al., *Org. Process Res. Dev.*, **14**, 234-237 (2010).
20. Hailes, H.C., Dalby, P.A., et al., *J. Chem. Technol. Biotechnol.*, **82**, 1063-106 (2007).
21. Tufvesson, P., Lima-Ramos, J., et al., *Biotechnol. Bioeng.*, **108(7)**, 1479-1493 (2011).
22. Woodley, J.M., *Curr. Opin. Chem. Biol.*, **17(2)**, 1-7 (2013).
23. Itabaiana Jr., I., Miranda, L.S., et al., *J. Mol. Catal. B: Enzym.*, **85-86**, 1-9 (2013).
24. Tufvesson, P., Fu, W., et al., *Food and Bioprod, Process.*, **88(1)**, 3-11 (2010).
25. Malik, M.S., Park, E.S., et al., *Appl. Microbiol. Biotechnol.*, **94(5)**, 1163-1171 (2012).
26. Bodla, V.K., Seerup, R., et al., *Chem. Eng. Technol.*, **36(00)**, 1–11 (2013).
27. Manz, A., Graber, N., et al., *Sens. Actuators, B*, **1-6**, 244-248 (1990).
28. Cervera-Padrell, A.E., Morthensen, S.T., et al., *Org. Process Res. Dev.*, **16(5)**, 888-900 (2012).
29. Burns, J., R., Ramshaw, C., *Chem. Eng. Res. Des.*, **77(3)**, 206-211 (1999).
30. Wootton, R.C.R., deMello, A.J., *Chem. Commun.*, 266-267 (2004).
31. Hartman, R.L., Naber, J.R., et al., *Org. Process Res. Dev.*, **14(6)**, 1347-1357 (2010).
32. Jensen, K.F., *Microchemical systems for Discovery and Development, in New Avenues to Efficient Chemical Synthesis: Emerging Technologies*. Edited by Seeberger, P.H., Blume, T., Ed. Springer-Verlag, Berlin, Heidelberg, Germany (2007).
33. Hartman, R.L., *Org. Process Res. Dev.*, **16(5)**, 870-887 (2012).
34. Klianov, A.M., *Trends in Biotechnol.*, **15(3)**, 97-101 (1997).
35. Tufvesson, P., Lima-Ramos, J., et al., *Org. Process Res. Dev.*, **15(1)**, 266-274 (2011).
36. Lu, H., Koo, L.Y., et al., *Anal. Chem.*, **76(18)**, 5257-5264 (2004).
37. Mateo, C., Palomo, J.M., et al., *Enzyme Microb. Technol.*, **40(6)**, 1451-1463 (2007).
38. Garrett, C.E., Prasad, K., *Adv. Synth. Catal.*, **346(8)**, 889-900 (2004).
39. Corbet, J-P., Mignani, G., *Chem. Rev.*, **106(7)**, 2651-2710 (2006).
40. Wiles, C., Watts, P., *Review*, **2(11)**, 1487-1503 (2007).
41. Aota, A., Mawatari, K., Kitamori, T., Lab Chip, 9(17), 2470-2476 (2009).
42. Hartman, R.L., Sahoo, H.R., Yen, B.C., Jensen, K.F., *Lab Chip*, **9(13)**, 1843-1849 (2009).
43. Kralj, J.G., Sahoo, H.R., Jensen, K.F., *Lab Chip*, **7(2)**, 256-263 (2007).
44. Losey, M.W., Schmidt, M.A., et al., *Ind. Eng. Chem. Res.*, **40**, 2555-2563 (2001)
45. Cervera-Padrell, A.E., Nielsen, J.P., et al., *Org. Process Res. Dev.*, **16(5)**, 901-914 (2012).
46. Chew, W., Sharratt, P., *Anal. Methods*, **2(10)**, 1412-1438 (2010).

Review

Ulrich Krühne, Søren Heintz, Rolf Ringborg, Inês P. Rosinha, Pär Tufvesson, Krist V. Gernaey and John M. Woodley*

Biocatalytic process development using microfluidic miniaturized systems

Abstract: The increasing interest in biocatalytic processes means there is a clear need for a new systematic development paradigm which encompasses both protein engineering and process engineering. This paper argues that through the use of a new microfluidic platform, data can be collected more rapidly and integrated with process modeling, can provide the basis for validating a reduced number of potential processes. The miniaturized platform should use a smaller reagent inventory and make better use of precious biocatalysts. The EC funded BIOINTENSE project will use ω-transaminase based synthesis of chiral amines as a test-bed for assessing the viability of such a high throughput biocatalytic process development, and in this paper, such a vision for the future is presented.

Keywords: biocatalysis; microfluidics; process development; transaminase.

***Corresponding author: John M. Woodley,** Center for Process Engineering and Technology, Department of Chemical and Biochemical Engineering, Technical University of Denmark, 2800 Lyngby, Denmark, e-mail: jw@kt.dtu.dk
Ulrich Krühne, Søren Heintz, Rolf Ringborg, Inês P. Rosinha, Pär Tufvesson and Krist V. Gernaey: Center for Process Engineering and Technology, Department of Chemical and Biochemical Engineering, Technical University of Denmark, 2800 Lyngby, Denmark

1 Introduction

The increasing academic and industrial interest in biocatalytic processes (chemical reactions catalyzed by an isolated enzyme, immobilized enzyme, or whole cell containing one or more enzymes) is to a large extent driven by the need for selective chemistry [1]. Even more remarkable is that such selectivity is achieved with enzymes under mild reaction conditions. While high selectivity may be easily achievable using biocatalysis, for implementation in industry, it is also necessary to develop a process that is sufficiently efficient that it can be economically feasible. For example, for a pharmaceutical intermediate, a product concentration over 50 g/l must leave the reactor and a high yield of product on biocatalyst (termed biocatalyst yield) must also be achieved [2, 3]. The exact threshold values depend on the type of catalyst and the industry sector (or more accurately the selling price of the product relative to the cost of the substrate). However, almost without exception, a new biocatalytic process studied in the laboratory will not fulfill these requirements, since enzymes are usually evolved to convert natural substrates at low concentrations. This presents an interesting challenge for process chemists and engineers, since the wish to implement a new (non-natural) substrate at high concentrations can only be addressed by a concerted development effort with a combination of biocatalyst modification and process modification. The driver for such process development is economic and while targets can be evaluated in a given case, there remains a further problem, because there are many options to choose from and different routes to solve a given problem [4]. While some solutions are more effective than others, and some are easier to implement than others, there remain many choices to be made. One consequence of such complexity is that to date such an analysis has inevitably been carried out on a case-by-case basis, meaning that often the final scale-up and implementation does not even take place, because it takes too long and is too difficult. Furthermore, in many cases, at an early stage it is not clear which way to develop the process and where to put the research effort. In order to overcome this, one potential vision for the future could be a systematic procedure for automated data collection, followed by testing of a more limited number of alternatives at a miniature scale, such that operations can be carried out with a reduced reagent inventory and potentially even in parallel. Indeed, such schemes already exist for chemical synthetic systems and while the level of complexity with biocatalysis is frequently greater, it is also the case that their value might be the greater. At the very least, it would enable more process options to be evaluated in a shorter time (see Figure 1 for a schematic representation of the philosophy).

Combined with process modeling techniques (Krühne et al., 2013, submitted for publication), this could provide

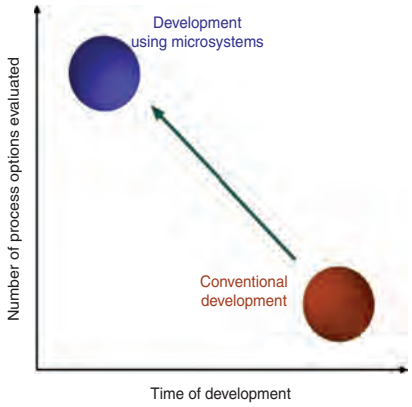

Figure 1 Philosophy underlying miniaturization in the context of process development for biocatalytic processes.

a way to map the solution space and enable design decisions to be made more rapidly and with greater confidence. This is one of the main objectives of the EC-funded BIOINTENSE project. In this brief article, the rationale behind high throughput biocatalytic process development will be discussed, together with the challenges and opportunities such an approach can bring. One of the most important application areas of biocatalytic processes is in the synthesis of pharmaceutical intermediates, where speed of development (and integration with the neighboring catalytic steps) is of the utmost importance.

2 Biocatalytic process development in the pharmaceutical sector

In the pharmaceutical industry, process development time is critical (both for chemical as well as biocatalytic synthetic steps) and therefore it is essential to evaluate and screen process options rapidly. For biocatalytic processes, in order that resources spent on development are used in the most efficient manner possible, a systematic method is necessary to help identify the process constraints (reaction related constraints as well as biocatalyst related constraints). The constraints form the basis of a methodology to identify suitable improvement strategies.

For biocatalytic processes, several strategies are available to improve the process from the initial laboratory reaction, so that it is suitable for industrial application. Strategies focused on reducing the cost contribution of the biocatalyst include fermentation technology (e.g., optimization of the production host platform, carbon feeding strategy, oxygen supply and media composition) to reduce the cost of producing the biocatalyst, as well as protein engineering and biocatalyst immobilization to ensure that the biocatalyst (irrespective of its cost) is subsequently used in the most effective way possible (maximum biocatalyst yield: kg product/kg biocatalyst). Strategies focused on reducing the other cost contributions include reaction engineering (e.g., addition of an organic solvent or use of substrate excess), reactor engineering (e.g., substrate feeding), or process engineering (e.g., *in situ* product removal), to enable the process to run as effectively as possible (maximum reaction yield, biocatalyst yield and product concentration). Additionally, it is important to recognize the interaction between the strategies.

Interestingly, several recent reviews about the application of protein engineering strategies to solve biocatalytic process challenges have argued that the advances in protein engineering now make it possible to 'fit' the biocatalyst to the process [5, 6], as originally proposed by Burton and coworkers [7]. Therefore, once initial activity for the desired reaction has been detected, the enzyme performance can indeed be enhanced by protein engineering, to improve the desired properties, such as substrate repertoire and selectivity, as well as activity and stability [8]. Today, there are many examples where new biocatalytic routes have been established through significant improvement of an existing enzyme, via iterative rounds of mutagenesis and screening [5, 6, 9, 10]. However, despite the remarkable advances in protein engineering, we are yet to be convinced that it is possible to fit the biocatalyst to all process conditions. For example, while optimal operating conditions for a biocatalyst can be expanded significantly from pH 7 and ambient temperature, enzymes still have limitations when compared to chemical catalysts (which in general operate at high concentrations of substrates and products, as well as elevated temperatures [11]), meaning that operation under extreme conditions may not be possible. However, of even greater importance is the fact that the thermodynamic constraints of the process cannot be addressed by biocatalyst modifications directly. While in nature, enzymes usually catalyze thermodynamically favorable reactions, for non-natural substrates as well as reactions run in synthetic mode, this is frequently not the case. Thus, the design of any process needs to also consider the likely operating space for the biocatalyst and the implication of changing key parameters on the process feasibility and cost [4].

3 Process development using microfluidic miniaturized systems

Microfluidic technologies concern the use of fluids in small compartments (e.g., with a size in the order of µl

volumes and with dynamic flow driven by pressure gradients or other methods). Such technologies are sometimes referred to as micro unit operations (MUOs), where the basic concept is to have conventional large scale equipment mimicked at a micro scale (e.g., reactors and separators [12]). However, microfluidic devices also enable novel process development methods [13–15]. At small scale, different physical effects dominate the flow compared to larger scale technologies. Microfluidic technologies exploit these effects in a way that simply cannot be achieved at a larger scale. Often these dominant effects are described by dimensionless numbers [16]:

- In microfluidic devices, the Reynolds number (*Re*), the ratio of convective to viscous forces, is low (*Re*<100 and usually around 1) indicating that viscous forces are dominating and thereby laminar flows are obtained:

$$Re=\frac{\rho v d_h}{\mu}$$

  where ρ is the fluid density, v is the fluid velocity, d_h is the hydraulic diameter (4A/P, where A is the cross sectional area and P the wetted perimeter) and μ is the fluid viscosity.
- The Péclet (*Pe*) number, the ratio of mass transfer rate due to convection compared to that of diffusion, becomes small in microfluidic devices, indicating that the rate of mass transport is dominated by diffusion:

$$Pe=\frac{va}{D}$$

  where D is the diffusion coefficient and a is the radial length scale.
- The bond number (*Bo*), the ratio of gravitational forces to those caused by surface tension, is small in microfluidic devices, as a consequence of dominant surface tension forces, i.e., *Bo*<<1:

$$Bo=\frac{\rho g a^2}{\gamma}$$

  where g is the gravitational acceleration ($9.81\ \frac{m}{s^2}$) and γ is the surface tension.
- The Damköhler number (*Da*) is another important dimensionless number for the characterization of microfluidic systems. This number is used to relate the chemical or biochemical reaction timescale to other phenomena that occur in miniaturized systems. This can, for instance, be the material transport due to diffusion, interphase transport and fluid dynamic convective driving forces. The mathematical description is omitted here due to the dependency on the specific case considered.

At a larger scale these effects do not have such a significant impact, which may result in problems when transferring processes from micro to large scale and *vice-versa*. However, it is quite common with conventional technologies to experience problems when transferring knowledge obtained at the lab scale to the industrial scale. Alternatively, rather than scaling-up by increasing dimensions, microfluidic systems can be numbered-up/parallelized in order to obtain the desired process throughput (although clearly there is a cost penalty since 'economies of scale' are lost). Indeed, this scaling strategy is, in many cases, not straightforward due to operating and handling issues of many systems in parallel [17].

Nevertheless, for screening of reactions, biocatalysts and processes, many possibilities exist and therefore, even with the potential limitations for scale-up of processes developed in microfluidic systems, there are many motivators for using microfluidic systems for process development. Indeed, in our opinion it seems most likely that process development will benefit most from the application of miniaturized systems. There is a growing group of bioprocess practitioners that share this view, working not only on development problems related to applied biocatalysis [18–20], but also fermentation [21] and protein recovery for biopharmaceutical applications [22]. Some of the key motivators are reduced development costs and accelerated process development, compared to conventional technologies in the ml scale. In many cases, microfluidic technologies have been applied for chemical synthesis, for example, where otherwise difficult syntheses have been operated and controlled under new and in some cases extreme conditions [23, 24]. However, there is an increasing interest in applying microfluidic technologies for the development of biocatalytic processes, due to the many general benefits and advantages highlighted in the scientific literature [25]. Examples of potential, advantages and benefits for process development based on microfluidic devices are discussed below, where special attention is given to how this will influence the development of new biocatalytic processes.

The first obvious benefit of performing process development in microfluidic systems is the reduced consumption of valuable and scarce resources. The reduced consumption of resources makes it possible to obtain greater process knowledge with the available resources and at the same time reduce the development costs. For biocatalytic processes, this is especially important, since the availability of a generally expensive biocatalyst is initially limited and will continue to be so until the process has been validated. For example, when improving the performance of biocatalysts through protein engineering,

only small quantities of different putative mutants need to be tested for their performance before larger scale production is initiated. The reduced consumption is in general, especially for the fine chemicals and pharmaceutical industries, a major driver for using microfluidic systems. Development costs can therefore be reduced since resources are so valuable.

Process development requires the testing and optimization of different biocatalyst and process options [e.g., reactors and downstream unit operations (separations)], which can in principle be performed relatively easily in microfluidic systems. For example, scientific literature can be found on membrane based microfluidic separation units [26]. Furthermore the liquid-liquid extraction in microsystems has also been proven to be successful [27], especially operated in a continuous way. The extraction in microsystems in two phase systems is also being investigated more [28]. Furthermore, the most promising microfluidic unit operations can easily be tested in combination, to get an indication of how they influence one another. It should though be mentioned that individual reaction systems or processes benefit differently from miniaturization and in some cases it will not be advantageous to use microsystems. In the scientific literature, it has been argued, with good justification, that micro-reactors benefit faster reactions [29]. However, there are also examples where slower reaction systems, e.g., biocatalytic reaction systems, have proven to greatly benefit from being operated at a micro scale [30]. The easy testing and optimization of process options in microfluidic systems opens the possibility of greatly accelerating the development of new processes, which is especially important in intellectual property (IP)-dominated industry sectors, such as pharmaceuticals. Assuming that miniaturized microfluidic systems contribute to easy testing and optimization of processes, such systems open the possibility of greatly accelerated process development, realized through parallelization and automation of the microfluidic systems. Operating the systems in parallel potentially increases screening and testing throughput. This potentially makes it possible to test different process conditions and options relatively quickly, thus generating knowledge that can be used to select and focus on feasible process options, eliminating infeasible processes. The information collected could also serve well the regulatory needs for Quality-by-Design (QbD) of the US Food and Drug Administration [31]. However, a certain degree of automation will be required in order to run the systems in parallel and ensure high throughput, and certainly there is still a major effort in software development required in order to reach automated and parallelized experimental microfluidic platforms [32]. Nevertheless, in principle at least, microfluidic systems already require a certain degree of automation in order to be operated. For example, it is not possible to achieve controlled flows through the devices without automated pumps. Automated systems will also aid in increasing the throughput of the parallel systems, since they in principle are able to operate continuously, with minimum downtime. Automated systems also have the advantage of having consistent systematic errors, making results comparable, unlike manual sample handling which may vary from operator to operator and from day to day.

Furthermore, microfluidic systems can be manufactured in a modular way, thus allowing the user to combine the different fluidic modules to test the influence of different process steps on the process efficiency [33–35]. It will therefore be possible to test the entire miniaturized process before making any efforts to scale-up the best process option.

Microfluidic systems have the advantage of enhanced process control (e.g., controlled flow scenarios and with rapid heat and mass transfer). The characteristic high surface-to-volume ratio in microfluidic systems enables fast and highly controlled heat and mass transfer. This opens up possibilities for dynamic process scenarios (e.g., fast transition between hot and cold regions for reactions operated in cascades). Likewise, laminar flows in microfluidic systems make it possible to operate with different flow scenarios (e.g., parallel, plug flow, slug flow). This can be very useful in order to precisely control mass transfer in these systems and enables the possibility of obtaining valuable mass transfer knowledge for the processes of interest. Also, it makes it much easier to simulate and model the processes in a microfluidic device.

Having laminar flows also enables easy liquid separation in the systems, based on capillary forces or controlled phase (or flow) splitting. This is very useful for extractive purposes and provides an option to operate biocatalytic processes in new ways. For example, this could enable the possibility of having substrate(s) continuously fed to the reaction stream. Other possibilities are *in situ* product removal or *in situ* co-product removal operating scenarios, where an auxiliary phase is used to continuously remove products or co-products from the reaction stream. For biocatalytic processes, these scenarios could potentially be useful in order to improve process feasibility by shifting unfavorable reaction equilibria and overcoming the inhibitory effects of substrates and products on the biocatalyst.

The laminar flows correspond to having a membrane free separation or supply system. It is also possible to inject an auxiliary phase between two reacting phases (i.e., liquid membrane operation using hydrodynamic

focusing, and thereby control the reaction rate). It is, however, also possible to implement ordinary membranes into these systems, as for example demonstrated by Cervera-Padrell and co-workers [36]. The driving force for the laminar flow and membrane operations is the concentration gradient between the different fluids.

Biocatalytic processes are operated in different ways dependent on the formulation of the biocatalyst, i.e., free, surface immobilized, immobilized in/on support particles, or in whole cell form. In relation to microfluidic systems, the different immobilization scenarios can be exploited in order to perform controlled sequential cascade reactions, or actually replicate metabolic pathways. For example, in Figure 2A, a micro packed bed reactor performing a cascade reaction is illustrated and in Figure 2B, an illustration of a packed bed reactor can be seen, where laminar side-by-side flow is used to perform continuous adsorption and desorption of products.

4 Transaminases

One of the most important functionalities in pharmaceutical molecules is the amine group and in recent years, therefore, routes to optically pure chiral amines have attracted considerable academic and industrial interest. Of the possible routes for synthesis of such molecules, which include selective crystallization and chemical catalytic methods, biocatalysis is particularly attractive. Biocatalytic methods offer high selectivity, under mild conditions with a renewable and tunable catalyst. In principle, several biocatalytic options exist, but the use of ω-transaminases (EC 2.6.1.X) in synthetic mode has driven significant research to find not only S-selective, but also R-selective enzymes for specific applications, and process routes to effectively implement the technology. Despite the excellent selectivity of this reaction and its unique ability to create a chiral center, in principle with 100% yield, in reality the ω-transaminase is one of the more challenging of the biocatalytic reactions; the substrates and products are often poorly water-soluble, the equilibrium is frequently unfavorable [37] and the substrate(s) and product(s) are more often than not inhibitory to the reaction (see Table 1) [38, 39]. This means that at first glance such a process is not only economically infeasible, but indeed far away from the targets which would be required for economic industrial exploitation [3]. Interestingly, in common with many other biocatalytic reactions, via a combination of protein engineering and clever use of reaction, reactor and process engineering, a cost effective process can be established (see Figure 3), and excellent precedent has already been set with the synthesis of sitagliptin by Merck and Co (USA) [42, 43], and other examples by Cellgene/Cambrex (USA and Sweden) [44] and Astra Zeneca (UK and Sweden)[45].

However, there are many other potential molecules to be synthesized using ω-transaminases, where the challenges have not yet been overcome and in general no standardized procedure exists to design an appropriate reaction, reactor and process for a given transaminase conversion. For this reason, we decided to use this reaction as a test system for the microfluidic development platform in the BIOINTENSE project.

Transaminases catalyze the transfer of an amine (-NH2) group from a donor molecule, usually an amino acid or a simple non-chiral amine such as 2-propylamine, to a pro-chiral ketone acceptor, yielding a chiral amine as well as a co-product ketone (or alpha-keto acid) (Figure 4). The enzyme requires the cofactor pyridoxal phosphate

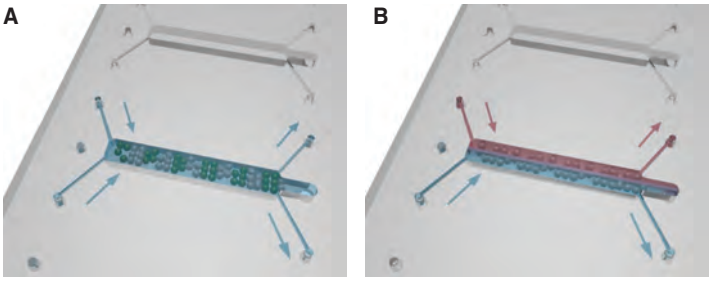

Figure 2 (A) Example of a micro packed bed reactor operated with a cascade reaction performed by immobilized enzyme on particles arranged in a sequential order. Green and gray particles represent different immobilized biocatalysts; (B) example of a novel way to operate micro packed bed reactors in which a simultaneous adsorption (blue stream) and desorption (red stream) flow is established with the help of a side by side laminar flow. This flow concept is currently under investigation and can be achieved by an appropriate design of the length and depth ratio of the Micro Packed Bed Reactor (μ-PBR). The channeling effects which also occur in miniaturized systems should in this way be limited to each side of the separated flow.

Table 1 Overview of challenges, solutions and implementation issues for ω-transaminase based reactions. The table is read by identifying a potential 'solution' (from the list on the left hand side of the table) to address a given reaction or biocatalyst 'challenge' (listed at the top of the table). In order to decide between solutions, the list of 'issues' (on the right hand side of the table) should be consulted.

Solutions	Reaction challenges			Biocatalyst challenges				Implementation issues
	Low thermodynamic equilibrium	Low substrate solubility	Substrate and product degradation	Inhibition by substrates or products	Stability of biocatalyst	Low catalyst activity or specificity	Separation of biocatalyst	
Excess amine donor	✓							Inhibition of catalyst; insufficient equilibrium shift; stability; costs; separation
Whole-cell biocatalyst	✓				✓			Selectivity; separation (foaming); Genetically Modified Organism
Degradation or recycling of co-product (cascade)	✓			✓				Compatibility of biocatalysts; added cost of biocatalysts; co-factor recycling
Distillation of (co-)product	✓							Co-distillation of water and/or solvent
Extraction of (co-)product, Resin/membrane/solvent	✓	✓		✓				Selectivity between substrates, co-products and products
Co-solvent/2-phase system		✓		✓				Enzyme stability; compatibility with free enzymes/cells; separation down-stream
In situ substrate supply/fed batch		✓	✓	✓				Capacity; compatibility with free enzymes/cells
Alter catalyst (Directed evolution, etc.)					✓	✓		Development time and cost
Immobilization					✓		✓	Deactivation; development costs; higher catalyst costs

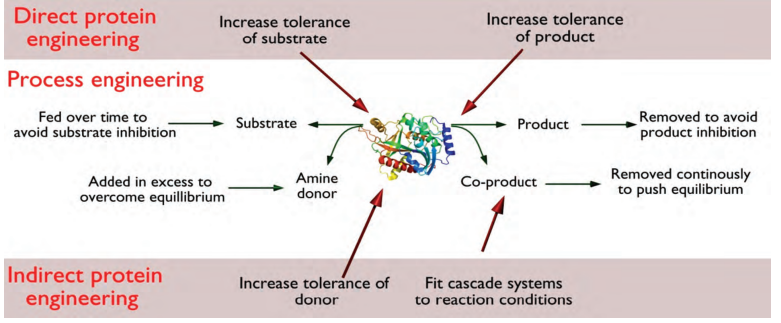

Figure 3 Illustrative presentation of different strategies which can be applied to improve transaminase based biocatalytic technology for chiral amine synthesis. Protein engineering can be used to improve the biocatalyst to withstand harsh process relevant conditions (e.g., overcome inhibition), while process engineering strategies can be applied to shift the equilibrium in a favorable direction (e.g., by *in situ* product removal (ISPR) and/or *in situ* co-product removal (IScPR) [40, 41].

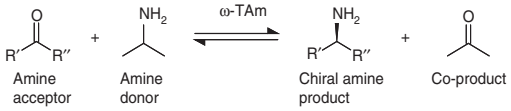

Figure 4 Asymmetric synthesis of chiral amines by ω-transaminase.

(PLP) to act as a shuttle to transfer the amine group. The cofactor is tightly bound to the enzyme and therefore does not pose the cofactor regeneration problems so often encountered in biocatalytic oxidation and reduction reactions [46, 47].

The asymmetric synthesis of chiral amines by ω-transaminase consists of three major steps (Figure 5); fermentation, biocatalytic reaction and product recovery. In order to avoid unnecessary costs, the biocatalyst is used in the crudest possible form (either as whole cells or cell free extract). Immobilization of the enzymes can be used to facilitate recovery and recycle, thereby improving the biocatalyst yield (g products/g biocatalyst).

After the reaction is complete, the biocatalyst is removed (biocatalyst separation) and the product is isolated from the substrate (which may also be recycled dependent upon the cost contribution to the process) prior to purification.

There are many challenges inherent to transaminase processes that need to be dealt with and numerous reports have been published that address one or more of these challenges. Frequently, the suggested strategies solve more than one problem, for instance the use of an auxiliary phase may solve issues related to substrate and product inhibition as well as low water solubility; by contrast, the solution might pose other problems, such as lower biocatalyst stability. An overview of transaminase process challenges has been compiled in Table 1, along with the suggested technologies and strategies used to overcome these, as well as the further implications of using a specific technology.

5 Discussion

Although there is a great potential for the application of microfluidic miniaturized systems in process development, there are also several challenges related to their operation.

One of the main challenges is the large number of samples required for analysis due to the sensitivity of the measurements and manual sample handling for off-line measurements. The implementation of on-line measurements could be a possible solution. However, the standard on-line measurement methods [e.g., near-infrared (NIR) and ultraviolet (UV)] can be quite problematic. The compounds involved in the processes studied by BIOINTENSE, amines and ketones, have peaks appearing in critical regions of the NIR and UV spectra. For instance, the amines are shadowed by water in the NIR spectrum, and in the UV spectrum, the peaks appear in the lower region, where common materials used for fabrication of microfluidic devices will have shadowing effects.

The integration of the hardware such as pumps, valves, analytical equipment and the heating/cooling zone can be quite challenging when working at the micro scale. For this reason, it is necessary to standardize connections to simplify their application. There is a similar constraint related to the available technology that can be applied to process development. Here, there is a need for readily and commercially available platforms, modules and methodologies. For instance, for biocatalytic processes, there is no guidance and there has been a trend towards starting from the very beginning each time. For that matter, methodologies should also cover development and scale-up procedures and/or strategies. This is one of the tasks that will be undertaken in BIOINTENSE.

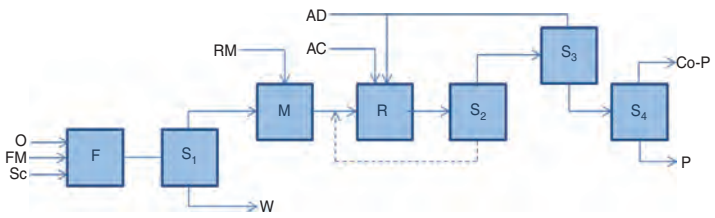

Figure 5 Generalized process flow sheet for transaminase-catalyzed reactions. Unit operations: fermenter (F), mixer (M), reactor (R), cell/fermentation broth separator (S_1), biocatalyst/reaction medium separator (S_2), amine donor/acceptor separator (S3) and chiral amine product/co-product separator (S4). Process streams: amine acceptor (AC), amine donor (AD), product (P), co-product (Co-P), fermentation media (FM), oxygen (O), reaction media (RM), starter culture (SC), waste fermentation broth (W).

Likewise, the formation (or use) of solids in microsystems can cause severe channel clogging due to surface adhesion. The large surface to volume ratio supports adhesion and it is difficult to prevent [48]. This is a great bottleneck, since the biocatalyst formulation can vary, e.g., free solubilized enzymes, immobilized enzymes on solid support, or whole cells. Biocatalysts are usually expensive and it is intended to use them in as crude as possible a state, or at least for as many cycles as possible [3]. Another challenge that should be considered is the catalyst immobilization in strategic locations of the micro-reactor surface for topology studies. These studies can involve complex biocatalyst distribution patterns determined by simulations using biocatalyst immobilization and can be difficult to replicate experimentally.

6 Future outlook

In the BIOINTENSE project, we are developing entirely new tools and only time will tell if the results and the performance of the microsystem based platform will reveal a new 'high throughput' paradigm. However, based on the preliminary results obtained, it can already now be seen that the developed 'microtools' contribute to entirely new results, including deepening the understanding and knowledge of mass transfer parameters (like diffusion velocities of the substrates and products). With the help of this information, it will become possible to understand the complex interactions of the biocatalytic system better and hence it can also be expected that in the long run, this information can contribute to the rapid development of the identified processes. Indeed, we are convinced that it will be necessary to develop a miniaturized toolbox for the investigation and screening of process options. Nevertheless, the exact composition of that toolbox is today unknown. The project will show, in the end, if the full advantages of microsystems can be applied for rapid process development and if this is, from an economic point of view, worthwhile. However, the highest expectations are at the moment to prove if the miniaturized process toolbox will contribute to the acceleration of the process development and thereby to the reduction of development time.

Acknowledgements: Financial support by the European Union FP7 Project BIOINTENSE – Mastering Bioprocess integration and intensification across scales (KBBE 2012.3.3-03 Grant Agreement Number 312148) is gratefully acknowledged.

Received October 2, 2013; accepted November 2, 2013; previously published online December 6, 2013

References

[1] Pollard DJ, Woodley JM. *Trends Biotechnol.* 2007, 25, 66–73.
[2] Straathof AJJ, Panke S, Schmid A. *Curr. Opin. Biotech.* 2002, 13, 548–556.
[3] Tufvesson P, Lima-Ramos J, Nordblad M, Woodley JM. *Org. Proc. Res. Dev.* 2011b, 15, 255–274.
[4] Tufvesson P, Lima-Ramos J, A-Haque N, Gernaey KV, Woodley JM. *Org. Proc. Res. Dev.* 2013, 17, 1233–1238.
[5] Bornscheuer UT, Huisman GW, Kazlauskas RJ, Lutz S, Moore JC, Robins K. *Nature* 2012, 485, 185–194.
[6] Woodley JM. *Curr. Opin. Chem. Biol.* 2013, 17, 310–316.
[7] Burton SG, Cowan DA, Woodley JM. *Nat. Biotech.* 2002, 20, 35–46.
[8] Turner NJ. *Nat. Chem. Bio.* 2009, 8, 567–573.
[9] Bommarius AS, Blum JK, Abrahamson MJ. *Curr. Opin. Chem. Biol.* 2011, 2, 194–200.
[10] Reetz MT. *Angew. Chem. Int. Ed.* 2011, 50, 138–174.
[11] Vennestrøm PNR, Christensen CH, Pedersen S, Grunwaldt J-D, Woodley JM. *ChemCatChem* 2010, 2, 249–258.
[12] Aota A, Mawatari K, Kitamori T. *Lab Chip* 2009, 9, 2470–2476.
[13] Whitesides GM. *Nature* 2006, 442, 368–373.
[14] Baraldi PT, Hessel V. *Green Proc. Synth.* 2012, 1, 149–167.
[15] Wirth T. *Microreactors in Organic Chemistry and Catalysis*, 2nd ed., Wiley-VCH Verlag GmbH & Co KGaA: Weinheim, Germany, 2013.
[16] Bruus H. *Theoretical Microfluidics*, Oxford University Press: Oxford, 2008.
[17] Roberge DM, Gottsponer M, Eyholzer M, Kockmann N. *Chem. Today* 2009, 27, 8–11.
[18] Cull S, Lovick J, Lye G, Angeli P. *Bioprocess Biosyst. Eng.* 2002, 3, 143–153.
[19] O'Sullivan B, Al-Bahrani H, Lawrence J, Campos M, Cázares A, Baganz F, Wohlgemuth R, Hailes HC, Szita N. *J. Mol. Catal. B* 2012, 77, 1–8.
[20] Dencic I, de Vaan S, Noël T, Meuldijk J, de Croon M, Hessel V. *Ind. Eng. Chem. Res.* 2013, 52, 10951–10960.
[21] Betts J, Baganz F. *Microb. Cell Fact.* 2006, 1, 21.
[22] Nfor BK, Verhaert PDEM, van der Wielen LAM, Hubbuch J, Ottens M. *Trends Biotechnol.* 2009, 27, 673–679.
[23] Jensen KF. *Chem. Eng. Sci.* 2001, 56, 293–303.
[24] Hartman RL, Jensen KF. *Lab-on-a-Chip* 2009, 9, 2495–2507.
[25] McMullen JP, Jensen KF. *Annu. Rev. Anal. Chem.* 2010, 3, 19–42.
[26] De Jong J, Lammertink R, Wessling M. *Lab Chip* 2006, 6, 1125–1139.
[27] Kralj JG, Sahoo HR, Jensen KF. *Lab Chip* 2007, 7, 256–263.
[28] Žnidaršič-Plazl P, Plazl I. *Lab Chip* 2007, 7, 883–889.
[29] Roberge DM, Ducry L, Bieler N, Cretton P, Zimmermann B. *Chem. Eng. Technol.* 2005, 28, 318–323.

[30] Bodla VK, Seerup R, Krühne U, Woodley JM, Gernaey KV. *Chem. Eng. Technol.* 2013, 36, 1017–1026.
[31] U.S. Food and Drug Administration, Department of Health and Human Services. Pharmaceutical CGMPs for the 21st Century - a Risk-Based Approach: Progress Report. U.S. Food and Drug Administration, Department of Health and Human Services: 2007: http://www.fda.gov/AboutFDA/CentersOffices/Officeof-MedicalProductsandTobacco/CDER/ucm128080.htm#mission.
[32] Gernaey KV, Baganz F, Franco-Lara E, Kesny F, Krühne U. Luebberstedt M, Marx U, Palmqvist E, Schmid A, Schubert F, Mandenious C-F. *Biotechnol. J.* 2012, 7, 1308–1314.
[33] Perozziello G, Simone G, Candeloro P, Gentile F, Malara N, Larocca R, Coluccio M, Pullano SA, Tirinato L, Geschke O. *Micro Nanosyst.* 2010, 2, 227–238.
[34] Shaikh KA, Ryu KS, Goluch ED, Nam J, Liu J, Thaxton CS, Chiesl TN, Barron AE, Lu Y, Mirkin CA. *Proc. Natl. Acad. Sci.* 2005, 102, 9745–9750.
[35] Yuen PK. *Lab Chip* 2008, 8, 1374–1378.
[36] Cervera-Padrell AE, Morthensen ST, Lewandowski DJ, Skovby T, Kiil S, Gernaey KV. *Org. Proc. Res. Dev.* 2012, 16, 888–900.
[37] Tufvesson P, Jensen JS, Kroutil W, Woodley JM. *Biotech. Bioeng.* 2012, 109, 2159–2162.
[38] Ward JM, Wohlgemuth R. *Curr. Org. Chem.* 2010, 14, 1914–1927.
[39] Tufvesson P, Lima-Ramos J, Jensen JS, Al-Haque N, Neto W, Woodley JM. *Biotech. Bioeng.* 2011a, 108, 1479–1493.
[40] Goldberg K, Edegger K, Kroutil W, Liese A. *Biotech. Bioeng.* 2006, 95, 192–198.
[41] Lima-Ramos J, Neto W, Woodley JM. *Top. Catal.* 2013, DOI 10.1007/s11244-013-0185-0.
[42] Savile CK, Janey JM, Mundorff EC, Moore JM, Tam S, Jarvis WR, Colbeck JC, Krebber A, Fleitz FJ, Brands J, Devine PN, Huisman GW, Hughes GJ. *Science* 2010, 329, 305–309.
[43] Truppo MD, Strotman H, Hughes G. *ChemCatChem* 2012, 4, 1071–1074.
[44] Martin A, DiSanto R, Plotnikov I, Kamat S, Shonnard D, Pannuri S. *Biochem. Eng. J.* 2007, 37, 246–255.
[45] Frodsham L, Golden MD, Hard S, Kenworthy MN, Klauber DJ, Leslie K, MacLeod C, Meadows RE, Mulholland KR, Reilly J, Squire C, Tomasi S, Watt D, Wells AS. *Org. Proc. Res. Dev.* 2013, 17, 1123–1130.
[46] Pannuri S, DiSanto R, Kamat S. Biocatalysis. In *Kirk-Othmer Encyclopedia of Chemical Technology*, Wiley: Hoboken, NJ, USA, 2003.
[47] Hwang BY, Cho BK, Yun H, Koteshwar K, Kim B-G. *J. Mol. Catal.* B. 2005, 37, 47–55.
[48] Hartman RL. *Org. Proc. Res. Dev.* 2012, 16, 870–887.

Systematic Development of Miniaturized (Bio)Processes using Process Systems Engineering (PSE) Methods and Tools

U. Krühne,* H. Larsson, S. Heintz, R. H. Ringborg, I. P. Rosinha, V. K. Bodla, P. A. Santacoloma, P. Tufvesson, J. M. Woodley, and K. V. Gernaey

Center for Process Engineering and Technology, Department of Chemical and Biochemical Engineering, Technical University of Denmark (DTU), Building 229, DK-2800 Lyngby, Denmark

doi: 10.15255/CABEQ.2014.1940

Original scientific paper
Received: February 14, 2014
Accepted: March 3, 2014

The focus of this work is on process systems engineering (PSE) methods and tools, and especially on how such PSE methods and tools can be used to accelerate and support systematic bioprocess development at a miniature scale. After a short presentation of the PSE methods and the bioprocess development drivers, three case studies are presented. In the first example it is demonstrated how experimental investigations of the bi-enzymatic production of lactobionic acid can be modeled with help of a new mechanistic mathematical model. The reaction was performed at lab scale and the prediction quality analyzed. In the second example a computational fluid dynamic (CFD) model is used to study mass transfer phenomena in a microreactor. In this example the model is not only used to predict the transient dynamics of the reactor system but also to extract material properties like the diffusion velocities of substrate and product, which is otherwise difficult to access. In the last example, a new approach to the design of microbioreactor layouts using topology optimization is presented and discussed. Finally, the PSE methods are carefully discussed with respect to the complexity of the presented approaches, the applicability with respect to practical considerations and the opportunity to analyze experimental results and transfer the knowledge between different scales.

Key words:

Computational Fluid Dynamics (CFD), modeling, Process Systems Engineering (PSE), (bio)processes

Introduction

The development of new chemical engineering design tools is essential for the implementation of the latest technology in the manufacture of chemical and other products. The focus of this paper is on process systems engineering (PSE) methods and tools, and especially on how such PSE methods and tools can be applied to speed up or support systematic bioprocess development at miniature scale. In this context, the term bioprocess is interpreted broadly, and includes both biocatalysis (enzyme or resting cell conversion) as well as fermentation (growing cell conversion). In the following section, we first provide a brief introduction to the main drivers of biocatalysis and fermentation process development. The paper also contains a short overview of PSE methods and tools. The use of such tools is illustrated on the basis of three examples, which summarize some of our recent experiences in the area. The paper ends with a discussion on future perspectives with respect to the use of PSE methods and tools in miniaturized bioprocess systems and for extrapolation of results across reactor scales (scaling up).

*Corresponding author: ulkr@kt.dtu.dk

Bioprocess development drivers – biocatalysis

The need for selective chemistry is the main driver behind the increasing academic and industrial interest in biocatalytic processes (chemical reactions catalyzed by an isolated enzyme, immobilized enzyme or whole cell containing one or more enzymes).[1] While biocatalysis may easily hold the promise of high selectivity, economic process feasibility is also necessary for implementation in industry. Economic feasibility translates into a minimum required product concentration that must leave the reactor, as well as a yield of product on biocatalyst that is to be achieved, as has been illustrated by Tufvesson and coworkers for a number of different scenarios.[2] The exact threshold values for minimum product concentration and yield of product on biocatalyst will indeed depend on the particular industry sector as well as the selling cost of the product relative to the cost of the substrate. In fact, most new biocatalytic processes studied in the laboratory do not fulfill these requirements, mainly because enzymes are usually evolved to operate under mild conditions converting natural substrates at low concentrations. Hence, achieving an economically feasible biocatalytic process in terms of minimum re-

quired product concentration and yield of product on biocatalyst is therefore often challenging, and can only be addressed by a combination of process modifications as well as biocatalyst modifications. Indeed, in many cases it is not clear at an early stage how to develop the process. In order to overcome this, one potential vision for the future could be automated data collection and systematic testing of alternatives at a miniature scale such that operations can be carried out in parallel and with a reduced reagent inventory. This is the main aim of the EC-funded BIOINTENSE project, and the experimental and practical challenges of such an approach have recently been discussed by Krühne and co-workers (2014).[3]

When considering the list of potential process and biocatalyst modifications, analyzing all potential options is a combinatorial problem that is too difficult and time-consuming to be addressed by evaluating options one-by-one in the laboratory, even at miniature scale. However, specifically at this point, mathematical models can be used to supplement biocatalytic process development, and to support the rapid identification of the most promising biocatalytic process options among many. This also matches the above-mentioned ideas on automated data collection and systematic testing of alternatives at a miniature scale. Automated data collection can indeed be combined with automated model structure selection and parameter estimation, as recently illustrated for a conventionally-catalyzed Diels-Alder reaction with complex kinetics in a microreactor.[4]

Bioprocess development drivers – fermentation

Fermentation processes have been used for hundreds of years in the production of food, including beer and wine. However, partly due to the scarcity of fossil fuels, fermentation processes have become increasingly attractive during the past decades to produce proteins (including enzymes), fine and bulk chemicals as well on the basis of renewable raw materials. The essential difference between a biocatalytic process and a fermentation process is that the catalyst in the fermentation process is a living microorganism – most often a genetically modified organism overexpressing the genes required to produce the product of interest – that grows on a carbon substrate which usually also forms the substrate for the formation of the product of interest. As a consequence, successful implementation of an economically feasible fermentation process relies on achieving a high enough product yield on substrate (especially for lower value products) as well as maintaining a delicate balance between using substrate for biomass growth on the one hand and product formation on the other hand. If biomass growth is not sufficiently prioritized, the product formation rate will be too low, resulting in suboptimal exploitation of the available reactor volume. On the other hand, if biomass growth is promoted too much, the final yield of product on substrate achieved in the fermentation process and the product concentration will be suboptimal. Thus, the main economic drivers of an industrial fermentation process are the yield of product on substrate and the final product concentration that can be achieved – the higher the better, since less water needs to be removed from the product in the downstream processing. Furthermore, for aerobic fermentations the energy cost for oxygen supply is also an important cost.

Mathematical models are often used to study laboratory scale fermentation processes. However, their use in industry is rather limited, and fermentation process development has traditionally relied on an extended series of experiments at lab-scale and pilot-scale in order to find the operating conditions that result in an economically feasible fermentation process. In recent years, microliter and milliliter scale devices capable of performing fermentations have been developed as well,[5] and have been promoted for use in fermentation process development. However, it is quite clear that additional research work is needed before the use of microscale or milliliter scale devices will be the generally accepted process development strategy or support tool. Mechanistic models could, according to us, be helpful in realizing that future vision.

PSE methods and tools

Process systems engineering (PSE) is an interdisciplinary field within chemical engineering that focuses on the design, operation, control, and optimization of chemical, physical, and biological processes through the aid of systematic computer-based methods. A systems approach is generally model-based, i.e. different types and forms of mathematical models play a prominent role in process design/operation, evaluation and analysis as they have the potential to provide the necessary process understanding, supplement the available knowledge with new data, and reduce time and cost for process-product development.[6,7] PSE methods and tools have been applied successfully to many industries, such as the chemical and petrochemical, the pharmaceutical[8] and biotechnological industries.

While working on a process development task, independent of scale, mathematical models are often used to summarize the available process knowledge and to describe the dynamics of the most important process variables. Such ‘dynamic models’ are usually mechanistic models of a process or a

unit operation, for example consisting of a set of ordinary differential equations (ODEs) which represent the input-output dynamics. Once available, such a model can be supplemented by a set of well-established model analysis tools,[9–11] for example also including uncertainty and sensitivity analysis to assess the statistical quality (reliability) of the simulated scenarios.[12] Perhaps most importantly from a process development point of view, the calibrated dynamic models can be used for *in-silico* testing of a set of potential process operating strategies, e.g. by comparing different control strategies in a series of dynamic simulations, without disturbing process operation. The latter is a major advantage, but requires a dynamic model which has been calibrated on the basis of available process data.

Case study examples

Example 1: Bi-enzyme production of lactobionic acid (Santacoloma, 2012)[3]

The main goal of this first example was to analyze the reliability of a mechanistic mathematical model describing a biocatalytic reaction in a lab-scale reactor in terms of its prediction quality. During the process the temperature was controlled at 30 °C and pH was maintained at 3.9. Furthermore, concentrations of lactose, lactobionic acid and oxygen were measured for 6 hours. After that time, the lactose was completely consumed. The sampling interval for lactose and lactobionic acid was 1 hour and the samples were measured by High-performance liquid chromatography (HPLC). The dissolved oxygen measurements were recorded every 10 seconds.

Production of lactobionic acid (4-O-β-D-galactopyranosyl-D-gluconic acid), a compound used in the production of high-value products, pharmaceutical and food applications, is primarily achieved by the oxidation of lactose. The general scheme for the biocatalytic production of lactobionic acid is shown in Fig. 1. A first enzyme, cellobiose dehydrogenase (CDH), catalyzes the dehydrogenation of lactose to lactobiono-lactone, which is spontaneously hydrolyzed to lactobionic acid. In this case, the double action of the redox mediator 2,2'-azinobis(3-ethylbenzothiazoline-6-sulfonic acid) (ABTS) is exploited. In the first reaction, ABTS acts as an electron acceptor regenerating the initial oxidation state of the first enzyme (CDH). In the second reaction, ABTS serves as electron donor to obtain the reduction by laccase (lacc), which is the second enzyme added to the system. The reduced state of laccase catalyzes the second reaction where oxygen (the co-substrate) is fully reduced to water.[14,15]

The mathematical model for this system was obtained from the literature, including the kinetic parameters of the multi-enzyme process.[16] and was implemented in MATLAB. Both enzymes involved in the process (CDH and lacc) follow the substituted enzyme mechanism. Kinetic parameters for each enzyme were obtained from the literature.[14,15,17] Interaction due to the combination of enzymes was not taken into account in these studies. In this case study, the bi-enzyme process was carried out in batch mode, in a membrane bioreactor. The main purpose of this reactor was to provide bubble-free oxygenation. Furthermore, the mass transfer of oxygen from the gas to the liquid phase was included in the mathematical model.[16]

The following assumptions were made for the mathematical model: (1) Substrate and product inhibition are neglected in the process; (2) pH and temperature are maintained constant during the operation; (3) Perfect mixing in the reactor.

The model for the system consists of six differential equations, and can be written down in a compact matrix notation,[18] as shown in Table 1. An example of how the matrix in Table 1 should be read is shown in Eq. 1 with the oxygen balance:

$$\frac{\mathrm{d}C_{o_2}}{\mathrm{d}t} = r_{omt} - \frac{1}{2} r_2 \qquad (1)$$

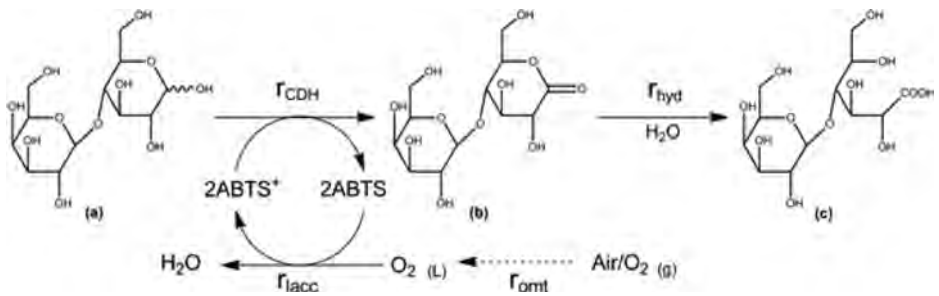

Fig. 1 – *General reaction scheme for bi-enzyme production of lactobionic acid: (a) lactose, (b) lactobiono-lactone and (c) lactobionic acid*

Table 1 – *Mass balances of the batch process for lactobionic acid production represented by the stoichiometric matrix notation*

Component / Process	C_{lact} (mM)	C_{LBL} (mM)	C_{LBA} (mM)	C_{O_2} (mM)	C_{ABTS} (mM)	C_{ABTS+} (mM)	Process rates
Enzyme 1- CDH	–1	1			2	–2	r_{CDH}
Enzyme 2- Lacc.				–1/2	–2	2	r_{lacc}
Hydrolysis		–1	1				r_{hyd}
Aeration				1			r_{omt}

Table 2 – *Reaction rate expressions for lactobionic acid production*

Reaction rate (symbol)	Reaction rate expression
r_{CDH}	$r_{CDH} = V_{max\_1} \dfrac{C_{Lact} \cdot C_{ABTS+}}{K_{M_{Lact}} \cdot C_{ABTS+} + K_{M_{ABTS+}} \cdot C_{Lact} + C_{Lact} \cdot C_{ABTS+}}$
r_{lacc}	$r_{lacc} = V_{max\_2} \dfrac{C_{O_2} \cdot C_{ABTS}}{K_{M_{O_2}} \cdot C_{ABTS} + K_{M_{ABTS}} \cdot C_{O_2} + C_{O_2} \cdot C_{ABTS}}$
r_{hyd}	$r_{hyd} = K_{hyd} \cdot C_{LBL}$
r_{omt}	$r_{omt} = K_L a \cdot (C_{O_2}^{sat} - C_{O_2})$

The enzymatic reactions follow the bi-bi ping-pong (or substituted-enzyme[19,20]) kinetics. In this case study, both enzymes follow the same type of mechanism. Hence, two coupled substituted-enzyme mechanisms are suggested to describe both enzymatic reactions. The process rates are summarized in Table 2.

Progress curves for lactic acid, dissolved oxygen and lactobionic acid formed the basis of a parameter estimation. Details of the parameter estimation procedure can be found in Santacoloma (2012).[13] The resulting model fit is illustrated in Fig. 2. The parameter estimates, including confidence intervals, are provided in Table 3.

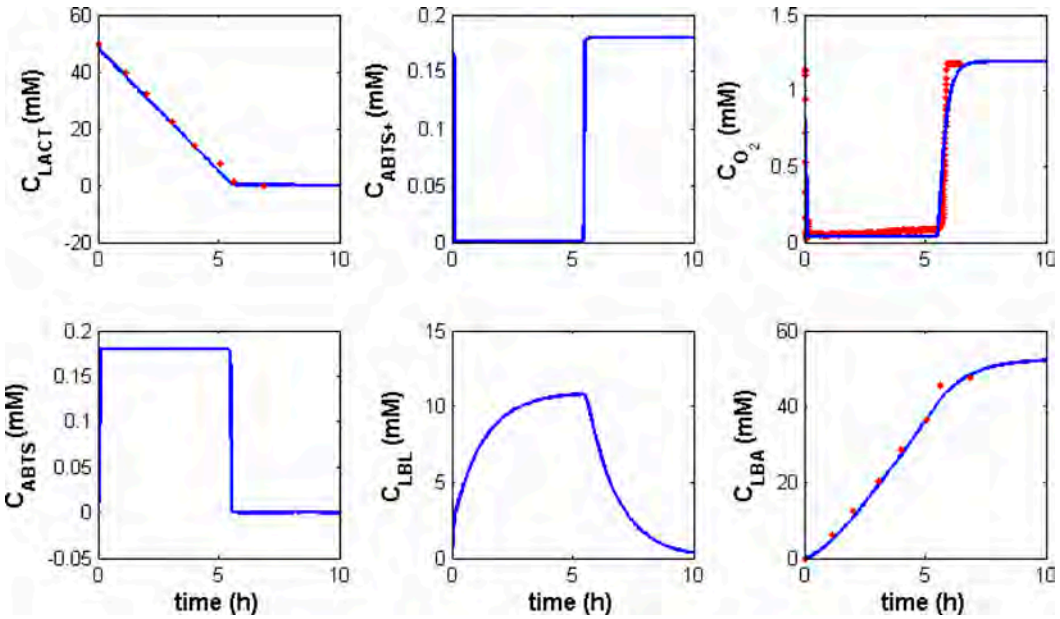

Fig. 2 – *Comparison between experimental data and simulation of the system using the estimated parameters (line – simulation, dots – measurement)*

Table 3 – *Lactobionic acid example: parameter estimates with 95 % confidence intervals and correlation matrix of the estimated parameters*

Parameter	Estimates with 95 % C. intervals		Units	Correlation matrix						
				θ_1	θ_2	θ_3	θ_4	θ_5	θ_6	θ_7
$V_{max\ 1}$	23.33	± 16.4	mM h^{-1}	1						
$K_{M\ lact}$	1.27	± 3.06	mM	–0.47	1					
$K_{M\ ABTS+}$	4.10 e–5	± 0.09	mM	0.85	–0.71	1				
$V_{max\ 2}$	58.48	± 34.7	mM h^{-1}	0.29	0.13	–0.08	1			
$K_{M\ ABTS}$	8.74 e–3	± 0.51	mM	0.42	0.18	–0.06	0.83	1		
K_La	3.84	± 0.10	h^{-1}	0.13	0.13	0.23	–0.07	–0.22	1	
K_{hyd}	0.655	± 0.44	mM h^{-1}	–0.00	0.00	–0.00	–0.00	–0.00	0.00	1

Despite the assumptions, the suggested mathematical model can in general describe the process dynamics. Seven parameters were found to be identifiable based on the given dataset, but the kinetic parameters (K_M) for both oxidation states of the intermediate redox mediator ABTS are very small which physically means fast dynamics in the system as the lactic acid approaches depletion. That effect could probably also explain – at least to some extent – the uncertainty in those parameters, observable in Table 2 as a large confidence interval. Several other parameters show rather large confidence intervals as well. This means[12] that the absolute values of the parameters should be interpreted with care, i.e. the model can describe the process dynamics but the physical meaning of the parameters is limited. Improved quality of the parameter estimation (reduced confidence intervals) could be achieved by collecting measured data on other model variables as well.

Example 2: CFD to study mass transfer phenomena in microreactors (Bodla *et al.*, 2013)[21]

The second case study demonstrates the combination of microreactor technology and computational fluid dynamics (CFD) to contribute towards understanding of the diffusional properties of substrate and product in a biocatalytic reaction. Such knowledge can then be applied to design new reactor configurations.

As a case study, an ω-transaminase catalyzed transamination for the synthesis of chiral amines was selected. Biocatalytic transamination is studied intensively nowadays, mainly because the transamination reaction is attractive for synthesis of optically pure chiral amines (which are valuable building blocks for pharmaceuticals and precursors). However, in the synthetic direction the reaction is often limited by unfavourable thermodynamics, as well as substrate and product inhibition of the enzyme activity.[22] The reaction is catalysed by ω-transaminase, in the presence of a co-factor, pyridoxal-5'-phosphate (PLP), by transferring the amine group from the amine donor to a pro-chiral acceptor ketone, yielding a chiral amine along with a co-product ketone. The reaction follows the bi-bi ping pong mechanism where the substrate is first bound to the enzyme while co-product is released before the second substrate is bound and the final product leaves the enzyme.[23] Thus diffusion of the substrate to the enzyme binding site and the product diffusion potentially have a significant effect on the reaction performance. Hence, it was specifically intended here to study the diffusion characteristics of the substrate and the product under operating conditions.

Transient experiments were performed in a microchannel under continuous flow conditions. Following a step input of the diffusing species at the inlet at time $t = 0$, the phenomenon of species transport in uniform poiseuille flow is explained by the convection-diffusion equation.[24] A species that is diffusing relatively fast creates a more radial mixing profile, while a species diffusing more slowly has less effect. Under laminar flow conditions, residence time distribution (RTD) experiments were performed by inducing a step input at the inlet of the channel after reaching steady-state, while the concentration over time is subsequently measured at the outlet in order to obtain the response curves, $E(t)$ as shown in Eq. 2. These distribution profiles are helpful in understanding the diffusional properties of each species. Slowly diffusing species have more lag time, and thus it takes more time to reach the normalized concentration at the outlet. The first molecules of the species will also break through sooner at the end of the channel compared to relatively faster diffusing species (Fig. 3).

$$E(t) = \frac{C(t)}{C_o} \tag{2}$$

Where C_o is the species concentration at the inlet for a step input, and $C(t)$ is the concentration measured at the outlet at time t. The RTD experiments were performed in the microchannel at a flow rate of 7.5 μL min^{-1} for the amine acceptor substrate (acetophenone), for the amine product (methylbenzylamine), and for glucose, as shown in Fig. 3. The channel dimensions (width $0.5 \cdot 10^{-3}$ m, height $1 \cdot 10^{-3}$ m, length 0.1 m) are sufficiently small and the flow rate is sufficiently low to maintain a laminar flow (Reynolds number is 0.2). Glucose is a compound with a known aqueous diffusion coefficient of $0.67 \cdot 10^{-9}$ m^2 s^{-1} and was therefore used as a reference.

Computational fluid dynamics (CFD) models of the flow behaviour were also constructed for a range of diffusion coefficients with the intention of distinguishing between fast and slowly diffusing compounds (i.e. compounds with orders of magnitude differences of their diffusion coefficients). ANSYS CFX version 12.5 was used as software package for this purpose. Response curves were obtained from the simulations, after inducing a step input at the inlet, and by measuring the area average of the species concentration at the outlet of the channel and are also plotted in Fig. 3.

The results in Fig. 3 provide a comparison of the experimental data obtained from transient experiments with the RTD curves resulting from CFD simulations. The simulation result, with a diffusion coefficient of $0.67 \cdot 10^{-9}$ m^2 s^{-1}, fits well with the data for the product, indicating that the diffusion coefficient of the product is close to that of glucose. With respect to acetophenone, the results indicate an increased lag time to reach the normalized concentration at the outlet compared to the product implying that the substrate is diffusing slower than the product. Compared to the simulations, the experimental data does not fit exactly, although the behaviour of the response curve is closer to that of the simulation with a diffusion coefficient of $0.67 \cdot 10^{-12}$ m^2 s^{-1}. Hence it can be interpreted that the diffusion coefficient is in the order of magnitude of 10^{-12}. Thus it can be concluded that the substrate is diffusing considerably slower than the product (around 10^3 fold slower).

For experimental values, a standard deviation of about 10 % from the mean has been observed. This could account for an error of 10 % in determining the value of the diffusion coefficients. Further errors in numerical simulations will have a combined effect on determining the value of the diffusion coefficients. CFD simulations for solving the Navier -Stokes equations for fluid dynamics are well established in various applications. It is important to replicate the exact geometry including the wall effects and boundary conditions in the simulation since the response curve is a function of these variables. Appropriate meshing of the geometry is also crucial to minimize the numerical error. The finer the mesh size or the higher the number of mesh elements, the more precise will the numerical calculations be. For transient simulations, the time-step is also important when the error has to be minimized. However, there is a tradeoff between the mesh size, the time-step and the required computational time and effort. Thus a compound (such as glucose in this case study) with a known diffusion coefficient can be used to confirm if the simulations are able to predict the experimental data. Assuming about 5 % error in the numerical simulations, the combined error could be in the order of 5 % – 30 %.

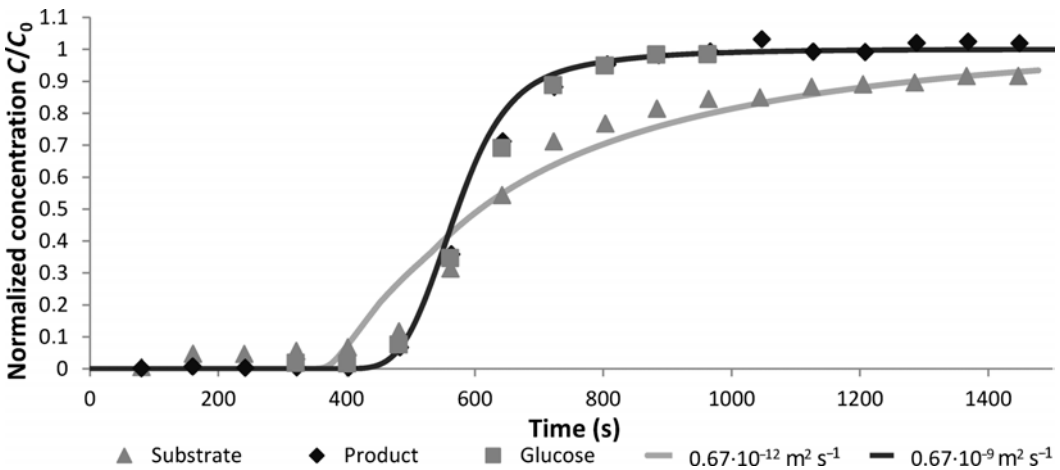

Fig. 3 – *CFD simulations with induced diffusion coefficients of $0.67 \cdot 10^{-9}$ m^2 s^{-1} and $0.67 \cdot 10^{-12}$ m^2 s^{-1} plotted as continuous lines; Experimental results are plotted as markers. Figure adapted from (Bodla et al., 2013)*[25]

In this case, the substrate is estimated to be diffusing 1000 fold slower compared to the product, where the real value could thus be about 700–1300 times slower compared to the product (assuming maximum 30 % error). So when comparing the numerical response curves with the experimental data, errors in both numerical simulation and experimental data can result in incorrect estimation of the diffusion coefficients.

The knowledge of substrate and product diffusion coefficients is crucial for the choice and design of reactors for biocatalytic reactions. Different reactor configurations can be achieved based on the flow and species transport characteristics. It has been demonstrated that the reactor configurations built from this knowledge perform better than the traditional well mixed batch reactor.[21] In order to build reactor configurations for industrial purposes, it is furthermore also crucial to be able to extrapolate the results from microscale to larger industrial scale. Although it is challenging to obtain the selectivity of a microreactor configuration in a conventional reactor, the data acquired at microscale can be used as a guide to understanding the process limitations during scale-up.

Example 3: Topology optimization (Schäpper *et al.*, 2011)[25]

The third case study (Schäpper *et al.*, 2011),[25] presents a new approach to the design of microbioreactor layouts using topology optimization, a method which had previously been successfully applied in the design of optimal catalytic microreactors.[26] Topology optimization is an iterative mathematical optimization technique which can optimize a design according to the value of a pre-defined objective function. In this case the design was the spatial distribution of immobilized yeast cells and their carrier material inside a small bioreactor, which was optimized based on the yeast cells' total production of a given protein as the objective function.

The yeast *Saccharomyces cerevisiae* was chosen for this study for several reasons: it is one of the best known model systems, and *S. cerevisiae* is furthermore one of the microorganisms most commonly used in the biotechnology industry.

Simulations were carried out using the software COMSOL coupled to MATLAB and the optimized reactor was a rectangular microbioreactor with a length of 1.2 mm and a width of 1.2 mm. A constant pressure difference between inlet and outlet provided a continuous flow of glucose containing medium inside the reactor.

Inside the reactor, the distribution of a carrier material with immobilized yeast cells was then optimized. The carrier was modeled as a porous, sponge-like material which gave rise to an additional so called Darcy friction anti-parallel to the flow medium. For the volumes inside the reactor with no carrier present, i.e. those regions only containing culture medium, the Darcy friction was set to zero.

For a given distribution of carrier material in the reactor, the flow velocities of the medium were calculated from the steady state Navier-Stokes equation, taking the Darcy friction of the carrier material into consideration. These flow velocities were then used in the second part of the calculations, where kinetic models were applied to model the protein production in the reactor.

Topology optimization was then applied in order to find a better reactor design with a more beneficial distribution of carrier material, and each candidate was evaluated based on how high a protein production the configuration could achieve.

The kinetic model in this study was based on the work of Bránýik *et al*. (2004)[27] and Zhang *et al*. (1997),[28] and describes the yeast metabolism through the three metabolic events described in Fig. 4.

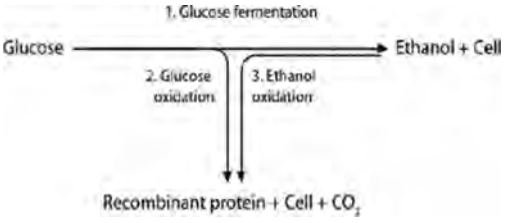

Fig. 4 – *The three pathway model for yeast metabolism suggested by Zhang et al. (1997).[28] (Figure adapted from (Schäpper et al., 2011)[25])*

According to the model, glucose may be oxidized to carbon dioxide along the respiratory metabolic pathway 2. However, if the glucose flow becomes too large for the respiratory capacity of the cell, excess glucose is fermented to ethanol according to pathway 1, and the activity of the enzymes in the glucose oxidation pathway is reduced. When glucose approaches depletion, ethanol begins to be metabolized by pathway 3. The cells grow exclusively on ethanol when glucose is exhausted.

In this model, the production of the desired protein is assumed to be associated with growth and is exclusively associated to the oxidative metabolism (pathways 2 and 3) in the yeast cells. This means that the production of the protein will be negatively affected by, for example, too high glucose concentrations.

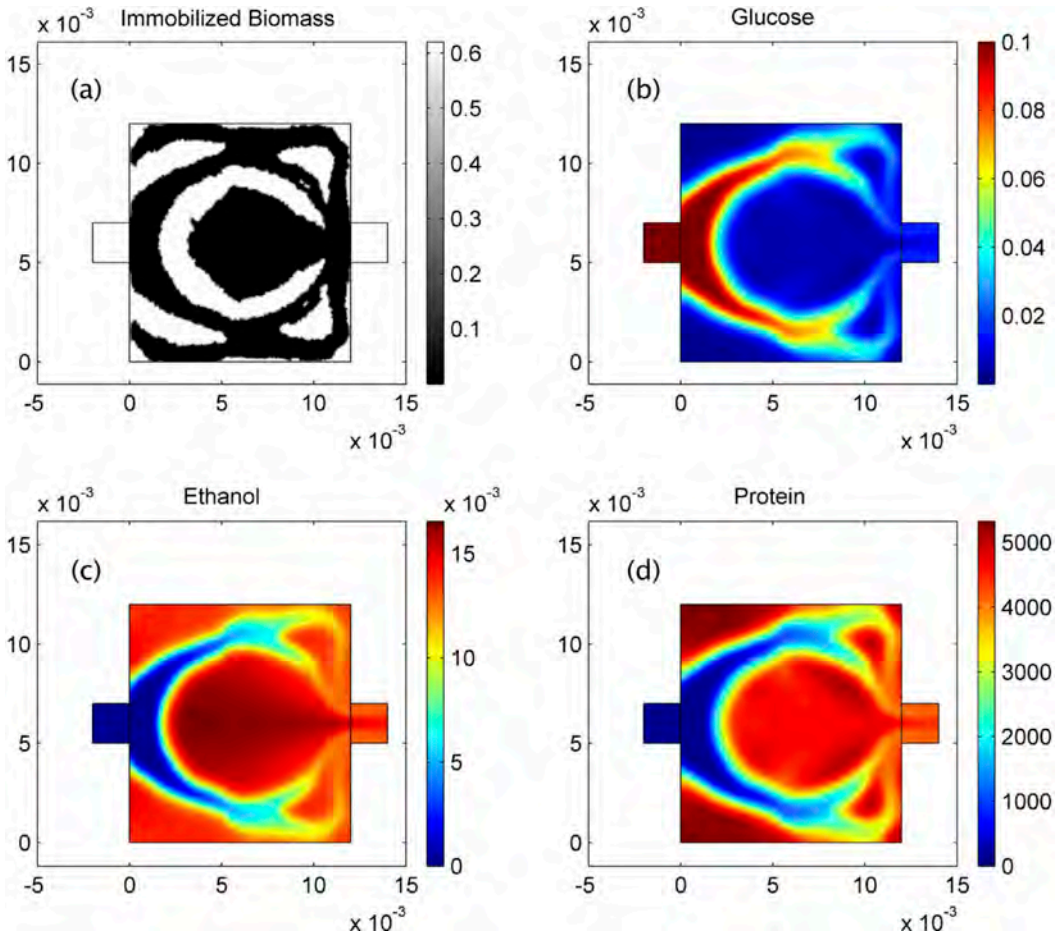

Fig. 5 – *Resulting structure and concentrations for a glucose inflow concentration of 0.1 g L^{-1}. (a) Distribution of biomass where white = cells and black = fluid, (b) glucose concentration [g L^{-1}], (c) ethanol concentration [g L^{-1}] and (d) protein concentration [units L^{-1}]. From Schäpper et al. (2011).*[26]

With this as a basis, a set of equations describing glucose consumption, ethanol production and consumption, protein production as well as both immobilized and suspended biomass was implemented as a kinetic model. The concentrations of glucose, ethanol, protein and biomass were then calculated at steady state based on the kinetic models coupled to their diffusion in the medium as well as their convection, based on the previously calculated flow velocities. From this the objective function, which was the total production of protein in the system, was calculated and the carrier distribution re-organized in order to try to find a more optimal distribution, by repeating the flow and kinetic calculations.

The total protein production in the optimized bioreactors (i.e. in the reactors with an optimized distribution of carrier) was then compared to the calculated performance of non-optimized reactors (i.e. in reactors where the carrier material was homogeneously distributed).

This comparison was made for different glucose concentrations in the feed and the results can be seen in Table 4, which shows that the protein mass flow rate at the outlet increased at least fivefold for all the simulated glucose concentrations when topology optimization was applied. The resulting structure for the case with a glucose concentration of 0.1 g L^{-1} in the feed can be seen in Fig. 5, together with its resulting glucose, ethanol and protein concentrations at steady state.

The significant gain in protein concentration can be explained by the fact that a structurally optimized distribution, where flow is distributed and islands of biomass are surrounded by streams of liq-

Table 4 – *Comparison of the total protein outputs for the homogeneous and the optimized reactor at different glucose feed concentrations*

Glucose feed conc. (mg L^{-1})	Protein flow at the reactor outlet (U sec^{-1})		
	homogeneous reactor	structurally optimized reactor	increase (fold)
1	0.3	2.7	5.8
5	1.4	12.9	9.1
10	2.7	23.1	8.4
30	7.2	57.4	8.0
50	10.7	91.7	8.5
100	17.6	170.3	9.7
200	25.2	229.5	9.1
500	39.0	325.2	8.3
1000	63.8	380.4	6.0

uid flow, allows for a more balanced distribution of glucose across the reactor leading to higher local protein production rates.

This first theoretical investigation of the potential of topology optimization for improvement of microbial cultivation processes at micro scale has clearly shown that the use of this methodology can potentially lead to microbioreactors with a significantly higher productivity than conventional reactor designs where immobilized biomass is homogeneously distributed.

Discussion

The presented case studies have different levels of complexity, and address different experimental scales as well. For the first case a lab-scale biocatalytic reaction is described by a system of coupled algebraic and ordinary differential equations that have been solved for a number of state variables, while for the second case, a microreactor, the Navier-Stokes equation has been solved with a mass balance for two different slow diffusing species. Finally in the last case study the partial differential equation systems for momentum and mass transport have been coupled with the kinetic rate laws of a relatively simple biological model, and this model of a microbioreactor was then linked with an optimization routine.

In the case studies, different types of information can be gathered from the calculations. In the first example, a model is confirmed with respect to the prediction quality, which by calibration may be further improved. In the second example a CFD model is applied in order to gain a better understanding of existing experimental data collected in a microscale reactor. Here new insight is quickly gained from a rapidly performed experiment, and this new information – the diffusion coefficient – can subsequently be used for the prediction of later experiments. Finally, the third example is completely theoretical and describes how an advanced model is used with the intention of generating new design configurations of an otherwise relatively well known fermentation system. The future challenge here is to verify experimentally whether new and intensified reaction systems can be generated. An evolutionary algorithm is furthermore implemented in order to achieve this goal.

Such examples are interesting from a scientific point of view, but also the more practical oriented scientist or engineer should consider the more systematic use of PSE methods and tools, since these methods and tools offer a range of convincing opportunities, as well as saving considerable resources. Indeed guiding experimentalists to the most valuable experiments is a key role of PSE methods and tools in general, and modeling in particular.

In most cases it is impossible to investigate all potential process configurations experimentally. Indeed, there is often not enough material (substrate, enzymes and other reactants) available, and if so the time/manpower for the experiments is limited. PSE methods can assist here as well. A broad range of theoretical configurations can be tested in relatively simple simulations and hence the impact of product inhibition, substrate inhibition, co-factor inhibitions and especially also mass transfer limitations due to reactor designs can be tested. A sensitivity analysis[12] is helpful for planning of experiments which can be used for the Design of Experiments (DoE) or Optimal Experimental Design (OED). The sensitivity analysis – local or global – will for example give an indication of which variables to measure in order to allow estimation of specific parameters. New process options can be investigated as well, before they are experimentally tested. In this way, PSE methods and tools can support process development. Even more importantly, PSE methods and tools can support process development in a structured way, meaning that the tools can be used over and over again each time a new process development task is started up.

Another area of application is the direct coupling of experimental data and mathematical simulations. Here well-established models will help to access requested but not available information. For example in case study 2 the diffusion characteristics of acetophenone and methylbenzylamine were not known and could not be found in literature. A surprising result was that by an appropriate experimental design (again planned with help of a model) it was discovered that one of the species diffuses sub-

stantially slower than the other. This was unexpected, since the molecular weight and the chemical structure are very similar. The acquired material properties are fundamentally important for the mass transfer limitations in the reaction and hence this information can also be used for scale up and scale out of reactors and processes.

From an intellectual point of view most interesting is the application of models for testing of concepts and even generation of entirely new ideas. It is not important, that the model predicts correctly from a quantitative point of view. As long as the qualitative prediction capacity is sufficient, the models can be used for the generation of understanding, insight and evaluation of new ideas. The user can visit the virtual laboratory in order to test simple relationships, complex interactions between different kinetic formulations and material transport limitations or simply to obtain a different view of a problem which the user is assumed to have been working with already for a long time. The more exact and experimentally validated the models are, the user might even omit the experimental validation of the simulation. This is classically done in engineering areas like turbine design or ship design, where the fabrication of prototypes is too demanding with respect to the costs.

The impact of the PSE tools can be substantial when the interdisciplinary nature of the project is guaranteed by a proper collaboration of different experts, such as protein scientists, chemists, process engineers, mathematicians and physicists. Then today futuristic appearing models can be used for advanced optimization routines, where under the assumption that the model is right, complex configurations can be automatically produced and hence reactors can be optimized with respect to topology and shape.

A last important potential application area for PSE methods is the transfer of experimentally established knowledge across scales. Miniaturized reactor technology is receiving increased attention due to the economic potential with respect to reduced time and costs in process development. But even though more and more companies are using or experimenting with such technology it is still unknown to what extent the experimental results can be used for the comparison with setups at another scale.

As presented in Table 5, the experimental setup of micro-scale experiments is dominated by laminar flow conditions and hence the mixing is poor and often diffusion limited. This results in considerable material transfer limitations and hence partial differential equations (PDE) have to be solved, for instance by use of CFD models, in order to predict the conditions in such systems. When changing to bench or pilot scale experiments it can be assumed that the systems are relatively well mixed and the mathematical description can be reduced to ordinary differential equations (ODEs), which simplifies the mathematical description of those systems. At full scale the situation is again such that there are mixing limitations due to the physical reactor design and a limited transfer of kinetic energy in comparison to bench/pilot scale setups. The fluid dynamic conditions are here highly turbulent and hence more complex PDE systems (CFD models) have to be applied which also consider turbulence modeling. Under the assumption that

1. The kinetics can be transferred across scales and
2. The model analysis tools can be used at all scales

it will be possible to answer many open questions with respect to the varying performances of systems at different scales, which is a research area in biochemical process technology which receives considerable attention nowadays.

Table 5 – *Summary of the variation of reactor characteristics and model tools across reactor scales*

Scale	Characteristics	Models
Micro-scale	Not well mixed, laminar flow, material transport limitations	PDEs (CFD)
Lab scale	Well-mixed	ODEs
Pilot scale	Usually well-mixed	ODEs
Full scale	Often not well mixed, gradients	PDEs (CFD), ODEs (compartment model)

According to the complexity of the presented case studies also the requested mathematical skills, knowledge and experience of the user has to be appropriately matching the task. For the first case study an experienced student, working for instance on a master project, might be the appropriate person to perform the task. As here presented, the system is modelled with help of MATLAB and mass balances which are coupled with the governing kinetic reaction rate expressions. In the second case study a commercial CFD software (ANSYS CFX 12.5) has been used, which made the numerical investigation simple with respect to the CFD work (days). But it should be considered that a commercial license of such software might not be available at all companies or research institutions. This would then demand either an investment into a license or the use of open software, where the latter then would need considerable training for the person involved. Finally in the third case, again a commercial CFD software (COMSOL) has been used and coupled with an evolutionary algorithm written in MATLAB. Clearly this is the most advanced PSE example that is presented here and a considerable experience

with this software tool has been a requirement. Consequently, the user of this software has been an advanced user and has nevertheless spent a considerable amount of time (month) on this task.

Conclusions and perspectives

This article has briefly presented an overview about how Process System Engineering (PSE) methods can be used for the systematic development of (bio) reactor systems. Three case studies have been presented with different applications, reactions and scales. The intention of the studies is to present different applications of PSE tools. One important focus area is the use of PSE methods for the development of miniaturized reactor systems. It was demonstrated, how models can assist in achieving a better understanding of the process conditions, the prediction of process performance and the theoretical investigation of reaction conditions with computer based algorithms for reactor improvement. The manuscript gives the reader a motivation for the use of PSE models and tools at different scales and level of detail of applications. This included practical aspects like determination of material constants or reaction performance as well as more academic use like in optimization routines. The future and experimental studies will show if such *in silico* investigations will contribute to the reduction of process development costs and improved understanding of processes across scales.

ACKNOWLEDGEMENTS

Financial support by the European Union FP7 Project BIOINTENSE – Mastering Bioprocess integration and intensification across scales (Grant Agreement Number 312148) is gratefully acknowledged. The research work furthermore received financial support from the Danish Council for Independent Research | Technology and Production Sciences (project number: 10-082388), and from the Novo Nordisk Foundation (project: Exploring biochemical process performance limits through topology optimization).

List of symbols and nomenclature

Abbreviations

CDH – Cellobiose dehydrogenase
ABTS – 2,2'-azino-bis(3-ethylbenzothiazoline-6--sulfonic acid) diammonium salt
$ABTS^+$ – 2,2'-azino-bis(3-ethylbenzothiazoline-6--sulfonic acid) diammonium salt cation radical
HPLC – High-performance liquid chromatography

Nomenclature

V_{max} – Maximum initial velocity of an enzyme, mM h^{-1}
K_M – Michaelis-Menten constant, mM
K_La – Volumetric mass transfer coefficient, h^{-1}
K_{hyd} – Hydrolysis constant, h^{-1}
C_0 – Initial concentration of any species, mM
C – Concentration of any species, mM
r – Reaction rate, mM h^{-1}

Subscripts

lact – Lactose
LBL – Lactobiono-lactone
LBA – Lactobionic acid
O_2 – Oxygen
ABTS – Reduced redox intermediate
$ABTS^+$ – Oxidized redox intermediate
omt – Oxygen mass transfer

Superscripts

CDH – Cellobiose dehydrogenase
lacc –Laccase
$ABTS^+$ – Oxidized redox mediator
ABTS – Reduced redox mediator
sat – Saturation

References

1. *Pollard, D. J., Woodley, J. M.*, Trends Biotechnol. **25** (2007) 66. doi: dx.doi.org/10.1016/j.tibtech.2006.12.005
2. *Tufvesson, P., Lima-Ramos, J., Nordblad, M., Woodley, J. M.*, Org. Process Res. Dev. **15** (2011) 266. doi: dx.doi.org/10.1021/op1002165
3. *Krühne, U., Heintz, S., Ringborg, R., Rosinha, I. P., Tufvesson, P., Gernaey, K. V., Woodley, J. M.*, Green Processing Synth. **3**, 1, (2014) 23.
4. *McMullen, J. P., Jensen, K. F.*, Org. Process Res. Dev. **15** (2011) 398. doi: dx.doi.org/10.1021/op100300p
5. *Schäpper, D., Zainal Alam, M. N. H., Szita, N., Eliasson Lantz, A., Gernaey, K. V.*, Anal. Bioanal. Chem. **395** (2009) 679. doi: dx.doi.org/10.1007/s00216-009-2955-x
6. *Klatt, K., Marquardt, W.*, Comput. Chem. Eng. **33** (2009) 536. doi: dx.doi.org/10.1016/j.compchemeng.2008.09.002
7. *Stephanopoulos, G., Reklaitis, G. V.*, Chem. Eng. Sci. **66** (2011) 4272. doi: dx.doi.org/10.1016/j.ces.2011.05.049
8. *Gernaey, K. V., Cervera-Padrell, A. E., Woodley, J. M.*, Comput. Chem. Eng. **42** (2012) 15. doi: dx.doi.org/10.1016/j.compchemeng.2012.02.022
9. *Asprey, S. P., Macchietto, S.*, Comput. Chem. Eng. **24** (2000) 1261. doi: dx.doi.org/10.1016/S0098-1354(00)00328-8

10. *Sales-Cruz, M., Gani, R.*, Comp. Aid. Chem. Eng. **16** (2003) 209.
doi: dx.doi.org/10.1016/S1570-7946(03)80076-7
11. *Marquardt, W.*, Chem. Eng. Res. Design **83** (2005) 561.
doi: dx.doi.org/10.1205/cherd.05086
12. *Sin, G., Gernaey, K. V., Eliasson Lantz, A.*, Biotechnol. Progr. **25** (2009) 1043.
doi: dx.doi.org/10.1002/btpr.166
13. *Santacoloma* (2012) Multi-enzyme process modelling. PhD thesis, Technical University of Denmark, Kgs. Lyngby, Denmark. p 197.
14. *Van Hecke, W., Bhagwat, A., Ludwig, R., Dewulf, J., Haltrich, D., Van Langenhove, H.*, Biotechnol. Bioeng. **102** (2009) 1475.
doi: dx.doi.org/10.1002/bit.22165
15. *Ludwig, R., Ozga, M., Zámocky, M., Peterbauer, C., Kulbe, K. D., Haltrich, D.*, Biocatal. Biotranfor. **22** (2004) 97.
16. *Van Hecke, W., Ludwig, R., Dewulf, J., Auly, M., Messiaen, T., Haltrich, D., Van Langenhove, H.*, Biotechnol. Bioeng. **102** (2009) 122.
doi: dx.doi.org/10.1002/bit.22165
17. *Galhaup, C., Goller, S., Peterbauer, C. K., Strauss, J., Haltrich, D.*, Microbiol. **148** (2002) 2159.
18. *Sin, G., Ödman, P., Petersen, N., Eliasson Lantz, A., Gernaey, K. V.*, Biotechnol. Bioeng. **101** (2008) 153.
doi: dx.doi.org/10.1002/bit.21869
19. *Cornish-Bowden, A.*, Fundamental of enzyme kinetics, Third Edition, Portland Press Ltd., London, 2004.
20. *Leskovac, V.*, Comprehensive Enzyme Kinetics, Kluwer Academic/Plenum Publishers, New York, 2003.
21. *Bodla, V. K., Seerup, R., Krühne, U., Woodley, J. M., Gernaey, K. V.*, Chem. Eng. Technol. **36** (2013) 1017.
doi: dx.doi.org/10.1002/ceat.201200667
22. *Tufvesson, P., Lima-Ramos, J., Jensen, J. S., Al-Haque, N., Neto, W., Woodley, J. M.*, Biotechnol. Bioeng. **108** (2011) 1479.
doi: dx.doi.org/10.1002/bit.23154
23. *Al-Haque, N., Santacoloma, P. A., Neto, W., Tufvesson, P., Gani, R., Woodley, J. M.*, Biotechnol. Progr. **28** (2012) 1186.
doi: dx.doi.org/10.1002/btpr.1588
24. *Bruus, H.*, Theoretical Microfluidics, First Edition, Oxford University Press, Oxford, 2008.
25. *Schäpper, D., Lencastre Fernandes, R., Lantz, A. E., Okkels, F., Bruus, H., Gernaey, K. V.*, Biotechnol. Bioeng. **108** (2011) 786.
doi: dx.doi.org/10.1002/bit.23001
26. *Okkels, F., Bruus, H.*, Physical Review E. **75** (2007) 16301.
doi: dx.doi.org/10.1103/PhysRevE.75.016301
27. *Bránýik, T., Vicente, A. A., Kuncová, G., Podrazký, O., Dostálek, P., Teixeira, J. A.*, Biotechnol. Progr. **20** (2004) 1733.
doi: dx.doi.org/10.1021/bp049766j
28. *Zhang, Z., Scharer, J. M., Moo-Young, M.*, Bioprocess Eng. **17** (1997) 235.
doi: dx.doi.org/10.1007/s004490050380

Reaction Chemistry & Engineering

REVIEW

View Article Online
View Journal | View Issue

Cite this: *React. Chem. Eng.*, 2016, **1**, 10

The application of reaction engineering to biocatalysis

R. H. Ringborg and J. M. Woodley*

Received 30th September 2015,
Accepted 4th January 2016

DOI: 10.1039/c5re00045a

rsc.li/reaction-engineering

Biocatalysis is a growing area of synthetic and process chemistry with the ability to deliver not only improved processes for the synthesis of existing compounds, but also new routes to new compounds. In order to assess the many options and strategies available to an engineer developing a new biocatalytic process, it is essential to carry out a systematic evaluation to progress rapidly and ensure decisions are made on firm foundations. In this way, directed development can be carried out and the chances of implementation of a commercially successful process can be much improved. In this review we outline the benefits of reaction engineering in this development process, with particular emphasis of reaction kinetics. Future research needs to focus on rapid methods to collect such data at sufficient accuracy that it can be used for the effective design of new biocatalytic processes.

Introduction

In recent decades a growing branch of synthetic chemistry has been established which uses enzymes to catalyze interesting reactions for the production of valuable molecules.[1,2] Such an approach is termed biocatalysis and today finds application in the synthesis of many chemical products, ranging from bulk commodities to pharmaceutical intermediates.[3–6] Several hundred industrial processes have already been implemented, mostly in the pharmaceutical industry, with more in development.[3,7] The motivation for the application of such catalysts stems from their ability to perform highly selective chemistry under mild conditions in water based solutions, making them attractive as 'green' catalysts.[8] In the last decade the ability to alter the properties of the enzyme *via* protein engineering[9–11] has enabled the synthesis of entirely new molecules and reactions (without precedent in nature).[10,12] Multi-step sequences of enzymes, operating sequentially or in tandem,[13,14] as well as chemo-enzymatic combinations[15,16] have now also been established. In short, biocatalysis provides a valuable tool to complement many established synthetic approaches. Despite these scientific developments biocatalysis is still often limited in application due to a poor transition from the laboratory to the process plant. There are several good reasons for this, but amongst the most important is the complexity of enzyme kinetics, combined with the fact that the enzymes need to carry out synthetic reactions under conditions far away from those found in Nature. This makes the

CAPEC-PROCESS Research Center, Department of Chemical and Biochemical Engineering, Technical University of Denmark, DK-2800 Lyngby, Denmark. E-mail: jw@kt.dtu.dk

R. H. Ringborg

Rolf H. Ringborg is currently a postdoctoral researcher at the Technical University of Denmark (DTU). In 2015 he received his Ph. D in chemical engineering researching enzyme kinetics with the aim of accelerating biocatalytic process development. His research interests revolve around how biocatalytic processes can be developed at the interface of reaction-, process- and biocatalyst-engineering.

J. M. Woodley

John M. Woodley (originally from the UK) is currently Professor of Chemical Engineering at the Department of Chemical and Biochemical Engineering at the Technical University of Denmark (DTU, Lyngby, Denmark). His research group is focused on thermodynamics, kinetics and process integration of new bioprocesses, including laboratory and pilot scale experimentation. He is a Fellow of the Institution of Chemical Engineers (UK) and a Fellow of the Royal Academy of Engineering (UK).

collection of parameters in kinetic models especially difficult. For conventional chemical reactions (including catalytic conversions), reaction engineering has long provided an efficient and effective methodology for the design and sizing of appropriate reactors in which to synthesize valuable industrial chemicals.[17–20] At the heart of the discipline lies the determination of rate laws, collection of kinetic parameters and the application of these models to mass balances to enable *in silico* prediction of product concentration and reactant conversion as a function of residence time. It is an essential activity to inform chemical engineers charged with the design of pilot-scale or full scale plant. The time is now right for the development of such a paradigm for biocatalytic reactions where suitable methods are established for deriving kinetic expressions, not solely aimed at the mechanistic understanding required by biochemists, but now also of appropriate accuracy to be used by (bio)chemical engineers to design (bio)reactors. Such design should also include options for defining suitable biocatalyst loadings and operating schemes to make optimal use of existing equipment, which is often the requirement in the pharmaceutical industry. Likewise such design should also enable considerations for improvement of the enzyme itself[21] (*via* protein engineering) as well as the process plant and operation to be considered.

In order for the new biocatalytic synthesis routes to reach industrialization it is necessary to have models describing the kinetic properties of the biocatalyst. Chemical engineering tools can then be used to scale and design facilities. Ideally, for the biocatalyst to reach this stage several requirements need to be met.

- An enzyme has been developed to thrive in the operational conditions required in the industrial process, frequently much harsher than those found in Nature. For example, a process for pharmaceutical synthesis, requires product concentrations of >50 g L^{-1},[3,6,22,23] with a biocatalyst yield of 10–100 $g_{Product}\ g_{Immobilized\ Biocatalyst}^{-1}$.[22,23]
- The enzyme has been characterized comprehensively in terms of kinetics and stability.
- A model has been fitted to describe the rate of reaction in the full conversion range.
- A process concept has been made to define targets for the performance of the enzyme.

These four requirements are often attained in an iterative manner, leading to inefficiencies. Systematic procedures would be far more preferable to give the opportunity to assess the feasibility of processes quickly and where appropriate design optimum development strategies. Enzyme kinetics lies at the center of this procedure.

Today processes are developed first with an emphasis on protein engineering to broaden substrate scope, and secondly by process engineering to enable implementation. However, it is our contention that investigation of potential processes should be considered much earlier in the development procedure, so that it is possible to use reaction engineering as a guide for protein engineering such that biocatalytic properties match the process requirements. Indeed, without such guidance there is even a danger of 'over'-engineering an enzyme. We believe judicious use of process engineering in concert with protein engineering may ultimately prove more effective.

With this background to the importance of kinetics, we will in this review describe different kinetic models of enzymes important to synthesis and production, and describe methods available for determination of rate laws (and associated kinetic parameters). Importantly, we will describe the application of such models in process evaluation and design and give a future outlook, emphasizing where they can be used to assist the targeted improvement of the biocatalysts themselves.

Biocatalytic process features

As described in numerous texts, chemical reaction engineering is built around the determination of a rate law (defining the relationship of the rate of reaction with the concentration of reactants and catalyst, under given conditions). Although in essence the rate law is similar whether an enzymatic or a chemical catalyst is used (*e.g.* Michaelis–Menten kinetics are equivalent to Langmuir–Hinshelwood), in reality extra terms are required in enzyme catalysis to account for reactant and product inhibition at the extraordinarily high concentrations required for an industrial process, compared to those found in Nature. This added complexity needs to be built into the rate law and becomes particularly important when multiple reactants are used and/or products produced. Hence the rate law may prove particularly complex and while the estimation of macro-kinetic parameters is difficult, the estimation of micro-kinetic parameters is in many cases impossible due to problems of identifiability.

A second feature of enzyme reactions is that they usually take place in the liquid phase. This means that operating a simple continuous plug flow reactor for catalyst characterization, is frequently limited due to high pressure drops. The many chemical reactions that take place in a gas phase can easily overcome such problems, due to much lower viscosities and higher diffusion rates. Additionally, enzyme reactions in Nature mostly take place in an aqueous environment, and while many enzymes have the ability to work in organic media (to a greater or lesser extent), clearly the kinetics are affected.[24] In many cases the requirement for addition of an organic solvent is essential based on the poor water-solubility of many of the most interesting industrial compounds. The complex structure of an enzyme also means that the protein is subject to unfolding under exposure to extremes of pH, temperature, ionic strength and interfacial effects.[25] In general, conditions such as the solvent, pH and temperature will therefore be predefined, but in principle this also provides room for optimization, provided suitable kinetic data is available as a function of these variables. In itself this also implies a vast space of reaction conditions.

The third important feature of biocatalysis, with respect to reaction engineering, concerns thermodynamics. The early

days of biocatalysis focused in particular on hydrolytic reactions, in the presence of water. Since then we now know that the amount of water required to maintain structure is minimal (although essential) meaning such reactions can be run in reverse.[26,27] Biocatalysts lowers the activation energy for both directions of a reaction and thermodynamics determines the favourable direction. Nonetheless, it can be desirable to operate reactions in the unfavourable direction for synthetic purposes. Specific products, low cost substrates or natural substrates can be the motivator for such a direction of reaction, but makes the process considerable more difficult to design. Substrate and consequently product pairs can however be chosen so that the direction of the reaction will be overall favourable. This has been shown for amine transaminases[28] and can also be obtained by coupling the main reaction with enzymatic cascades.[29] In cases where reactions are operated against the thermodynamically favourable direction it is necessary to collect thermodynamic data to establish the reaction equilibrium as well as the kinetic data. Unlike chemical catalysts where the variables of pressure and/or temperature can be used to shift equilibrium, for biocatalysis other methods are required such as use of an excess of a reactant (provided it is beneath its inhibitory threshold) and *in situ* product removal (ISPR technologies).[30,31] This also needs consideration in reaction engineering.

For all these reasons we argue that biocatalysis is deserving of a separate treatment in reaction engineering. The variables available to improve the process metrics, as well as the targets required, are quite different depending on whether one develops a chemo-catalytic reaction or a biocatalytic reaction. For example, the operational temperature for chemo-catalysts can span hundreds of degrees and investigation of rate constants can be extrapolated by activation energies to describe this change. The different activation energies of parallel reactions can then be used to tune selectivity. In contrast, the temperature range for enzymes is rather limited and selectivity rarely a concern.

Operational window for kinetic studies

Historically and still today for biocatalysis, activity assays are used for the investigation of enzyme kinetics. These preliminary studies include an investigation of the effect on reaction rate of changes in temperature, pH, ionic strength, enzyme and component concentration. The results have not always been presented in a rate law, but have most often provided a useful starting point for more detailed studies by fixing some of the environmental variables such as ionic strength, pH and temperature. Experiments have usually been carried out by mixing all components together at the same time and thereafter monitoring the development of the individual component concentrations. The rate of reaction has then been defined as either the disappearance or production of a component over time. The initial testing of enzymes usually includes an investigation of the linear activity/enzyme concentration range and the optimal pH. After this has been established, enzyme concentration can be fixed so as to obtain subsequently measured initial rates in a reasonable time period. pH is then also fixed in accordance with the highest activity observed, which usually also represents the most stable condition for the enzyme. Care should however be taken here to investigate the protonation of the different compounds in solution. The activity dependence on temperature for enzymes is similar to that of chemo-catalysts. Here also the empirical rule of a 10 °C increase in temperature resulting in a two-fold increase in rate holds true.[32] However, with enzymes, denaturation can also occur at higher temperatures, resulting in a trade-off of activity and stability – most usually reported as an optimum temperature. The temperature at which an enzyme is fully denatured is termed its melting temperature.[33] Technology for measuring this is available and can be done either with differential scanning calorimetry (DSC)[34] or the recently developed thermal shift methodology.[35] At temperatures beneath the melting temperature, denaturation will still occur but at a slower rate, and can easily be mistaken for inhibition. An optimal temperature will require a minimum enzyme stability and will therefore lie significantly below the melting temperature. In order to avoid stability issues, experiments are therefore often carried out at ambient temperatures similar to these in their natural environment. After fixing the enzyme concentration, pH and temperature, the concentration of the different compounds can be investigated. To put the above analysis into perspective the general workflow for developing a kinetic model for an enzyme can be represented diagrammatically as shown on Fig. 1, without the dashed processes. An overview of the different analysis methods are given later in the article.

The determination of the rate law is the last part of such a workflow. Modelling chemo-catalytic reactions can be done by fitting or testing zero, first or second order rate laws which are relatively straight forward since these will remain constant under specific conditions.[17,36] However, for biocatalytic reactions, the identification of rate laws is more complex since they display mixed order kinetics. The strategy has therefore been to elucidate reaction mechanisms and in turn develop models, prior to parameter estimation based on rigorous experimental data. Not surprisingly, the field of biocatalytic model construction has therefore produced several textbooks covering the common mechanisms.[37,38] Enzyme classification has long been based on the reaction catalysed and according to the convention of the International Union of Biochemistry and Molecular Biology, IUBMB, an agreed nomenclature falls into 6 Enzyme Commission (EC) groups, each of which have a further 3 levels of sub-classes. In this way each enzyme can be characterized by a 4 digit number (*e.g.* transketolase is EC 2.2.1.1). The generalized reactions that are carried out by these enzymes in the 6 groups are summarized in Table 1.

The third column of Table 1 indicates the general reaction equation of these conversions. This is important in order to identify the basic structure of the rate law. For synthetic

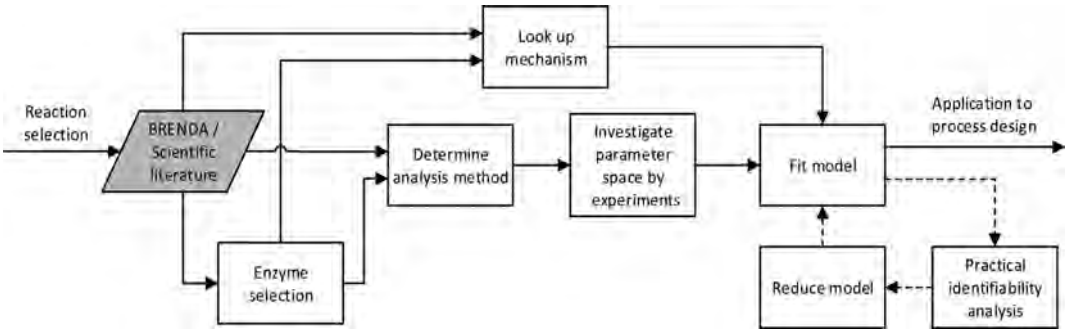

Fig. 1 Proposed workflow for developing a kinetic model, here BRENDA refers to the data base.[115] The dashed line introduces statistical analysis of the model applied.

Table 1 Enzyme commission categories with generalized reaction schemes

Group	Reaction catalyzed	Typical reaction	Enzyme example(s) with trivial name
EC 1 oxidoreductases	To catalyze oxidation/reduction reactions; transfer of hydrogen and oxygen atoms	$A + B \rightleftharpoons P + Q$ $A + O_2 \rightleftharpoons P + H_2O_2$	Dehydrogenase, oxidase
EC 2 transferases	Transfer of a functional group from one substance to another. The group may be methyl-, acyl, amino- or phosphate	$A + B \rightleftharpoons P + Q$	Transaminase, transketolase
EC 3 hydrolases	Formation of two products from a substrate by hydrolysis	$A + H_2O \rightleftharpoons P + Q$	Lipase, amylase, peptidase
EC 4 lyases	Non-hydrolytic addition or removal of groups from substrates. C–C, C–N, C–O or C–S bonds may be cleaved	$A \rightleftharpoons P + Q$	Aldolase decarboxylase
EC 5 isomerase	Intramolecular rearrangement, *i.e.* isomerization changes within a single molecule	$A \rightleftharpoons P$	Isomerase, mutase
EC 6 ligases	Join together two molecules by synthesis of new C–O, C–S, C–N or C–C bonds with simultaneous breakdown of ATP	$A + B + ATP \rightleftharpoons P +$ ADP + Pi	Synthetase

purposes, the emphasis lies with EC groups 1–4,[1,2,5,6] where typical reaction schemes involve two reactants and two products (with the exception of EC 4 that in the synthesis direction only has a single product). General models for EC groups 1–3 are summarized in Fig. 2 and represent so-called ordered, random and ping pong bi–bi mechanisms, reflecting the order in which multiple substrates and products are bound to or released from the enzyme complex, respectively. Enzymes in EC group 4 will also follow these models but in a reduced form since this group has a reaction equation with one less specie. Examples of synthetically useful enzymes from these different EC categories are listed in Table 2. It is well known that the three mechanisms listed do not represent all enzymes, and both more complex as well as simpler mechanisms exist. Nonetheless, for synthetic purposes these are the most common and further discussion will therefore be based on the identification and parameter fitting of these models in particular.

Mechanistic models

In cases where no mechanism has previously been determined for an enzymatic catalyst of interest, it can be determined by an inhibition study. The initial rates are studied under the conditions where one substrate is varied while the other is kept constant. The mechanism can hereafter be

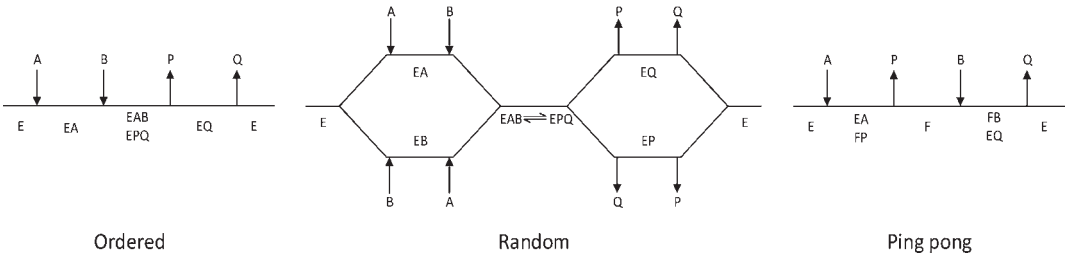

Fig. 2 Cleland representation of ordered bi–bi, random bi–bi and ping pong bi–bi, substrates are denoted A and B, products are denoted P and Q, free enzyme species are denoted E, F, enzyme complexes are denoted EA, EB, EP, EQ, EAB, EPQ.

Table 2 Kinetic mechanisms of different enzymes in different EC categories

EC category	Sub EC #	Reactive group	Case enzyme	Kinetic mechanism	Ref.
EC 1 oxidoreductases		Acting on			
	1.1	Alcohol groups	Alcohol dehydrogenase	Random bi–bi, ordered bi–bi, theorell-chance	39–41
	1.1	Alcohol groups	Galactose oxidase	Ping pong bi–bi	42
	1.2	Aldehyde or oxo groups	Pyruvate dehydrogenase	Ping pong bi–bi	43
	1.4	Amino groups	Mono amino oxidase	Ping pong bi–bi	44
EC 2 transferases		Transferring			
	2.7	Phosphorous-containing groups	Non-specific protein-tyrosine kinase	Random bi–bi	45
	2.4	Glycosyl groups	Glycogen phosphorylase	Random bi–bi	46
	2.1	One-carbon groups	Thymidylate synthase	Ordered bi–bi	47
	2.3	Acyl groups	Histone acetyltransferases	Ordered bi–bi	48
	2.6	Nitrogenous groups	Transaminases	Ping pong bi–bi	49–51
	2.2	Carbon–carbon	Transketolase	Ping pong bi–bi	52, 53
EC 3 hydrolases		Acting on			
	3.1	Ester bonds	Lipase	Ping pong bi–bi	26
	3.2	Glycosyl bonds	Amylase	Ping pong bi–bi	54
	3.5	Carbon–nitrogen bonds	Amidase	Ping pong bi–bi	55, 56
EC 4 lyases		Acting on			
	4.1	Keto acid	Aldolase	Random bi–uni ordered bi–uni	57
	4.3	Carbon–nitrogen	Methylaspartate ammonia-lyase	Ordered bi–uni	58

identified by plotting them in a Lineweaver–Burk plot, see Fig. 3. The relative position of the intercept depends on whether the substrates hinder or favour one another, resulting in an intercept above or below the abscissa, respectively. Commonly, the intercept will appear to the left of the ordinate above the abscissa. If both substrates bind independent of one another then the intercept should lie on the abscissa, indicating a random mechanism. When parallel lines are observed, then a ping-pong mechanism is inferred. As can be observed in Fig. 3, the enzyme is either in the form of one or other complex (EX) or alternatively activated enzyme (F). Experiments need to be designed such that the substrate concentration greatly exceeds that of the enzyme. This is not required in order to saturate the enzyme but rather to have a negligible amount of the substrate bound to the enzyme.[59] The required sensitivity of the analysis method for measuring the different enzymatic species can thereby only be achieved by the sensitive fluorescence methods. Aside for mechanistic studies, for reaction engineering the inability to measure the species restricts model fitting substantially and estimation of micro-kinetic constants will therefore only make sense in cases where the individual species can be measured. The necessary simplification of the models is achieved primarily by the steady state assumption, which states that the concentration of enzymatic species reaches steady state after milliseconds of reaction. Additionally, the rate constants are collected together in the form of equilibrium-like constants, K, which are termed macro-kinetic constants. For example the model for the ping pong bi–bi mechanism without dead-end inhibition[37] is shown in eqn (1)

$$v = \frac{V_f V_r \left([A][B] + \frac{[P][Q]}{K_{eq}} \right)}{V_r K_{m_B}[A] + V_r K_{m_A}[B] + \frac{V_f K_{m_Q}[P]}{K_{eq}} + \frac{V_f K_{m_P}[Q]}{K_{eq}} + V_r[A][B] + \frac{V_f K_{m_Q}[A][P]}{K_{eq} K_{iQ}} + \frac{V_f[P][Q]}{K_{eq}} + \frac{V_r K_{m_A}[B][Q]}{K_{iQ}}} \quad (1)$$

where K_{eq} are described by the following Haldane equations see eqn (2)

$$K_{eq} = \frac{V_f K_{mQ} K_{iP}}{V_r K_{iA} K_{mB}} = \frac{V_f K_{mP} K_{iQ}}{V_r K_{iB} K_{mA}} = \frac{K_{iP} K_{iQ}}{K_{iA} K_{iB}} = \left(\frac{V_f}{V_r} \right)^2 \frac{K_{mP} K_{mQ}}{K_{mA} K_{mB}} \quad (2)$$

There are 8 degrees of freedom (DOF) in this model and fitting it all at once without proper initial guesses and/or constraints is not advised. This is due to the high level of correlation, explained later, where many parameter sets can be a solution that satisfies the objective function. It is therefore rare that a non-linear regression of the complete dataset would result in a global optimum. Recently, our group has published a stepwise approach for the fitting of the ping pong bi–bi mechanism,[51] based on deriving the rate equations for the forward and backward rates independently (eqn (3) and (4)). The remaining model parameters are then adjusted and validated against high conversion experiments. In total, one can

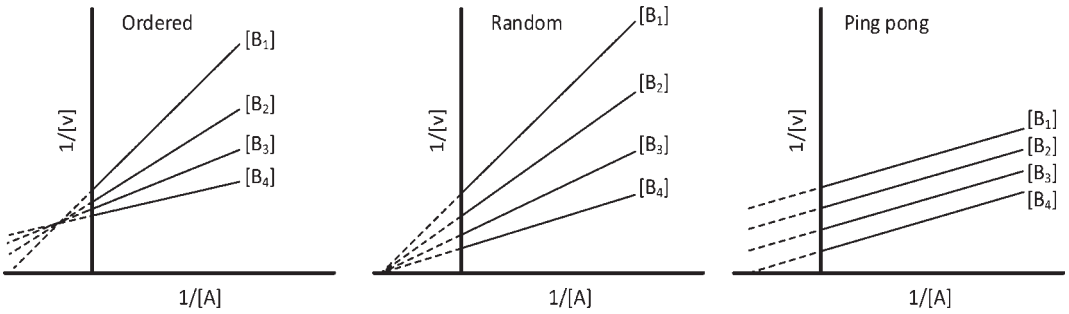

Fig. 3 Lineweaver–Burk plots for the determination of ordered, random and ping pong bi–bi mechanisms.

expect to carry out 45–55 different experiments to have a robust platform for fitting such a mechanism.[51]

$$v_{\text{forward}} = \frac{V_f[A][B]}{K_{m_B}[A] + K_{m_A}[B] + [A][B]} \quad (3)$$

$$v_{\text{reverse}} = \frac{V_r[P][Q]}{K_{m_Q}[P] + K_{m_P}[Q] + [P][Q]} \quad (4)$$

However, such a methodology is not particularly robust since a strong correlation between some parameters exists. A change in one parameter can therefore be compensated by another, *i.e.* the parameters become unidentifiable.

In the scientific literature, makrokinetic reaction networks with sequential, competitive or consecutive steps are models recognized to have highly correlated parameters.[60] This causes problems with finding a global minimum for the objective function, and therefore a unique solution. The estimated parameters from the previously described method rely on "independent estimation", first fitting the forward rate, then fitting the backward rate and finally fitting the remaining parameters. However, because correlation persists further measures need be taken. Model-based design of experiments (MBDoE), uses the model to design new experiments which will yield information in terms of reducing uncertainty or correlation.[60,61] In order for this method to be applicable it is necessary to have a good initial guess of the individual model parameters. The stepwise approach is currently the best way of fitting the data and thus the best "initial-guess" available. MBDoE aims at devising experiments that will yield the most informative data, in a statistical sense, for use in parameter estimation and model validation. The method applies the maximization of the Fisher information matrix (FIM) or minimization of the covariance matrix, which is the inverse of the FIM. The calculated experimental conditions required to reach this point can then be identified and tested. Specific, anti-correlation criteria for experimental design have been described by Franceschini *et al.*[62] In the case where correlation cannot be eliminated, the parameters should be collapsed into a new variable. This variable may lose physical meaning but, as with the case of the rate and equilibrium constants described previously, it is better to have an practically identifiable model.

Methods for obtaining kinetic data

The term 'reaction progress kinetic analysis', coined by Blackmond,[17,36] stresses the importance of on- or in-line analysis to elucidate mechanisms of catalytic systems. Ideally, this would also be routinely applied to the study of enzyme kinetics and Johnson[63] has reported an excellent case applying this to determine the micro-kinetic parameters for the rate law of invertase and the more complex case of EPSP synthase.[64] The goal of that research was to investigate the structure–activity relationship, which is quite different from the process engineering objective, which is the primary target addressed in this paper. In principle, for process design and development all that is desired is a sufficiently accurate model that can describe the kinetic dynamics of a biocatalytic reaction. The stepwise fitting procedure presented in the mechanistic model section is heavily reliant upon initial rates. For this reason determination of macro-kinetic parameters is probably more practical, although correlation remains a challenge. A suitable technology and methodology for determining enzyme kinetics would therefore be very desirable. Ideally it could be used to reliably determine initial rates at low conversion and likewise have the possibility of conducting high conversion experiments. Recent developments include exciting new ways of collecting data at microscale,[65–68] although the associated FT-IR and Raman spectroscopy do not yet deliver the required sensitivity. All the methods are summarized in Table 3.

Spectrophotometric assays

Proteins and enzymes are in general detectable by UV-vis absorption spectroscopy, and can in this way be quantified, although the absorption maxima of many substances, *e.g.*, carbonyl groups or peptide bonds, lie in the far-UV region (122–200 nm), which is not easily accessible. From the perspective of synthesis, many small molecules are used which absorb in the mid-UV region (200–300 nm). Therefore, for determination of enzyme kinetics, both the absolute absorption and spectral changes must be considered. In fact, in many cases

Table 3 Comparison of the different methods for collection of enzyme kinetics, in this context 'continuous' data acquisition implies the measurement can be made in-line or on-line whereas 'discontinuous' implies the transfer of samples (manually) between instruments

	Micro wells	Spectrophotometric assays	Batch	Continuous flow	Stopped-flow	Isothermal titration calorimetry
Detector	UV-plate reader HPLC	UV-vis	HPLC	NIR, IR, Raman	—	Heat flow
Advantages	Automated	In-line	Omnipotent	Automated batch kinetics	Studying reactions in the millisecond range	Direct non-destructive measurement
	Mixing	Cheap	Mixing	Controlled environment		Constant error
	Running many reactions in parallel		Running many reactions in parallel			Determination of ΔH_r
Disadvantages	Generally not sealed	Generally not sealed No mechanical mixing	Manual handling	Long term experiments	Long term experiments	Expensive External validation for ΔH_r Fitting of heat flow
Examples of application	Oxygen dependent systems	Kinetics at benign conditions	Long term experiments	Exo and endothermic reactions	Very fast reactions	Complex and opaque solutions
	Small quantity of consumables			Small quantity of consumables	Assays	
Time range	Seconds–hours	Seconds–few hours	Minutes–days	Few minutes–few hours	Millisecond–few minutes	Second–few hours
Time resolution	Single wavelenght: 1/10 Hz for 96 wells	Up to 100 Hz	Minutes	1-1/15 Hz	Up to 300 Hz	Up to 100 Hz
Data acquisition	Parallel-semicontinuous	Single-continuous	Parallel-discontinouos	Single-continuous	Single-continuous	Single-continuous
Ref.	75–77	40, 41, 43, 49, 50, 78–81	51, 53, 54, 57, 76	65–68	39, 44, 82–86	87–90

the spectral differences in solutions with enzyme, substrate(s) and product(s) are not very large and only small shifts can be observed. Even with curve resolution techniques, the quantification of small molecules proves to be very dependent upon local calibration. Historically, this has been circumvented by determination of the cofactor $NAD(P)^+$, which upon reduction to NAD(P)H forms a new absorption band at 340 nm.[69] This is not only an easily accessible region but has the great advantage that the oxidized form does not absorb at this wavelength, meaning any observed change in absorption is directly proportional to the reaction rate. This technique is directly applicable to dehydrogenases[39–41,43] and these enzymes can also be coupled with other reactions in cascades.[70–72] The reaction conditions of such 'coupled assays' are rather complex to ensure that the test reaction and not the 'indicator' reaction becomes limiting. In general, coupled assays are helpful for the determination of enzyme activity, but cannot be recommended for enzyme kinetic studies for this exact reason. In an analogous way, oxidases can be used to produce hydrogen peroxide which can then oxidize phenol red[73] or xylenol orange[74] detected at 610 and 560 nm, respectively.

Batch reactors

The slowest and most labor intensive method for collecting kinetic data is in batch mode. However, this is also the most robust in terms of wide applicability. Vessels can range from micro wells to laboratory scale equipment, although vessels are commonly chosen in the scale of a few mLs. Such reactors can fit into thermoshakers and aliquots can be drawn without affecting the reaction. The samples can then be measured off-line, most commonly by HPLC. The frequency of sampling is usually quite high for measuring initial rates and 5–10 points can be collected within an hour. Many batch experiments can be carried out in parallel and for a prolonged time, making them ideal for the measuring of progress curves. Here the sampling frequency is in the order of hours.

Flow reactors

More recently systems based on the principles of flow chemistry have been developed to ensure rapid, low-volume and high precision analysis. This can replace many tedious and high volume requirements of conventional analysis. Use of flow systems implies the use of pumps and this environment leads quite naturally towards automation. The implications of computer controlled liquid handling can give rapid characterization throughputs and cost savings. Furthermore, automated operation can remove manual errors and in principle will give more reliable results.

Flow strategies can best be classified dependent upon how the reacting stream is manipulated after merging of the reactant and enzyme. The different types considered here are "continuous flow" which is a non-interrupted flow from introduction to waste, "stopped flow" which holds the mixture in a chamber fit for spectrophotometric measurements and "quench flow" which involves either physically or chemically stopping the reaction at the exit of the system and thereafter analyzing the samples off-line.

Generally flow systems struggle to circumvent the problem of laminar flow, which introduces dispersion into the system. Dispersion elongates the flow profile and hence time required to reach steady state. This is a problem because the concentration profile in the reactor will change over time until steady-state is reached. A comparison of different performance under non-steady state reactor conditions should therefore only be made when the flow conditions are exactly the same, such as constant residence time and Reynolds number. Flow injection analysis (FIA) solves this to some extent by measuring pulses of samples. Here the distribution of the sample is followed over time and the area of the pulse is measured. This method is very similar to that of an HPLC and it is calibrated likewise. What further complicates things for enzymes are their size, which in solution translates to a factor 100 slower diffusivity compared to small molecules (10^{-11} to 10^{-9} m^2 s^{-1}).[91,92] The dispersion of enzymes will therefore be much more pronounced, meaning they are more dispersed through the channel compared to the small molecule reactants and resulting products. Homogeneity of the pulses is therefore questionable for FIA applied to enzyme catalysis. The effect of enzyme diffusion in 83–283 μm wide channels with side-by-side flow has been investigated by Swarts and co-workers.[93] A Michaelis–Menten model was constructed for a β-galactopyranoside enzyme (V_{max} = 20.9 μmol s^{-1} g $enzyme^{-1}$, K_M = 1.04 mM), the model was combined with a computational fluid dynamics (CFD) model. The pure model and the CFD model were subsequently compared to understand the effects of diffusion. Even though the enzyme only occupies half of the reactor volume, the reaction rate was not limiting due to the short characteristic mixing time of the reactant. Consequently, only at high enzyme concentrations (>1 g L^{-1}) in this case would rate limiting effects be observed. Clearly, this is very dependent on the kinetic constants of the enzyme of interest. The investigation was assumed to have been carried out at steady-state, and so the impact of enzyme diffusion on non-steady state methods is yet to be described.

Microfluidic flow reactors

Developments towards carrying out chemical reactions in flow micro-reactors has in recent years received much attention.[94–98] This can also be applied to the collection of kinetic data. In many cases it is likely this will replace the traditionally used flasks or stirred vessels operated in batch mode. The small scale makes it possible to conduct experiments with low material input but yielding the same degree of information about the reaction performance. There are three methods reported in the scientific literature used for conducting such investigations, namely: (1) steady-state, (2) measurements at multiple positions at steady-state and (3) non-steady state. The measurements at non-steady-state are made possible by reconsidering low disperse flow[99] that was originally described by Taylor[100] and Aris.[101] Low-disperse flow

behaves similar to that of plug flow but at relatively small flow rates. What makes this so interesting is that a plug-flow reactor has the same integrated mass balance model as a batch reactor. Sampling from an ideal batch reactor will provide concentration over time data and such data is exactly what is used for kinetic modelling. Low-disperse flow reactors can therefore also be used to obtain this type of data without correction for flow dynamics.

Steady-state. Steady-state measurements of "continuous flow" should represent the kinetic behavior of batch systems. The method will generally be slower for measuring kinetics compared to that of a batch reactor as one will have to wait for steady-state to be attained, prior to making measurements. Normally, operational steady state is measured as a dependence on substrate or product concentration, a small drift might be neglected but could indicate that the mass balance of the enzyme is yet to reach steady state. Looking through the literature this is often not considered and it is expected that this is commonly attributed to uncertainty of the experiments.

Steady state multi point readings. Making microfluidic reactor designs in transparent materials offers the possibility of probing the concentration at different locations along the length of the reactor. These locations represent different residence times according to the flowrate and channel dimensions. Such a combination was recently reported by Fagaschewski and co-workers[67] using IR-spectroscopy. Absorption saturation of water was avoided by substitution with deuterium oxide.

Non-steady state. Mozharov and co-workers have developed a method in which the contents of the reactor are quickly pushed out and measured.[65] It was subsequently possible to correlate concentrations with residence times. The Jensen group at MIT has reconsidered the low-disperse flow,[99] and investigated a method to exploit this region further by implementing a flow ramp after obtaining steady-state. This gradually changes the residence time of the reactor and in this way it was possible to monitor the development of the reaction by coupling the system to FT-IR analysis.[68] The progress curve obtained was compared to steady-state values and thereby validated. The method has already been adopted by others and shown to work as well coupled to analysis using Raman spectroscopy.[66]

Stopped-flow techniques

This technique has been developed for the study of reactions in the millisecond to minutes time range. Transient kinetics can be measured in the lower time range[102–104] if the method is in place. The system can otherwise be used to study steady-state kinetics with the common assays as described previously. Experiments can be carried out by rapidly injecting solutions into a mixing device. The liquid is then led into the flow cell from the mixer, replacing the previous sample, the displaced liquid then fills a stop syringe moving the plunger towards the trigger leaf. After hitting the leaf the flow is stopped and measurement begins. The flow cell is illuminated and data is collected over time. The usual properties exploited are absorbance and fluorescence measurements, as well as application of light scattering, turbidity and fluorescence anisotropy technologies see Fig. 4. In the absence of a spectrophotometric method, quench flow can be applied. Directly after mixing, the solution is be chemically quenched, which can be used to study reactions in the millisecond range. Instead of holding the solution in an observation cell the quenched sample is collected and analyzed elsewhere (*e.g.* by HPLC).

Isothermal titration calorimetry (ITC)

In contrast to spectral methods, measurements performed with ITC, are independent of the optical properties of the solution. ITC instruments have the objective of keeping the temperature constant in the reaction chamber, achieved either by heating or cooling the chamber. The required energy added or subtracted is logged and can be directly translated into reaction rate by relating the heat flow (dQ/dt) to the enthalpy change of reaction (ΔH_r).[105] From a practical perspective this is usually done with a single injection experiment where reactant is inserted into the reaction chamber. In the chamber it is possible to follow the burst of energy as the reaction initiates. From this point the reaction will follow a 1st order reaction development until the return to steady state (zero energy flow). It is necessary to know the exact amount of reactant converted by performing an independent concentration determination. The enthalpy change of reaction can thereafter be calculated by dividing the total heat transferred to the measurement cell by the total number of moles of substrate converted, $n_{\text{sub,converted}}$.

$$\Delta H_r = \frac{\int_{t=0}^{t=\infty} \frac{dQ}{dt} dt}{n_{\text{sub,converted}}}$$

The reaction rate can thereafter be determined by

$$v = \frac{1}{V \Delta H_r} \frac{dQ}{dt}$$

where V denotes the volume of the reaction chamber.

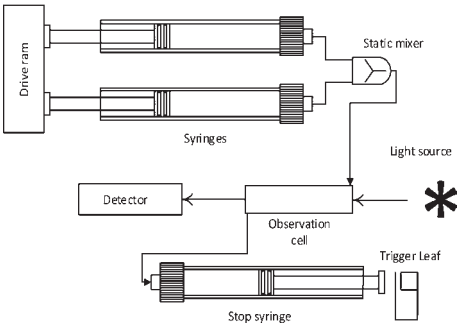

Fig. 4 Concept of stopped flow methods.

The technique of ITC is particularly potent since it can essentially measure any event occurring in a reaction chamber. This is also its problem, since dilution, binding events, interaction of impurities and buffer protonation effects[106] will influence the readout. Pure formulations and materials for experiments are therefore required to ensure accurate measurements. Furthermore, dialysis of macromolecular solutions is also recommended, and preparation of small molecule solutions should be made from dialysate. After satisfying the rather high entrance requirements, it is necessary to match the energy development (rate of reaction) with the lower and upper detection limits. The enthalpy changes for most enzyme-catalyzed reactions range from −40 to −400 kJ mol^{-1}, allowing reaction rates from 10 to 100 pmol s^{-1} to be accurately measured.[107] Despite the fact that ITC has been used to measure enzymatic activity[87,89,90] and that the technology dates back to 1965,[108,109] the method is not found to be frequently applied in the field of enzyme kinetics. The advantage of a direct non-invasive measurement is though obvious and could be applied to a greater extent.

Application of kinetic data for process development

A powerful tool in assessing how a process can be developed is by coupling mass balances in a process design. This can only be carried out if kinetic and thermodynamic models for all the different parts of the process are available. Biocatalytic processes most often deal with the relatively low reaction rates prior to any biocatalyst engineering and this emphasizes the importance of having a reliable kinetic model. Theoretical evaluation is thereafter possible and requirements for the different elements of a process can be set. In the development of new processes one of the most difficult parts is to assess where the bottleneck lies. Moreover, it is not expected that biocatalyst engineering alone will be able to overcome all problems in relation to carrying out reactions at industrial conditions. Today, process engineering is most often only carried out at the end of a protein engineering development phase, where the biocatalyst engineer hands over the enzyme to the chemical engineer. It would be hugely advantageous were process engineers able to be involved earlier such that they could obtain enzymatic kinetic data and fit the different mechanisms (as they do for chemo-catalytic processes) prior to setting targets for enzyme development.

Recent reviews on the application of biocatalytic models,[110,111] show that models are applied to find performance limitations, to define optimal operating conditions, different reactor choices and compare different process configurations. Example: Berendsen and co-workers[112] combined models of two enzymes to optimize the enantiomeric excess as a function of conversion. Schaber and co-workers[113] carried out an economic assessment of a full process. It is therefore clear that these models can be applied to obtain this kind of information, and from a development perspective it is necessary to use these for identification of the bottleneck. For example enzymatic reactions are often hampered by product inhibition at high product concentrations. The introduction of ISPR to the simulation could here reveal targets for a given removal method, which would assist process engineering in terms of improving the method as well as protein engineering in terms of increasing tolerance.

Hence the input from the process engineering gives direction for protein engineering, which in turn drives a better process. While the order of the necessary tasks in process development is still not fixed[22] it remains certain that in order to move the field forward collaboration between chemical engineers and protein engineers must be emphasized.

Discussion

Many spectrophotometric assays require alterations to the original reaction in order to be carried out effectively. This is can be achieved either by derivatization of the reactant with a chromophore or by an analytical enzyme cascade. The widely used indirect spectrophotometric assays rely on the stability of not only the target enzyme but also the assay enzyme and cofactors (*e.g.* NAD(P)H). Testing rather harsh conditions also requires a robust assay and this should therefore be carefully considered in the experimental planning phase. The industrial development environment is rarely able to conduct comprehensive investigations, so both speed and resources are important factors, driving automated and flexible methods similar to those that have been developed for classic organic synthesis.[66,68] However, more sensitive concentration measurement methods are required and preferably in the order of 0.1 mM. The UV-vis spectrophotometer-based assays are therefore still advantageous, and if these fail one can turn to classic chromatographic measurements.

The microfluidic FT-IR method developed by Moore and Jensen[68] can be further developed to automatically propose experiments in the parameter space (*e.g.* concentration, temperature) based on the Fisher information matrix.[114] However, focus in the paper by Schaber and co-workers was to have a fluid dynamic model of the reactor to circumvent the problems of dispersion. We propose that focus should rather be on fitting more complex models while applying the low-disperse flow regime.[99] Having this in mind one can envisage automation of the kinetic models for enzymes. This may be possible after the realization of a versatile and sensitive on-line method.

The different parts of the development required could conceivably be combined into a methodology as proposed in Fig. 1, including the dashed processes. The theory and methods have already been developed, but appropriate models are yet to be produced as a basic step in biocatalytic process development.

Conclusion

In order to find the real bottleneck for the development of a new biocatalytic process, it is necessary to have a kinetic

model of the reaction. The increasing interest in biocatalytic processes and the constant change of catalysts justifies a more streamlined development. Here, the common bi-substrate mechanisms covering most enzymes for synthetic purposes have been shown, the models for these can be found in textbooks and a method for fitting them has been presented. Methods for collecting kinetic data are available and assays can be found for almost any enzyme. The general methods of stopped flow, quenched flow or ITC in combination with HPLC provide an almost universal detection method. Analytical tools coupled with microfluidics are rapidly developing and it can be assumed that a method for enzymatic systems will be available in the near future. The entry barrier of fitting biocatalytic kinetic models is therefore lowered, this enables others to find bottlenecks, quantify the process problem and conduct a fast feasibility analysis of what is at hand. In this way the application of validated models will therefore be able to drive the field biocatalytic process development, as a whole, forward.

Nomenclature

In this article, reactants are designated by the letters A and B in the order in which they are added to the enzyme. Products are designated the letters P and Q in the order in which they leave the enzyme. Stable enzyme forms are designated E and F, complexes between *e.g.* E and A are designated EA. K_{i_x} is the dissociation constant of EX, K_{M_x} is the Michaelis–Menten constant for the individual compound X. The number of kinetically important reactants in a given direction is indicated by the prefix or postfix uni, bi, ter and quad. A reaction with two reactants and two products is therefore termed a bi–bi reaction.

Acknowledgements

R. H. Ringborg kindly acknowledges that he is funded by the European Union Seventh Framework Programme (FP7/2007-2013) BIOINTENSE under grant agreement no. 312148 and the Technical University of Denmark.

References

1 K. Faber, W.-D. Fessner and N. J. Turner, *Science of Synthesis: Biocatalysis in Organic Synthesis*, Georg Thieme Verlag KG, 2015.
2 K. Drauz, H. Groger and O. May, *Enzyme Catalysis in Organic Synthesis, Third, Completely Revised and Enlarged Edition*, WILEY-VCH Verlag, 3rd edn, 2012.
3 D. J. Pollard and J. M. Woodley, *Trends Biotechnol.*, 2007, **25**, 66–73.
4 B. M. Nestl, B. A. Nebel and B. Hauer, *Curr. Opin. Chem. Biol.*, 2011, **15**, 187–193.
5 H.-P. Meyer, E. Eichhorn, S. Hanlon, S. Lütz, M. Schürmann, R. Wohlgemuth and R. Coppolecchia, *Catal. Sci. Technol.*, 2012, **3**, 29–40.
6 G. W. Huisman and S. J. Collier, *Curr. Opin. Chem. Biol.*, 2013, **17**, 284–292.
7 A. Schmid, J. S. Dordick, B. Hauer, A. Kiener, M. Wubbolts and B. Witholt, *Nature*, 2001, **409**, 258–268.
8 Y. Ni, D. Holtmann and F. Hollmann, *ChemCatChem*, 2014, **6**, 930–943.
9 N. J. Turner and M. D. Truppo, *Curr. Opin. Chem. Biol.*, 2013, **17**, 212–214.
10 G. A. Strohmeier, H. Pichler, O. May and M. Gruber-Khadjawi, *Chem. Rev.*, 2011, **111**, 4141–4164.
11 U. T. Bornscheuer, G. W. Huisman, R. J. Kazlauskas, S. Lutz, J. C. Moore and K. Robins, *Nature*, 2012, **485**, 185–194.
12 J. B. Siegel, A. Zanghellini, H. M. Lovick, G. Kiss, R. Abigail, J. L. S. Clair, J. L. Gallaher, D. Hilvert, M. H. Gelb, B. L. Stoddard, K. N. Houk, F. E. Michael and D. Baker, *Science*, 2011, **329**, 309–313.
13 E. Ricca, B. Brucher and J. H. Schrittwieser, *Adv. Synth. Catal.*, 2011, **353**, 2239–2262.
14 R. C. Simon, N. Richter, E. Busto and W. Kroutil, *ACS Catal.*, 2014, **4**, 129–143.
15 H. Gröger and W. Hummel, *Curr. Opin. Chem. Biol.*, 2014, **19**, 171–179.
16 A. Bruggink, R. Schoevaart and T. Kieboom, *Org. Process Res. Dev.*, 2003, **7**, 622–640.
17 D. G. Blackmond, *J. Am. Chem. Soc.*, 2015, **137**, 10852–10866.
18 V. Hessel, D. Kralisch, N. Kockmann, T. Noël and Q. Wang, *ChemSusChem*, 2013, **6**, 746–789.
19 J. P. McMullen and K. F. Jensen, *Annu. Rev. Anal. Chem.*, 2010, **3**, 19–42.
20 S. G. Newman and K. F. Jensen, *Green Chem.*, 2013, **15**, 1456–1472.
21 J. M. Woodley, *Curr. Opin. Chem. Biol.*, 2013, **17**, 310–316.
22 P. Tufvesson, J. Lima-Ramos, N. Al Haque, K. V. Gernaey and J. M. Woodley, *Org. Process Res. Dev.*, 2013, **17**, 1233–1238.
23 J. Lima-Ramos, W. Neto and J. M. Woodley, *Top. Catal.*, 2014, **57**, 301–320.
24 A. M. Klibanov, *Nature*, 2001, **409**, 241–246.
25 C. R. Thomas and D. Geer, *Biotechnol. Lett.*, 2011, **33**, 443–456.
26 A. L. Paiva, V. M. Balcão and F. X. Malcata, *Enzyme Microb. Technol.*, 2000, **27**, 187–204.
27 P. J. Halling, *Enzyme Microb. Technol.*, 1994, **16**, 178–206.
28 R. J. Meier, M. T. Gundersen, J. M. Woodley and M. Schürmann, *ChemCatChem*, 2015, **7**, 2594–2597.
29 R. Abu and J. M. Woodley, *ChemCatChem*, 2015, **7**, 3094–3105.
30 J. M. Woodley, M. Bisschops, A. J. J. Straathof and M. Ottens, *J. Chem. Technol. Biotechnol.*, 2008, **83**, 121–123.
31 W. van Hecke, G. Kaur and H. De Wever, *Biotechnol. Adv.*, 2014, **32**, 1245–1255.
32 H. Bisswanger, *Perspect. Sci.*, 2014, **1**, 41–55.
33 C. Vieille, G. J. Zeikus and C. Vieille, *Microbiol. Mol. Biol. Rev.*, 2001, **65**, 1–43.
34 G. Bruylants, J. Wouters and C. Michaux, *Curr. Med. Chem.*, 2005, **12**, 2011–2020.

35 C. G. Alexander, R. Wanner, C. M. Johnson, D. Breitsprecher, G. Winter, S. Duhr, P. Baaske and N. Ferguson, *Biochim. Biophys. Acta, Proteins Proteomics*, 2014, **1844**, 2241–2250.
36 D. G. Blackmond, *Angew. Chem., Int. Ed.*, 2005, **44**, 4302–4320.
37 I. H. Segel, *Enzyme kinetics: behavior and analysis of rapid equilibrium and steady-state enzyme systems*, John Wiley & Sons, 1975, vol. 2.
38 W. W. Cleland, in *The enzymes, vol II: kinetics and mechanism*, ed. P. D. Boyer, Academic Press, 3rd edn, 1970, pp. 1–61.
39 H. W. Adolph, P. Maurer, H. Schneider-bernlöhr, C. Sartorius and M. Zeppezauer, *Eur. J. Biochem.*, 1991, **201**, 615–625.
40 P. W. Heinstra, G. E. Thörig, W. Scharloo, W. Drenth and R. J. Nolte, *Biochim. Biophys. Acta*, 1988, **967**, 224–233.
41 K. Dalziel and F. M. Dickinson, *Biochem. J.*, 1966, **100**, 34–46.
42 K. J. Humphreys, L. M. Mirica, Y. Wang and J. P. Klinman, *J. Am. Chem. Soc.*, 2009, **131**, 4657–4663.
43 C. S. Tsai, M. W. Burgett and L. J. Reed, *J. Biol. Chem.*, 1973, **248**, 8348–8352.
44 H. Suzuki, Y. Ogura and H. Yamada, *J. Biochem.*, 1972, **72**, 703–712.
45 J. A. Adams, *Chem. Rev.*, 2001, **101**, 2271–2290.
46 V. T. Maddaiah and N. B. Madsen, *J. Biol. Chem.*, 1966, **241**, 3873–3881.
47 C. W. Carreras and D. V. Santi, *Annu. Rev. Biochem.*, 1995, **64**, 721–762.
48 S. Y. Roth, J. M. Denu and C. D. Allis, *Annu. Rev. Biochem.*, 2001, **70**, 81–120.
49 C. P. Henson and W. W. Cleland, *Biochemistry*, 1963, **3**, 338–345.
50 J. S. Shin and B. G. Kim, *Biotechnol. Bioeng.*, 1998, **60**, 534–540.
51 N. Al-Haque, P. A. Santacoloma, W. Neto, P. Tufvesson, R. Gani and J. M. Woodley, *Biotechnol. Prog.*, 2012, **28**, 1186–1196.
52 M. Gyamerah and A. J. Willetts, *Enzyme Microb. Technol.*, 1997, **20**, 127–134.
53 B. H. Chen, E. G. Hibbert, P. A. Dalby and J. M. Woodley, *AIChE J.*, 2008, **54**, 3–5.
54 B. A. van der Veen, G. J. W. M. van Alebeek, J. C. M. Uitdehaag, B. W. Dijkstra and L. Dijkhuizen, *Eur. J. Biochem.*, 2000, **267**, 658–665.
55 M. Maestracci, A. Thiery, A. Arnaud and P. Galzy, *Agric. Biol. Chem.*, 1986, **50**, 2237–2241.
56 D. Fournand, F. Bigey and A. Arnaud, *Appl. Environ. Microbiol.*, 1998, **64**, 2844–2852.
57 W. Wang, P. Baker and S. Y. K. Seah, *Biochemistry*, 2010, **49**, 3774–3782.
58 N. P. Botting and D. Gani, *Biochemistry*, 1992, **31**, 1509–1520.
59 R. Schulz, *A, Enzyme Kinetics*, Cambridge University Press, 1994.
60 G. Franceschini and S. Macchietto, *Chem. Eng. Sci.*, 2008, **63**, 4846–4872.
61 D. Telen, F. Logist, E. van Derlinden, I. Tack and J. van Impe, *Chem. Eng. Sci.*, 2012, **78**, 82–97.
62 G. Franceschini and S. Macchietto, *AIChE J.*, 2008, **54**, 1009–1024.
63 K. A. Johnson, *FEBS Lett.*, 2013, **587**, 2753–2766.
64 K. S. Anderson, J. A. Sikorski and K. A. Johnson, *Biochemistry*, 1988, **27**, 7395–7406.
65 S. Mozharov, A. Nordon, D. Littlejohn, C. Wiles, P. Watts, P. Dallin and J. M. Girkin, *J. Am. Chem. Soc.*, 2011, **133**, 3601–3608.
66 S. Schwolow, F. Braun, M. Rädle, N. Kockmann and T. Röder, *Org. Process Res. Dev.*, 2015, **19**, 1286–1292.
67 J. Fagaschewski, D. Sellin, C. Wiedenhöfer, S. Bohne, H. K. Trieu and L. Hilterhaus, *Bioprocess Biosyst. Eng.*, 2015, **38**, 1399–1405.
68 J. S. Moore and K. F. Jensen, *Angew. Chem., Int. Ed.*, 2014, **53**, 470–473.
69 H. B. Burch, M. E. Bradley and O. H. Lowry, *J. Biol. Chem.*, 1967, **242**, 4546–4554.
70 J. V. Passonneau and O. H. Lowry, *Enzym. Anal. A Pract. Guid.*, 1993, pp. 229–305.
71 H. Bisswanger, *Practical Enzymology*, Wiley-VCH Verlag GmbH & Co. KGaA, 2nd edn, 2011.
72 D. L. Purich and R. D. Allison, *The enzyme reference: a comprehensive guidebook to enzyme nomenclature, reactions, and methods*, 1st edn, 2003.
73 E. Pick and Y. Keisari, *J. Immunol. Methods*, 1980, **38**, 161–170.
74 O. Erel, *Clin. Biochem.*, 2005, **38**, 1103–1111.
75 L. Rios-Solis, N. Bayir, M. Halim, C. Du, J. M. Ward, F. Baganz and G. J. Lye, *Biochem. Eng. J.*, 2013, **73**, 38–48.
76 L. Rios-Solis, P. Morris, C. Grant, A. O. O. Odeleye, H. C. Hailes, J. M. Ward, P. A. Dalby, F. Baganz and G. J. Lye, *Chem. Eng. Sci.*, 2015, **122**, 360–372.
77 F. Galgani, Y. Cadiou and G. Bocquene, *Biotechnol. Bioeng.*, 1991, **38**, 434–437.
78 S. Schätzle, M. Höhne, E. Redestad, K. Robins and U. T. Bornscheuer, *Anal. Chem.*, 2009, **81**, 8244–8248.
79 L. A. DeLouise and B. L. Miller, *Anal. Chem.*, 2005, **77**, 1950–1956.
80 Y. Kim, K. G. Tanner and J. M. Denu, *Anal. Biochem.*, 2000, **280**, 308–314.
81 P. Baker, D. Pan, J. Carere, A. Rossi, W. Wang and S. Y. K. Seah, *Biochemistry*, 2009, **48**, 6551–6558.
82 B. J. Burke and F. E. Regnier, *Anal. Chem.*, 2003, **75**, 1786–1791.
83 B. Faller, M. Cadène and J. G. Bieth, *Biochemistry*, 1993, **32**, 9230–9235.
84 B. Kintses, Z. Simon, M. Gyimesi, J. Tóth, B. Jelinek, C. Niedetzky, M. Kovács and A. Málnási-Csizmadia, *Biophys. J.*, 2006, **91**, 4605–4610.
85 S. K. Hartwell and K. Grudpan, *J. Anal. Methods Chem.*, 2012, 2012.
86 L. P. Saunders, W. Cao, W. C. Chang, R. A. Albright, D. T. Braddock and E. M. De La Cruz, *J. Biol. Chem.*, 2011, **286**, 30130–30141.

87 M. J. Todd and J. Gomez, *Anal. Biochem.*, 2001, **296**, 179–187.
88 G. D. Watt, *Anal. Biochem.*, 1990, **187**, 141–146.
89 I. Haq and B. Hill, *Microcal, LLC Appl. note*, 2002, p. 44.
90 M. L. Bianconi, *Biophys. Chem.*, 2007, **126**, 59–64.
91 E. L. Cussler, *Diffusion: Mass Transfer in Fluid Systems*, 1997, vol. Second.
92 M. E. Young, P. A. Carroad and R. L. Bell, *Biotechnol. Bioeng.*, 1980, **22**, 947–955.
93 J. W. Swarts, R. C. Kolfschoten, M. C. A. A. Jansen, A. E. M. Janssen and R. M. Boom, *Chem. Eng. J.*, 2010, **162**, 301–306.
94 K. Jähnisch, V. Hessel, H. Löwe and M. Baerns, *Angew. Chem., Int. Ed.*, 2004, **43**, 406–446.
95 C. Wiles and P. Watts, *Green Chem.*, 2012, **14**, 38.
96 R. L. Hartman and K. F. Jensen, *Lab Chip*, 2009, **9**, 2495–2507.
97 R. Wohlgemuth, I. Plazl, P. Žnidaršič-Plazl, K. V. Gernaey and J. M. Woodley, *Trends Biotechnol.*, 2015, **33**, 302–314.
98 J. I. Yoshida, H. Kim and A. Nagaki, *ChemSusChem*, 2011, **4**, 331–340.
99 K. D. Nagy, B. Shen, T. F. Jamison and K. F. Jensen, *Org. Process Res. Dev.*, 2012, **16**, 976–981.
100 G. Taylor, *Proc. R. Soc. London, Ser. A*, 1953, **219**, 186–203.
101 R. Aris, *Proc. R. Soc. London, Ser. A*, 1956, **235**, 67–77.
102 D. L. Zechel, L. Konermann, S. G. Withers and D. J. Douglas, *Biochemistry*, 1998, **2960**, 7664–7669.
103 S. L. Lawson, W. W. Wakarchuk and S. G. Withers, *Biochemistry*, 1997, **36**, 2257–2265.
104 J. P. Huddleston, G. K. Schroeder, K. A. Johnson and C. P. Whitman, *Biochemistry*, 2012, **51**, 9420–9435.
105 J. A. Thomson and J. E. Ladbury, in *Biocalorimetry 2: Application of Calorimetry in the Biological Sciences*, ed. J. E. Ladbury and M. L. Doyle, 2004.
106 H. Fukada and K. Takahashi, *Proteins: Struct., Funct., Genet.*, 1998, **33**, 159–166.
107 M. W. Freyer and E. A. Lewis, *Methods Cell Biol.*, 2008, **84**, 79–113.
108 J. J. Christensen, R. M. Izatt, L. D. Hansen and J. A. Partridge, *J. Phys. Chem.*, 1966, **70**, 2003–2010.
109 L. D. Hansen, J. J. Christensen and R. M. Izatt, *Chem. Commun.*, 1965, 36–38.
110 D. Vasić-Rački, Z. Findrik and A. Vrsalović Presečki, *Appl. Microbiol. Biotechnol.*, 2011, **91**, 845–856.
111 G. Sin, J. M. Woodley and K. V. Gernaey, *Biotechnol. Prog.*, 2009, **25**, 1529–1538.
112 W. R. Berendsen, G. Gendrot, A. Freund and M. Reuss, *Biotechnol. Bioeng.*, 2006, **96**, 883–892.
113 S. D. Schaber, D. I. Gerogiorgis, R. Ramachandran, J. M. B. Evans, P. I. Barton and B. L. Trout, *Ind. Eng. Chem. Res.*, 2011, **50**, 10083–10092.
114 S. D. Schaber, S. C. Born, K. F. Jensen and P. I. Barton, *Org. Process Res. Dev.*, 2014, **18**, 1461–1467.
115 M. Scheer, A. Grote, A. Chang, I. Schomburg, C. Munaretto, M. Rother, C. Söhngen, M. Stelzer, J. Thiele and D. Schomburg, *Nucleic Acids Res.*, 2011, **39**, 670–676.

APPENDIX D – LABVIEW

The ramp control virtual instrument is here illustrated and is presented in the following order:

- Front panel
- Sequence control
- Pump control
- Injection valve and sample volume calculation

All LabVIEW virtual instruments are available here:

https://www.dropbox.com/sh/r07zkoulqm6wv6v/AABCANJ08IFuAfcKxFU-M2Yba?dl=0

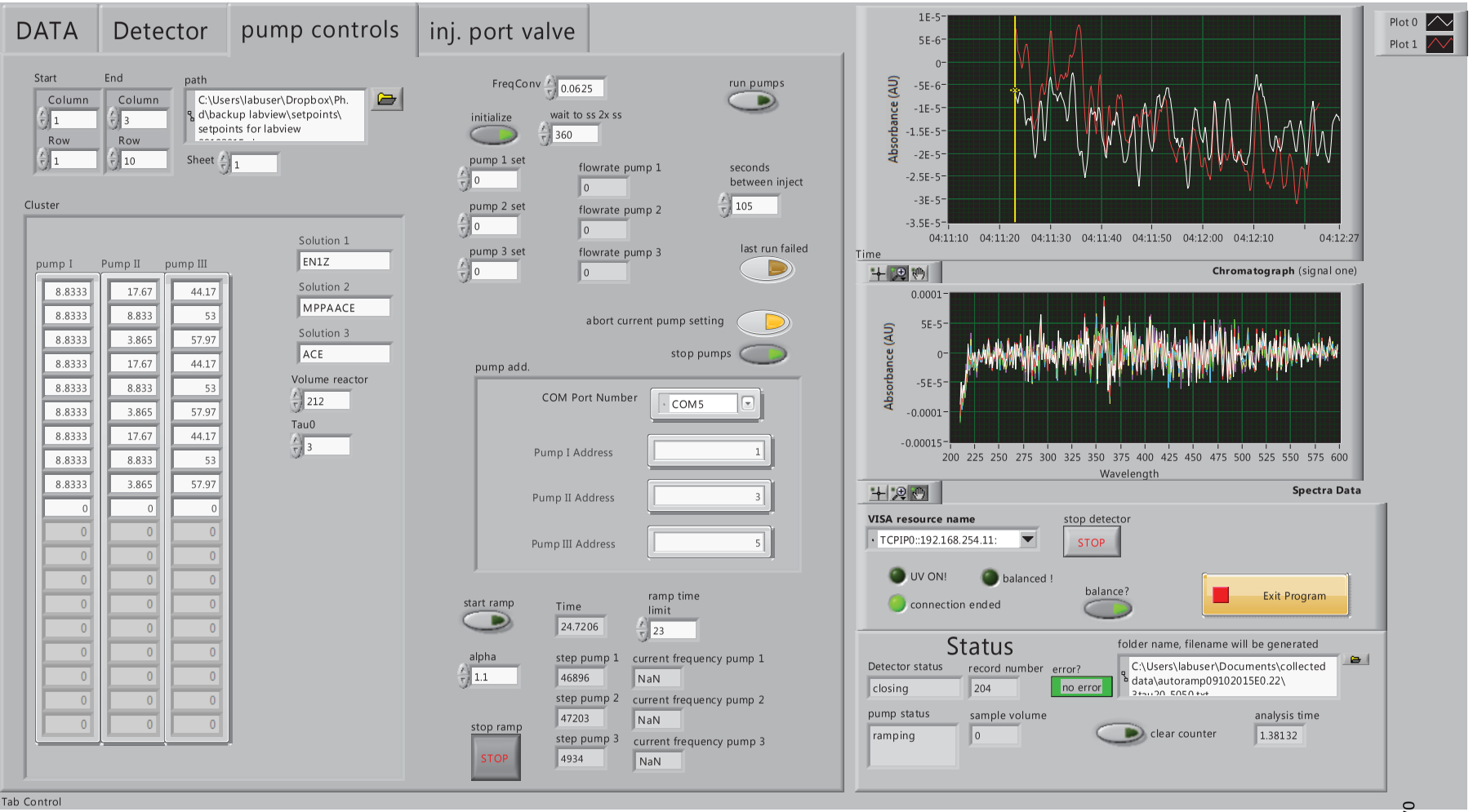
DATA
Detector
pump controls
inj. port valve
Start
End
Column
Row
path
C:\Users\labuser\Dropbox\Ph. d\backup labview\setpoints\ setpoints for labview
Sheet
Cluster
pump I
Pump II
pump III
Solution 1
EN1Z
Solution 2
MPPAACE
Solution 3
ACE
Volume reactor
212
Tau0
FreqConv
0.0625
initialize
wait to ss 2x ss
360
run pumps
pump 1 set
pump 2 set
pump 3 set
flowrate pump 1
flowrate pump 2
flowrate pump 3
seconds between inject
105
last run failed
abort current pump setting
stop pumps
pump add.
COM Port Number
COM5
Pump I Address
Pump II Address
Pump III Address
start ramp
Time
24.7206
ramp time limit
23
alpha
1.1
step pump 1
step pump 2
step pump 3
current frequency pump 1
current frequency pump 2
current frequency pump 3
stop ramp
STOP
Absorbance (AU)
Time
Chromatograph (signal one)
Wavelength
Spectra Data
VISA resource name
TCPIP0::192.168.254.11:
stop detector
STOP
UV ON!
balanced !
connection ended
balance?
Exit Program
Status
Detector status
closing
record number
204
error?
no error
folder name, filename will be generated
C:\Users\labuser\Documents\collected data\autoramp09102015E0.22\
pump status
ramping
sample volume
clear counter
analysis time
1.38132
Plot 0
Plot 1
Tab Control

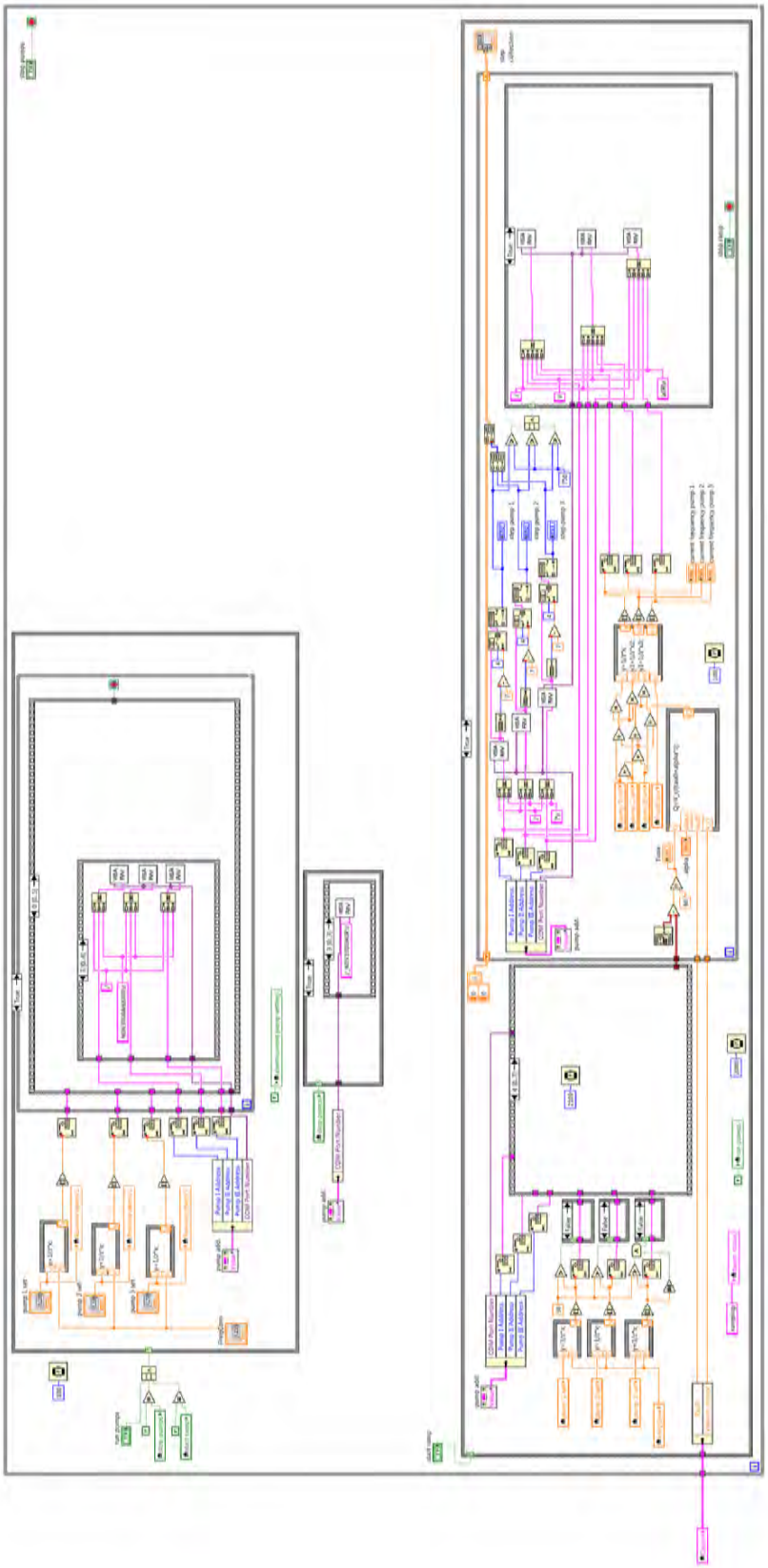

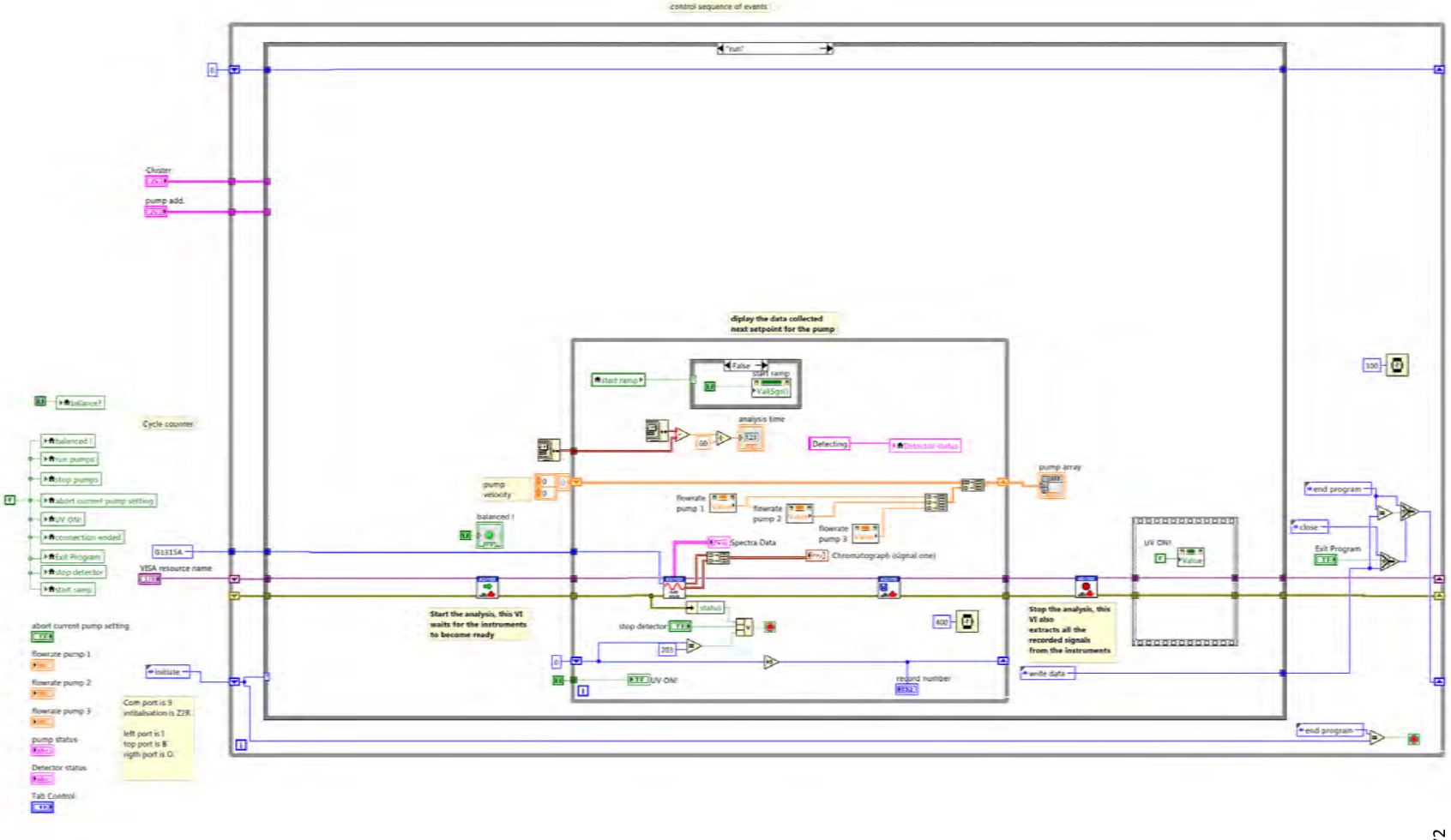
control sequence of events
"run"
Cluster
pump add.
balance?
Cycle counter
balanced !
run pumps
stop pumps
abort current pump setting
UV ON!
connection ended
Exit Program
stop detector
start ramp
G1315A
VISA resource name
abort current pump setting
flowrate pump 1
flowrate pump 2
flowrate pump 3
pump status
Detector status
Tab Control
initiate
Com port is 9
initialisation is Z1R
left port is 1
top port is 8
rigth port is 0.
diplay the data collected
next setpoint for the pump
False
start ramp
analysis time
Detecting
Detector status
pump velocity
balanced !
flowrate pump 1
flowrate pump 2
flowrate pump 3
pump array
Spectra Data
Chromatograph (signal one)
Start the analysis, this VI
waits for the instruments
to become ready
status
stop detector
UV ON!
record number
write data
Stop the analysis, this
VI also
extracts all the
recorded signals
from the instruments
UV ON!
end program
close
Exit Program
end program

Calculate sample volume based on flowrate

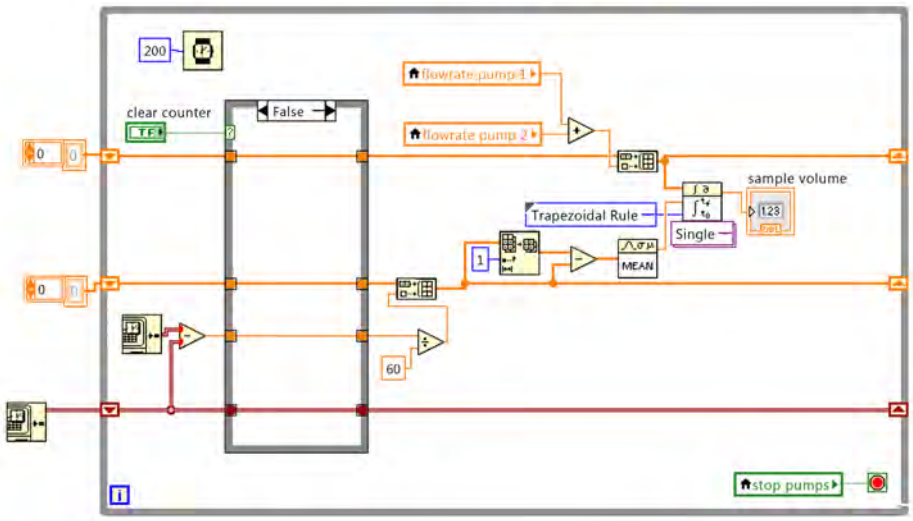

control injector valve

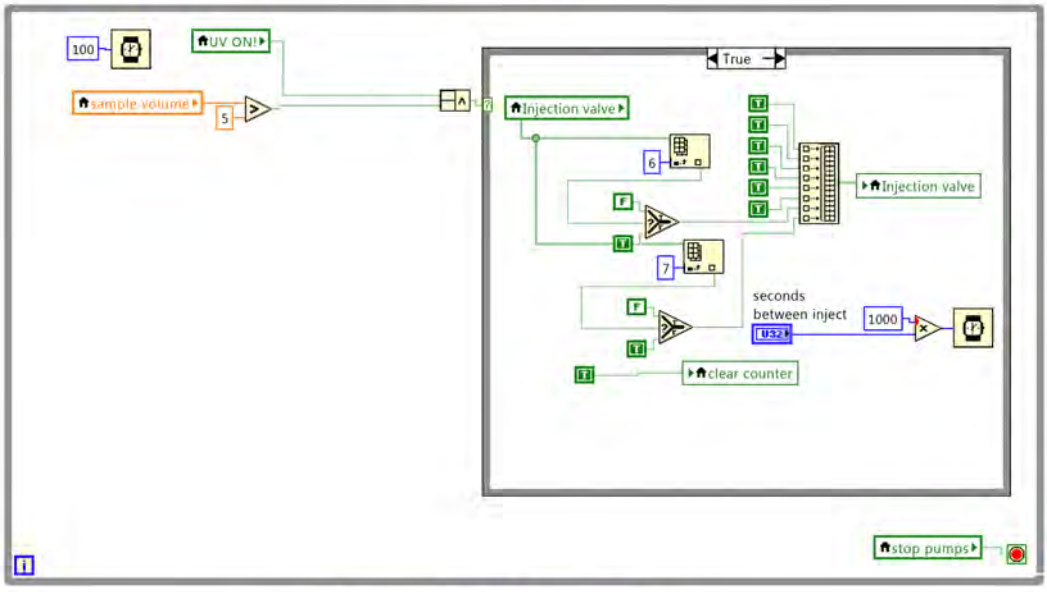

send commands to control of the injection valve

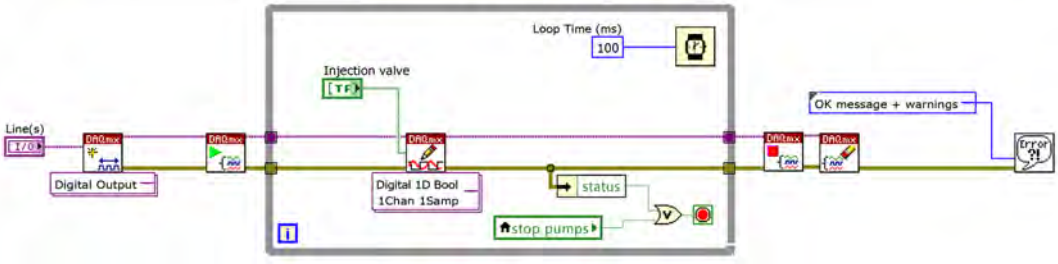

Channel Settings

APPENDIX E – MATLAB SCRIPTS

Icoshift and parafac (N-way toolbox) can be obtained at www.models.life.ku.dk, ApplyiCoshift is scheduled to be released at the end of 2015.

All the scripts developed here are available at

https://www.dropbox.com/sh/r07zkoulqm6wv6v/AABCANJ08IFuAfcKxFU-M2Yba?dl=0

calibration

```
%% load calibration data
dirName = 'folder path';                %# folder path
files = dir( fullfile(dirName,'*.txt') );   %# list all *.txt files
[r idx] = sort({files.date});
files = files(idx);
files = {files.name}';                      %# file names

data = cell(numel(files),1);                %# store file contents

for i=1:numel(files)
    fname = fullfile(dirName,files{i});     %# full path to file
    data{i} = csvread(fname);               %# load file
end

for k=1:numel(files)
xdata{k}=data{k}(38:200,15:end-140);        %extract usefull data
end

for i=1 :numel(files)
    appxcali(i,:,:)=[xdata{i}];             % Cell to array
end

%% Align samples
clearvars localdata Xmax Xint Mint invervals indexes
[n,m,l]=size(appxcali);
Xhatcoshiftapp=zeros(n,m,l);
Xmax = max(appxcali(:,:,45:end),[],3);              % Align after
maximum of 285-460;
Xint = interp1((1:m)',Xmax',linspace(1,m,m*2-1))';  % interpolate
chromatrogram in respect to residence time
Mint = max(Xint); Mint(1:200) = Mint(5);            % define target
for alignment
[AlignedUVData, intervals, indexes] = icoshift (Mint, Xint, 'whole',
6,[2 1 0]); % the shifts are calculated and stored

Y = reshape(appxcali(:,:)',[m n*l]); % The three way data is reshaped
Yint = interp1((1:m)',Y,linspace(1,m,2*m-1)); % All data are
interpolated
YRes = reshape(Yint,[l*(2*m-1) n]);
YResT = YRes';
Xhat = reshape(YResT,[n 2*m-1 l]);   % data is transformed back to
three way
[Xhatcoshift] = ApplyiCoshift(Xhat, intervals(:,1:3), indexes, true,
2); % apply transformation of alignment to all data
Xhatcoshiftapp(:,:,:) = Xhatcoshift(:,1:2:end,:);   % resample


%% Create alignment profile from aligned data
clearvars localdata Xmax Xint Mint invervals indexes
```

```
[n,m,l]=size(Xhatcoshiftapp);

Xmax = max(Xhatcoshiftapp(:,:,45:end),[],3);
Xint = interp1((1:m)',Xmax',linspace(1,m,m*2-1))';
Mint = max(Xint); Mint(1:200) = Mint(5);
% Define target for alignment
[AlignedUVData, intervals, indexes] = icoshift (Mint, Xint, 'whole',
6,[2 1 0]);
%% Save aligned data in workspace
Aligneddata = Xhatcoshiftapp;

%% Create calibration PARAFAC model
[Factors,it,err,corcondia]=parafac(Aligneddata,4,[1e-
6,0,0,0],[2,2,2]);                    % fit PARAFAC model
for (i = 1:3);sh(i) = subplot(2,2,i); plot(Factors{1,i});
title(sprintf('mode. #%i',i));end % model
```

Make concentration array based on filenames

```
n=length(files);
c=[];
conc=[];

%Example of how combinations of ACE and mppaace was found
for i=1:n
    Str=files{i};
    Key   = 'ACE';
    Key2   = 'mppaace';
    Index = strfind(Str, Key);
    Index2 = strfind(Str, Key2);
%check string if both names occur
    if isempty(Index)==0 && isempty(Index2)==0
        c1 = num2str(sscanf(Str(Index(1) + length(Key):end), '%g',
2));
        c2 = num2str(sscanf(Str(Index2(1) + length(Key2):end), '%g',
2));
        if isempty(c1)==0 && isempty(c2)==0;

% input weight of compound (mass(g)/molar weight(g/mol)/Volume(L)) /
100%
            %ACE set concentrations based on ACE stock solution
            cmppa1=0;
            cba1=0;
            cace1=0.6591/58.08/0.1*1000/100;
            cenz1=0;

            %mppaace set concentrations based on mppaace stock
solution
            cmppa2=0.6723/149.21/0.1*1000/100;
            cba2=0;
            cace2=0.6582/58.08/0.1*1000/100;
            cenz2=0;

        % calculate actual concentrations of the different compounds
as a combination of setpoints(defined from LabVIEW in percent
integers) and concentration of the two stock solutions
        conc(i,1)=str2num(c1)*cmppa1+str2num(c2)*cmppa2;
        conc(i,2)=str2num(c1)*cace1+str2num(c2)*cace2;
        conc(i,3)=str2num(c1)*cba1+str2num(c2)*cba2;
        conc(i,4)=str2num(c1)*cenz1+str2num(c2)*cenz2;
        end

    end
```

```
%after concentrations have been calculated extract the solutions has
been defined scores are extracted from the parafac model (Factors)

%conc & scores
% 1 MPPA
% 2 Ace
% 3 ENZ
% 4 BA


scores=Factors{1,1};

comp1=createFit(scores(:,1),,conc(:,1),'MPPA');
p(1,1)=comp1.p1;
p(1,2)=comp1.p2;
comp2=createFit(scores(:,2),conc(:,2),'ACE');
p(2,1)=comp2.p1;
p(2,2)=comp2.p2;
comp3=createFit(scores(:,3),conc(:,3),'ENZ');
p(3,1)=comp3.p1;
p(3,2)=comp3.p2;
comp4=createFit(scores(:,4),conc(:,4),'BA');
p(4,1)=comp4.p1;
p(4,2)=comp4.p2;
```

createFit - Fit scores and concentration of samples for calibration

```
function [fitresult, gof] = createFit(scores, conc,i)
%% Fit: 'untitled fit 1'.
[xData, yData] = prepareCurveData(scores, conc );

% Set up fittype and options.
ft = fittype( 'poly1' );
opts = fitoptions( 'Method', 'LinearLeastSquares' );
opts.Robust = 'Bisquare';

% Fit model to data.
[fitresult, gof] = fit( xData, yData, ft, opts );

str= (['Calibration of ' i]);
% Plot fit with data.
figure( 'Name', str);
hold on
h = plot( fitresult, xData, yData);
set(h,'LineWidth',2);
set(h,'MarkerSize',14);
legend( h,[i 'data'], 'fit', 'Location', 'NorthWest' );
title(str);
% Label axes
xlabel(i)
ylabel('concentration [mM]')
grid on
set(gca,'FontName','Calibri');
set(gca,'FontSize',16);

p(1)=fitresult.p1;
p(2)=fitresult.p2;
yfit = p(1)*xData+p(2);
yresid = yData - yfit;
```

```
SSresid = sum(yresid.^2);
SStotal = (length(yData)-1) * var(yData);
rsq = 1 - SSresid/SStotal;


str1={'R^2 =' str2num(sprintf('%.3f',rsq))};
text(0.6*max(xData),0.1*max(yData),str1,
'FontSize',14,'BackgroundColor','w','EdgeColor','b')
hold off
```

Apply calibration model to experimental data

```
%% load experimental data
clearvars -except Aligneddata Factors Mint predicted p %
dirName = 'folder path';
files = dir( fullfile(dirName,'*.txt') );   %# list all *.txt files
[r idx] = sort({files.date});
files = files(idx);
files = {files.name}';                      %# file names

data = cell(numel(files),1);                %# store file contents

for i=1:numel(files)
    fname = fullfile(dirName,files{i});     %# full path to file
    data{i} = csvread(fname);               %# load file
end

for k=1:numel(files)
time{k}=data{k}(1,394);                     %extract start time !393
for calidata!
xdata{k}=data{k}(38:200,15:end-141);        %extract usefull data
end

for i=1 :numel(files)
    appxdata(i,:,:)=[xdata{i}];             % cell to array
    apptime(i)=[time{i}];                   % cell to array

end
apptime1=(apptime(:)-apptime(1))/60;        % time development from 0
in mintues

% correct time for midnight shift
neglocs=find(apptime1<0);
if isempty(neglocs)==0

    for i=neglocs(1)+1:length(apptime1)
    apptime1(i)=apptime1(i)-
apptime1(neglocs(1))+10+apptime1(neglocs(1)-1);

    end
    apptime1(neglocs(1))=apptime1(neglocs(1))-
apptime1(neglocs(1))+10+apptime1(neglocs(1)-1);
end



%% align data
clearvars localdata Xmax Xint invervals indexes
[n,m,l]=size(appxdata);
```

```
Xhatcoshiftapp=zeros(n,m,l);
Xmax = max(appxdata(:,:,45:end),[],3);              % Align after
maximum of 285-460;
Xint = interp1((1:m)',Xmax',linspace(1,m,m*2-1))';  % interpolate
chromatrogram in respect to residence time
%Mint = max(Xint); %Mint(1:230) = Mint(5);
[AlignedUVData, intervals, indexes] = icoshift (Mint, Xint, 'whole',
30,[2 1 0]);  % the shifts are calculated and stored with Mint from
the calibration

Y = reshape(appxdata(:,:)',[m n*l]);    % The three way data is
reshaped
Yint = interp1((1:m)',Y,linspace(1,m,2*m-1)); % All data are
interpolated
YRes = reshape(Yint,[l*(2*m-1) n]);
YResT = YRes';
Xhat = reshape(YResT,[n 2*m-1 l]); % data is transformed back to three
way
[Xhatcoshift] = ApplyiCoshift(Xhat, intervals(:,1:3), indexes, true,
2); % apply transformation of alignment to all data
Xhatcoshiftapp(:,:,:) = Xhatcoshift(:,1:2:end,:); % resample

%% parafac for new data
Factors{1}=zeros(k,5);
[Factorsdata,it,err,corcondia]=parafac(Xhatcoshiftapp,5,[1e-
6,0,0,0],[0,0,0],Factors,[0,1,1]);
figure
for (i = 1:3);sh(i) = subplot(2,2,i); plot(Factorsdata{1,i});
title(sprintf('Mode. #%i',i));end

[n,m,l]=size(appxdata);
predicted=zeros(n,4);
corrcoeff=Factorsdata{1,1};
% convert scores into concentration data
predicted(:,1)=p(1,1)*corrcoeff(:,1)+p(1,2);
predicted(:,2)=p(2,1)*corrcoeff(:,2)+p(2,2);
predicted(:,3)=p(3,1)*corrcoeff(:,3)+p(3,2);
predicted(:,4)=p(4,1)*corrcoeff(:,4)+p(4,2);
```

Calculate initial rates

```
% Divide data into setpoint sets
for i=2:numel(data)
    if i==numel(data)
        sets(a,2)=i;
    elseif abs(apptime1(i)-apptime1(i-1))>3;
        sets(a,2)=i-1;    %start of set
        sets(a+1,1)=i;
        a=a+1;
        if sets(a-1,2)-sets(a-1,1)<8 % filter error sets
            a=a-1;
            sets(a,1)=sets(a+1,1);
        end
    end
    sets(1,1)=1;
end

% calculate space time for each sample

alpha=0.5;
S=1-exp(-alpha); %slope of real time versus residence time
tau0=5; %steady state residence time
```

```
for i=1:length(sets)
    clearvars localdata
    localdata=apptime1(sets(i,1):sets(i,2))-apptime1(sets(i,1)-1);

    for j=1:length(localdata)
    if localdata(j)<5
        spacetime{i}(1,j)=localdata(j)-
tau0*(1/alpha*log((tau0+alpha*localdata(j))/tau0)-1);
    else
        spacetime{i}(1,j)=S/alpha*tau0+S*localdata(j);
    end
    end
end


% calculate initial rates based on BA predicted(:,4)
for i=1:length(sets)
    clearvars xData yData yfit yresid SSresid SStotal rsq
    xData = spacetime{i}';
    yData = predicted(sets(i,1):sets(i,2),4);
    ft = fittype( 'poly1' );
    opts = fitoptions( 'Method', 'LinearLeastSquares' );
    opts.Robust = 'Bisquare';

    % Fit model to data.
    [fitresult, gof] = fit( xData, yData, ft, opts );
    vba(i,1)=fitresult.p1;
    vba(i,2)=fitresult.p2;
    % Calculate squared residuals
    yfit = fitresult.p1*xData+fitresult.p2;
    yresid = yData - yfit;
    SSresid = sum(yresid.^2);
    SStotal = (length(yData)-1) * var(yData);
    rsq = 1 - SSresid/SStotal;
    vba(i,3)=rsq;
end

% find enzyme concentration for the individual sets
for i=1:length(sets)
Econc(i,1)=mean(predicted(sets(i,1):sets(i,2),3));
end

% calculate specific activity
for i=1:length(sets)
vspfba(i,1)=vba(i,1)/Econc(i,1);
end
```

CAPEC-PROCESS Research Center
Department of Chemical and Biochemical Engineering
Technical University of Denmark
Søltofts Plads, Building 227
Dk-2800 Kgs. Lyngby
Denmark

Phone: +45 45252800
Web: www.capec-process.kt.dtu.dk